

Design and Analysis of an Energy Efficient Dehumidification System for Drying Applications

Wen-Chung Wang

A thesis submitted in partial fulfilment of the requirements of the
University of Hertfordshire for the degree of Doctor of Philosophy

The programme of research was carried out in the School of Engineering &
Technology, University of Hertfordshire, Hatfield, UK.

December 2015

Abstract

The motivation of this research project was in response to problems of re-condensation in drying, reduced drying rate encountered by the food and beverage packaging industry which led to the aim of developing a better performing drying system as well as achieving high energy efficiency. A hybrid dryer suited for rapid drying applications is designed, constructed and experimentally tested and considered in atmospheric environment only. The system employs a heat pump in conjunction with a heat reactivated desiccant wheel to provide an efficient drying capability and supply low dew point temperature (DPT) conditions. The combined system utilises the heat dissipated by the condenser in regenerating the desiccant wheel, to increase the economic feasibility of such a hybrid system. Up to 60% heat energy can be saved by using the hybrid system in the rapid surface drying applications.

Mathematical models are developed to obtain the correlations among the design operating and performance parameters of the dehumidification systems. The mathematical models can be used to estimate the performance of the hybrid system as well as the performance of the individual components of the system. A prototype model was designed, fabricated and tested. The experimental facility consisted of a heat pump desiccant dehumidifier with the new ecological R134a as a refrigerant which used the heat dissipated by the condenser.

An analysis of the experimental data was conducted to determine the practical relationship between the operational parameters (COP, m_a and T_R) and performance parameters (SMER, DPT and ε) of the system. The observed behaviours of the test cases are suggested to be governed by a specific combination of the operation parameters. The analysis shows that the proposed hybrid system can deliver supply air at a much lower DPT compared with the single refrigerant circuit and a desiccant wheel. It is shown that the specific moisture extraction rate (SMER) for conventional dryers is 0.5 - 1 kg/kWh and SMER for heat pump based system is 3 - 4 kg/kWh whereas the hybrid system achieves SMER >5 kg/kWh. By operating the combined system in tandem, a greater amount of dehumidification could be realised due to the improved ratio of latent to the total load. The present research also confirms the importance of improving heat recovery to improve the performance of a heat-pump-assisted drying system.

Key words: Dehumidification, Drying, Desiccant wheel, Heat recovery, Hybrid system

Acknowledgments

I would like to acknowledge my supervisory team: Dr. Rodney Day and Dr. Pandelis Kourtessis for the guidance and support they have provided.

I am particularly grateful to Dr. Raj Calay for her guidance, not only in engineering, also in other aspects of life. To Dr. Yong-Kang Chen for providing the relevant software training for this study and to Mr. David Dell for his encouragement and support that enabled me to complete this study

I would like to thank my classmates Rajeev Vishwakarma, Claudia Pisac, Ian Campbell, Lazaros Aresti, Behrad Vahedi, Chuanli Zhao and Xu Zhang for providing encouragement, support and the help in making the initial steps towards research.

Many thanks must go to Mrs. Lorraine Nicholls, the Research Students Administrator, for her continuing support.

Of course, my greatest gratitude goes to my family for their infinite support, my parents, my wife Hsing-Chen Lin, my daughter Ya-Chun Wang and my son Wei-Chun Wang, who always believed in me.

Nomenclature

A	heat transfer surfaces area (m^2)
a_1-a_{38}	coefficients of empirical equations to calculate refrigerant thermodynamic properties
A_{co}	condenser outside finned tube surface area (m^2)
A_{eo}	evaporator outside finned tube surface area (m^2)
b_1-b_4	coefficients of empirical equations to calculate steam properties
BF	bypass factor
COP	coefficient of performance
COP_{HP}	COP of the heat pump
COP_R	COP of the refrigerator
c_p	specific heat at constant pressure (kJ/kg K)
c_{pa}	specific heat of dry air (kJ/kg K)
c_{pam}	specific heat of moist air (kJ/kg K)
c_{pf}	specific heat of condensate refrigerant film (kJ/kg K)
c_{pv}	specific heat of water vapour (kJ/kg K)
D	diameter of tubes (m)
DBT	dry bulb temperature ($^{\circ}C$)
D_p	diameter of compressor cylinder (m)
DPT	dew point temperature ($^{\circ}C$)
DW	desiccant wheel
P_{comp}	compressor power requirement (kW)
P_{fan}	fan power requirement (kW)
f	friction factor
G	mass velocity (kg/m^2s)
h	specific enthalpy of refrigerant (kJ/kg)
h_a	specific enthalpy of air (kJ/kg dry air)
h_{fg}	specific latent heat of vaporisation of refrigerant (kJ/kg)
h_{fg}	specific latent heat of vaporisation of water at reference temperature of $0^{\circ}C$ (kJ/kg)
h_g	specific enthalpy per unit mass of saturated vapour (kJ/kg)
HP	heat pump
HPD	heat pump dryer
$HPDW$	heat pump desiccant wheel
h_v	specific enthalpy of water vapour (kJ/kg)
h_v	specific enthalpy per unit mass of water vapour (kJ/kg)
h_{we}	specific enthalpy of condensed water at evaporator surface temperature (kJ/kg)

<i>IEC</i>	indirect evaporative cooling
<i>K_{lf}</i>	load factor
<i>L</i>	length of main tube (<i>m</i>)
<i>L_{ad}</i>	length of air duct (m)
<i>LMTD</i>	log mean temperature difference
<i>L_p</i>	stroke of compressor piston (m)
<i>L_{rs}</i>	tube row spacing (m)
<i>L_t</i>	tube length (m)
<i>m</i>	mass (kg)
<i>M</i>	molecular mass (kg/mol)
<i>m_a</i>	mass of dry air (kg)
<i>M_a</i>	molecular mass of dry air (kg/mol)
<i>q_{ma}</i>	mass flow rate of dry air (kg/s)
<i>MER</i>	moisture removal capacity (kg/s)
<i>m_p</i>	dry mass of the product (kg)
<i>q_{mr}</i>	mass flow rate of refrigerant (kg/s)
<i>m_v</i>	masses weight of water vapour (kg)
<i>M_v</i>	molecular mass of water vapour (kg/mol)
<i>m_w</i>	mass of moisture (kg)
<i>M_w</i>	molar mass moisture (kg/mol)
<i>m_{wd}</i>	mass of moisture removed during drying (kg)
<i>q_{mwe}</i>	rate of moisture condensed at the evaporator surface (kg/s)
<i>n</i>	moles (mol)
<i>n_a</i>	moles of dry air (mol)
<i>N_{fin}</i>	number of fins per meter
<i>N_s</i>	no. of cylinders
<i>n_v</i>	moles of water vapour (mol)
<i>p</i>	absolute pressure of refrigerant (kPa)
<i>p_a</i>	partial pressures of dry air (Pa)
<i>p_g</i>	partial pressure of saturated vapour (Pa)
<i>p_i</i>	pressure of inlet air (Pa)
<i>Pr</i>	Prandlt number
<i>p_s</i>	saturated vapour pressure (kPa)
<i>p_v</i>	partial pressure of water vapour (Pa)
<i>w</i>	partial pressure of moisture vapour (Pa)
<i>Q</i>	heat transfer rate (kW)
<i>Q_c</i>	cooling rate (kJ)
<i>R</i>	gas constant (J/mol K)

Re	Reynolds number
RF	radio frequency (Hz)
RH	relative humidity (%)
RSHF	room sensible heat factor
SHR	ratio of sensible load to total load
$SMER$	specific moisture extraction rate (kg/kWh)
T	temperature of refrigerant (K)
T_R	regeneration temperature (K)
t	temperature of air (K)
T_{wb}	wet-bulb temperature (K)
u	specific internal energy (J/kg)
U	overall heat transfer coefficient (kW/m ² K)
u	velocity (m/s)
V	volume (m ³)
q_{va}	volumetric air flow rate (m ³ /s)
v_a	specific volume of air (m ³ /kg dry air)
q_{vp}	piston displacement (m ³ /s)
v_{r1}	specific volume of refrigerant vapour at suction (m ³ /kg)
v_W	specific molar volume (m ³ /mol)
W	humidity ratio of air (kg water/kg dry air)
y_a	mole fraction of dry air
y_v	mole fraction of water vapour
ΔT	temperature drop (K)
ΔT_c	cold air temperature reduction (K)
η_{is}	isentropic of efficiency (%)

Greek letters

ε	desiccant wheel efficiency
ω	humidity ratio
ϕ	relative humidity
γ	specific heat ratio
α	heat transfer coefficient (kW/m ² K)
η_{mech}	mechanical efficiency of compressor
η_{motor}	compressor motor efficiency
η_{sf}	surface fin efficiency of coil
η_v	volumetric efficiency of compressor
θ_{dr}	total drying time (s)
u	viscosity (kg/m s)

ρ	density (kg/m ³)
λ	thermal conductivity (kW/m K)

Subscripts

<i>a</i>	air
<i>c</i>	condenser
<i>co</i>	condenser outlet
<i>cs</i>	condenser surface
<i>d</i>	at dry-bulb temperature
<i>di</i>	dryer inlet
<i>do</i>	dryer outlet
<i>dr</i>	dryer
<i>e</i>	evaporator
<i>eo</i>	evaporator outlet
<i>es</i>	evaporator surface
<i>ext</i>	external
<i>f</i>	condensate refrigerant film
<i>i</i>	inside
<i>int</i>	internal
<i>l</i>	liquid refrigerant
<i>o</i>	outside
<i>r</i>	refrigerant
<i>rc</i>	refrigerant in condenser
<i>re</i>	refrigerant in evaporator
<i>s</i>	saturated
<i>tw</i>	tube wall
<i>w</i>	at wet-bulb temperature
<i>1, 2, 3....</i>	State number

TABLE OF CONTENTS

Abstract	ii
Acknowledgments	iii
Nomenclature	iv
Chapter 1 Introduction	1
1.1 Problem Statement	1
1.2 Aim and Objectives	3
1.3 Outline of the Thesis	4
1.3.1 Methodology Flow Chart	4
1.3.2 Thesis Layout	6
Chapter 2 Theoretical Background	7
2.1 Fundamental Aspects of Drying	7
2.2 Classification and Selection of Dryers	9
2.2.1 Classification	9
2.2.2 Selection of dryers	9
2.2.3 Effect of Energy and Environmental Factors on Dryer Selection 10	
2.2.4 Energy Aspects in Drying	11
2.2.5 Drying Efficiency	12
2.2.6 Principles for Energy Efficient Design	15
2.3 Psychrometrics	19
2.4 Moisture Load Sources	24
2.5 Summary	27
Chapter 3 Advances on Drying Systems	28
3.1 Review of Hybrid Assisted Heat Pump Dryer	28
3.1.1 Exergy Analysis of an Isothermal Heat Pump Dryer	29
3.1.2 Solar Source Assisted Heat Pump Dryer	32
3.1.3 Ground Source Assisted Heat Pump Dryer	33
3.1.4 Chemical Assisted Heat Pump Dryer	34
3.1.5 Two Stage Heat Pump System for Drying	35
3.1.6 Modelling of Heat Pump Dryer	39
3.2 Desiccant Dehumidifier	45
3.2.1 Regeneration methods of desiccant in drying applications	46
3.2.2 Thermal Transfer Coefficients of Desiccant Wheel	51
3.2.3 Effect of Desiccant Isotherm	60
3.2.4 Desiccant Applications	67
3.3 Vortex Tube	69

3.3.1 Summary of Experimental Studies on Vortex Tube.....	73
3.3.2 Vortex Tube for Drying in Further Research	75
3.4 Summary.....	77
Chapter 4 Methodology	79
4.1 Justification of Objectives	79
4.2 Theoretical Design.....	80
4.3 Summary.....	85
Chapter 5 Analysis of Hybrid Systems.....	86
5.1 Assumptions.....	86
5.1.1 Heat Pump	86
5.1.2 Desiccant Wheel	89
5.2 Analysis of Different Hybrid Dryers	92
5.3. Summary.....	101
Chapter 6 Design & Construction of a Hybrid Dryer	102
6.1 Description of the System.....	102
6.2 Experiment Setup.....	105
6.3 Summary.....	108
Chapter 7 Results and Discussion.....	109
7.1 Realisation of the Operation Cycle of Hybrid System.....	109
7.2 Effect of Inlet Air Temperature	111
7.3 Effect of Airflow Rate	127
7.4 Influence of Varying Operation Parameters in Desiccant Wheel.....	138
7.5 Influence of Varying Operation Parameters in Heat Pump.....	140
7.6 Summary.....	142
Chapter 8 Conclusions and Recommendations for Future Work	143
8.1 Conclusions.....	143
8.1.1 Overall Performance of the Hybrid Drying System	143
8.1.2 Theoretical & Experimental Analysis of Various Parameters	144
8.1.3 Other Practical Implications.....	145
8.2 Recommendations for Future Work.....	145
References	147
List of Publications	155
Appendix-A Journal Paper	156
Appendix-B ASHRAE Psychrometric Chart	163
Appendix-C Auxiliary Calculations	169

Chapter 1 Introduction

1.1 Problem Statement

The many applications of drying can be found in chemical, agricultural, pharmaceutical, mineral processing and biotechnology industries. Its high latent heat of vapourisation and inherent inefficiency of using hot air as the most common drying medium marks its reputation as one of the most energy-intensive unit operations. Studies have shown that the industrial drying operation in the US, Canada, France and the UK consumes 10-15% of the nations' energy, with Denmark and Germany using up to 20-25%. Latter figures were obtained from mandatory energy audit data given by industry [1]. It is important to realise that most studies available in the literature are aimed at specific applications, and not a general overview of all the drying processes. In particular, there is currently no comparison among the different hybrid dryer systems based on desiccant wheels in the literature, thus the results of this study are not suitable as a guideline to other applications other than product drying.

The rapid transfer of heat and mass in the drying operation often leads to changes of product quality, such as crystallisation, puffing, shrinkage and other physical. Sometimes chemical and biochemical reactions also occur, which may or may not be desirable; these usually involve changes in colour, odour and texture. In addition, the drying operation could potentially alter the effectiveness of certain catalysts by changing the internal surface area, which in turn generates discrepancy in the expected catalytic activity.

Drying process is an energy intensive activity and plays a significant role in many industrial applications such as food, textile and paper and in many other processing industries. The largest amount of investment is often spent on the operation itself, not the initial installation of equipment. Capital expenditure in the US is estimated to only reach \$800 million per annum. Operations such as papermaking hold 35% of the energy consumption, whereas chemical processing only uses under 5%. In general, the current drying processes are very inefficient. Typically the energy efficiency is between 20% and 60% [2], depending on the type of dryer and product used for drying. Stefano De Antonellis et al. [3], developed and investigated of simulation and energy efficiency analysis of desiccant wheel systems for drying processes of hybrid dryer system configurations based on desiccant wheels and the evaluation of primary energy consumption for different hybrid dryer systems are the main purposes of this work. Both aim to reduce the overall energy consumption, and both the simulation and analysis processes operate on similar ideas and use

comparable control parameters.

Different values of sensible to latent ambient load ratio are used in simulations, in order to evaluate the effect of ambient and outside air conditions under different configurations. Reference technology that is based on a cooling coil is compared with the hybrid system. At first investigation, primary energy savings of hybrid system is found to achieve up to 70 – 80%. Hybrid dryer systems with sorption wheels are in our particular interest in this case. The analysis is carried out between 2°C and 25°C, at a relative humidity between 50% and 75%, which are the standard conditions in drying processes for salami and cheese etc. The results obtained in this study serve as good indicators to general approach in drying applications and are helpful in the preliminary process of assessing and selecting the appropriate applications.

In the current environment when the shortage of energy is experienced in every country, it is very important that energy is conserved and used with caution. Use of hydrocarbon fuels also has problems such as CO₂ and other emissions and there are very strict environmental regulations are imposed on industry and businesses and industries are expected to reduce their carbon footprint. The global impact of the use of non-replenish able fossil fuel resources has reached to an unacceptable level and is now reflected in the ever increasing cost of energy. It is obvious that the energy costs will continues to increase; therefore like any other industry for drying industry also there are economic implications of using energy.

Thus it is important that drying industry explores low energy drying options and employ innovative methods to achieve efficient drying. A drying process involves heat and mass transfer in a dynamic process and how to achieve proper drying conditions is an important research field. The innovative methods are sought to develop low energy or efficient drying systems. An ideal drying condition for an application would offer an optimized drying time and energy consumption. Currently various technologies and strategies can be used in drying industry may use to achieve energy savings. Table 1.1 shows the most promising options for energy savings that can then be selected.

Drying of paper accounts for the highest demand of equipment, as the process is continuous. There are several types of essential drying methods in the industries: thermal drying is largely adapted in the textile, agricultural and foodstuffs fields, but spray and freezing dryings are also commonly used. The possible shrinkage that may occur must be taken into consideration for humidity control, as this is vital for the ceramic industry, for the drying process determines the quality of the products. Over-drying should be avoided. Internal moisture gradients within particles and

inter-particle moisture content variation are important.

Table 1.1 Potential Energy Savings for Selected Dryer [4]

Option	Potential energy savings		Penetration rating ^a
	(109 MJ/y)	(% Total)	
Heat recovery from dryer exhaust (other than heat pump)	18.9	15	High
Heat pumps (closed cycle)	8.9	6	Medium
Vapor compression	26.2	20	Low
Better instrumentation and control	4.3	3	Medium/high
Optimization of dryer design and operation	11	9	High
Improved dewatering of feedstock	5.3	4	High

^aPenetration rate is a guess of the degree of penetration of the potential market for the development that will eventually be achieved

Rapid surface drying is a special form of drying which is widely used in food and beverage packaging industry such as bottles, cans and food packets and response. .

For dry bulb temperatures (DBT) of 20 ~ 30°C, products will be dried at dew point temperatures (DPT) of -10 ~ -20°C for product quality optimisation. As the machine operates at ambient temperatures of 20 ~ 30°C, we will only consider drying processes above 0°C, thus the system will not reach its frost point. The big issue in these applications is re-condensation and the moisture interference with the drying processes which adversely affects the product quality and reduces production process speeds. For example, when the cold cider is bottled, it quickly causes condensation to form on the neck and body of the bottles' surface. This moisture must be completely removed prior to labelling, coating and date stamps otherwise the label can easily slip out of alignment and water can accumulate under the foil wrap around the neck presenting possible hygiene concerns to customers. Drying in these cases is very rapid; compressed air is blown over the bottle on the conveyor belt, moving at very high speeds which can be up to 2000 bottles per minute. Therefore, firstly it is necessary to expose as much of the drying surface to the drying effect in a shortest time as possible. Secondly, values of the temperature and humidity need to be optimised in order to achieve best performance and maximum efficiency.

1.2 Aim and Objectives

The aim of the presented thesis is to develop a *high energy efficiency system for*

rapid surface drying applications from recycled heat produced by the condenser to reduce the impact on the environment. To achieve this aim, the following objectives of the investigation were set. A necessary research methodology was pursued to achieve the proposed objectives:

- A critical review of the literature on current energy efficient technologies for dehumidification in various applications
- A feasibility study of using a hybrid drying system consisting of different technologies i.e. heat pump, desiccant wheel etc. This would consist of an analysis of design and operating parameters for optimal performance with desired drying quality
- Identifying the primary control variables of the drying process and optimisation of these variables to improve drying performance
- Mathematical modelling for determining correlations between design and operating parameters and for estimating drying efficiency and performance of the proposed dryer
- Proposal of a hybrid system for drying applications optimized for specifically surface drying in order to reduce energy consumption
- Construction of experimental testing of the proposed system
- Construction of a novel dehumidification machine in rapid drying processes for a low energy conditioning process unit that would meet the existing application. The chosen method will be used to perform a range of heat energy reclaimed to reduce power consumption

1.3 Outline of the Thesis

1.3.1 Methodology Flow Chart

Figure 1.1 represents diagrammatically the proposed methodology. It shows three main parts of the research, with the central part, representing the bulk of the study split into three main sections which are heat pump, desiccant and vortex tube. These relate to design and analysis of the developed construction of a hybrid drying system for industrial drying application.

From the initial analysis I found that the drying method involving vortex tube consumes way too much energy to be an appropriate candidate to developing an efficient system, therefore it was omitted from the research at the beginning already.

Firstly, critical evaluation of existing systems and products in dehumidification/air-conditioning applications is carried out; secondly, a proposal of a

hybrid system consisting of the benefits of more than one system is made and finally, design and manufacture of the proposed system for rapid drying is presented. The performance and energy efficiency of the system is theoretically and experimentally tested in the second stage. At the end a comparison of energy efficiency of the hybrid system with various existing systems is discussed.

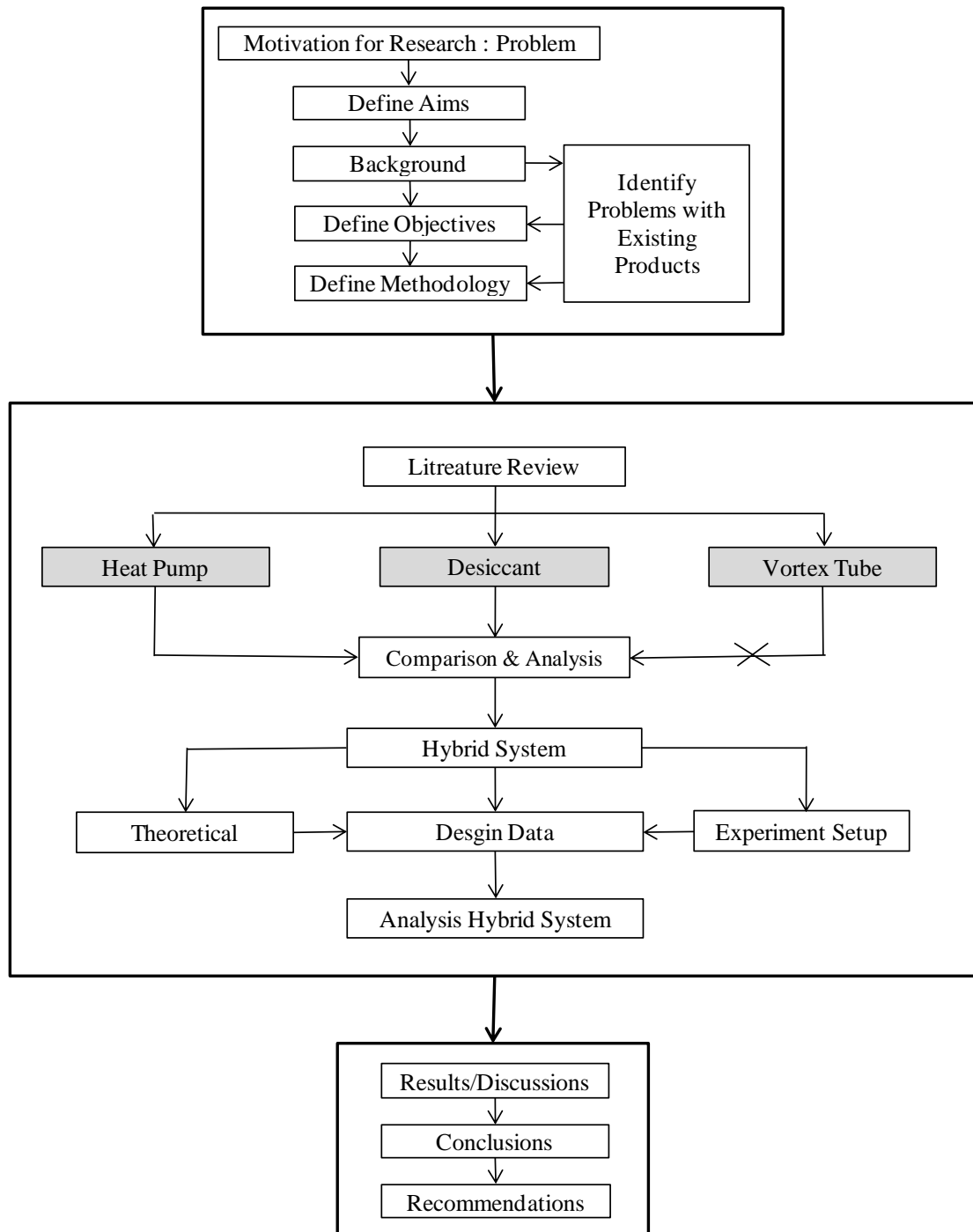


Fig 1.1 Flow Chart of Research Methodology

1.3.2 Thesis Layout

This thesis comprises of eight chapters. Chapter 1 is to introduce the problem to be solved and to lay down the aim and objectives of the research. The Chapter 2 of this thesis provides theoretical background of the subject in order to comprehend the energy aspects of drying applications. Other aspects such as safety and environmental factors for dryer selection are presented and external conditions of drying are also described in detail. Chapter 3 presents a critical review of published scientific literature on heat pump, desiccant wheel and vortex tube, as these systems are relevant to the current field of investigation. Purpose of this review is to: a) ensure that the proposed research offer ample scope for a significant contribution to the knowledge of the proposed field of study and to avoid any duplication; b) know the pitfalls that may lay ahead in the required experimental and/or theoretical work; c) carry out a critical evaluation of the claims made in each paper on the basis of evidence (theoretical or experimental) presented in the paper. The existing systems are analysed for their applicability in drying applications and potential for energy efficiency.

Chapter 4 discusses the methodology to achieve the objectives of the work. The approach during the various stages is highlighted to establish a logical procedure of this research. Design considerations are outlined and a hybrid system is proposed as an alternative method for rapid drying applications. Chapter 5 describes the mathematical model of hybrid system descriptions. In this chapter mathematical models are developed and equations are presented for heat and mass balance of heat pump, desiccant and air circuits in all components of the system. These models can be used for design and for the analysis of the complete hybrid system. It was theoretically found that hybrid system consisting of heat pump and desiccant wheel offers the energy savings when compared with the individual systems.

Chapter 6 presents the design, construction and experiment setup of the heat pump desiccant wheel hybrid dryer. The experiments were performed to investigate the effect of various operational and design parameters on the performance of the proposed hybrid system. Chapter 7 provides results of these experiments and discussion of the test results. The present study confirms the importance of improving heat recovery to improve the performance of hybrid drying systems. Finally, Chapter 8 offers conclusions and suggestions for obtaining improved predictions and recommendations for further research are offered at the end of this chapter.

Chapter 2 Theoretical Background

2.1 Fundamental Aspects of Drying

Through the application of heat that leads to the evaporation of liquid, solids, semisolids or liquid substances are turned into solid products as volatile substances leave the product. Two processes take place simultaneously as a moist/wet solid undergoes thermal drying. The first being the transfer of energy: the surface moisture is converted into vapours by the heat from the surrounding environment. The second process involves the transfer of internal moisture to its surface, by which the first process follows. Drying of fruits and vegetables etc., is an example that operates on the principle of such process.

Industrial drying yields various rates, which are determined by the way energy is transferred: heat from the surrounding environment could be transferred by means of convection, radiation or conduction, or the combined effect of the above, and the dryers employed by each industry would adapt to the method that produces the ideal drying effect.

Most drying processes removes excess water by transferring heat from the surface to the interior, of which the said process' outcome and efficiency depends on external conditions such as pressure, temperature, area and flow of exposed surface and air humidity. In the case of radio frequency, microwave freeze drying or dielectric, heat is generated from the interior by an external energy supply and spread out to the surface. It is worth mentioning that the process of freeze drying is a special case where drying occurs through sublimation, not evaporation, since the process takes place under the liquid's triple point: the solid phase of the substance is changed directly into the vapour phase.

The only exception that differs from the conventional evaporation method is the dielectric, which operates on the principle of conduction. The dielectric involves sending radio frequency that causes vibrations at the boundaries of the object, for which the liquid molecules are then agitated throughout the object. The liquid travels to the boundary of the material, and then is transported away from the material either by a medium gas, or by going through a vacuum. A good example of such drying method is microwave.

We now discuss the mechanisms of transport of moisture within the material. There exist several ways in which one can remove moisture from an object. Sometimes the combination of methods might even be desirable in terms of efficiency

and maintaining product quality. There are four types of diffusion mechanisms:

- 1) Vapour diffusion: where the liquid vaporises within the material
- 2) Liquid diffusion: if the liquid to be removed has a higher boiling point as the wet material itself
- 3) Knudsen diffusion: freeze drying is an example. The process takes place in very low temperatures and pressures
- 4) Surface diffusion: a method that is possible, but is yet to be testified

The above mechanisms could be combined with each other, or with a fifth type of drying process, called hydrostatic pressure differences, where the internal vaporisation rates exceed the rate of vapour transport through the material to its surroundings. The pressure differences forces the liquid to leave the solid.

For convection dryers, the rate of heat transfer (kcal/h) is given by $q = (h_a)(V)(t - t_m)$ for the batch type and $q = (h_a)(V)(t - t_m)_{l_m}$ for the continuous type. For the conduction dryer $q = UA(t_k - t_m)$ In these equations, t_m is the product temperature; t is the inlet temperature; $(t - t_m)_{l_m}$ is the logarithmic mean of the temperature differences between the hot air and the product at the inlet and outlet respectively; h_a is the volumetric heat transfer coefficient (kJ/s K m³); U is the overall heat transfer coefficient (kJ/s K m²); A is the heating area in contact with the product (m²); and t_k is the temperature of the heat source. Table 2.1 shows the heat transfer rate h_a (kcal/h °C m³) for various dryer types.

Table 2.1 Approximate Values of h_a for Various Dryer Types [5]

Type	h_a	$(t-t_m)_{l_m}$ (°C)	Inlet Hot Air Temperature (°C)
<u>Convection</u>			
Rotary	100–200	Countercurrent: 80–150 Cocurrent: 100–180	200–600 300–600
Flash	2000–6000	Parallel flow only: 100–180	400–600
Fluid bed	2000–6000	50–150	100–600
Spray	20–80 (large five)	Counterflow: 80–90 Cocurrent: 70–170	200–300 200–450
Tunnel	200–300	Counterflow: 30–60 Cocurrent: 50–70	100–200 100–200
Jet flow	$h = 100–150$	30–80	60–150
<u>Conduction</u>			
	U (kcal/h °C m ²)	$t_k - t_m$ (°C)	
Drum	100–200	50–80	
Agitated through rotary with steam tubes, etc.	60–130 (smaller for sticky solids)	50–100	

2.2 Classification and Selection of Dryers

2.2.1 Classification

Dryer types have been identified and classified by Sloan [6] through their methods of heat exchange – whether they are batch or continuous, through direct contact with gases or by heat exchange through walls of vessel. This also takes the motion of the equipment into account. McCormick's [7] classification method differs from Sloan's: according to how well they deal with and handle materials, 19 types of dryers are classified. Lastly, Schulunder [8] [9] put the dryers into categories by identifying the physical state of the product and how long the production time is. The classification is based on methods of heat transfer, namely, (a) conduction heating (b) convection heating (c) radiant heating, and (d) dielectric heating. Freeze drying is classified as a special case of conduction heating. The next subdivision is the type of drying vessel: tray, rotating drum, fluidized bed, pneumatic, or spray [10] [11].

In some cases two or more different types of dryer are required to carry out the drying process, depending on the material's conditions. Extra costs may need to be taken into account for treating the material into confirming a particular dryer's functioning mechanism.

One needs to be aware that many of the new dryers cannot be so readily categorised into the existing classification system. Many are better than their older versions and have the potential of replacing them in some industrial applications; therefore a new classification system was employed. In 1977, Dittman [12] proposed a system that puts dryers into two general classes, which are adiabatic and non-adiabatic, and five subclasses stemming from the two general classes.

For the adiabatic class, it is further broken down into whether the drying gases pass through the material or across the surface of the material. As for non-adiabatic dryers, it is the method of heat supply that determines the categorisation; for example, heat applied through a heat exchange surface, or through direct radiation. How the extracted moisture is carried away from the material is also taken into consideration in categorising the dryer.

2.2.2 Selection of dryers

The lack of standardised apparatus to select the appropriate drying system for different materials, based on their drying characteristics, has been problematic in selecting the most suitable mechanism for drying materials. The afore-mentioned

classification of dryers is still yet to be fully agreed upon, so in order to determine which system is the most apt, some initial information on the physical and chemical characteristics of the material and drying substances and the dried product (end product) are needed.

The physical characteristics include the particle size distribution in the wet feed, the presence of previous and the method of supplying material to the dryer etc. Knowledge on the temperature limitations, fire and explosion hazards and corrosive properties is also vital in the process of selection. Chemical characteristics of the feed include the toxicity, odour issues and whether hot combustion gases which contain carbon dioxide, nitrogen oxides and sulfur oxides could be used to dry the material.

The five types of dryer used in continuous operation are [1]:

- 1) continuous band circulation,
- 2) spray,
- 3) pneumatic,
- 4) continuous rotary, direct or indirect and
- 5) fluidised bed

Each of them serves different purposes, depending on the desired product outcome. It is best to select the drying method using previous experiences. Drying process requires a lot of trial and error, a slight alteration in quantity, concentration, temperature or impurity content of material could make a significant difference in the process, so there are no definitive ways of treating the materials.

One needs to keep in mind the compromises that need to be made between product quality, costs, equipment installations and safety concerns, therefore it is always wise to run preliminary tests, sometime a full-scale assessment, to establish the feasibility of employing such mechanism. On top of that, the aftermath is just as important as the drying process itself: the dryer's emissions will need to be dealt with carefully, and the post-processing that involves cooling, blending and granulation etc, also plays a vital role in selecting the mechanism.

2.2.3 Effect of Energy and Environmental Factors on Dryer Selection

A few environmental and health concerns must be taken into consideration when selecting the drying method. Many involve legal conflicts, energy efficiency and hygiene issues, which arise at different stages of drying. Possible scenarios have been compiled by Lang [13] as a reference when assessing the system's potential

problems:

- 1) Explosion vents
- 2) Direct combustion systems malfunction or failing heat exchanger surfaces caused by dust in recycling streams
- 3) Product build-up caused by fire-extinguishing equipment leading to fire hazard
- 4) High pressure drop and increased fan noise for high product collection efficiency

When selecting an energy-saving drying system, the thermal sensitivity of the material, the recycling process and the heat economy of the system must be taken into consideration, which sometimes requires the drying process to be split into multiple stages, where the intermediate stages are often too humid to work with easily.

The potential air pollution that accompanies drying installations should be below a certain standard. The particulates in exhaust air must be kept under 20-50 mg/nm³, depending on the type of particulate. Cyclones, scrubbers, electrostatic precipitators and bag filters are common like adsorption, absorption and incineration. Incineration is becoming more frequently used.

Dealing with sound pollution has shown to cost up to 20% of the total system spending, in the most stringent case. Difficulties exist in trying to achieve a balance between high collection efficiency and low noise production. This issue could be resolved by using a simple direct-fired dryer with once through airflow heating, which generates little noise, whilst still keeping a relatively high productivity the in drying process.

2.2.4 Energy Aspects in Drying

The unit energy for evaporating 1 kg of moisture is the standard measure of energy consumption in drying processes. For continuous timer drying, the quantity of drying agent required ranges from 3000 to 4000 kJ/kg, with counter current circulation. In general the value is between 2700 and 6500 kJ/kg in bate dryers [14]. It varies from 5000 to 8000 kJ/kg for the drying of thin and flexible materials like paper or fabrics. In theory, under standard conditions 1 kg of moisture requires 2200 to 2700 kJ/kg of heat to be evaporated, where 2700 kJ/kg indicates the upper limit of removal of bound moisture.

Today as the prices of energy thrive, many techniques are used to make the drying process a lot more energetically-efficient, due to the strict legislations on

working condition, pollution and safety. For example, using mechanical devices such as centrifuges or presses for liquids; the multistage evaporator results in much lower energy consumption. As previously mentioned, small-scale tests must be run to determine the materials' characteristics, in order to decide for the optimal drying procedure that is cost-efficient, environmentally-sustainable and safe. Table 2.2 presents the overall pattern of energy usage for drying in France and the United Kingdom.

Table 2.2 Overall Pattern of Energy Usage for Drying [15]

Subsector	French Industry	British Industry		% Due to Drying
	Drying (10 ⁹ MJ/y)	Drying (10 ⁹ MJ/y)	Total (10 ⁹ MJ/y)	
Food and agriculture	46.3	35	286	12
Chemicals	8.6	23	390	6
Textiles	1.9	7	128	5
Paper	38.8	45	137	33
Ceramic and building materials	15.7	14	127	11
Timber	7.9	4	35	11
Total	168	128	1103	12

2.2.5 Drying Efficiency

A study on industrial drying showed that 17 types of the dryers have the drying efficiency ranging from 20% for the convective tower dryer (convective), to about 90% for contact dryers (contact), such as drum, agitated pan dryer, cylinder and rotary dryers [16]. The heat required for moisture evaporation is supplied by conduction from tubes, vanes or heated walls as shown in Table 2.3.

It is not possible to standardise dryer efficiency as there is a vast variety of drying materials and equipment. However, Bakker-Arkema et al [17] established a standard index called the Dryer Performance Evaluation Index (DPEI), where the total energy needed by the dryer to remove one gram of moisture from the grain under specified conditions is defined. This concerns only the grain drying.

This method is not accepted in the manufacturing industry due to testing conditions related issues, and the high costs that accompany the incongruity. The hybrid systems are also not taken into account for the existing DPEI standard.

Table 2.3 Average Annual Energy Requirements and Drying Efficiency for Industrial Dryers [16]

Type of Dryer	Energy Requirement, 10 ⁹ MJ/y	Drying Efficiency, %	Energy Consumption by Equipment 10 ⁹ MJ/y
<u>Direct continuous</u>			
Tower	137+32	20-40	(Kiln) 2.6
Flash	528+211	50-75	8.4
Sheeting (stenters)	2.8	50-90	(Air floater dryer) 7.3
Conveyor	1.9	40-90	1.8
Rotary (bundle)	66	40-70	27
Spray	9.5	50	13.2
Tunnel	<1	35-40	7.6
Fluidized bed	23	40-80	1.97
<u>Batch</u>			
Tray	<1	85	(Bin dryer) 13.2
<u>Indirect continuous</u>			
Drum	2.4	85	32
Rotary (bundle)	53	78-90	(Tube bundle dryer) 4.4
Cylinder	127÷53	90-92	(Drying tenter) 1.68
<u>Batch</u>			
Agitated pan	<1	90	
Vacuum rotary	<11	Up to 70	
Vacuum tray	<1	-60	
Infrared	<1	60	
Dielectric	<1		
<u>Total</u>	1261		118.5

Source 1 : Richardson, A.S. and Jenson, W.M.P. Aerojet-Nuclear Company Report No. E (10-1)-1375, 1976

Source 2 : Larreture, A and Laniau, M., *Drying Tech.*, 9(1), 263-275, 1991

Testing individual drying procedures would be extremely expensive; therefore it is proposed that a few general drying mechanisms are set to be evaluated under similar testing conditions, and the results assimilated by computers. The performances of other non-standard drying operations are then simulated by the computers from existing data, to give an approximate estimation for their efficiencies. One thing to keep in mind is that the simulated or predicted efficiency for a system is always higher than the experimentally measured value, due to several reasons such as fuel combustions being not entirely efficient, losses by radiation and convection to the surroundings and heat losses through leaks in ducts etc.

There is a way to take into account the discrepancy between the theoretical and experimental efficiency values, which is called the Dryer Efficiency Factor (DEF). It is a ratio of the two values; the higher the DEF, the better the system is in terms of construction.

However, the first step in any energy saving program is to balance material and energy flow to and from the dryer. This often makes it possible to reveal areas in

which changes of operating conditions could result in a significant improvement in the efficiencies of the dryer operation and can bring about energy savings amounting to 10 to 30% [1]. The heat balance measurements required include airflow rate, temperature, and humidity, as well as material moisture content at various points of the drying system. An example of the installation of measuring points is given in Figure 2.1 showing a conveyor dryer, measured parameters for testing of the drying system: (1) ambient airflow rate, temperature, humidity; (2) supply steam flow rate, temperature, pressure; (3) condensate temperature; (4) process air temperature; (5) feed solids moisture content, temperature; (6) product solids flow rate, moisture content, and temperature; and (7) exhaust airflow rate, temperature, and humidity.

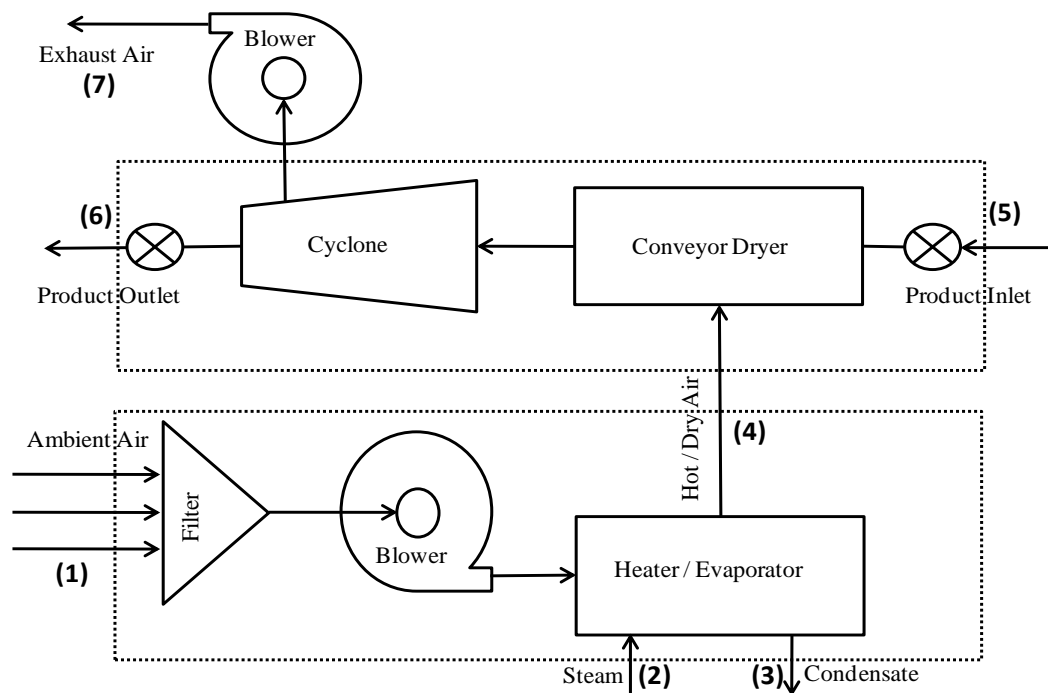


Fig 2.1 Measured Parameters for Testing of Conveyor Drying System [14]

Data presented in Table 1.1 (Chapter 1) show that, in order to increase energy efficiency, the method applied to achieve fast heat recovery must be given much attention to.

Traditionally, it is possible to recover heat from a dryer outlet, such as the outlet gas or the hot dried product. The flow arrangement and type of construction are taken into consideration when classifying conventional heat exchangers of such types. Typical devices for heat recovery are presented in Figure 2.2.

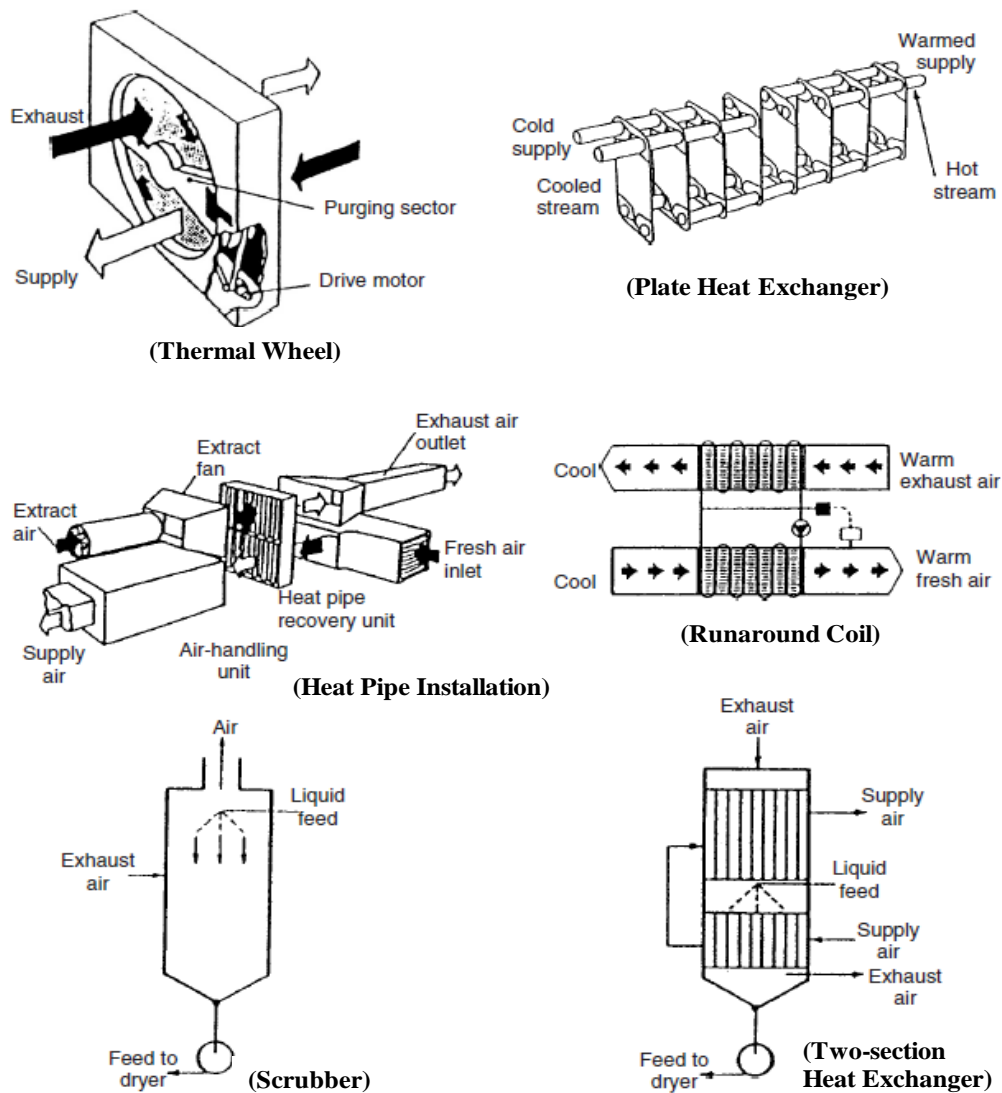


Fig 2.2 Heat-recovery Systems in Dryers [14]

2.2.6 Principles for Energy Efficient Design

In order to design a drying system, bench-scale and pilot-plant tests needed to be carried out, and previous experience on the dryers sold and the feedback from the customers are also needed. In general, a computer program based on hard data and experience is written to formulate the necessary parameters. Pilot-plant conducts the physical examinations of the material in which a desired procedure is tested to see if the material can be processed in such a manner.

However, the program is not entirely perfect, since the data used might have been misled by some arbitrary measurements that were not consistent, or not universal enough to adapt to every measuring standards. This should be kept in mind when using a computer to estimate for energy efficiency and such.

Dryer designs must be constantly re-evaluated, since the equipment is subject to exhaustion by changes in properties of the materials and/or the products, the types of solvents and the post-drying procedures, therefore it is essential to keep the conditions of the designs updated.

Many cases are to be considered when carrying out calculations. For example, the design of the dryer – whether the size is able to offer an optimal capital expense and operating costs. For real-time controls, the calculations on the input and output rates need to be performed almost instantly. In most cases neural network models are required for this task.

2.2.6.1 Intensification of Heat and Mass Transfer

There exists several ways in which energy consumption could be lowered. One can enhance the mechanism by supplying heat more precisely to the exact locations to avoid wasting energy to the peripheral regions, using less drying agents and by shortening the process time and machine length to reduce energy losses within the production frame.

For most convective dryers, the dominating energy demand comes from moisture evaporation and airstream exits. Up to 25% of energy could be used to heat up the material, 3 to 10% is contributed by heat losses to walls and atmosphere and 5 to 20% for other losses [18].

Methods of saving energy can be costly. The schemes that involve large capital expenditure are product cooler, use of exhaust gas to preheat inlet air and use direct instead of indirect heating. There are also ways that comprise of little or no costs to reduce energy consumption. One can simply change the dryer inlet temperature and dryer mass flow rate, or improve dryer and heater insulation. The most effective method is found to be heat recovery from outlet gas, by Bahu, Baker, and Reay [19].

It is important to specify the test conditions of the drying process. A drying material that has a high resistance to internal mass transfer could cause a significant drop in energy efficiency. Inadequacy in theoretical knowledge of energy consumption still exists for most industrial practices, therefore more research on the models of determination and methods of energy reduction is still in high quest.

2.2.6.2 Thermal Wheel

The thermal wheel is a type of heat exchanger that is situated inside the system of exhaust air handling in order to recover heat energy from the process, and is driven

by a small electric motor and belt drive system. The heat exchange matrix is often made of aluminium, or plastics and synthetic fibres.

Heat is picked up from the exhaust air as the wheel rotates to 180°, and then transferred to fresh air stream as the wheel completes its full circle. The temperature of the supply air stream raised in this procedure creates a thermal gradient between itself and the fresh air streams, meaning that the increase is proportional. The increase also depends on the efficiency of the device.

2.2.6.3 Plate Heat Exchanger

Another means of heat transfer is to use the plate heat exchanger. One major advantage of using such exchanger is that the fluids are exposed to a much greater surface area of the plate, as the fluids are spread over it. This greatly speeds up the temperature change, therefore plate heat exchangers are now commonly used in many hot-water sections of combination boilers.

2.2.6.4 Scrubber

Scrubber is a primary device that monitors the gaseous emissions from a drying process. It operates on the principle of injecting a dry reagent or slurry into the waste exhaust to eliminate the particulates gases, in particular, acid gases. Flue gas condensation in wet scrubbers can be used for heat recovery, by circulating the water through a cooler to the nozzles at the top of the system, where the hot gas enters from the bottom. Condensation of water releases heat, and this heat can be recovered for district heating purposes by the cooler, for example. The gas is initially cooled by evaporation of water drops, so even though the gas leaves the scrubber at its dew point, it is still likely that a large amount of water vapour will accumulate.

2.2.6.5 Two-Section Heat Exchanger

This is commonly known as a regenerator, where the flow through the heat exchanger periodically changes direction, working on a similar mechanism to a counter-current heat exchanger, but only that it mixes the two fluid flows.

Fluids flow through both sides of the two-section heat exchanger and reach high temperatures, and the incoming fluid is heated using the existing energy in the exiting fluid that is already contained in the process. The substantial net save in energy in two-section heat exchanger is achieved by its thermodynamically reversible heat exchanges, which could have up to 50% of thermal efficiency in transferring the relative heat energy from one end to another.

2.2.6.6 Heat Pipe

Heat pipes require little to no maintenance since they contain no mechanical moving parts. They are usually made of material like aluminium or copper, which are with high thermal conductivities, at both hot and cold ends. Air is eliminated from the pipe by a vacuum pump and the pipe is partly filled with a coolant such as water, sodium, ethanol, mercury or acetone. The fluid needs to match the operating temperature.

The partial vacuum is near or below the vapour pressure of the fluid, therefore it causes the fluid to be in either the liquid phase or the gas phase, and it conveniently removes the need for the operating gas to diffuse through, so that the bulk transfer occurs at the moving molecules' speed. Therefore the only existing practical limit is the speed for which the condensation of gas into liquid occur, in the rate of heat transfer.

Conventional heat exchangers have the following efficiency indices: thermal wheel, 75 to 90%; plate exchanger, $\approx 70\%$; heat pipe, $\approx 60\%$; scrubber, $\approx 60\%$; and two-section exchanger, $\approx 50\%$. Heat may also be recovered from a hot product if this does not cause its rewetting. Heat recovery from a hot stream of outlet gases is not difficult from the technical point of view, provided the outlet gases do not contain dust or condensable volatiles. Such conditions are encountered in drying of timber, paper, and so on, where dust filters and heat exchangers that are easy to disassemble and clean should be used. As an alternative, scrubbers can be used.

2.2.6.7 Heat Pump

In a system where there are regions of higher temperature relative to other parts of the system, a heat pump acts as a diverter of the heat energy from the source of heat to the heat sink. Using mechanical work or other means of heat transfer, the gaseous working fluid is pressurised and circulated by a compressor to go through the system, then is cooled in a heat exchanger on the discharge side of the compressor.

Next, the condensed refrigerant passes through a metering device to lower its pressure through devices like a turbine or a capillary tube, before it leaves the expansion device and enters the evaporator, where it absorbs heat and boils. The whole cycle repeats as the refrigerant returns to the compressor. A reversing valve can help exchanging the condenser and evaporator coil, and this is helpful because it means that a heat pump can serve both as a heating and cooling device.

2.2.6.8 Heat Pump Dryer

Dehumidification drying recycles heat that is usually vented to the atmosphere. The outlet gas should measure a temperature similar to the wet bulb temperature with high humidity if the dryer is operating efficiently.

An efficiency parameter, the specific moisture evaporation rate (SMER), is defined as [20]:

$$SMER = \frac{\text{Amount of water evaporated}}{\text{Energy used}} = \frac{kg}{kWh} \quad (2.1)$$

The variation in cost of energy in each country determines the profitability of a device, since the electricity used may cost more than the value of the heat recovered; the payback time may vary largely due to this reason.

There are a number of ways to optimise heat pump dryer. For example, the temperature control of the evaporator and condenser in a single-stage compression should be kept under 40°C, and the heat pump should operate at a constant heat load under the same condition. The compressors should be designed to function for several days in continuum as well [21].

2.3 Psychrometrics

The important variables for drying operations are temperature, humidity, rate and direction of airflow. External drying conditions are especially important during the initial stages of drying when unbound surface moisture is removed. In addition to these the physical form of the objects to be dried and the rate of agitation are also important. Surface evaporation is controlled by the diffusion of vapour from the surface of the solid to the surrounding atmosphere through a thin film of air in contact with the surface.

Since drying involves the inter phase transfer of mass when a gas is brought in contact with a liquid in which it is essentially insoluble, it is necessary to be familiar with the equilibrium characteristics of the wet solid. Also, because the mass transfer is usually accompanied by the simultaneous transfer of heat, due consideration must be given to the enthalpy characteristics. The ability to perform psychrometric calculations forms a basis on which all drying models are built. One principal problem is how to determine the solid temperature in the constant drying rate conditions.

In psychrometric calculations three thermodynamics phases: one consider inert

gas phase, moisture vapour phase, and moisture liquid phase. Two gaseous phases form a solution (mixture) called humid gas. To determine the degree of complexity of our approach make the following assumptions are needed:

- 1) Inert gas component is insoluble in the liquid phase
- 2) Gaseous phase behaviour is close to ideal gas; this limits the total pressure range to less than 2 bar
- 3) Liquid phase is incompressible
- 4) Components of both phases do not chemically react with themselves

2.3.1 Humidity Ratio, Relative Humidity, and Mixture Enthalpy

The humidity ratio ω of a moist air sample is defined as followed:

$$\omega = \frac{m_v}{m_a} = \frac{M_v p_v V / \bar{R}T}{M_a p_a V / \bar{R}T} = \frac{M_v p_v}{M_a p_a} \quad (2.2)$$

which is the ratio of the mass of vapour to mass of dry air. Using Equation 2.5, an alternate expression can be obtained in terms of partial pressures and molecular weights, by solving for m_a and m_v , respectively. The above equation is found by substituting the results into Equation 2.2.

Introducing $p_a = p - p_v$ and noting that the ratio of the molecular weight of water to that of dry air is approximately 0.622, this expression can be written as

$$\omega = 0.622 \frac{p_v}{p - p_v} \quad (2.3)$$

Moist air also can be described in terms of the relative humidity ϕ , given by

$$\phi = \left(\frac{p_v}{p_g} \right)_{T,P} \quad (2.4)$$

A hygrometer can be used in laboratory measurements for a moist air sample, under which is exposed to the appropriate chemicals until all the moisture is absorbed, and the water present is then determined by weighing the chemicals. Transducers with resistance- or capacitance-type sensors are for obtaining continuous recordings of relative humidity, since their electrical characteristics change accordingly with the relative humidity.

The values of h and U for moist air modelled as an ideal gas mixture can be found by adding the contribution of each component at the condition at which the component exists in the mixture. For example, the enthalpy h of a given moist air

sample is

$$h = h_a + h_v = m_a h_a + m_v h_v \quad (2.5)$$

Dividing by m_a and introducing the humidity ratio gives the mixture enthalpy per unit mass of dry air

$$\frac{h}{m_a} = h_a + \frac{m_v}{m_a} h_v = h_a + \omega h_v \quad (2.6)$$

The enthalpies of the dry air and water vapour appearing in Equation. 2.6 are evaluated at the mixture temperature.

Evaluation of the internal energy of moist air can be done in a similar fashion to the enthalpy. Enthalpy of the vapour h_v in Equation. 2.6 can be taken as h_g at the mixture temperature:

$$h_v \approx h_g(T) \quad (2.7)$$

and is given by the saturated vapour value corresponding to the given temperature for a superheated vapour at low pressures, according to the Mollier diagram and reference to steam table data.

2.3.2 Evaluating the Dew Point Temperature

To study the partial condensation of water vapour, consider a system made up of a moist air sample that is cooled at a constant pressure, as shown in Figure 2.3. The diagram indicates the states of the water vapour and their locations. At state 1, the vapour is superheated, and then is cooled under constant system pressure, with a constant moist air composition. The partial pressure of the vapour would remain constant since $p_v = y_v p$, and the vapour would cool at constant p_v from state 1 to state d, the dew point. The saturation temperature corresponding to p_v is called the dew point temperature and is indicated.

During the cooling process, some of the water vapour that is present initially would condense as the system eventually cools below the dew point temperature. The system would consist of a gas phase of dry air and water vapour that is saturated in equilibrium, with a liquid water phase at the final state. There is a decrease between the partial pressures, p_{g2} and p_{v1} , as the amount of water vapour present at the final state is less than that at the initial state since condensation occurs.

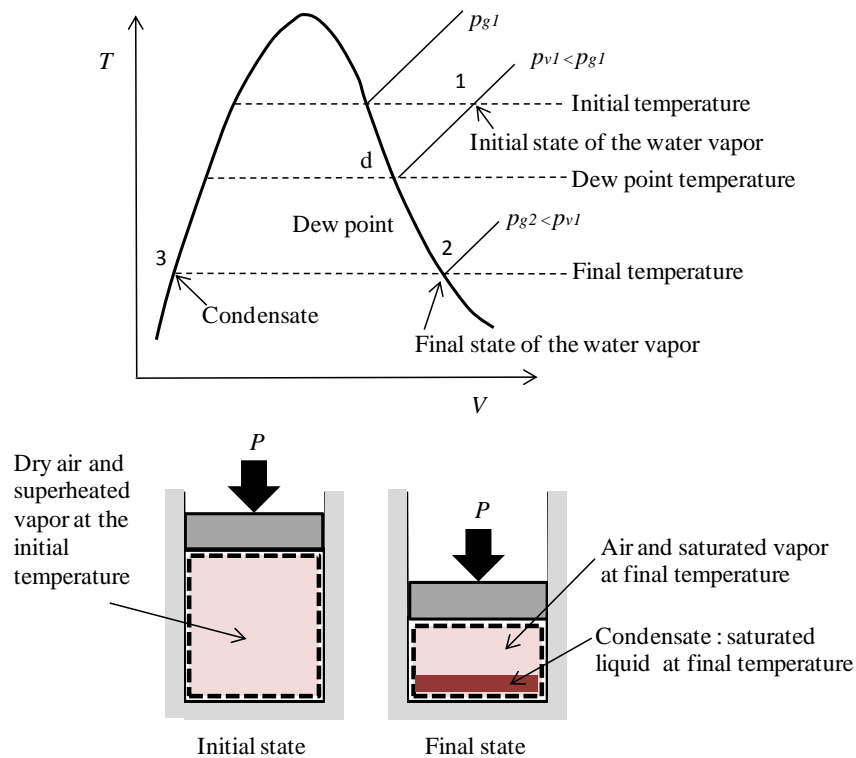


Fig 2.3 States of Water for Moist Air Cooled at Constant Mixture Pressure [22]

2.3.3 Measuring the Wet-Bulb and Dry-Bulb Temperatures

For air–water vapour mixtures in the normal pressure and temperature range of atmospheric air, the wet-bulb temperature is an important psychrometric parameter that can be related to the humidity ratio, the relative humidity, and other psychrometric parameters. As considered next, the wet-bulb temperature is measurable.

The wet-bulb temperature is read from a wet-bulb thermometer, which is an ordinary liquid-in-glass thermometer whose bulb is enclosed by a wick moistened with water. The term dry-bulb temperature refers simply to the temperature that would be measured by a thermometer placed in the mixture. Often a wet-bulb thermometer is mounted together with a dry-bulb thermometer to form an instrument called a psychrometer.

2.3.4 Psychrometric Charts

There are three popular types of psychrometric charts constructed by a computer, which are Grosvenor chart, Mollier chart and Salin chart, which can also be called the psychrometric chart, the enthalpy-humidity chart and the deformed enthalpy-humidity chart, respectively. These graphs exhibit several important properties of moist air.

These are shown in Figure 2.4.

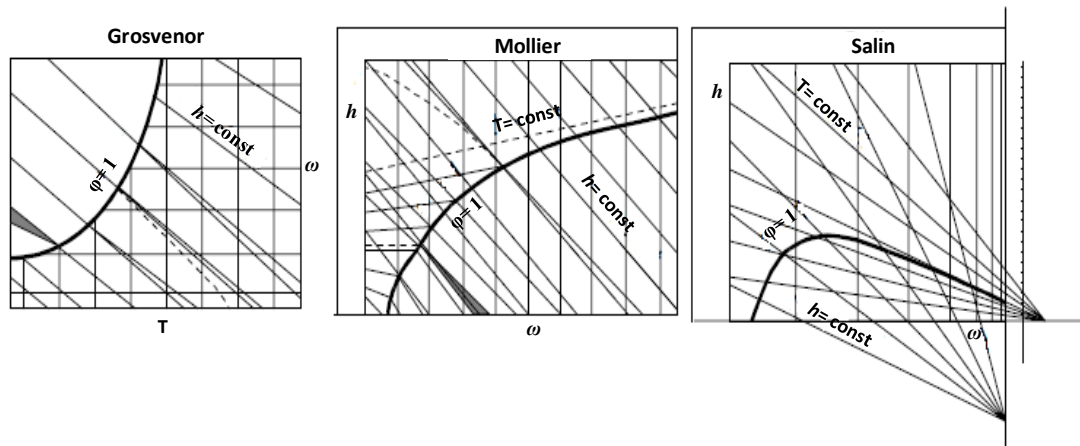


Fig 2.4 Schematics of the Grosvenor, Mollier, and Salin Charts [22]

Figure 2.5 shows the main features of one form on chart; the charts shown are constructed for a mixture pressure of 1 atm, but charts for other mixture pressures are also available.

- **Dry-Bulb Temperature:** The temperature of air read on a standard thermometer indicating its thermal state.
- **Wet-Bulb Temperature:** The equilibrium temperature reached as water evaporates from a thoroughly wetted psychrometer wick into an airstream. While this process is not one of adiabatic saturation, by applying only small corrections one can obtain the thermodynamic wet-bulb temperature.
- **Dew Point Temperature:** The temperature of moist air saturated at the same pressure and humidity ratio. Or more simply the temperature at which water vapour will begin to condense from a sample of air.
- **Enthalpy:** The thermodynamic property defined as energy per unit mass commonly used to define the internal energy of moist air. The enthalpy of a sample of moist air is the sum of enthalpies of the air and the water vapour. On the psychrometric chart Enthalpy is expressed in terms of energy per weight of dry air.
- **Humidity Ratio:** The ratio of the mass of water vapour to the mass of dry air of a sample.
- **Relative Humidity:** The ratio of mole fraction of water vapour in a given moist air sample to the mole fraction in a saturated air sample at the same temperature and pressure.
- **Specific Volume:** The ratio of the total volume of air to the mass of dry air in a sample.

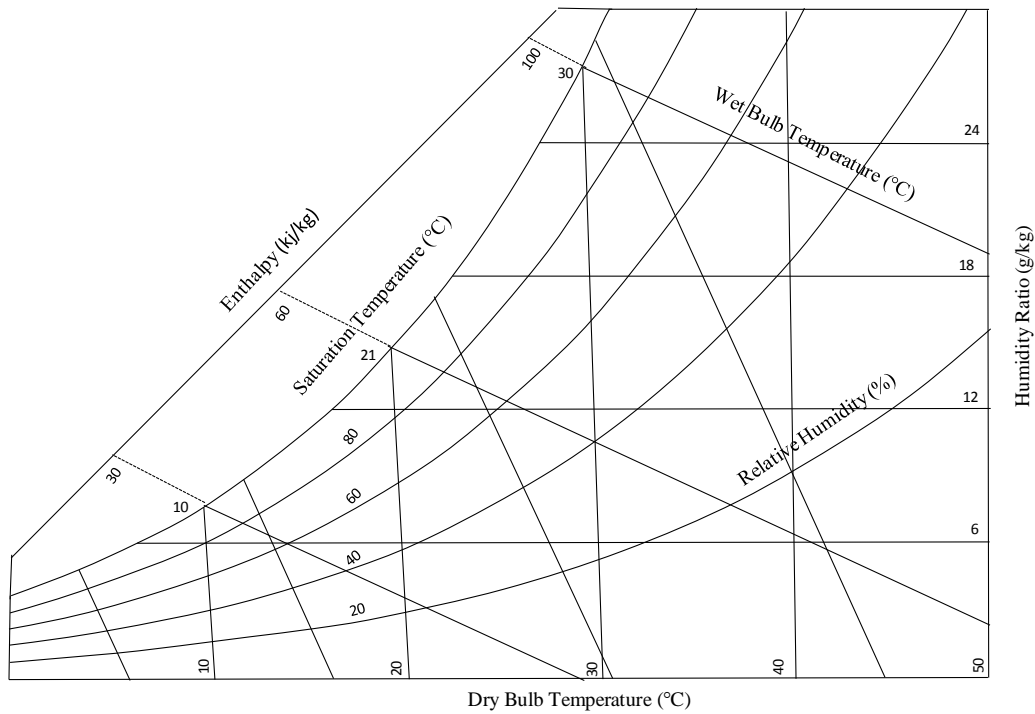


Fig 2.5 Psychrometric Chart

The software used for mathematical analysis is Psychrometric Analysis by ASHRAE. It was chosen for its convenient and clearly laid-out user interface and powerful analysis of fluid properties. Procedure of using the software is given in Appendix-2. Psychrometric Algorithms used are shown in Appendix-3. The following is the methodology the program uses in determining the psychrometric properties of moist air.

2.4 Moisture Load Sources

When designing dehumidification installations, one must quantify the moisture loads that must be removed by the system. This section will discuss the basic elements of moisture loads, how they can be quantified, and most importantly, the relative importance of each element in different situations. There are seven principal sources of moisture:

- Permeation through floors, walls and ceiling
- Evaporation from peoples clothing, breath and perspiration
- Desorption from moist products, including packaging materials
- Evaporation from wet surfaces or open tanks
- Generation from combustion — open flame in the space
- Air infiltration through leaks, holes and door openings
- Fresh air ventilation from outside the space.

By considering individual circumstances, the importance of the sources will vary with its size relative to the other sources.

2.4.1 Moisture from combustion

The heat of combustion is the energy released as heat when a compound undergoes complete combustion with oxygen under standard conditions. The chemical reaction is typically a hydrocarbon reacting with oxygen to form carbon dioxide, water and heat. The heating value or energy value of a substance, usually a fuel or food, is the amount of heat released during the combustion of a specified amount of it. It is measured in units of energy per unit of the substance, usually mass, such as: kJ/kg, kJ/mol, kcal/kg and btu/m³. Heating value is commonly determined by use of a bomb calorimeter. It may also be calculated as the difference between the heat of formation of the products and reactants.

In spaces where open gas burners are used for heating, the moisture resulting from combustion can be a significant load. The exact amount of water vapour produced will vary with the composition of the gas, but where the value is unknown; the engineer can estimate that each m³ of gas burned produces 1488 grams of water vapour. Equation $W_g = G * 1488$, where W_g are moisture load from gas combustion (g/hr), G are gas firing rate (cubic. meter./hr) and 1448 are moisture produced per cubic meter of gas burned (g/cubic. meter).

2.4.2 Moisture evaporated from wet surfaces

The fastest evaporation rates occur when the wet surface is warm, with the surrounding air dry and travelling at a high speed across the surface, as this airflow provides high heat transfer rates from air to the water film, leading to high mass transfer rates from the water to the air. The rate of evaporation is directly proportional to the difference in vapour pressure between the surface and the surrounding air and also to the rate for which the heat is transferred to the surface water film.

The most critical condition in determining the evaporation rate is the velocity in which the air passes across the surface, and also when the wet surface is warm. The effects of these conditions are shown in Figure 2.6.

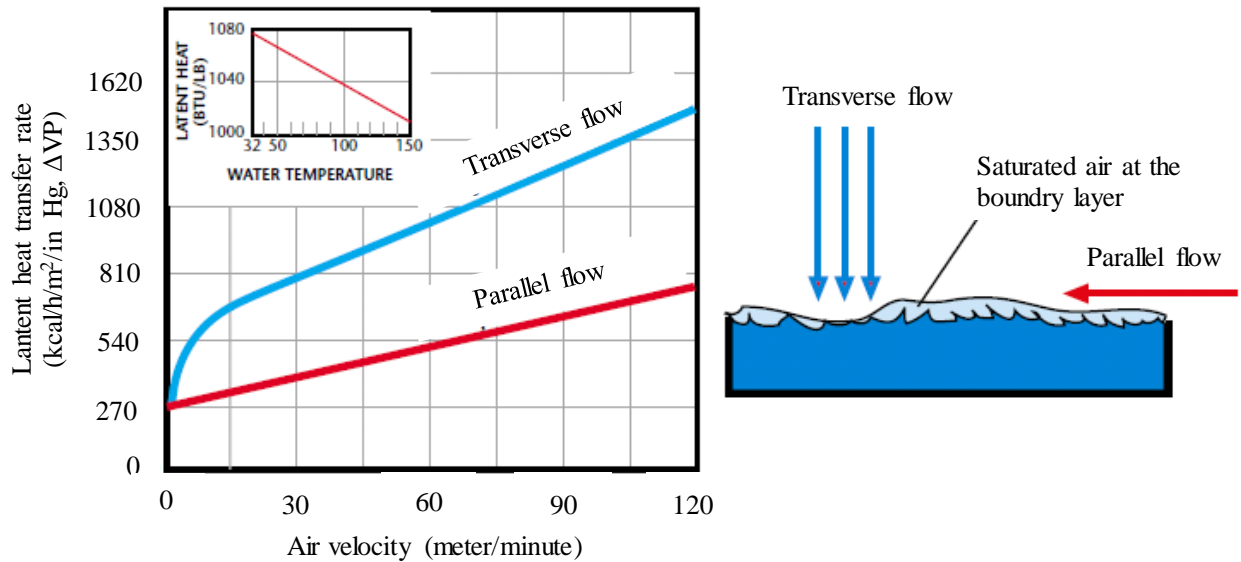


Fig 2.6 Moisture Evaporated from Wet Surfaces [23]

2.4.3 Moisture from air leaks through cracks and holes

The moisture load carried into the room by air flowing through cracks and wall penetrations is far more important than the load which results from diffusion through materials. No building or air handling system is hermetically sealed. All rooms and ductwork will leak a certain amount of air, which carries a certain amount of moisture into the conditioned space. Typical air leak locations include:

- Cracks at duct joints
- Gaps in the vapour barrier film at wall-ceiling, wall-floor and wall-wall joints
- Gaps between wallboard and electrical fixtures that penetrate the wall
- Electrical conduits through which wires pass into a room
- Oversized holes for pipe and duct wall penetrations
- Gaps where strips of vapour barrier film are overlapped but not taped
- Cracks at access doors of air handling equipment casings
- Wall or ceiling penetrations to pass products in and out of the room
- Old ventilation louvers in walls and doors
- Cracks between the doors and their frames and sills
- Open construction above hung ceilings
- Open doorways, loading docks or doorways with plastic strip curtains

2.4.5 Fresh air moisture load

In general moisture loads are the downstream of the system as they are internal, but for a dehumidifier, the fresh air brought to the system upstream is where the

largest moisture load originates.

It is important to separate the ventilation load calculation from the internal loads, in order to maintain the dry air requirement of the system. Eliminating moisture from the ventilation air will greatly decrease the cost and size of the dehumidification system; therefore it is desirable to achieve this condition.

2.5 Summary

The physical mechanisms of drying, governing equations and factors that influence drying and basic definitions are presented in this chapter. Various types of dryers that are available for a range of drying applications are reviewed for their suitability in different conditions, depending on the product and the aim. For more complicated drying methods, more care needs to be given for a balanced compromise made between costs and quality; selection of a dryer for a particular application should consider not only the investment costs, but also energy consumption and environmental effects such as pollution, dust and hygiene, which is important for a rapidly growing industry in any aspect of the society.

Chapter 3 Advances on Drying Systems

A review of various systems used to dehumidify/condition air in different applications is presented in this chapter. Three types of systems i.e. heat pump, desiccant and vortex-tube are discussed.

3.1 Review of Hybrid Assisted Heat Pump Dryer

Hybrid energy effectively eliminates many disadvantages and difficulties in using the traditional method of using heat pumps separately. Quality control of the products is much better due to the low temperature and well-controlled drying conditions. This contributes to the high quality of the products.

We only consider the case where heat pump operates at atmospheric pressure for the purpose of this research. Heat pump operation below or above atmospheric pressure is not the same as the drying application discussed in this thesis; however, significant differences in air density and water vapour pressure must be accounted for when considering different altitudes. The effects can be calculated or from reading a psychrometric chart at such altitude.

On top of improved quality control, high coefficient of performance and thermal efficiency and reduced energy consumption were also observed in solar heat pump drying systems. Figure 3.1 illustrates a classification of heat pump dryers, with air, ground and chemical source being the most common means of drying methods in heat pumps. The focus of research and development in the field of solar-assisted drying systems ought to be the theoretical and experimental analysis, and possible replacement, of the conventional solar dryer. This poses greater possibilities for future advancements in drying technologies.

In order to produce a high quality product that has a prolonged shelf life, low temperature of 30-35 °C is crucial to preserve the active and fresh ingredients inside the food, therefore drying is an operation that needs to be both efficient and timely. The overall thermal performance can be achieved with higher efficiency with a heat pump dryer than a conventional dryer, as latent heat can be recovered from the exhaust air. It also has the ability to operate at lower temperatures.

Dryers such as kilns, tray dryers and batch shelf are common dryers that use convection as a primary mean of heat input, of which their designs is aptly intended to implement a heat pump. On the contrary, dryers like spray or flash dryers are examples which require a large amount of drying air, therefore are not suited for heat pump operation. The main advantage of using a heat pump dryer comes from the fact that it is able to recover energy from exhaust gas. It is also sensitive and competent

enough to control drying gas humidity and temperature, making them the optimal apparatus in controlling product quality.

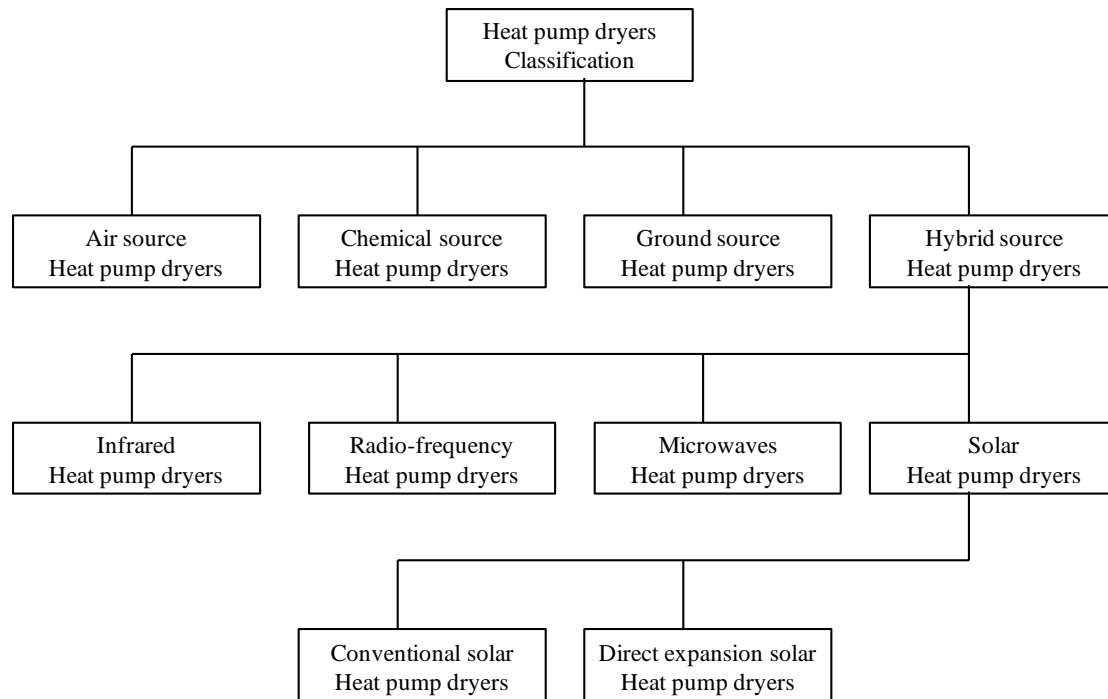


Fig 3.1 Classification Scheme for Heat Pump Dryers [24]

3.1.1 Exergy Analysis of an Isothermal Heat Pump Dryer

Exergy is a term defined as the maximum useful work that a system is able to perform with a given amount of energy. Figure 3.2 is a sketch of the refrigeration components that are incorporated in the drying chamber. At point 3, the inlet drying air is passed through the drying chamber and the air takes up the moisture from the product. This air goes through point 1 and is directed to the evaporator coil which the refrigerant goes through a phase change from liquid to vapour in order to cool and dehumidify the air. The air is cooled to its dew point from point 1 to point 2, and later on the cooling results in condensation of water from the air. The evaporator absorbs the latent heat of vaporisation in order to boil the refrigerant, and this recovered heat is then transferred to the condenser.

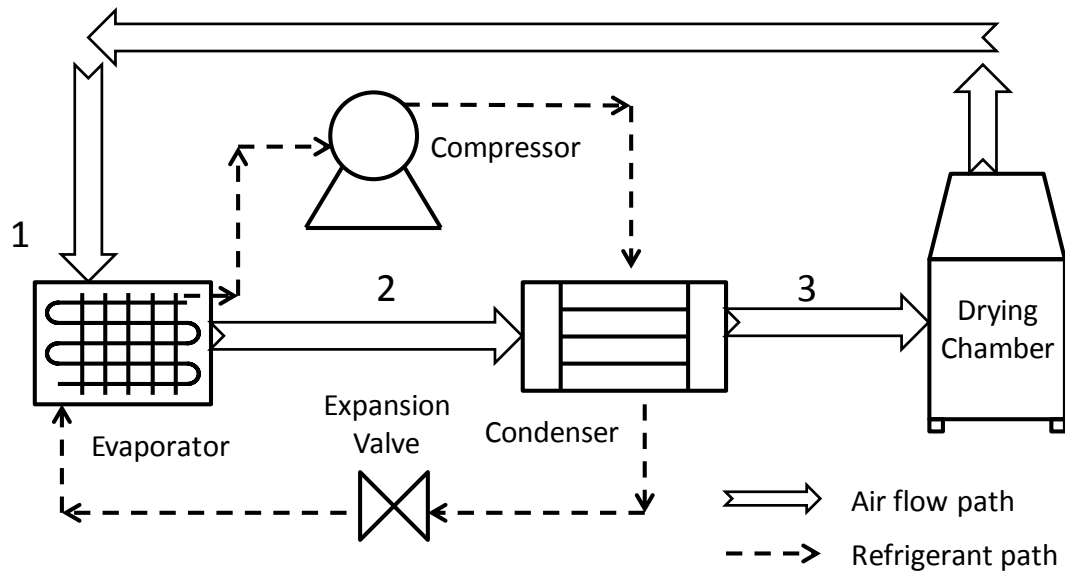


Fig 3.2 Schematic Representation of Heat Pump Drying System

A schematic diagram of a cross flow heat pump dryer system is shown in Figure 3.3. The numbers denote the direction of the forward refrigerant cycle. The energy efficiency improvement of this system is examined by a numerical simulation of a contact-type isothermal heat pump dryer, in order to make a comparison with a conventional heat pump dryer. However, albeit the usable design, a practical application still has not been found thus far. The simulation consists of a detailed plate, product and air flow model that solve the mass, momentum and energy balances within the dryer to a preliminary model of the remaining components of the heat pump dryer. The idealised model is not entirely perfect as local system temperature variations are found to be causing a fluctuation in the general accuracy of the model, but fortunately, this is not enough to lead to any significant errors when integrated into the complete heat pump dryer model. Irreversibility in the refrigerant cycle is reduced by contact heat transfer in isothermal heat pump dryer. The amount of heat transfer in this cycle is found to be approximately the same as that from the condenser to the product. A factor of between 2 and 3 is found to be associated with the isothermal contact heat pump dryer; an exergy analysis is used to investigate this gain in performance efficiency.

Carnot's principle of the second law of thermodynamics states that no engines can operate realistically at a higher efficiency than the Carnot engine. However, the work done by a system can theoretically reach 100% exergy efficiency as this is an indication of the input's potential to do work. In other words, this is a calculation of the system's realistic work output.

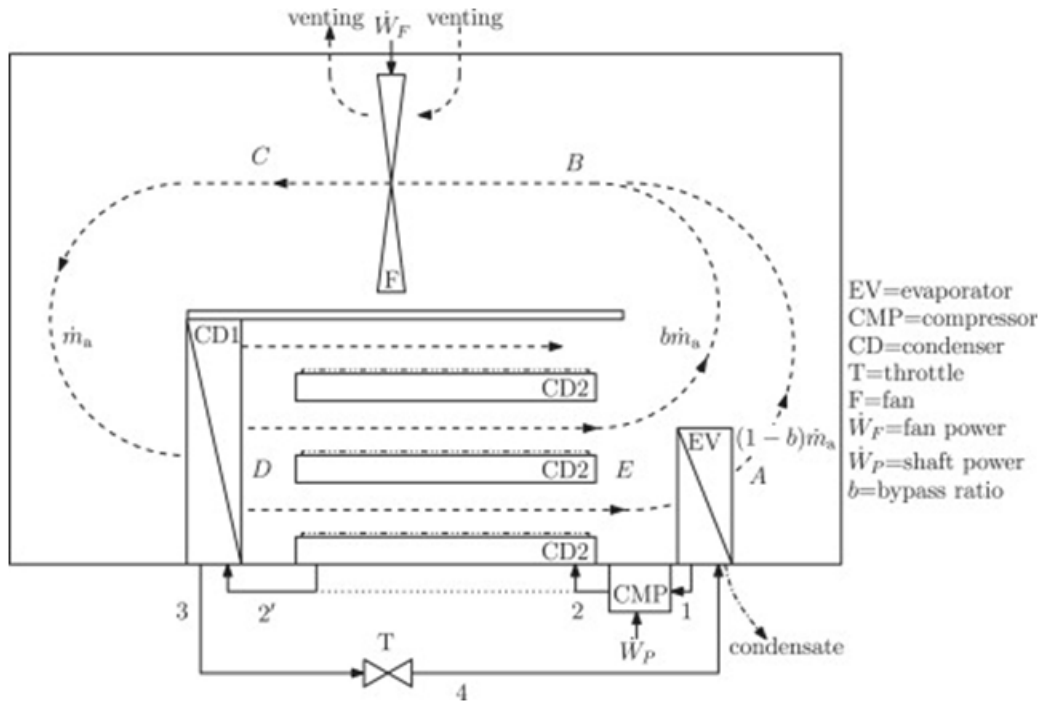


Fig 3.3 Schematic of Heat Pump Dryer System [25]

The energy efficiency of a heat pump is defined by the coefficient of performance (COP). COP_{HP} is given by

$$COP_{HP} = \frac{\text{useful heat output}}{\text{power input}} \quad (3.1)$$

The maximum theoretical heat pump efficiency is given by the Carnot efficiency as

$$COP_{carnot} = \frac{T_{condenser}}{T_{condenser} - T_{evaporator}} \quad (3.2)$$

The COP_{carnot} cannot be realised physically but is used as a gauge to determine such as a refrigeration system is from the ideal system. The SMER (Specific Moisture Extraction Rate) is a common performance indicator used to express the performance of a certain dryer. It is defined as below [26]:

$$SMER = \frac{\text{amount of water evaporated}}{\text{energy input to the year}}, \text{ kg/kWh} \quad (3.3)$$

The real efficiency of a heat pump ranges from 40 to 50% to the theoretical Carnot efficiency [27].

3.1.2 Solar Source Assisted Heat Pump Dryer

Figure 3.4 shows a simple sketch of the Solar Assisted Heat Pump Dryer (SAHPD) system, which illustrates the different refrigeration components and the integration of solar systems in the drying chamber. This combination of solar energy collectors with heat pump dryer effectively increases the drying temperature and energy efficiency of the overall system.

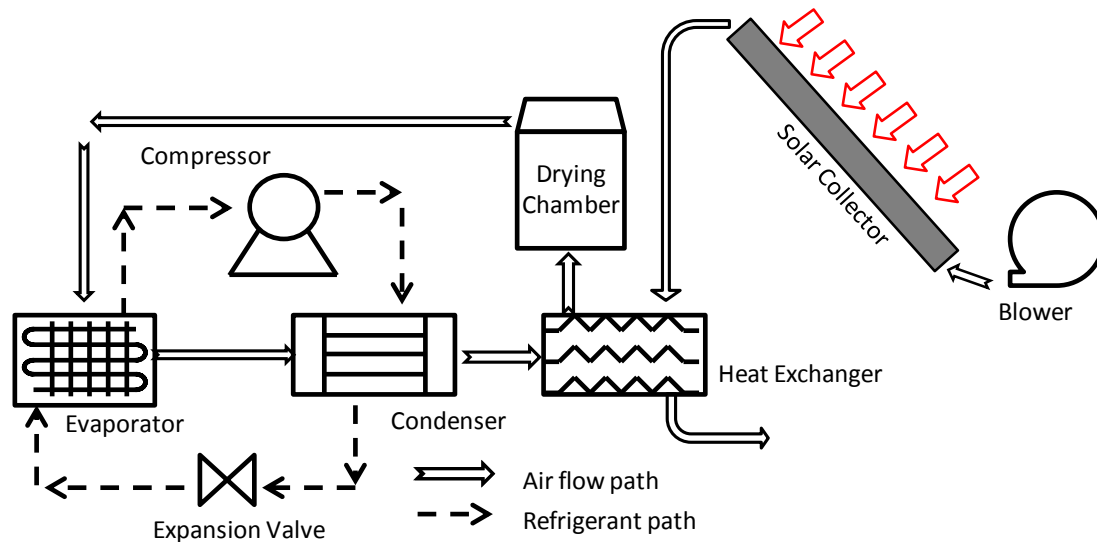


Fig 3.4 Schematic of a simplified SAHPD system

Figure 3.5 is an illustration of the solar-ambient hybrid source heat pump drier in a hot-humid weather condition. The COP of a SAHPD shows to vary between 2.31 and 2.77, with an average of 2.54; the heating capacity of the condenser varies between 2.9 kW and 3.75 kW, with an average of 3.325 kW. SMER is calculated to be 0.79kg/kWh. The moisture content was observed to reduce from about 52% to about 9.2% and 9.8% in 40h for trays at the bottom and the top on wet basis of the copra. Copra obtained in a SAHSHPD has been found to have a higher quality than in other drying methods.

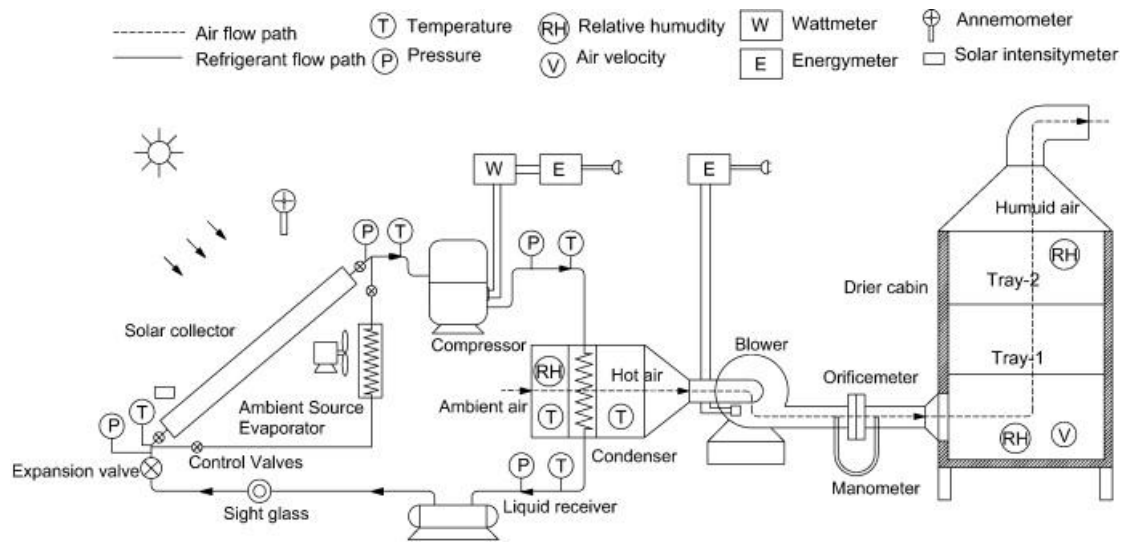


Fig 3.5 Schematic view of SAHPD [28]

3.1.3 Ground Source Assisted Heat Pump Dryer

Figure 3.6 is a diagram of the components of the ground-source heat pump drying system (GSHP). Heat from the ground is used as a heat source and heat sink in cooling mode operations. This works by absorbing the heat and using it to heat the working fluid. This is unarguably a more efficient alternative as it does not use ambient air, which is a less thermally-stable heat exchange medium than the ground. Due to this reason, the GSHPs can even maintain an outstanding performance in colder climates.

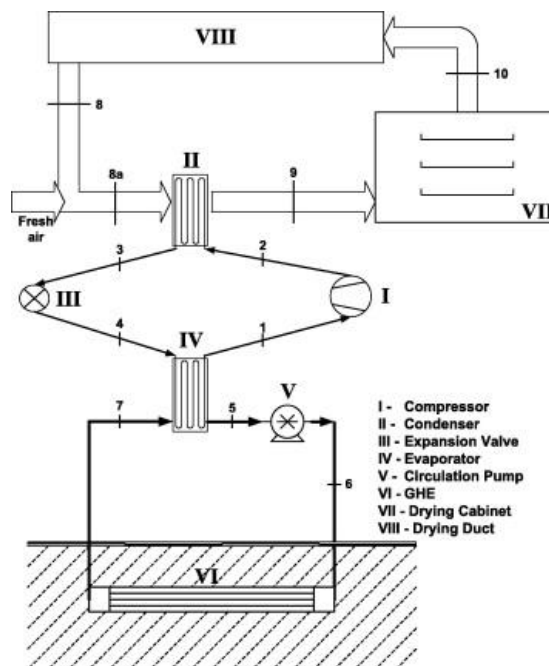


Fig 3.6 A schematic of the ground-source heat pump drying system [29]

An exergetic assessment of a ground source heat pump (GSHP) drying system presented by Hancioglu [29]. Exergy efficiencies of the system components are determined to assess their performances and to elucidate potentials for improvement. COP values for the GSHP unit and overall GSHP drying system are found to range between 1.63–2.88 and 1.45–2.65, respectively, while corresponding exergy efficiency values on a product/fuel basis are found to be 21.1 and 15.5% at a dead state temperature of 27°C, respectively. Specific moisture extraction rate (SMER) on the system basis is obtained to be 0.122 kg kW⁻¹h⁻¹. For drying systems, The SMER of the whole GSHP drying system is found to be 5.11 kg kW⁻¹h⁻¹.

3.1.4 Chemical Assisted Heat Pump Dryer

. The use of chemical heat pumps requires no mechanical energy input and allows several functions to simultaneously take place, including improving heat quality, heat pumping, refrigeration and thermal energy storage. Unit operations that deal with vast enthalpy changes in industrial processes such as distillation, drying, evaporation and condensation, can benefit from using chemical heat pumps.

Figure 3.7 is an illustration of a solar-assisted chemical heat pump dryer by Fadhel [30]. Note that the performance of the system was tested and studied under the meteorological conditions in Malaysia. The system comprises of four major components: solar collector (evacuated tubes type), storage tank, solid-gas chemical heat pump unit (consists of reactor, condenser and evaporator) and dryer chamber. The reaction studied in this system is between that of CaCl₂–NH₃. Both a simulation and an experiment were carried out. Theoretical results and experimental results were compared: The maximum value of solar fraction from the simulation was found to be 0.795, with the experiment yielding 0.713. The maximum efficiency of the solar collector was predicted to be 80%, against the experimental efficiency of 74%, but the COP of the chemical heat pump obtained from both simulation and the experiments gave 2.2 and 2.0, respectively, showing that a decrease in solar radiation – leading to a reduction of energy at the condenser – decreases the COP of the chemical heat pump and thus the efficiency of drying.

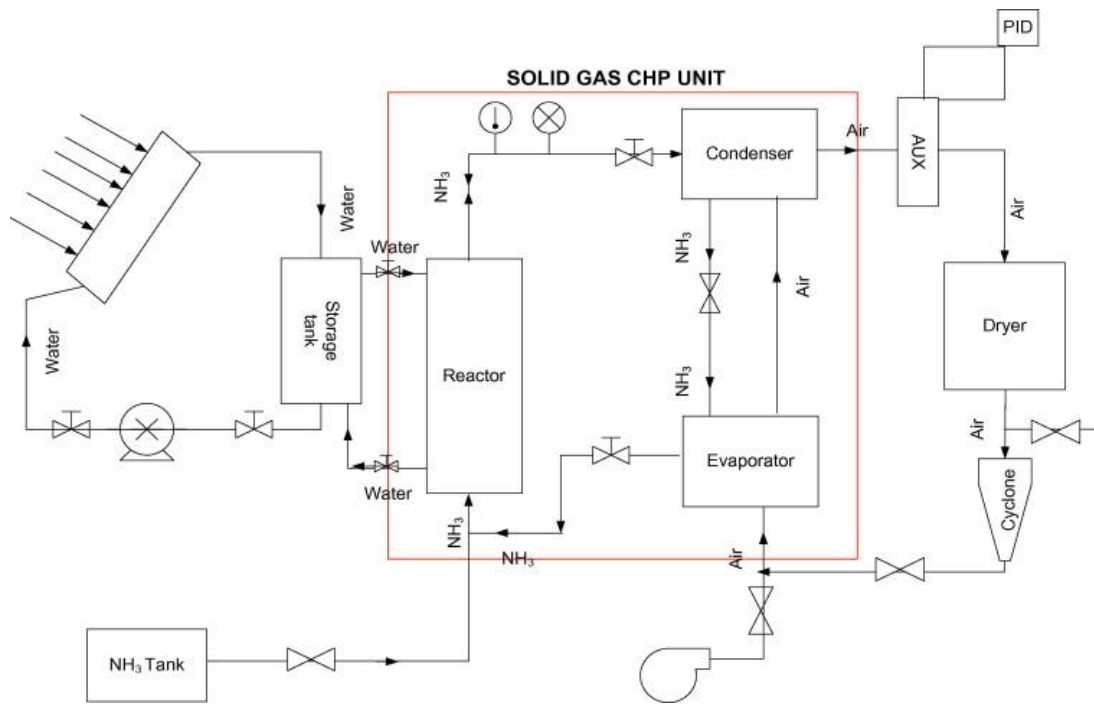


Fig 3.7 Schematic diagram of solar-assisted chemical heat-pump dryer [30]

3.1.5 Two Stage Heat Pump System for Drying

The single-stage vapour compression cycle used in many commercial heat pump dryers has many disadvantages comparing to a two-stage or multi-stage heat pump dryer. In a single-stage drying system, there is only one evaporator for all the operations involved in dehumidifying, cooling and recovering latent heat from the drying air, as there is a limit to the amount of heat recovered due to the lack of available area for heat transfer. One huge downside of a single-stage dryer is its inability to provide streams of drying with varying humidity and temperature in order to adapt to several independent drying chambers.

The study conducted by Chua et al [31] focuses on the performance of a two-stage heat pump system for drying. Figure 3.8 illustrates the application of both low- and high-pressure internal evaporators for cooling and dehumidification in the system. Two sub-coolers are placed at the condenser for additional sensible heating and a passive-evaporator economiser is also further integrated for pre-cooling and pre-heating before the air enters the evaporators and the condenser, respectively. The amount of heat recovered at the evaporators and the system's COP and SMER are factors to consider when evaluating the performance of the system. Up to 35% or more of the heat could be recovered by the two-stage evaporator compared to the

one-stage evaporator system. To further recover heat, one can vary the pressure level of the high-pressure evaporator as the ratio of latent to total load at the two-stage evaporator is improved.

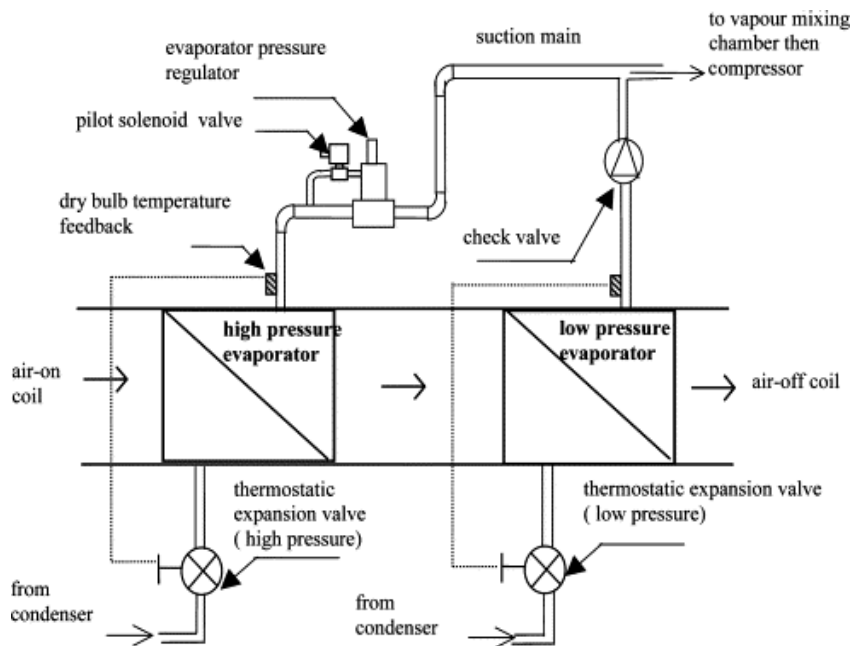


Fig 3.8 Schematic Diagram of the Two Stage Evaporator System [31]

Figure 3.9 shows a substantial improvement in the heat pump energy efficiency going from a single- to a two-stage dryer. The implementation of a multi-stage heat pump cycle is that it permits regulations of humidity of the air, which is a huge advantage over the conventional single-stage heat pump cycle.

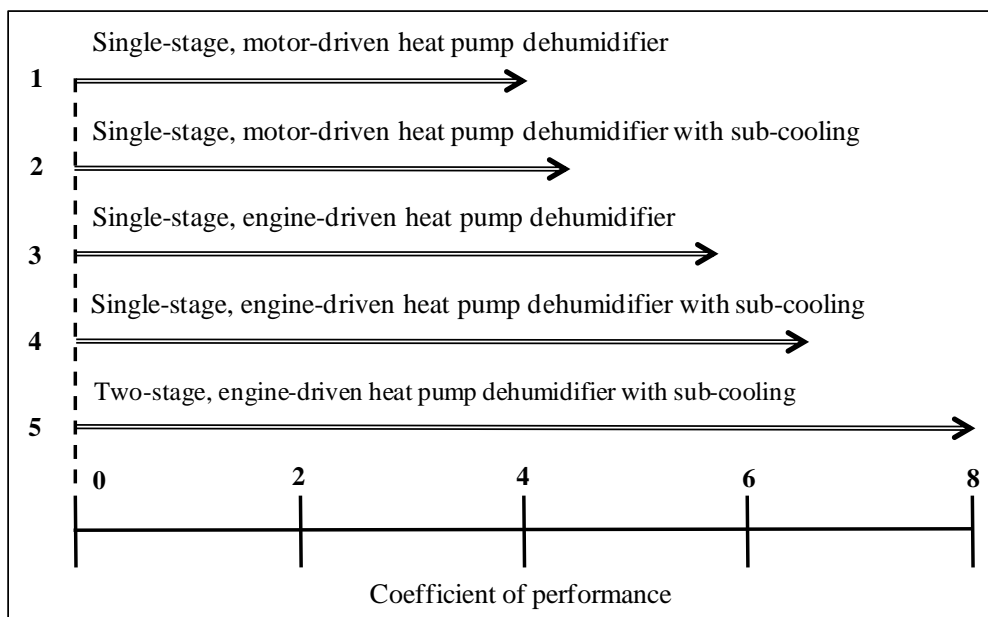


Fig 3.9 Coefficient of Performance of Various Heat Pump Configurations [31]

3.1.5.1 Advantages and Limitations

Since the 1970s heat pump has been gradually replacing conventional hot air dryers in various industries for food and timber drying, due to its high energy efficiency. However, there are some technical difficulties in trying to achieve the optimal performance for the drying system. This section discusses these aspects of the development of the dryer.

Heat pump dryer have several advantages and limitations. Which drying system is right for a given installation, or even whether to use a drying system, depends on the circumstances of that particular installation.

The key advantages and limitations of the heat pump dryer include a high SMER ratio (in the range of 1.0 to 4.0), meaning that a significant amount of heat can be recovered from the moisture-laden air, and not only does it improves the overall thermal performance, it also yields effective air conditions control. Secondly, it is a very versatile system in that its environments can be easily altered to suit the product's value and needs; a wide range of drying conditions can be generated to adapt to different materials, without being influenced by weather conditions. And finally, it improves the product quality by drying at low temperatures, which is achieved by further reduction of the humidity of air.

Although heat pumps drying as many advantages to them, there are inevitably some limitations that are still being worked on. Some of the limitations include using CFCs as its refrigerant and a high machinery cost, due to regular maintenance of the components and refrigerant supply etc. But even if so, the heat pump dryers still gives a 40% reduction in energy in comparison to electrical resistance dryers, according to the literature [32].

3.1.5.2 Energy Efficiency

The ability of heat pump dryers to convert latent heat of condensation into sensible heat at the hot condenser makes them unique heat recovering devices for drying application. The energy efficiency of HPD can be reflected by the higher SMER values and drying efficiency when compared with other drying systems as shown in Table 3.1 Consequently, higher SMER would then be translated to lower operating cost, making the payback period for initial capital considerably shorter.

Table 3.1 Comparison between Heat Pump Drying and Other Drying Systems [33]

Parameter	Hot Air Drying	Vacuum Drying	Heat Pump Drying
SMER(kg water/kWh)	0.12-1.28	0.72-1.2	1.0-4.0
Drying efficiency (%)	35-40	≤ 70	95
Operating temperature range (°C)	40-90	30-60	10.0-65.0
Operating % RH range	Variable	Low	10.0-65.0
Capital cost	Low	High	Moderate
Running cost	High	Very High	Low

Source: Adapted from Perera, C.O. and Rahman, M.S., Trends Food Science Technology, 8(3),75,1990. With permission

3.1.5.3 Batch and Conveyor Heat Pump Dryer

In the drying chamber, the products are placed on trays, and as soon as the desired product moisture content is sufficiently reduced to a value, they are removed from the trays. This operation is illustrated in Figure 3.10 show a cross-flow dryer configuration, where the drying air can flow parallel or perpendicular to the surface of the product. Batch drying is commonly used in smaller production rates, but because of this high costs pursue. Since batch systems permits air to be re-circulated at very low leakage rates, heat pumps are more apt for such operations, but the thermal load of batch dryers decreases as the material gradually dries. This leads to drying processes that are time-dependent and thus having an impact on the performance and the thermodynamic cycle. A continuous conveyor drying system has shown to be a more suitable method of drying for crop harvests. Jia et al. [34] developed such a model that exhibited maximum efficiency. This model was later used by Clements et al. [35] for study purposes, and they used a wet foam rubber in the continuous bed dryer. This effectively doubled the SMER of the dryer from 1.25 to 2.5 kg kWh⁻¹ as the relative humidity of the air at the dryer inlet increased from 32% to 80%.

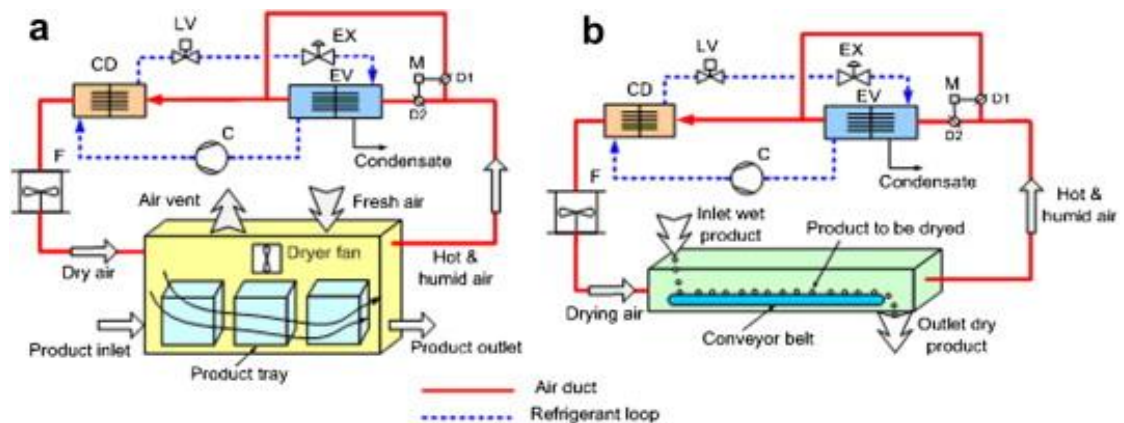


Fig 3.10 (a) Batch heat pump dryer; (b) conveyor heat pump dryer; C: compressor; CD: condenser; D: damper; F: fan; EV: evaporator; EX: expansion valve; LV: liquid valve; M: motor [36]

3.1.6 Modelling of Heat Pump Dryer

All components in a heat pump air dehumidifier that is coupled with a dryer are independent, thus the heat pump is a complex system that, as a consequence, leads to many proposal of models:

- Jolly et al.: a simulation model that considers detailed heat and mass transfer in each individual component of the heat pump continuous dryer system [37].
- Jia et al.: used the model of Jolly's to investigate the performance of such system [38].
- Teeboonma et al.: used the model of Jolly's to predict the performance of such system [39].
- Prasertsan et al.: developed a mathematical model to simulate results, using finite-difference method [40] [41].
- Achariyaviriya et al.: developed an empirical model to study the performance, leading to the discovery that results with closed-loop operation were yielded to be closer to the experimental data [42].
- Adapa et al.: reported an R134a heat pump drying system, that is a numerical model, for specialty corps [43] [44].
- Krokida et al.: proposed a mathematical model that accurately designs the desired and effective energy-saving system for thermal energy recovery of a convective dryer exhaust stream [45].
- Sarkar et al.: developed a mathematical model that studies the performance of a transcritical CO₂ heat pump dryer [46].

Even though empirical equations have contributed towards determining the thermodynamic properties and steam properties of the refrigerant, it is too complicated to apply different theories and designs to individual heat pump dryers, that all have different configurations and operating conditions. Simplified mathematical models are used to design for different components of a batch-type, closed-loop heat pump dryer, under a steady-state and constant conditions of drying rate.

3.1.6.1 Heat Pump Dryer Models

There are a few assumptions made for the heat pump dryer model, used by ASHRAE in the Psychrometric Analysis software for mathematical analysis.

For the heat pump unit:

- 1) The heat pump is operated at steady-state.

- 2) The component housing wall is adiabatic.
- 3) The expansion of the refrigerant is isenthalpic and the compression of the refrigerant is isentropic.
- 4) The tubes that connect the heat pump component is insulated, and in the pipe system, the pressure drop is negligible.
- 5) The refrigerant at outlet of condenser is saturated liquid, and saturated vapour at outlet of evaporator.

For the dryer unit:

- 1) The dryer is in a steady-state condition.
- 2) Both the drying chamber and the air duct are thermally insulated.
- 3) The air entering the evaporator has the same condition as the air leaving the dryer. The same applies to air entering the dryer and leaving the condenser.
- 4) The drying process is operating under constant rate period, and in this period, the working air follows the constant wet bulb temperature line in the psychrometric chart.
- 5) Both the specific heat capacity of air and the ambient conditions are constant.
- 6) There exists thermal equilibrium between the drying air and the product.
- 7) In the system, the air pressure stays constant at one atm, so is the mass flow rate of circulating dry air.

The mathematical model of a heat pump dryer consists of three sub models [32]; drying models, heat pump models, and performance models. Heat and mass balance of both refrigerant and air circuits are used for development of the mathematical models.

3.1.6.2 Drying Model

The following equation denotes the mass and energy balance between the material and the process air in the dryer.

$$\theta_{dr} - q_{ma}(W_{do} - W_{di}) = q_{mp}(M_{\theta i} - M_{\theta f})/100 \quad (3.4)$$

$$c_{pa}t_{di} + W_{di}(h_{fg} + c_{pv}t_{di}) = c_{pa}t_{do} + w_{do}(h_{fg} + c_{pv}t_{do}) \quad (3.5)$$

3.1.6.3 Evaporator Model

It is possible to derive the evaporator model based on the mass and energy balance of drying air making contact with the surface of the evaporator.

$$q_{mwe} = q_{ma}(1 - BF)(W_{do} - W_{es}) \quad (3.6)$$

$$Q_e = q_{ma}(1 - BF)(h_{do} - h_{es}) - q_{mwe}h_{we} = m_r(H_2 - H_1) \quad (3.7)$$

On the air side of a flat-finned tube coil, the forced convection heat transfer coefficient is calculated by the correlation below:

$$\alpha_a = 0.195 G_a c_{pam} P_{ra}^{-2/3} R_{ea}^{-0.35} \quad (3.8)$$

$$R_{ea} = \frac{G_a l_{rs}}{\mu_a} \quad (3.9)$$

$$P_{ra} = \frac{c_{pam} \mu_a}{k_a} \quad (3.10)$$

The range of $118 < N_{fin} < 787$ fins per meter is appropriate for this correlation.

The evaluation of the heat transfer coefficient of refrigerant for the force convection evaporation is as follows:

$$\alpha_{re} = 9.1825 \frac{k_l}{D_i} \left(\frac{D_i G_l}{\mu_l} \right)^{0.8} K_{lf}^{0.4} \quad (3.11)$$

$$K_{lf} = \frac{v_x H_{fg}}{L_t} \quad (3.12)$$

The total outside finned tube surface area for evaporator and condenser determines the overall heat transfer coefficient. This is calculated as follows:

$$U = \frac{1}{1/(\alpha_a \eta_{sf}) + A_o/(A_i \alpha_r) + (A_o \ln(D_o/D_i))/(2\pi k_{tw} L_t)} \quad (3.13)$$

$$LMTD_e = \frac{(t_{do} - t_{eo})}{\ln \left(\frac{t_{do} - T_{re}}{t_{eo} - T_{re}} \right)} \quad (3.14)$$

$$Q_e = U_e A_{eo} (LMTD)_e \quad (3.15)$$

3.1.6.4 Compressor Model

In order to predict a change in enthalpy of refrigerant, a mathematical model of a reciprocating compressor is used during compression and energy consumption.

$$P_{comp} = q_{mr}(h_3 - h_2)/(\eta_{mech} \eta_{motor}) \quad (3.16)$$

$$Vh = \frac{P_2 v_{r2}}{3600} \left(\frac{n}{n-1} \right) \left\{ \left(\frac{P_3}{P_2} \right)^{n-1/n} - 1 \right\} \quad (3.17)$$

$$n = a_{31} + a_{32}T_2 + a_{33}T_2^2 + a_{34}T_2(T_3 - T_2) + a_{35}T_2^2(T_3 - T_2) + a_{36}T_2(T_3 - T_2)^2 + a_{37}T_2^2(T_3 - T_2) + a_{38}(T_3 - T_2) \quad (3.18)$$

$$q_{mr} = \frac{\pi d_p^2 l_p N_p \eta_v N_s}{240 v_{r2}} \quad (3.19)$$

$$\eta_v = 1 + n - n \left(\frac{P_3}{P_2} \right)^{1/n} \quad (3.20)$$

3.1.6.5 Condenser Model

At the condenser coil, the condenser model can be used to predict the mass flow rate and the energy transfer of the refrigerant.

$$Q_c = q_{mr}(h_4 - h_5) \quad (3.21)$$

$$Q_{c,int} = q_{ma}(c_{pa} + W_{di}c_{pv})(t_{co} - t_{eo}) \quad (3.22)$$

The heat pumper dryer system's energy balance is given by:

$$Q_c = Q_e + \nabla h = Q_{c,int} + Q_{c,ext} \quad (3.23)$$

The heat transfer coefficients of the refrigerant side of the condenser for single phase:

$$\alpha_{rc} = 0.023 \frac{k_l}{D_i} \left(\frac{D_f G_i}{\mu_f} \right)^{0.8} \left(\frac{\mu_f c_{pf}}{k_f} \right)^{0.4} \quad (3.24)$$

Equation 3.14 calculated the air-side forced convection heat transfer coefficients.

Equation 3.18 calculated the overall heat transfer coefficients.

$$LMTD_c = \frac{(t_{co} - t_{eo})}{\ln \left(\frac{T_{rc} - t_{eo}}{T_{rc} - t_{co}} \right)} \quad (3.25)$$

$$Q_c = U_c A_{co} (LMTD)_c \quad (3.26)$$

3.1.6.6 Capillary Tube Model

A pressure reduction is achieved by using a capillary tube as a model for the expansion device. It is assumed that the expansion is isenthalpic:

$$h_6 = h_1 \quad (3.27)$$

There are several stages of temperature drop in the capillary tube: the frictional pressure drop and friction factor of each segment of drop is calculated, and using equation 3.28 and 3.29, the required length of capillary tube can be determined.

$$Vp_r = \frac{\rho_r f_r \nabla L u_r^2}{2D} \quad (3.28)$$

$$f_r = \frac{0.32}{Re_r^{0.25}} \text{ for turbulent flow} \quad (3.29)$$

3.1.6.7 Fan Power

The following equation calculated the air-side pressure drops:

$$Vp_a = \frac{2f_a l_{ad} G_a^2}{D\rho_a} \quad (3.30)$$

The correlations of ASHRAE determine the friction factor, f_a , of air in the evaporator, condenser, and air duct. The change in direction and velocity causes the dynamic pressure losses in ducts, and this change is calculated for the total pressure of fan.

$$\begin{aligned} \text{Fan power requirement}(P_{fan}) \\ = \text{Fan total pressure} \times \text{Volumetric air flow rate} \end{aligned} \quad (3.31)$$

3.1.6.8 Performance Model

COP evaluates the drying and dehumidification performance of the system, in particular the heat pump and the specific moisture extraction rate, SMER, and the moisture extraction rate, MER.

$$COP_{HP} = \frac{\text{Heat delivered in internal condenser}}{\text{Power input to compressor}} \quad (3.32)$$

$$SMER = \frac{\text{Water evaporated from product}}{\text{Total energy input}} \quad (3.33)$$

$$MER = \frac{\text{Water evaporated from product}}{\text{Drying time}} \quad (3.34)$$

3.1.6.9 Improving Performance Heat Pump System

The two interactive working fluids in heat pump dryer, which are the refrigerant and the drying air, influence its efficiency due to its complex system, therefore the question of whether an optimum design exists still remains. When a heat pump is coupled with a dryer, the interdependency of all components contribute to a complicated system, whereby the performance of the dryer depends on the configuration of the working fluids' flows. Both drying rate of the product and the ambient condition of the system determine the preferable operation configuration. In tropical climate and high drying rate, the best operating mode is usually the partially open system, but at a low drying rate, the operation is slightly more complicated, as the optimum configuration is sensitive to the drying rate and the ambient temperature. The heat pump dryer configuration design must be continuously changed for the low drying rate product. On top of that, it also requires an external condenser and cooler in order to function properly.

There are three factors that regulate the efficiency of the heat pump energy efficiency. One evaluates each component as follows: the compressor's efficiency is not within the control of the system's designer, as it is an off-the-shelf product; the choice of refrigerant has a small impact on the cycle efficiency, and it generally depends on the size and type of application. The last component is the heat exchanger, which now appears to be determining factor for the optimisation of the heat pump dryer system.

There exist two heat exchangers in the heat pump system, one being the condenser and the other being the evaporator. The condenser provides heat for the drying air, the medium, which means that it plays a vital role in the overall performance. Studies conducted by Saensabai and Prasertsan [47] [48] discovered that the COP could be improved up to 27.6% by changing the refrigerant flow path, and increasing the coil depth has shown to improve the COP by 12.3%, concluding that effects of the arrangement of the heat exchanger is not to be neglected.

The optimum performance of a heat pump drying system is achieved by using

an evaporator or a large surface area, minimum fin space, minimum depth, low airflow rates, no superheat across the coil, and uses the high evaporating temperature as the system can operate at. The coil performance is shown to improve by a change in the refrigerant's mass velocity along the flow path. This can reduce to up to 5% of the heat transfer area. This research done by Liang et al [49] reports the effects of condenser coil arrangement on the heat pump dryer, which aims for the optimal coil design. The mathematical model and simulations used in this study was developed based on the heat and mass transfer concept of both the refrigerant and the air side, plus the thermal process analysis.

The simulation procedure puts an emphasis on the small control volume approach, in order to take care of the working fluids' continuous change of their thermodynamic and thermo-physical properties.

- 1) Optimal design of condenser and evaporator coil: The heat exchanger coil configuration is represented by $xr-yc$, where x and y are the number of rows (r) and circuits (c) respectively.
- 2) Demand of refrigerant flow: The demand of refrigerant flow was the flow rate of refrigerant in each circuit of condenser coil for working with high efficiency. In condenser coil design, the optimum refrigerant flow rate must be used in order to maximize the heating capacity (heating COP).
- 3) Optimum heat exchanger arrangement: In some conditions, they need only one or two refrigerant circuits. But, for other conditions, three or four circuits are needed.

Many interrelated parameters must be taken into consideration whilst assessing the design of a heat exchanger of a heat pump dryer. Improvements can be made by alterations on the system's refrigerant mass flow rate and the air flow rate. The coil configuration, such as the number of rows, circuits and modules, can affect the heat transfer capability and the pressure drop of both the refrigerant and the air side. Verified mathematical models determine the optimum parameters, and the matching of the components was based on the heat pump dryer performance.

3.2 Desiccant Dehumidifier

There are two methods in which atmosphere air dehumidification can be achieved, one done by cooling the air below its dew point, then removing the moisture by condensation, the other completed by sorption by a desiccant material, as desiccants in either their solid or liquid forms have a natural tendency to remove

moisture. The latent heat released as the desiccant removes the moisture from air heats up the air itself. This warm air can then be cooled by sensible coolers, such as heat exchangers, evaporative coolers or evaporator coils, to the desired conditions. The desiccant can only be regenerated or reactivated when the moisture in it has been removed by means of heating. Energy sources to conduct such heating include waste heat, solar energy, waste heat, or simply electricity.

3.2.1 Regeneration methods of desiccant in drying applications

Higher energy efficiency can be achieved by using renewable energy or waste heat from other systems, or regenerating desiccant material at a low temperature. The process of regenerating materials typically uses electrical heat, solar energy and waste heat as a mean of energy drive. Here we discuss about the three methods and evaluate their effectiveness and economy.

3.2.1.1 Solar energy

This method for the regeneration process is highly researched and studied, as the source itself is considered “free”. The capital for producing solar panels and its additional accessories is high, but taking the payback period into consideration, the long term overall savings may be able to compensate for the initial cost. One major issue with solar energy is that its operation is weather-dependent, so there is a need for additional backup energy when the main energy supply fails, in order to keep the drying process running. Alosaimy and Hamed [50] developed and investigated the application of a flat plate solar water heater to regenerate the liquid desiccant. Xiong et al. [51] studied a two-stage solar-powered liquid desiccant dehumidification system with two types of desiccant solutions. Ahmed et al. [52] constructed an open test loop for the desiccant wheel to conduct experiments and thus validate the numerical model. Lu et al. [53] developed two solar desiccant dehumidification regeneration systems known as SDERC and SRAD.

3.2.1.2 Waste heat

This is arguably one of the best alternatives for regeneration as there is no regeneration cost. Whilst it is nearly the best option out of all, only equipment that is able to exhaust waste heat between 60 °C and 140 °C can use this method for desiccant regeneration, and they are not so readily available either. De Antonellis et al. [54] investigated seven HVAC configurations for drying based on desiccant wheels to find the most energy-efficient system. Zaltash et al. [55] reported on this topic. TA systems use the DG's hot exhaust gas for heating, cooling, and regenerating the desiccant material in dehumidification systems.

3.2.1.3 Electrical heater

This is a much more consistent heat source than solar energy. It is simple and reliable, but electrical heaters tend to have a high energy consumption and thus high operating cost, therefore they are only generally considered suitable as a backup energy source, or when waste heat is not sufficient to run on its own. Bassuoni [56] investigated the performance of the structured packing cross flow air–liquid desiccant contacting surfaces on the dehumidification and regeneration of the system. Mandegari and Pahlavanzadeh [57] introduced a novel efficiency definition for a desiccant wheel by comparing the process of air enthalpy between outlet and inlet.

3.2.1.4 Ultrasonic technology

Ultrasonic technology is a non-heating drying method. Studies have found that it improves drying kinetics and increases energy efficiency, but as it is ultrasonic after all, there have been safety concerns regarding health and the environment. Yao et al. [58][59] investigated five different drying models to quantify the drying kinetics of silica gel regeneration by hot air combined with ultrasonic power.

3.2.1.5 Electro-osmosis

In domestic applications, solid and liquid desiccant dehumidification is not viable, as the process requires large electricity consumptions in order to generate heat that regenerates the desiccant material. Researchers are seeking for alternatives with lower costs. Li et al. [60] experimented on using electro-osmosis (EO) for regeneration. In this technique, low voltage DC supply is used.

3.2.1.6 Vapour compression system (heat pump)

Low energy consumption is characteristic to a heat pump. This is particularly prominent with a system that combines heat pump and a desiccant system. It is a system with high energy efficiency and the processed air produced has a much lower humidity level. The dehumidification process carried out by an evaporator and a desiccant material can produce processed air with a better condition at low energy consumption as well. Furthermore, the heat released by the heat pump can be used to regenerate desiccant materials.

When the latent load is high in a desiccant system, it is particularly useful, as it removes moisture more economically than it removes sensible heat. In addition, when thermal energy comes into play, the cost of dehumidification with a refrigeration system falls under the cost of a dehumidification with a desiccant. When the desiccant

regeneration is done by waste heat, off-peak electricity, or natural gas, it is more economical compared to regular electric refrigeration, since there is no need to reheat with desiccant dehumidification systems, so another appropriate use is when conditioned air is reheated after exiting a coil to reach a suitable dry bulb temperature. The use of a desiccant is apt when dehumidification is required at levels below freezing dew-point temperatures; most solids are qualified as desiccant material as they attract moisture.

Desiccants have a low surface vapour pressure, and this is essential to their moisture collection characteristic, because if the desiccant is cool and dry, its surface vapour pressure will be low, therefore it is able to attract moisture in air, since the air has a higher vapour pressure when it is moist.

After moisture collection, the desiccant becomes wet and hot. As a result its surface vapour pressure increases and it re-releases water vapour into the surrounding air again. However, desiccant dehumidifiers use the change of vapour pressures to dry air continuously in a repeating cycle; therefore the mechanism ensures that the re-released vapour is re-absorbed into the desiccant material again. The equilibrium is illustrated in Figure 3.12.

At point 1 the desiccant begins its cycle. As the desiccant picks up the moisture, it changes from being dry and cool to wet and hot. This phenomenon is shown by point 2, which, at this point the desiccant cannot collect any more moisture, as its vapour pressure is now equal to that of the surrounding air and thus there is no pressure difference. After this point the desiccant is removed from the moist air and heated to be placed back into a different airstream. The surface vapour pressure of the desiccant is now higher than the surrounding air, so the moisture moves off the surface to the air to equalise the pressure difference. Whilst it is still hot at point 3, the desiccant is unable to collect moisture from air due to its high vapour pressure, but it can be cooled to restore its low pressure point, and the whole cycle starts again at point 1.

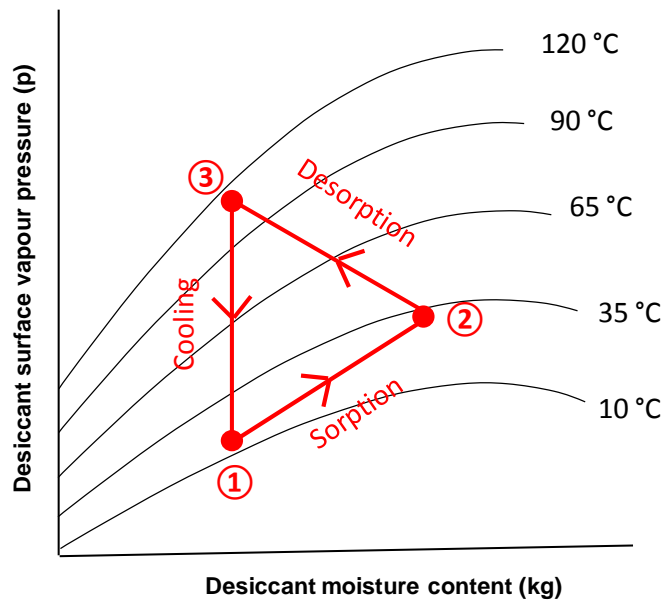


Fig 3.12 Repeating Cycle of Desiccant Dehumidifier

The cycle is driven by thermal energy. When the desiccant has a high moisture capacity and a low mass, the over efficiency of the process is improved. The required heating and cooling energy is directly proportional to the mass of the desiccant and the mass of the machinery that presents the desiccant to the airstream, so in an ideal world with an ideal desiccant dehumidifier, it would have an infinitely low mass and an infinitely high surface area to collect moisture.

The desiccant that collects moisture can be either a solid or a liquid. An example for a solid desiccant is the small packets inside camera cases and consumer electronic boxes. These often contain silica gel. As for the liquid example, triethylene glycol is a powerful desiccant that is similar to auto antifreeze. Apart from the phase difference, both solid and liquid desiccants function on the same principle, in which their surface vapour pressure dictates their temperature and moisture content.

There is one subtle distinction between the different types of desiccants however, and that is their reaction to moisture. There are two moisture collecting mechanisms, one is when the water is held on the surface of the material. This is called adsorption, which is how most solid desiccants work. The silica gel mentioned earlier is an example of such adsorbent. Other types of desiccants absorb moisture, which give rise to physical or chemical changes as they collect water, and this is how liquid and some solid desiccants work. An example is lithium chloride and sodium chloride, with are both salts.

The mechanism does not usually play a role in determining a system's final design, but the distinction exists and the engineers should be aware of the differences,

as it is still important to know what happens to the air when it is being dehumidified. The reverse of evaporation liberates heat, but in a cooling-based dehumidification process, the effect is not as distinct as the heat is removed almost instantly by the cooling coil. With a desiccant dehumidification system, the process air usually leaves the dehumidifier warmer with respect to how it was before it entered the desiccant unit, because the heat is transferred to the air and then to the desiccant.

Figure 3.13 shows a direct proportionality between the temperature rises to the amount of moisture removed from air. One can see on the psychrometric chart that, the drier the air when it leaves the dehumidifier, the warmer it will be. It is evident that desiccant dehumidification is different from cooling-based dehumidification. The total enthalpy of the air remains constant, due to the relationship illustrated in figure 3.13. On the other hand, the total energy increases due to a transfer of waste heat from the regeneration process to the air. This temperature rise is desirable in many cases, in particular, applications of notable product drying and unheated storage. It is, however, not desirable, nor it is an advantage; therefore the dry air is cooled before it is delivered to be used.

There are five typical equipment configurations for desiccant dehumidifiers, each of them has its own advantages and disadvantages, but nevertheless all have been commonly used in the industry.

- Desiccant wheel
- Liquid spray-tower
- Solid packed tower
- Rotating horizontal bed
- Multiple vertical beds

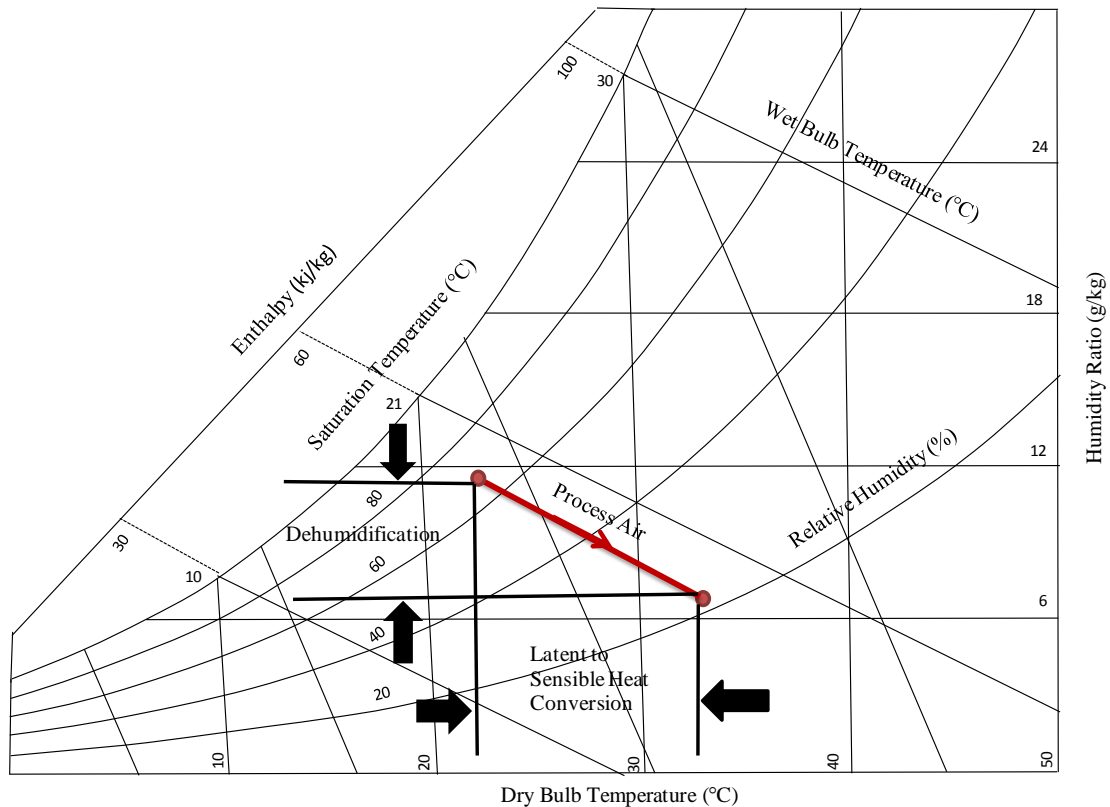


Fig 3.13 Heat from Desiccant Reactivation Carried Into the Dry Air Stream

3.2.2 Thermal Transfer Coefficients of Desiccant Wheel

A desiccant wheel dehumidifier works on the principle of relying on a rotating honeycomb wheel to deliver the desiccant to the operation and to present it to the reactivation airstreams. The semi-ceramic structure contains fine desiccant materials, which are integrated in a way that appears to be a grooved cardboard rolled up into a shape of a wheel. The wheel slowly rotates between the operation and the reactivation airstreams. Figure 3.14 shows a rotating cylinder containing small honeycomb-shaped channels covered with silica gel. Figure xx shows how the desiccant wheel is divided into two halves, with one being the desiccation part, where water vapour is adsorbed, and the other the regeneration part, where the water vapour is desorbed.

A model studied by Roula and Ghiaus [61] that is based on heat and a mass-transfer equation is developed with a gray-box approach in order to identify the thermal transfer coefficients experimentally. By defining the unknown parameters of the model as a function of a single parameter, the Nusselt number and heat and mass-transfer coefficients can be obtained.

Less than 10% of discrepancy is found between the literature and experimental values of the thermal transfer coefficients, thus the gray-box identification method is a reasonable estimation for the thermal coefficients of the desiccant wheels with

different design and operation conditions.

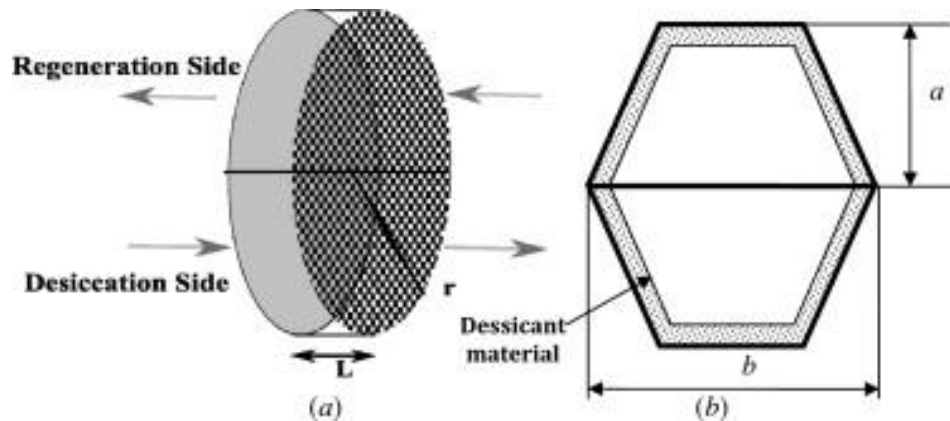


Fig 3.14 Desiccant wheel: (a) simplified illustration of a desiccant wheel; (b) cross-section view of a channel [61]

The design of the desiccant wheel is very flexible. It allows different kinds of desiccants, both liquid and solid, to be loaded into the structure, on top of that, the structure is also very lightweight and porous. This versatile characteristic allows the wheel to adapt to a wide range of specific applications. As the flutes of the structure are analogous to individual air ducts, the desiccant surface area exposed to the air is maximised even when the airflow of the system remains unstirred. This reduces the air pressure resistance compared to the packed beds. By combining a variety of desiccants into the same wheel, high capacity and low dew points can be reached, whilst the design remains energy-efficient. This is because the total rotating mass is low compared to its moisture removal capacity. Furthermore, the design is easy to maintain as it due to its simple and reliable nature.

One major concern with the design of a desiccant wheel is the cost of the rotating wheel. Its construction costs amounts to a higher value then if the system simply uses granules of dry desiccant, albeit the more energy-efficient approach. Great care should be taken to ensure that the wheel remains undamaged. Desiccant wheels are widely adapted into many desiccant dehumidifier configurations, so it goes to show that the results outweigh the equipment capital.

3.2.2.1 Liquid Desiccant

Figure 3.15 illustrates a typical liquid-desiccant dehumidifier system with its main five components: a dehumidifier, a regenerator to concentrate diluted solution from the dehumidifier, a heater powered by hot water and a chiller with vapour compression cycle to heat and cool the desiccant solution in the dehumidifier and

regenerator, and an internal heat exchanger to recover energy from two columns where desiccant solutions of different temperatures meet.

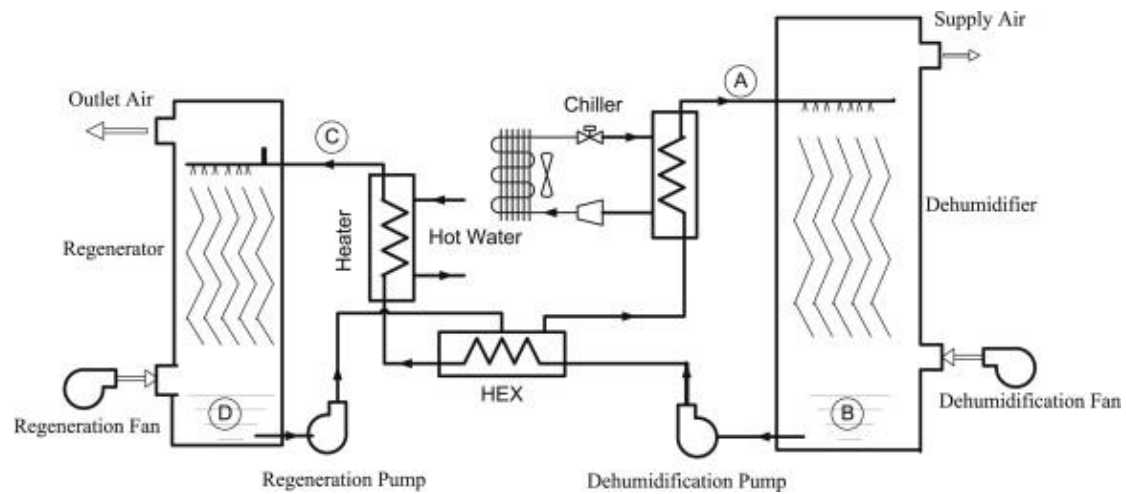


Fig 3.15 Schematic diagram of liquid desiccant dehumidifier system [62]

A model-based optimisation strategy for a chiller-driven dehumidifier of liquid desiccant dehumidification system with lithium chloride solution was presented by Wang et al. [62]. To reduce the energy consumption to a maximum while keeping the outlet air conditions at specific set-points, several measures are taken, including formulating an optimisation problem and the constraints of mechanical limitations and component interactions. Algorithm used in model-based optimisation strategy could obtain optimal set-points for desiccant solution temperature and flow rate, thus reducing energy consumption. The result of a comparison between experimental and theoretical optimisation shows a 12.2% reduction in the dehumidifier operation in the proposed optimisation strategy.

The minimum heating and cooling in a dehumidification process makes the liquid spray tower dehumidifiers a thermodynamically elegant operation. Only the necessary steps are carried out, for example, when the process needs to obtain a constant humidity, water can be freely added to the desiccant solution if the inlet air is dry, that the condition can act as a humidifier. If required, extra liquid can also be reproduced to provide energy storage in less than 20% of the floor space when being sent back to a holding tank. As well as the removal of the water vapour, particles in the air are also simultaneously removed as the liquid desiccant comes into contact with the air.

Liquid spray dehumidifiers are somewhat more complex than their solid desiccant units; therefore they are oftentimes arranged in large, central systems,

instead of small and free-standing units. Large systems' designs are more favourable for larger buildings with any dehumidification systems, since it is able to accommodate several conditioner units that are connected to a single regenerator, this gives an advantage in cost-savings, but the complexity in system control is a slight drawback to this setup.

There are a few potential disadvantages to liquid systems. These include the maintenance, first cost and response time of the smaller units. The slow response time may be caused by a long piping system and a large reserve sump for desiccant solution distributions. Information on rapid change in internal moisture loads and difference necessary outlet conditions may not be received by the system immediately. However, this slow response time may have a positive side to it: a large mass of re-circulating desiccant can protect an internal process from changing too quickly under the influence of weather moisture. For the maintenance aspect of it, the extend of protection and renewal varies from system to system, but since some desiccant materials are corrosive, more care needs to be taken. In addition, some liquid desiccant may dry out rapidly at low humidity levels, so in order to avoid desiccant solidification, liquid levels more be carefully monitored.

3.2.2.2 Solid Desiccant

There are two towers in a packed tower dehumidifier. Solid desiccants such as molecular sieve or silica gel are loaded into a vertical tower, and picks up moisture in the process air that flows through the tower. The process air is then diverted into a second drying tower after the desiccant has become saturated with moisture, whereas the first tower is cleared of its moisture with a small reactivated airstream and heated to ensure a dry environment is established for a new cycle to begin again.

The performance of molecular sieve desiccants when they absorb or release water studied by Tao [63] is evaluated by the weighing method. In a simulation of an environment with constant temperature, three types of saturated salt solutions of zinc bromide, Magnesium chloride and potassium acetate were employed to show the saturated water absorbing capability of molecular sieve desiccants. The experiment showed a clear dependence on the environmental condition of depositing, more specifically, a linear increase with the deposited time, with the temperature being a constant parameter. The slope varies with humidity. Relative humidity equilibrium exists between environment and molecular sieve desiccant after the water absorbing capability is saturated, while the molecular sieve desiccant's humidity varies in the range of 6.1 – 31.9%. The adsorbent water deposited on the surface of the molecular sieve desiccant was released once a lower humidity is reached in the silica gel and the

desiccant.

A composite material that consists of silica gel, sodium polyacrylate and polyacrylic acid developed by Chen et al. [64] were to be tested for its optimal mixing ratio, which was found to be 10:1:1. This material is originally developed for air-conditioning systems. The material exhibited a sorption capacity that is 41% higher than silica gel in a closed environment of a relative humidity of 70% at 25 °C. Tests on dehumidification capability at various air velocities, regeneration and inlet temperatures were performed, specifically at inlet air temperature of 30 °, regeneration temperature of 40 ° and relative humidity of 70% for 15 minutes, the material maintained 80% of itself being at its highest performance state. The material also showed a higher average dehumidification amount per minute (2.73 g/min compared to 2.46 g/min for silica gel). In addition, the airflow design of the composite material made a pressure drop of 149 mmAq/m in the system. From the above results, one can see that the composite material has a great potential in energy-saving.

The packed tower dehumidifier is often used to dry pressurised process air, as both drying and reactivation take place separately in sealed compartments. The same configuration is used to both gases and liquid chemicals. The process can achieve extremely low dew point like -40°C when a significant amount of desiccant are loaded into the towers, where the packed tower usually consists of desiccant dehumidifiers for compressed air. This design can lead to a change in outlet condition, even when the configuration permits low dew points. The desiccant can dry the air to a great extent when it first exposes to the process airstream, but as the process goes on and its moisture absorbing capacity reaches a limit, the drying speed slows down. Therefore a changing outlet condition must be closely monitored to avoid the process air condition becoming too wet.

Velocities of the air flow matters a great deal for packed tower dehumidifiers. The larger the process airflow requirements, the larger the dehumidifiers become, as the air velocities are usually kept low. The low air velocities gives an even air distribution through the bed for the air to be fully exposed to the desiccant. It also avoids lifting the desiccant, which would collide with other particles and with the vessel of the dehumidifier. This fractures the desiccant upon impact, and the specks would then be blown out of the unit as fine dusts. The configuration of units with fine dusts are used in small and low dew point air streams, and it offers compensating advantages to overcome the cost- and energy-related disadvantages in large-airflow, atmospheric pressure and higher dew point applications.

3.2.2.3 Limiting performance of desiccant

Goldsworthy [65] published a study on limiting performance in desiccant wheel dehumidification. At low temperature regeneration ($< \sim 80$ °C) the regeneration air relative humidity limits the supply air exit condition of a silica gel desiccant. It is easy for commercially available silica gel to reach relative humidity effectiveness that is higher than 85%.

The reduction in relative humidity to yield a useful dehumidification process can be achieved by keeping the temperature rise of the supply air to a minimum as it passes through the desiccant wheel. The desiccant dehumidification is at its most efficient when there is a minimal heat release in adsorption and low thermal mass to the supply air stream.

There are two ways to increase the capacity of the rotating bed, one is to increase the number of bed stacked on top of each other, and the other is to increase the diameter of the rotating trays in order to accommodate more desiccant materials. The rotating horizontal bed is able to provide relatively constant outlet moisture level if the desiccant is evenly placed on the trays, and less floor space is occupied than with a dual-tower unit as a high airflow capacity can be reached. However, it is never the case that the trays are completely filled with the desiccant until the top of the bed, as a result the desiccant settles slightly whilst in operation, causing air leaks from the side of the reactivation airstream to the process air side within the tray.

The rotating bed is usually designed to prevent this leakage by arranging the dry process airflow and moist reactivation airflow in parallel, rather than a counter flow configuration. Pressures between the process and reactivation sides are kept more or less equal using this format, therefore effectively reducing the leakage and enhancing the performance. As effective as this method appears to be, since the units are prone to low tolerance of moisture condition of the reactivation airstream, its energy consumption is significantly higher compared to other designs. However, this is compensated by the low first cost of the rotating horizontal bed design, as it is expandable and easy to manufacture. Problems such as fracture of desiccants and the desiccant debris in the airstream can be easily resolved by replacement of the material.

3.2.2.4 Effect of rotational speed of desiccant wheel

Angrisani [66] argues that there must be an optimal rotational speed on the performance of a desiccant wheel which depends on the operating conditions. The choice of the rotational velocity of the desiccant wheel is important as it affects how

the exiting temperature of the process air. It should lead to a high dehumidification performance and an outlet temperature that is low enough to reduce the cooling load on the cooling apparatus. Angrisani performed the experiments on a silica gel desiccant wheel. This puts an emphasis on the effect of the rotational speed on its performance. The results were used to calculate the main performance parameters of the wheel, which are the dehumidification coefficient of performance (DCOP), the dehumidification effectiveness and the sensible energy ratio (SER). The result showed that the dehumidification performance is optimised in the velocity range of 5-10 revolutions per hour.

3.2.2.5 Choosing between Desiccants and Cooling Dehumidifiers

Figure 3.16 shows the differences between a cooling-based dehumidifier and a desiccant dehumidifier in a psychrometric chart, as there already exists many circumstances, where both dehumidifiers remove moisture from air. Both dehumidifiers have their own advantages, to which could be applied depending on how close to saturation the air should be delivered from the system. The air leaving a cooling coil has a near 100% RH saturation. The two technologies are most competent when one compensates for the limitations of the other, therefore it is most efficient to use the two together.

- The optimum combination of the two drying materials in a particular situation depends on the difference in cost of thermal energy and electrical power. Given a cheap thermal energy and high power costs, it is more favourable to use desiccants to remove the bulk of the moisture, and vice versa.
- Cooling-based dehumidification is seldom used to dry air that is below a dew point of 5°C, as the condensate freezes on the coil and thus reduces the capacity in moisture removal. They are more economical than desiccants when operating at high moisture levels and high air temperature.
- They are efficient in different areas of drying. Cooling-based dehumidification is efficient when drying air to saturated air conditions, so if the air is drier than when it first entered the machine, whilst still saturated with moisture at a lower temperature, this method is more desirable. On the other hand, desiccants are efficient when drying air to create low relative humidity, and this is particularly useful when the air has a low relative humidity level.

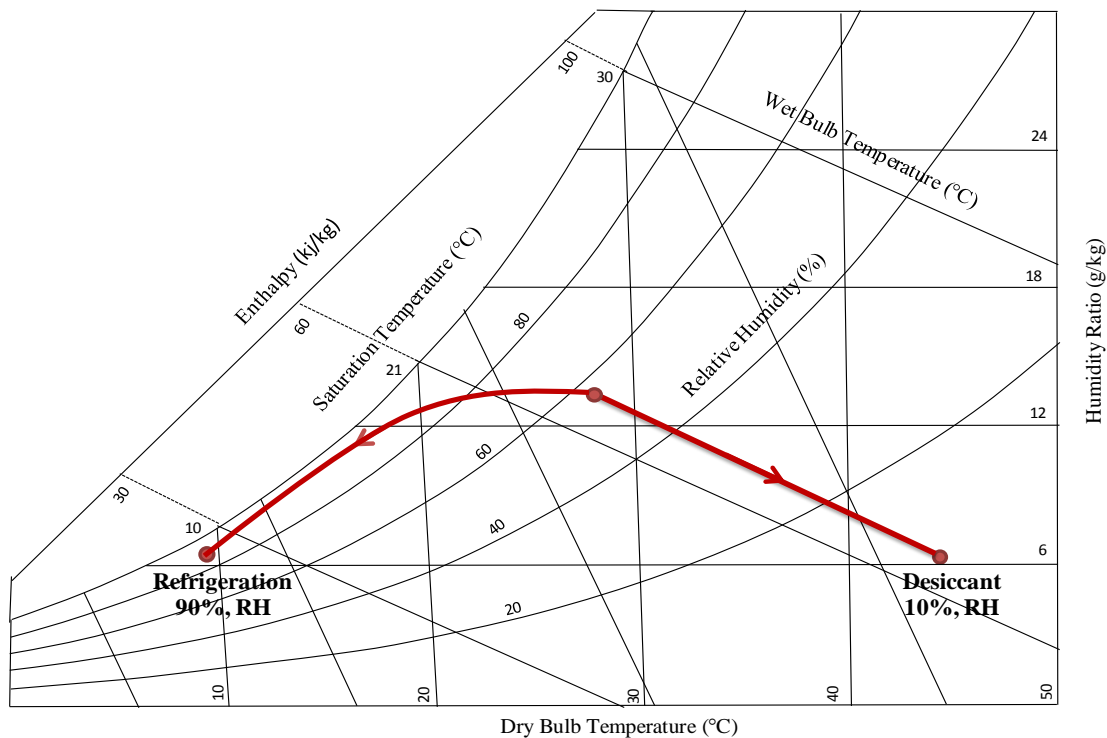


Fig 3.16 Difference between Cooling and Desiccant Dehumidifier in Psychrometric Chart

3.2.2.6 Desiccant Wheel Dehumidification Performance

Desiccant wheel removes water from air using the vapour pressure differences between the air and the desiccant surface to attract and release moisture. The equipment choice depends on the project requirements, especially the peak load requirements of a system, so it is vital to understand how the performance changes with difference operating conditions, bearing in mind the extreme peak design. Below is the discussion in engineering a desiccant system, in particular the mechanisms of the dehumidifiers and the relation between the operating variables of the equipment, and also their implications. There are eight key parameters which affect the performance of desiccant dehumidifiers [67-70]. These include:

- a) Process air moisture
- b) Process air temperature
- c) Process air velocity through the desiccant
- d) Reactivation air temperature
- e) Reactivation air moisture
- f) Reactivation air velocity through the desiccant
- g) Amount of desiccant presented to the reactivation and process airstreams
- h) Desiccant sorption-desorption characteristics

Desiccant dehumidifiers remove moisture from one airstream, called the “process” air, and move it to another airstream, called the “reactivation” air. High initial moisture in the process air, high reactivation air temperature and low process air velocity are combined to remove the largest amount of moisture from the process air.

Figure 3.17 shows what happens to the air on each side of the dehumidifier. As the process air is dehumidified, its temperature rises. Conversely, the reactivation air is being humidified, so its temperature drops as it picks up moisture. The process air leaves the dehumidifier warmer and drier than when it enters 40 °C and 5 g/ kg. On the reactivation side, a smaller air volume enters the dehumidifier from the ambience air. It passes through a heater and proceeds to the desiccant wheel. It heats the desiccant, which gives up moisture. The air is cooled as it absorbs the moisture from the desiccant, leaving the dehumidifier very moist, but much cooler than when it entered the desiccant wheel.

A desiccant dehumidifier moves latent heat from one airstream to another, analogous to a heat pump that shifts sensible heat from one airstream to another, so the operation has often been called a “humidity pump”. Since a desiccant dehumidifier removes moisture from the process air to a smaller reactivation airstream, it can be thought as a “moisture concentrator”.

First it needs to be known that the dehumidifier is assumed to operate at equilibrium from the beginning, meaning that the total energy on the process side is balanced by the energy in the reactivation side. The dehumidifier will not perform in a stable manner if the system is not in equilibrium. This is often caused by uncontrolled temperatures and airflows. Once this equilibrium is established, then other factors such as key variable changes can be considered for unit performance changes.

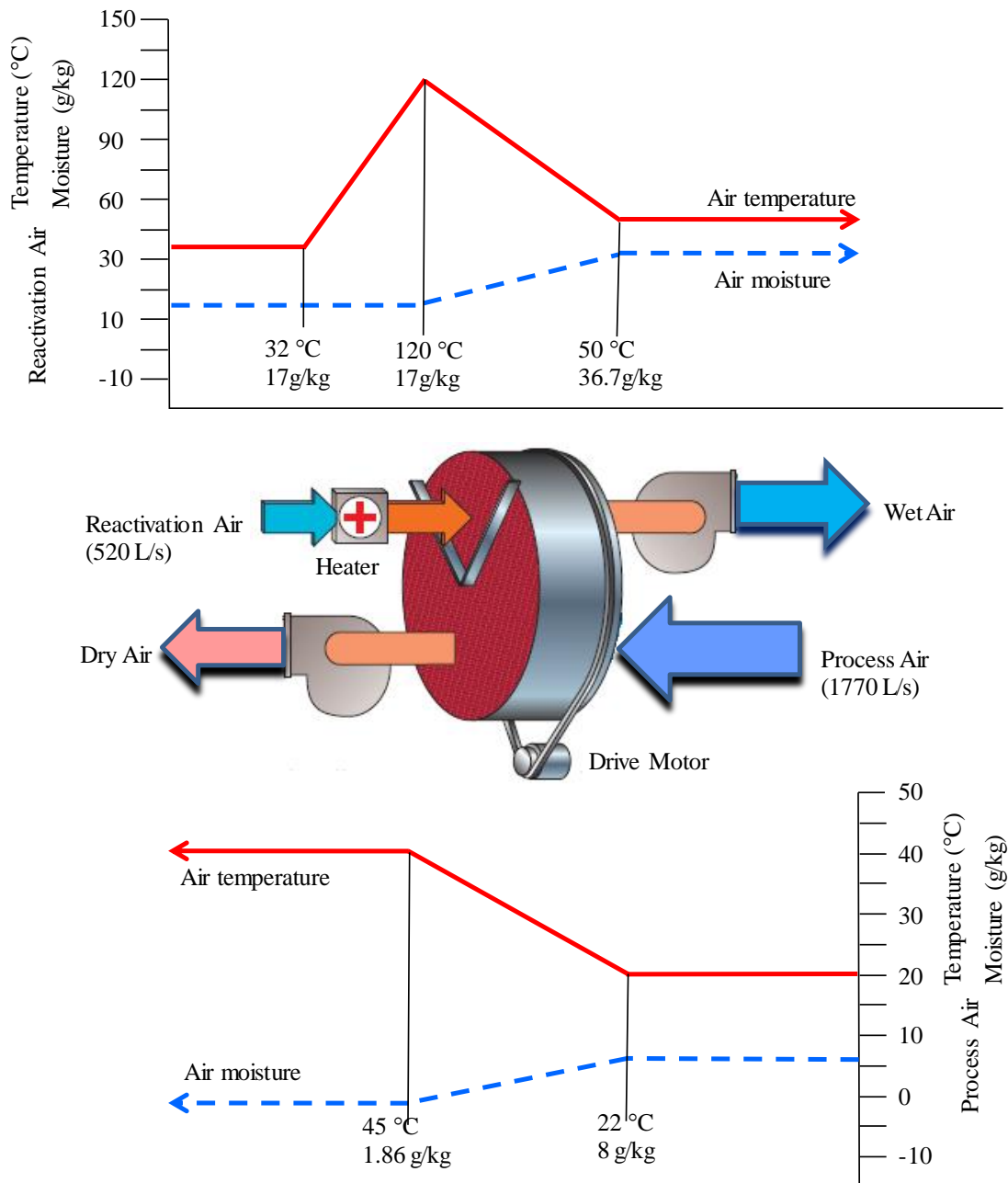


Fig 3.17 Process and Reactivation Airflow Temperature and Humidity Changes [23]

3.2.3 Effect of Desiccant Isotherm

The unique sorption characteristics of each individual desiccant can be demonstrated graphically as a capacity isotherm. These characteristics affect the performance of the dehumidifier and give a general indication of how moisture capacity changes as a function of relative humidity, under the condition that both the air and the desiccant have the same temperature.

Chung [71] uses numerical simulations in the study of the effect of desiccant isotherm on the performance of desiccant wheel, which focuses on the effect of

desiccant isotherm on the optimal conditions of operating and design parameters. A range of temperature from 50 °C to 150 °C was used to examine the rotation speed and the area ratio of regeneration to dehumidification. The range was found by an evaluation of the wheel performance by means of Moisture Removal Capacity (MRC). Effects of outdoor-air temperature and humidity were also examined for the optimum design parameters.

Figure 3.18 shows the illustration of a desiccant wheel. It is reasonable to represent the multiple-annular layers as in Figure xx due to geometrical similarities, and thus a three-dimensional cylindrical coordinates can be reduced to a two-dimensional, or more, a one-dimensional problem, which is a lot more unsteady than the previous two. The one-dimensional model is developed for coupled heat and mass-transfer process in rotary desiccant wheel. The model accepts the assumptions that the air flow is also one-dimensional, the axial heat conduction and mass diffusion in the fluid are negligible, and that the desiccant wheel is completely sealed, including the fact that all ducts are considered adiabatic and impermeable, with no change in thermodynamic properties. Finally, the heat and mass-transfer coefficient between air flow and the desiccant wall is taken to be constant along the channel as well.

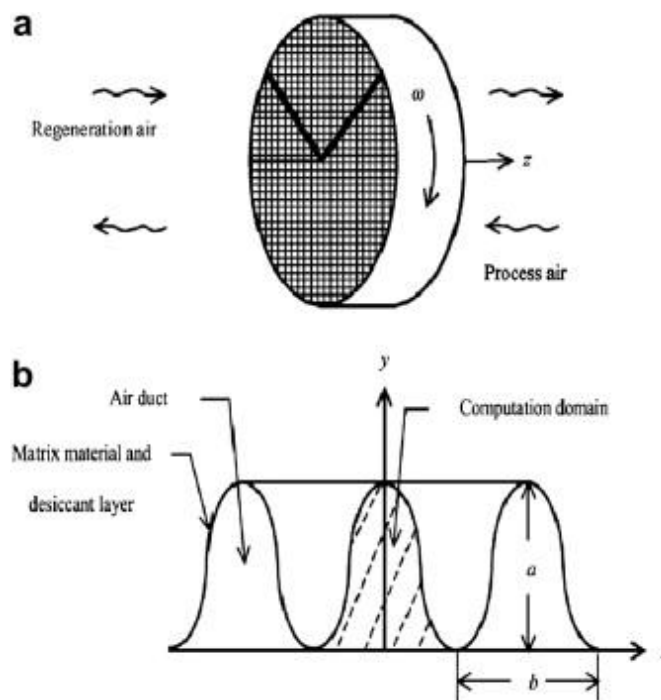


Fig 3.18 Schematics of (a) desiccant wheel and (b) computational domains [71]

The curve in Figure 3.19 shows the evolution of vapour pressure at the desiccant surface as a function of the moisture content in the desiccant wheel; for each angular position, the vapour pressure is averaged for the width of the wheel. C to D shows a heating zone at a constant adsorbed humidity, which is where the hot air meets the

wheel. From D to A there is an increase in partial vapour pressure caused by a transfer of moisture in the desiccant towards the air. There must be a corresponding cooling zone for a heating zone, and that is from A to B in the figure. This zone helps to decrease the water vapour pressure and the temperature at the surface of the desiccant, and it occurs at near-constant adsorbed moisture, as a result of the introduction of process air. Then, from B to C, the desiccant gradually loses its ability to adsorb water vapour in the air due to an increase in the vapour pressure. Over time, the performance of the desiccant material is influenced by the airstream contaminants and thermal cycling. Due to these reasons, desiccants are chosen on the ground of thermal durability and resistance to contamination effects.

Some contaminant materials can polymerise upon exposure to high reactivation heat, these over time would congest the desiccant's pores and potentially modify the surface characteristics. This may occur when organic vapours from indoor air are adsorbed by solid desiccants.

An example of alteration of chemical properties is when the presence of other chemicals affect liquid absorbents, such as triethylene glycol and lithium chloride. These chemicals can interfere with the reaction or modify the desiccant itself. Particle contamination in airstreams is inevitable as both thermal cycling high air velocities fragment a desiccant, regardless a desiccant is a solid or a liquid.

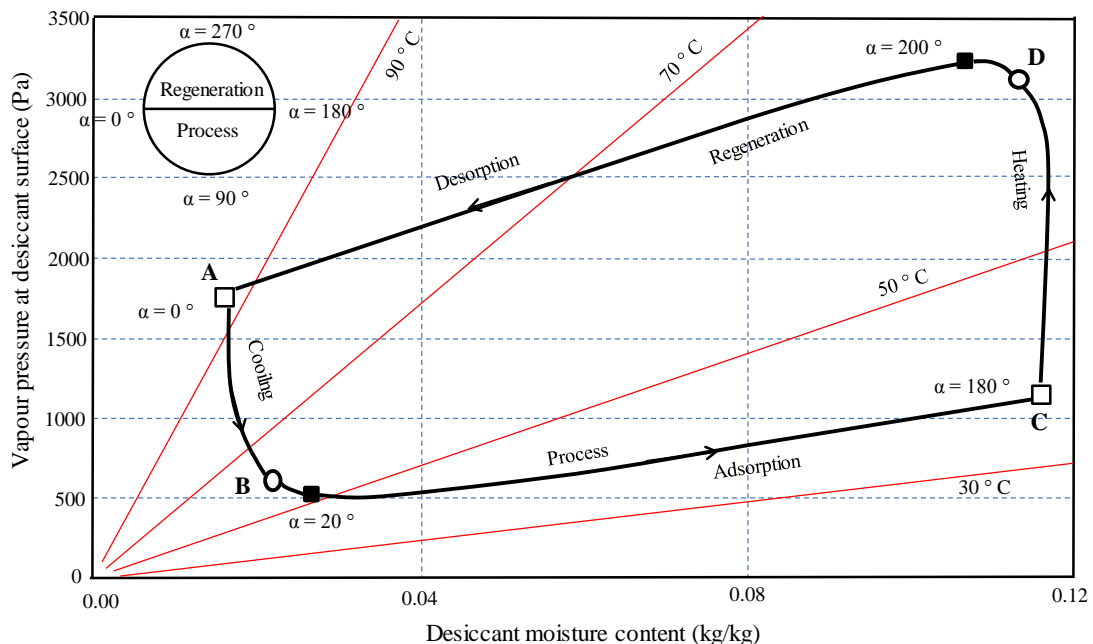


Fig 3.19 Vapour Pressure Evolution at Desiccant Surface [72]

3.2.3.1 Process inlet moisture

Changing the original content of moisture of the incoming air on the process side will have a predictable effect on the outlet moisture. If the moisture content entering is larger than expected, then the process air will be warmer as more moisture will have been removed and the air will leave the dehumidifier marginally more humid. This is when additional cooling might be needed if a constant temperature at the exit of the system is required.

3.2.3.2 Process inlet temperature

A desiccant's water content and temperature of the material dictates its surface vapour pressure, thus the temperature of the incoming air plays an important role in determining the performance of the desiccant. When other variables are kept constant, one can clearly see the relationship between inlet air temperature and performance: higher temperatures reduce performance and lower inlet temperatures enhance performance.

If higher temperatures cannot be exempted from the process, then firstly the highest temperature and the system's capacity at that temperature must be confirmed, then this information is used to select a desiccant that is less temperature sensitive. Alternatively, an extra cooling step could be added to achieve a desired outlet moisture. One reason why desiccant units are more often used than cooling-based dehumidifiers in cold-storage areas is because they do not require heating in the wintertime. Furthermore, performances are not worsened by having cooler process air conditions, so that is why desiccants are usually more desirable than cooling-based dehumidifiers.

3.2.3.3 Air velocity through the process side

Changing process air velocity, the slower the air moves through the desiccant bed, the drier the outlet moisture will be. Lowering process velocity allows more time for the air to contact the desiccant, so more moisture is removed. However, lower velocities mean larger equipment for a given airflow, so dehumidifiers are generally selected at the highest process air velocity that the application will allow.

The difference seems minor, and indeed, dehumidifiers are generally selected at the highest velocity that will accomplish the moisture removal because high velocities mean smaller, less costly equipment. The velocity of the process air plays an important role if the outlet moisture is very low, therefore an airflow monitoring device and control system might need to be implemented into the system to avoid unexpected changes in velocity. In contrary, the performance difference between low

and high velocities is small at high inlet moisture levels; therefore applying larger equipment may not be able to improve the performance significantly. More economical equipment that is smaller in size is sufficient; under the condition that high velocity is resulted from prioritising high inlet moisture levels over delivered air dew point.

3.2.3.4 Air temperature entering reactivation

The hotter the desiccant becomes by being heated by the air entering the reactivation side, the easier it releases moisture. This shows that the temperature of the reactivation air in a rotary dehumidifier influences the performance significantly. The moisture a desiccant can absorb as it rotates into the process airstream depends on how dry it can be made in reactivation. Therefore if the reactivation temperature needs to be used if a dry outlet conditions are desired.

Even with reactivation heat sources that have very low temperature, desiccant dehumidifiers can still make use of them. If necessary, hot water from cogeneration or steam condensate can be used to achieve the desired temperature, as this is more economical than energetically heating up the desiccant. But in order to do this, the size of the dehumidifier has to be bigger than the one that uses a high-temperature reactivation energy source, so that the same outlet condition is achieved in the process air. To maintain the equilibrium, larger reactivation airflows are required for the net energy added ($\dot{m} \times \Delta T$) to be kept the same. From ($\dot{m} \times \Delta T$), one knows that for an increase in temperature, there has to be a decrease in airflow.

The air is much cooler in autumn and winter than in the summer. For this reason, dehumidifiers are selected in the summer conditions, as the air entering the reactivation heats is already quite warm, even without it being heated. Lower entering-air temperature should be checked by the designer for the unit capacity, as the reactivation air temperature has a large influence on the performance of the dehumidifier. During some time in the other seasons other than the summer, it might be necessary to increase the capacity of the reactivation heat if the moisture load on the process side stays constant between summer and winter for a dehumidifier that dries make-up air downstream of a condensing cooling coil. In a storage application with recirculation, reactivation energy requirements are lower in a decrease in load during winter times, so heater made to adapt to the summer peaks would be sufficiently appropriate even when the reactivation air is much colder than in the summer.

3.2.3.5 Moisture of air entering reactivation

The desiccant is lithium chloride, which is not especially sensitive to moisture levels of the entering reactivation air. Having said that, some other desiccants such as molecular sieves are sensitive to reactivation inlet moisture. Air leakage between the moist air entering the reactivation side and the dry air exiting the process side is a mechanical concern of the unit. This leakage will raise the moisture level from reactive to process considerably. Rotary dehumidifiers must have good air seals between reactivation entering air and the dry process air leaving the unit. Any leakage at this point can raise the moisture level of the dry process air. For system designers, this suggests that when using rotary bed, multiple vertical bed or rotary honeycomb desiccant units:

The effect of any air leakage between the two sides needs to be consulted by the manufacturer in any given circumstances. Although there have been suggestions to avoid the leakage, in extremely dry outlet conditions, it is more sensible to mount the process air fan before the dehumidifier, rather than after it, or apply any mechanical changes. This ensures dry process air will be moved to reactivation if any leaks occur.

3.2.3.6 Velocity of air through reactivation

Heats, as well as moisture in a rotary dehumidifier, are both carried away by the reactivation air once it is being released by the desiccant. Higher velocity of this air is essential for heating than for carrying away moisture, and to keep the temperature and the reactivation airflow proportional to the moisture load absorbed by the desiccant, energy applied must be altered to keep the system in equilibrium: an increase in the moisture loading of the desiccant, the more energy is required to ensure a complete reactivation.

Since the net heat available to the desiccant is a function of the temperature difference between the desiccant and the air, multiplied by the airflow, having less reactivation air is comparable to having a lower reactivation temperature. Using this mathematical model, one can predict the heat applied to the desiccant: high reactivation airflows and high temperatures gives more heat to the desiccant, consequently its moisture absorption capacity increases, since the material would have been dried more thoroughly in the reactivation side. Energy could be carelessly wasted if the airflow is increased unnecessarily, whilst the temperature entering reactivation stays constant. Except the case where more moisture is needed to be removed from the desiccant – this means that the reactivation air would leave the dehumidifier at a higher temperature. Implications for the system designer include a

rough filtration of reactivation air. This is important as the built-up will eventually clog the filters, thus reducing airflow and degrade performance.

System control such as fixed or modulating airflow dampers for the reactivation air is also necessary to avoid unexpected high air velocities through the desiccant. There is a wide range in choice for operational conditions for reactivation, due to the various seasonal changes in the process air moisture load, even though there are limitations in the mechanical considerations for the selections of heaters and fans. Maximum load has to be the model but it must be realised that the fan and heat choices will be restricted, unless the owner is willing to raise the budget and install modulating controls.

3.2.3.7 Amount of desiccant presented to the airstream

The amount of moisture removed from the air depends on the quantity the desiccant that the air comes in contact with – the more desiccant in the dehumidifier, the drier the air becomes - along with other factors. Turning the wheel faster or making the wheel deep are ways to introduce the air to more desiccants in a rotary honeycomb dehumidifier, but both strategies increase the energy cost, albeit the effective moisture removal. The larger the depth of the wheel, the more resistance is posed to the air when it flows through the unit, as a larger surface area creates more air friction. The flow is turbulent in rotary tray, multiple vertical beds or packed towers, since the desiccant is granular, meaning that the resistance to airflow increases as the square of the velocity of air.

While the resistance still increases accordingly with the wheel depth, the effect in honeycomb dehumidifiers is less prominent than the others. Rather than a turbulent airflow, the air going through the straight passages is laminar. Other than the two strategies mention above, there are other methods to increase exposure to more desiccant for the air. For example, for solid desiccant units, the bed or wheel can be turned faster between the process side and the reactivation side. In liquid desiccant dehumidifiers, a desiccant solution can be pumped more quickly between the conditioner and the regenerator

The amount of heat in the desiccant when it returns from the reactivation side to the process side is proportional to the mass of the desiccant and the difference in temperature between the cooler process air and the warm desiccant. Consequently, more heat is moved over into the process side as more desiccant cycles between process and reactivation, and this means more energy is needed to cool the process air and the desiccant. Increasing the bed depth has a similar effect of transferring more

mass between the two sides, thus also requiring more energy for cooling.

3.2.4 Desiccant Applications

The applications of different categories of dehumidifiers will be discussed in this section, and how the diverse nature of them will lead to a creativity stimulation of system engineers. Working with such equipment is a rewarding task, and a good design is often profitable and could have a very positive impact.

The system of desiccant dehumidification is designed based on the application of product drying and all have different sizes and complexities. Of course, the cost of construction also varies. The main aim of the dehumidification system is to remove moisture from materials, and these materials include photographic film, plastic resins and pharmaceutical products etc. There is however, also another type of dehumidifier to remove moisture quickly from buildings that are damaged by water. These dehumidifiers are free-standing, and the process is similar to drying a product that cannot be damaged by the procedure, to which the damage is often caused by high air velocities or temperature. In this case, dry air simply becomes more economically advantageous.

It is important to understand the purpose of the project to achieve maximum efficiency. The preliminary preparations include establishing control levels and tolerances, calculating heat and moisture loads, selecting/locating controls and adjusting the components.

Prioritising the design concerns can double the processing speed of a production line, at the same time improving the quality of the product. This is achieved by using dehumidified air in many cases. A product drying dehumidification system with a good industrial building room control can pay back its construction and installation costs in months or even weeks.

3.2.4.1 Product Drying

It must be kept in mind that some products contain biologically substances, like enzymes, which can be easily destroyed by heat, and yeast will not be able to work if it is dried by very hot air. To that, conventional hot air drying cannot be used for such moisture removal. It is also sometimes too time-consuming to dry with just hot air.

The lower the temperature of the air, the more economical the dehumidifiers' performance is. It is often between to use dehumidified air rather than air that is simply heated when drying at temperature below 50°C. In a fluid bed, the drying

capacity is double when the dew point temperature of air is dropped from 18°C to -5 °C. This means that the size of the bed can be potentially cut in half, if the process does not need so much of the apparatus.

Over the years, companies have seen the improvement in quality in using dehumidifiers, without the sacrifice of the efficiency. The advantages of low-temperature drying meant an expansion in the range of product drying applications for dehumidifiers.

3.2.4.2 Condensation Prevention

Water vapour condenses on a surface when the surface's temperature is lower than the air, which contains moisture. This may cause a few problems which are often overseen by a good portion of our society, as people usually do not realise the intricate engineering in trying to resolve issues caused by condensation. This is surprisingly ubiquitous, for instance, glass doors of a refrigerator display will be covered in condensation in supermarkets, which would lead to a lost in revenue as the consumers are not able to see the products in the refrigerator.

A condensation control usually cannot fully prevent a problem, it can only make more economical opportunities. For example, in many production processes, chilled rollers that are blanketed by dry air are used to cool thin films or coatings. This technology allows much lower coolant temperatures to be used without the occurrence of condensation. Products can thus be cooled faster, and the whole process can potentially be completed in one machine alone.

3.2.4.3 Surface Preparation & Coating

When applying a coating to large and cool metal surfaces, such as chemical storage tanks and ship interiors, the coating manufacturers must ensure that the surface is clean and dry when the coating is applied, otherwise they cannot promise a lasting coating. Contractors nowadays use desiccant dehumidifiers to be able to blast and coat, even in adverse weather conditions, so the scheduling of a coating operation is much more flexible. It also means a cheaper cost and better coating for contractors.

3.2.4.4 Air Conditioning

Supermarkets are the first industry to realise the low capital cost and air conditioning applications of desiccant dehumidification. Currently, there are more than 500 supermarkets that integrated desiccant dehumidification into electrically driven refrigeration system in packaging [73-76]. The desiccant system operates as a

pre-conditioner for ventilation in these integrated designs, where it removes the latent load. Better humidity control, more efficient latent load removal and reduction of peak electric demands are all achieved by desiccant dehumidification, as this technology is extremely efficient in its energy usage. This greatly facilitates electric demands during peak periods where providing sufficient electricity is difficult. Applications of desiccant dehumidification are also seen in hotels, food restaurants, ice rinks and medical facilities etc.

3.3 Vortex Tube

The vortex tube (also called the Ranque–Hilsch vortex tube) is a mechanical device operating as a refrigerating machine without any moving parts, by separating a compressed gas stream into a low total temperature region and a high one. Such a separation of the flow into regions of low and high total temperature is referred to as the temperature (or energy) separation effect. The vortex tube was first discovered by Ranque [77] [78], a metallurgist and physicist who was granted a French patent for the device in 1932, and a United States patent in 1934. For many years, vortex tubes have been not considered to be used for its thermodynamically high inefficiency, it was only until a German engineer, Hilsch [79], who reported an improved efficiency of the vortex tube in his theoretical and experimental studies. Inlet pressure and geometrical parameters were systematically examined for their effects on the performance of the vortex tube, and Hilsch also gave a possible explanation to the process of how the energy separates.

It is very difficult to try to simulate the vortex flow in a vortex tube, since the phenomenon is compressible and complex. They are commonly used in low-temperature commercial applications, including cooling set solders, parts of machines, electric or electronic control cabinets, food, test-temperature sensors and to dehumidify gas samples etc. Other many practical applications are a liquefaction of natural gas, a quick start-up of steam power generation, temperature control of divers' air suppliers, hyperbaric chambers, cooling for nuclear reactors and separating particles in waste gas industry etc., many to be named. The vortex tube is known by many different names, commonly called Ranque vortex tube, Maxwell-Demon vortex tube, Hilsch vortex tube, Ranque-Hilsch tube or simply vortex tube.

There are two types of vortex tube in general, one being the standard type, which is the counter-flow vortex tube, and the other being the parallel/uni-flow vortex tube. They are respectively shown in Figure 3.20 and Figure 3.21.

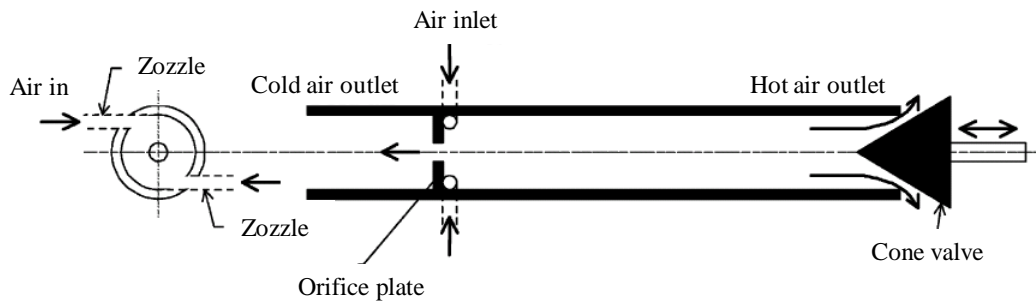


Fig 3.20 Ranque–Hilsch Standard Vortex Tube or Counter-flow Vortex Tube [80]

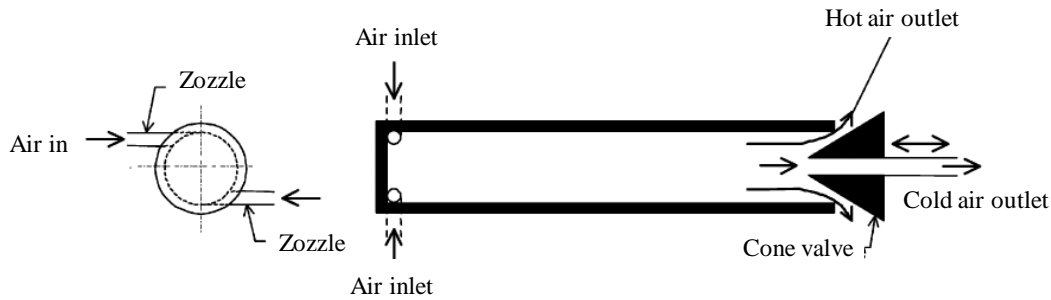


Fig 3.21 Ranque–Hilsch Vortex Tube Uni-flow or Parallel Flow Vortex Tube [80]

The components of a counter-flow vortex tube are as follow: a vortex/hot tube, an entrance block of nozzle connections with a central orifice and a valve that is cone-shaped. At a high velocity, a source of compressed gas with a high pressure enters the vortex tube tangentially, going through one or more inlet nozzles. A vortex that spins rapidly is then created inside the tube by the expanding air. Due to the small diameter of the orifice, the air flows through the tube, which has a larger diameter, rather than passing through the central orifice that is situated next to the nozzles. The length of the tube varies between 30 and 50 tube diameters, and depending on the system, the length has to be determined individually, as there is no general guideline for the optimal length. The pressure inside the tube drops sharply as the air expands down the tube, results in a pressure that is just slightly above atmospheric pressure. The air velocity at this point can reach near the speed of sound. This constrained vortex is kept close to the inner surface of the tube by the centrifugal motion.

The quantity of air that is made released at the other end of the tube varies between 30% and 70% of the total airflow, and this is regulated by a flow-control valve that is typically shaped as a cone. The remainder of the air is passed along the axis of the tube through the centre, acting as a counter-flowing stream. The air near the axis is cooled down in the tube as a vortex is established, while the air at the boundary increases in temperature, with respect to the inlet temperature, and this process is called the temperature separation effect, also known as the Ranque-Hilsch effect. Under this effect, the gas the escapes through the orifice is colder than the hot

gas flowing out in the other direction. This set up is remarkable in its high effectiveness and ease and simplicity of operation, without the need of heavy mechanics.

The uni-flow vortex tube consists of a vortex tube, an entrance block of inlet nozzles and a cone-shaped valve with a central orifice. On contrary to the counter-flow vortex tube, which is more popular, the cold air exit is found concentrically with the hot air annular exit. The mechanism of a uni-flow vortex tube is similar to that of counter-flow version. The temperatures at which a uni-flow vortex tube operates at ranges from 140°C to 160 °C, and generally speaking, –40 °C is the practical low-point temperature limit for cold airstream, and 190 °C for high temperature [81] [82]. Both higher and lower temperatures have been measured with research equipment [83]. Considering reliability, low equipment costs and compactness, vortex tube is an excellent choice over other drying mechanisms, if the operating efficiency is not of main concern. In cooling devices, such as for space units, mines, industrial process coolers, are typical applications of vortex tube.

This section defines some important terms in vortex tube work.

Equation 3.35 is an important parameter called the cold mass fraction, defined as cold air mass flow rate divided by inlet air mass flow rate. It serves the purpose of vortex tube performance indication and the separation of the temperature/energy inside the vortex tube. The cone valve located at the hot tube end controls the cold mass fraction.

$$\mu_c = \frac{M_c}{M_i} \quad (3.35)$$

where M_c is the mass flow rate of cold air and M_i is the mass flow rate of the entry air. The decrease in temperature, or the cold air temperature drop, is expressed as the difference in temperature between entry air temperature and cold air temperature:

$$\Delta T_c = T_i - T_c \quad (3.36)$$

in which T_i is the entry air temperature and T_c is the cold air temperature.

Cold orifice diameter ratio (β) is defined as the ratio of cold orifice diameter (d) to vortex tube diameter (D):

$$\beta = d/D \quad (3.37)$$

The principle of adiabatic expansion of ideal gas is applied in order to calculate

the cooling efficiency of the vortex tube. The expansion occurs in isentropic process as the air flows into the vortex tube. Equation 3.38 demonstrates the process:

$$\eta_{is} = \frac{T_i - T_c}{T_i \{1 - (P_a/P_i)^{(\gamma-1/\gamma)}\}} \quad (3.38)$$

where η_{is} , p_i , p_a and γ are the isentropic efficiency, inlet air pressure, atmosphere pressure and specific heat ratio, respectively.

The same principle of isentropic expansion of ideal gas is used to find the coefficient of performance (COP_{VT}). Equation 3.39 shows the calculation of the coefficient, and is defined as the ratio of cooling rate to energy used in cooling.

$$COP_{VT} = \frac{Q_c}{w} \quad (3.39)$$

in which Q_c is cooling rate per unit of air in the inlet vortex tube, and w is mechanical energy used in cooling per unit of air inlet.

The cause of vortex thermal separation is primarily the diffusion process of mean kinetic energy, past analysis showed. Low total and low static temperature are both found near the tube axis and lowers even more towards the standard vortex tube cold exit, or the orifice. The vortex tube generally serves two purposes, the first one is to obtain the maximum temperature separation, and the second one is to obtain the maximum efficiency. The same temperature separation can be achieved even by different parameters, on the basis that the same supply pressure is applied. The design parameter would consequently affect the vortex tube performance if it has an influence on the flow field.

Parameters to be considered when designing a standard vortex tube include the cold orifice diameter, the tube length, the tube diameter, the hot valve shape and the number, size and location of the inlet nozzles. The dimension of these parameters does not guarantee in a unique value of maximum temperature separation, but the knowledge on the temperature separation would indicate a more desirable design that is relative to the conditions applied. A vortex tube with a very small diameter would give significantly higher back pressures with fixed inlet conditions. Due to the lower specific air volume that is still high in density, the tangential velocities between the core and the periphery would not differ considerably, whereas the axial velocities remains high in the core region. Consequently, this results in low diffusion of kinetic energy that leads to low temperature separation. However, having evaluated the result of using a small diameter tube, the same would also be obtained with a very large tube diameter as well. Large diameters produce lower tangential velocities, in both the core

and the periphery region, leading to low diffusion of meant kinetic energy and low temperature separation.

Low temperature separation is also observed by using a very small cold orifice, which gives a higher back pressure in the vortex tube. Conversely, a very large cold orifice produces a weaker tangential velocities near the inlet region, due to its tendency to draw air from the inlet, resulting in low temperature separation. This phenomenon is also observed when using a very small inlet nozzle, because it leads to a significant pressure drop in the nozzle itself. Using a large inlet nozzle would not be appropriate either as it will not be able to establish a proper vortex flow. To yield a high tangential velocities near the orifice, the inlet nozzle should be located as close to the orifice as possible. Too far away will not generate a tangential velocity that is high enough to produce a high temperature separation.

3.3.1 Summary of Experimental Studies on Vortex Tube

Table 3.2 summarises the experimental data, where several operating conditions and tube dimensions are employed. Tube diameters range from 4.6mm to 800 mm. The table also presents the variations in the maximum temperature difference between the hot and cold streams and the inlet stream. Curley W and McGree Jr R [84] applied an inlet pressure of 2.0 atm (abs.), obtaining a temperature difference of about 8 °C, whereas Vennos [85] applied an inlet pressure of 5.8 atm (abs.) and obtained a temperature difference of 12 °C. Both used the same standard tube type. From this, one can conclude that it is not possible to predict the performance of a give tube, since the nature of the flow inside the tube is unknown, but if the mechanism of the energy separation is understood, the prediction may not be as far-fetched. Scheller and Brown [86] have reported that the static temperature exhibits a decrease in a radial-outwardly manner concerning the gradient of the radial static temperature, in contradiction to other researchers' findings of an increase in the static temperature.

Two categories in experimental investigations performed on vortex tubes are the parametric studies on the effects of the geometric variations of the vortex tube components, and the other is the studies of the mechanism of flow and energy separation inside the vortex tube. At various stations between the hot valve and the inlet nozzle, the pressure, temperature and velocity are measured. The latter category considers the operating condition and uses a uni-flow vortex tube. The cold orifice is blocked so all the air exits through the hot valve. There also exists two groups for the effective parameters on the temperature separation in the vortex tube, which are the thermo-physical and the geometrical parameters:

- 1) Increasing the inlet nozzles number results in a higher temperature separation
- 2) A small cold orifice ($d/D = 0.2, 0.3, \text{ and } 0.4$) produces a high back pressure, whereas a large cold orifice ($d/D = 0.6, 0.7, 0.8, \text{ and } 0.9$) permits high tangential velocities to enter the cold tube, causing lower energy/thermal separation in the vortex tube.
- 3) Optimum values for the cold orifice diameter (d/D), the angle of the control valve (φ), the length of the vortex tube (L/D), and the diameter of the inlet nozzle (δ/D) are found to be approximately $d/D \approx 0.5$, $\varphi \approx 50^\circ$, $L/D \approx 20$, and $\delta/D \approx 0.33$, respectively. These sets of standards are guidelines to a good vortex tube.
- 4) For optimal efficiency, the inlet gas pressure should be maintained at 2 bar. Higher temperature difference is given by helium in the inlet gas, in comparison to those containing methane, air and oxygen. The high inlet pressure is caused by high temperature separation.

Table 3.2 Summary of Experimental Studies on Vortex Tubes [80]

Year	Investigator	Dia., D (mm)	p_i , atm (abs.)	Total temperature (°C)		μ_c
				$T_h - T_i$	$T_c - T_i$	
1933	Ranque	12	7	38	-32	-
1947	Hilsch	4.6	11	140	-53	0.23
1950	Webster	8.7	-	-	-	-
1951	Scheper	38.1	2	3.9	-11.7	0.26
1956-7	Hartnett and Eckert	76.2	2.4	3.5	-40	-
1956	Martynovskii and Alekseev	4.4/28	12	-	-65	-
1957	Scheller and Brown	25.4	6.1	15.6	-23	9.506
1958	Otten	20	8	40	-50	0.43
1959	Lay	50.8	1,68	9.4	-15.5	0
1960	Suzuki	16	5	54	-30	1
1960	Takahama and Kawashima	52.8	-	-	-	-
1962	Sibulkin	44.5	-	-	-	-
1962	Reynolds	76.2	-	-	-	-
1962	Blatt and Trusch	38.1	4	-	-99	0
1965	Takahama	28/78	-	-	-	-
1966	Takahama and Soga	28/78	-	-	-	-
1968	Vennos	41.3	5.76	-1	-13	0.35
1969	Bruun	94	2	6	-20	0.23
1973	Soni	6.4/32	1.5/3	-	-	-
1982	Schlenz	50.8	3.36	-	-	-
1983	Stephan et al.	17.6	6	78	-38	0.3
1983	Amitani et al.	800	3.06	15	-19	0.4
1988	Negm et al.	11/20	6	30	-42	0.38
1994	Ahlborn et al.	18	4	40	-30	-
1996	Ahlborn et al.	25.4	2.7	30	-27	0.4
2001	Guillaume and Jolly III	9.5	6	-	-17.37	0.4
2003	Saidi and Valipour	9	3	-	-43	0.6
2004	Promvonge and Eiamsa-ard	16	3.5	-	33	0.33
2005	Promvonge and Eiamsa-ard	16	3.5	25	30	0.38
2005	Aljuwayhel et al.	19	3	1.2	-11	0.1

Note: p_i = inlet pressure before nozzle.

3.3.2 Vortex Tube for Drying in Further Research

3.3.2.1 Reversing System for Heat

When the Ranque Hilsch phenomenon is reversed, a substantial amount of heat rise that could reach up to 80°C in laboratory experiments is produced by a temperature separation. This heat rise can be applied to raise temperature for desiccant for regeneration. Furthermore, when the vortex tube system undergoes defrosting for performance maintenance, it is reversed temporarily to melt ice in the cooling-based system.

3.3.2.2 Condensation Water from Air

As the temperature drop occurs, a temperature below dew point can also be achieved, thus removing water from air. The inlet air is 30 °C at relative humidity 80%, and 10 °C with 0% humidity for exit conditions. A great advantage of this is that the water collected from air is considered clean. A closed system is represented in the following equation that determines the quantity of water generated, which is the relationship between volume and mass flow:

$$Q = q_{ma}(h_2 - h_1) + q_{ma}(w_1 - w_2)h_f \quad (3.40)$$

Q in equation 3.40 is the refrigeration capacity, determined by the vortex performance, w_1 is amount of water per kilogram of dry air (0.0216 kg water/kg dry air) and w_2 is (0.0098 kg water/kg dry air). Table 3.3 shows the water generation per hour, which is calculated by the mass balance and condensation of inlet air that is assumed to be complete. The inlet air temperature is 30°C and leaves at 10°C, with a relative humidity at 80% and a constant 0.6 cold fraction. The production may be significantly more substantial than predicted by the assumptions, as it largely depends on the environment of its installation.

Table 3.3 Water Produced from Variety of Vortex Tubes [87]

Vortex Tube Size (Siemens) Standard Liters Per Second (SLPS)	Predicted Water Produced (Liters/Hour)
1	0.03
2	0.05
4	0.11
5	0.15
7	0.2
12	0.34
17	0.47
24	0.68
35	1.01

3.3.2.3 Increased Vortex Efficiency

The overall efficiency of the system will be dramatically affected by an increase of the vortex's efficiency, as it is the least efficient measure of the process. Much research have gone into making it more effective as a refrigeration device. A great improvement in the overall performance in ice production is found in a paper written by Williams [87]. The cold production was increased by twisted airflow disturbance, and an increase in the refrigeration effect was observed by up to 25% in the rigid spiral.

3.3.2.4 Compressed Air

Compressed air is in itself a type of energy storage system. One of its benefits is that it could be used to power small electric generators to, for example, run lights. Another useful benefit is that it could help in fossil fuel combustions, since it is rich in oxygen. Care has to be taken when it is going to be used in this way, but when applied, it can minimise the consumption of fossil fuels.

3.3.2.5 Waste Usage

40% of the inlet mass flow generated by the vortex tube is a stream of waste air. Albeit being “waste” air, it could be used to power a thermoelectric Peltier cooler, run by a small electric generator. Temperatures can be maintained around 0 degree Celsius with these devices, and they are more efficiency at above freezing. Temperature of the mass flow is around the same as the ambient temperature, therefore it can be used as forced air convection over a heat sink, which helps to move heat from drying space.

3.4 Summary

The literature review presented in the preceding sections highlights the practicability of using heat pump, desiccant wheel and vortex tube in rapid/surface drying applications. Vortex tube requires compressed air and its energy efficiency is low for drying applications at industrial scale. Heat pump proves to be energy efficient when used in drying as it can use heat from the moisture laden exhaust air.

Rapid surface drying is a special case and the involved drying conditions are very different from general drying applications. The design and operating parametric conditions are further influenced by product type. Therefore requirements of different applications must be understood before using any drying system justified only on economic grounds. A detailed analysis is generally required to compare the cost-effectiveness of a hybrid system with a conventional drying system. These include maximum allowable moisture level in the drying space, ratio of the latent drying load to the total heating load, amount of dehumidification air required, design outlet dew point temperature, availability of exhaust hot air for regeneration heat, energy required, and the benefits of improved product quality.

Desiccant dehumidification systems are usually integrated with air conditioning or cooling systems in to control the humidity of the conditioned space and reduce system latent heat load. These systems are also used for condensation control at the surface in applications such as painting, coating and blasting. Usually the initial and operating costs are low for desiccant dehumidification systems. There are other

advantages such as environmental friendliness (no CFCs used), potential for energy saving due to the fact that waste heat and/or solar heat may be used for regeneration. Therefore the desiccant wheel may be considered an alternative way of drying by incorporation into a conventional heat pump drying system. The mechanism of removing water vapour from the air by desiccant material is analogous to water vapour condensing on an evaporator surface, and the latent heat corresponding to the extracted water liberated into the surrounding air is analogous to energy recovery through the condenser of a heat pump dryer. From the above analysis, the most suitable hybrid system is thus chosen to be composed of a heat pump and a desiccant wheel.

Chapter 4 Methodology

This chapter discusses the methodology to achieve the objectives of the project. The approach during the various stages of the project will be highlighted to establish a logical procedure of this research.

Mathematical models based on thermodynamics fundamentals were developed for predicting efficiencies of various components of the drying systems. These models were used in conjunction with Psychrometric Analysis software by ASHRAE to calculate the heat and moisture loads of the heat pump, desiccant wheel and the hybrid system. These calculations yield acceptable results for using in the design and estimating performance of dehumidification systems. The hybrid system was designed based on calculations for a range of operating conditions and manufactured. The performance and energy efficiency of the system was therefore experimentally tested.

4.1 Justification of Objectives

As discussed in previous Chapters the drying industry is facing challenges due to new regulatory environmental policies on combating global warming and increasing energy prices due to a shortage of supply of fossil fuels and other economical factors. To respond to these challenges, more energy efficient dehumidification technologies are needed.

There is a wide variety types of equipment available to choose from however it was observed from reviewing the literature that despite various types of dryers and drying techniques exist, the information and research on rapid surface drying techniques is not available in scientific literature. The producers of beverage are under increasing pressure from customers to produce high quality products at increasing speeds of production, since the quality and visual appearance of bottles and cans need to be maintained efficiently, to ensure maximum impact is achieved on supermarket shelves. Usually beverage and food products are dried at low dew point temperatures (DPT) of $-10 \sim -20^{\circ}\text{C}$ and low dry bulb temperatures (DBT) of $20 \sim 30^{\circ}\text{C}$ for product quality optimisation. Moisture can interfere with the drying processes, resulting in lower quality of product and reduced production speeds. For example in this case when the cold cider ($\approx 5^{\circ}\text{C}$) is bottled, it quickly causes condensation to form on the neck and body of the bottles' surface. This moisture must be completely removed prior to labelling, coating, date stamps or the label can easily slip out of alignment. Industry in general uses very inefficient methods such as blowing hot air or compressed air.

Therefore it is essential that the energy efficient and better performing methods/system are sought which dehumidifies air to overcome surface drying problems such as condensation removal, water removal and moisture removal. In order to compare the performance of existing systems for the considered drying application the design conditions were selected. There are three methods to remove moisture from air: by cooling it to condense the water vapour (e.g., cooling-based dehumidifier, heat pump dryer), by passing the air over a desiccant (e.g., desiccant dehumidifier, desiccant wheel), which pulls moisture from the air through differences in vapour pressures or by increasing its total pressure (e.g., compressed air, vortex tube), which also causes condensation.

Mathematical models were developed by software is Psychometric Analysis of ASHRAE to calculate the heat and moisture loads and performance of the heat pump, desiccant wheel and the hybrid system consisting of both the systems is compared. These calculations yield acceptable results for use in dehumidification drying industry work. Then the hybrid systems was designed and manufactured and its performance and energy efficiency of the system was experimentally tested.

The research also investigated the behaviour of heat pump dryer and desiccant wheel dehumidifier in order to propose improved correlations for design and construction of the process. As there are no standardized methods for determining the efficiency of dryers, correlations for determining efficiency are proposed.

4.2 Theoretical Design

Theoretical design of the proposed hybrid system consisting of a heat pump and desiccant wheel is presented in the context of an industrial case study where rapid drying of beverage bottles takes place. The bottles are dried on conveyer belt at the speed of about 2000 bottles per minute. The process air is taken from the surrounding inside the room, and blown into belt drying bottles. Inside air is at 22°C and 71% relative humidity (11.79 g/kg) in July. During summer the production rate is affected due to high moisture and drying at high speed becomes ineffective. Therefore it is essential to reduce humidity of the drying air, so the fast production rates of winter can be maintained year throughout. This particular case is chosen as it is the prime example of the aim of this research: to reduce the latent heat of the surface of the product by removing the surface moisture, without raising the temperature of either the surrounding or the product. Conventional drying method simply applies heat treatment to the product, consequently alters the quality and the properties of the product. The desiccant drying method of this research only removes the surface moisture and not more, which is a much desirable and energy efficient approach.

The drier the air, the faster the product will dry. The temperature of the product (in this case bottles) and the surrounding conditions establish the humidity level that affects the drying speed without over drying the product. Temperature and humidity must be controlled to meet the needs of products. Equipment energy consumption must modulate to follow the load, so the energy is not wasted. Humidity control is achieved through a set of modulating dampers which bypass air around the dehumidifier when the moisture load is low.

4.2.1 Design Conditions

Following Design data is needed for designing any drying system

- Required drying air temperature and relative humidity.
- Amount of material to be dried per batch.
- Initial and final moisture content of the product.
- Required drying time.

The internal condition is determined by the product or process, and there are as many possible specifications as there are different applications. The important point about the control level is that it must be specified in the absolute terms (grams per kilogram) before any calculations can proceed.

Figure 4.1 shows moisture load which depends on specific humidity difference between the two points, all other things being equal. The moisture load is proportional to the difference between the specific humidity inside room and the outside ambient environment. The larger the difference the greater the load.

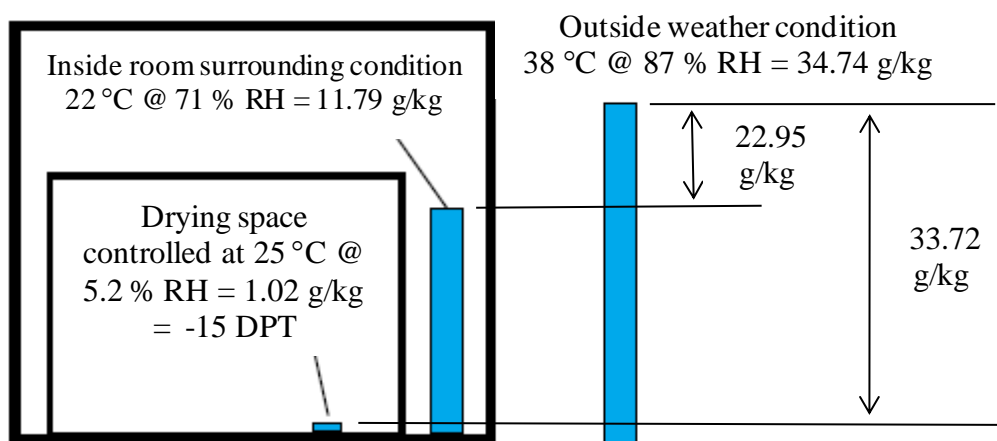


Fig 4.1 Moisture Loads Depend On Specific Humidity Difference [23]

Figure 4.2 (a) (b) and (c) show average temperature and relative humidity for London in the UK (Data from Would Weather & Climate Information). The weather conditions are assumed that in the summer time in July for area surrounding London. The drying room is controlled at 22°C and 5.2% RH (1.02 g/kg), each kilogram of infiltrating air brings 10.77 grams into the drying room. With this in mind, it becomes clear that the first and most important step in calculation of the moisture loads is to determine the temperature and moisture conditions inside and outside the controlled space. Inside room surrounding condition can be given:

- Dry bulb temperature : 22 °C
- Relative humidity : 71%
- Humidity ratio: 11.79 g/kg

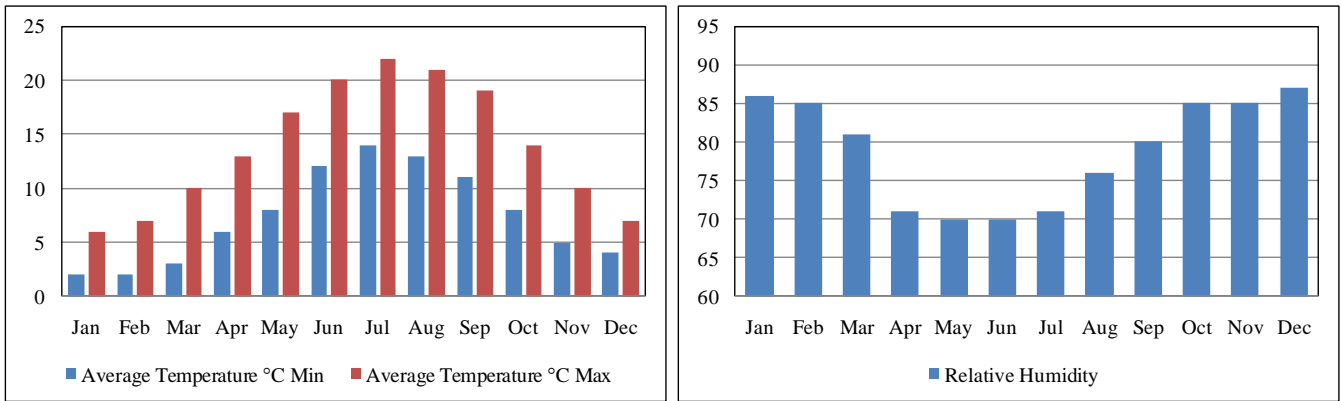
The minimum conditions of the delivered air for the heat pump and desiccant wheel are as follows:

Heat pump:

- Dry bulb temperature : 7 °C
- Dew point temperature : 5 °C
- Humidity ratio: 5.42 g/kg

London, United Kingdom						
Month	Average Temperature °C		Record Temperature °C		Relative Humidity	Average Rain fall (mm)
	Min	Max	Min	Max		
Jan	2	6	-10	14	86	54
Feb	2	7	-9	16	85	40
Mar	3	10	-8	21	81	37
Apr	6	13	-2	26	71	37
May	8	17	-1	30	70	46
Jun	12	20	5	33	70	45
Jul	14	22	7	34	71	57
Aug	13	21	6	38	76	59
Sep	11	19	3	30	80	49
Oct	8	14	-4	26	85	57
Nov	5	10	-5	19	85	64
Dec	4	7	-7	15	87	48

(a)



(b) (c)
 Fig 4.2 Average Temperature and Relative Humidity Data for the UK

Desiccant wheel:

- Dry bulb temperature : 25 °C
- Dew point temperature : -15 °C
- Humidity ratio: 1.02 g/kg

4.2.2 Control of the levels and tolerances

In this case drying room control levels are

- Dry bulb temperature : 25 °C ± 5 °C
- Dew point temperature : -15 °C ± 5 °C
- Humidity ratio: 1.02 g/kg (+0.59, -0.97 g/kg)
- 1300 kg/h airflow for every each drying cycle

4.2.3 Calculation of heat and moisture loads

If the air returns from the drying bottles directly, it will carry the moisture load from the bottles surface. If it comes back through the inside room, it will contain the moisture loads from the room as well as the inside room surrounding condition. These decisions have certainly simplified the moisture load calculation. The only heat and moisture loads on the system are contained in air taken from the inside room surrounding condition. There are no relevant outside weather loads or door openings. The system must simply take surrounding air and deliver it at 25 °C and 1.02 g/kg for the bottle coating and condensation prevention. The heat load consists of three factors:

- Total heat from the inside room surrounding air
- Sensible heat generated by product pieces cider in the drying bottles

- Latent heat in the inside room surrounding air, converted to sensible heat by the desiccant wheel

Therefore the total heating load and dehumidification rate are shown in below:

$$\text{Total heating load} = \frac{1300 \frac{kg}{h} * (52.08 - 20.67) \frac{kJ}{kg}}{3600 s} = 11.34 \frac{kJ}{s} (kW)$$

$$\text{Sensible heating load} = 6.6 \frac{kJ}{s} (kW)$$

$$\text{Latent heating load} = 5.84 \frac{kJ}{s} (kW)$$

$$\text{Evaporator dehumidification rate} = 1300 \frac{kg}{h} * (11.79 - 5.42) \frac{g}{kg} = 8.3 \frac{kg}{h}$$

$$\text{Desiccant wheel dehumidification rate} = 1300 \frac{kg}{h} * (5.42 - 1.02) \frac{g}{kg} = 5.7 \frac{kg}{h}$$

4.2.4 Input energy of hybrid system

Heat pump desiccant wheel dehumidification converts moisture to sensible heat, the dehumidifier must be selected and its performance determined before sizing the cooling system which follows the hybrid dryer. The size of the hybrid dryer depends on the temperature and moisture conditions of the entering air. Economically, it makes sense to pre-cool and dehumidify the inside surrounding air before it enters the desiccant unit. The power input to heat pump compressor and desiccant wheel efficient is shown in below:

$$\text{Power input to compressor} = \frac{11.34 \frac{kJ}{s}}{3.43} = 3.31 \frac{kJ}{s} (kW)$$

$$\text{Desiccant wheel efficient (\%)} = 1 - \frac{(27.72 - 20.67)}{20.67} * 100\% = 65.89\%$$

The total system airflow is large in surface drying applications because of the need to maintain high velocity across all surfaces of the product. But the dryer does not need to handle all that air. Thus the evaporator fan can be small in comparison to the airflow required to create high velocity within the drying chamber which can be achieved by adding large circulation blower in the chamber. In the present example the airflow, temperature and moisture can stay constant because product batches are identical in size, shape, type of coating and degree of dryness required.

4.3 Summary

In this chapter the problem and design considerations are outlined. The heat pump in tandem with the desiccant wheel is an alternative method for rapid drying products.

In order to achieve best performance of the hybrid systems, variables that affect the particular application need to be thoroughly understood, which include air temperature, air moisture, drying air velocity and moisture load through the system, quantity of desiccant introduced to the process and reactivation airstreams, the reactivation air temperature and the adsorption properties of the desiccant. These variables have a great influence on the energy use and the effectiveness of the hybrid system, and they vary accordingly to the weather and the moisture load in air. Understanding what the effects of these variations have on the system is useful to the system's designer.

Chapter 5 Analysis of Hybrid Systems

In this chapter mathematical models base on [88-94] for heat and mass balance of both refrigerant, desiccant and air circuits in all components of the system are developed. The developed mathematical model together with Psychrometric Analysis software is used to calculate the heat and moisture loads of the heat pump, desiccant wheel and the hybrid system. The software uses algorithms that are generally accepted by the HVAC (heating, ventilation, air conditioning) and drying industry for heat and moisture load in various components of the system. Complete state point, process report and charts produced by this software. The models are used for the design of different components of hybrid dryer operating under constant drying rate condition and for the analysis of the complete hybrid system.

In order to compute the energy input, work done and COP of a process, we need the following assumptions and mathematical equations to calculate the change in states.

5.1 Assumptions

Following assumptions are made in order to simplify the mathematical model:

- 1) Temperature difference between the heat exchanger surface and the refrigerant is 5°C
- 2) The bypass factor for evaporator and condenser coil is 0.2
- 3) 90% fin efficiency
- 4) 95% mechanical efficiency and 85% motor efficiency of compressor are assumed
- 5) 65% desiccant efficiency

To size the system the influence of operating parameters on the design is estimated. In particular, the effect of following factors influences the design:

- Necessary relative humidity and drying air temperature
- Drying time needed
- Quantity of material to be dried per batch
- Product's initial and final moisture content

5.1.1 Heat Pump

Following calculation steps are necessary for heat pump:

- Step 1: Calculate the required temperatures for the product

- Step 2: Calculate the specific heat, specific volume, enthalpy, wet-bulb temperature and humidity ratio of drying air using the psychrometric charts. Saturation vapour pressure at wet-bulb temperature, which is assumed to be less than the dry-bulb temperature, is calculated. This saturation temperature that corresponds to the pressure can be obtained by equating $p_s = p_{sw}$. The temperature must be assumed to be the wet-bulb temperature even when this temperature is not the same. Using a successive iteration method, the wet-bulb temperature is calculated.
- Step 3: Calculated the required heat for mass, drying and volumetric flow rate of the drying air.

$$Q_{dr} = q_{mwd} \times h_{fg} \quad (5.1)$$

$$q_{ma} = \frac{Q_{dr}}{c_{pam}(t_d - t_w)\theta_d} \quad (5.2)$$

$$V_a = v_a \times m_a \quad (5.3)$$

- Step 4: Calculate the humidity ratio and the temperature of the air at dryer outlet.
- Step 5: Determine the dew point temperature and the dryer exhaust air's partial water vapour pressure. The former is taken to be less than the dry-bulb temperature of the exhaust air, and the latter is calculated from W_{do} . p_d is the saturated vapour pressure at dew point temperature, and the corresponding saturation temperature is obtained from the assumed dew point temperature. When two consecutive readings are closing to be the same in an iteration process, a value of the dew point temperature can then be taken.
- Step 6: Calculate the saturated vapour pressure of air in close contact with evaporator surface, the humidity ratio and the temperature of the evaporator surface from the bypass factor.

$$W_{es} = \frac{W_{di} - BF \times W_{do}}{1 - BF} \quad (5.4)$$

the temperature of the evaporator surface is assumed to have a lower value than the dew point temperature of the exhaust air from the dryer. Successive iteration method is used again here to find out the corrected value.

- Step 7: Calculated the air temperature at the evaporator outlet and the refrigerant temperature inside the evaporator.

$$T_{re} = t_{es} - 5 \quad (5.5)$$

$$t_{eo} = t_{es} + BF(t_{do} - t_{es}) \quad (5.6)$$

- Step 8: Calculate the refrigerant temperature and also the temperature of the condenser surface inside the condenser.

$$t_{cs} = \frac{t_{di} - BF \times t_{eo}}{1 - BF} \quad (5.7)$$

$$T_{rc} = t_{cs} + 5 \quad (5.8)$$

- Step 9: Calculate the enthalpy of the refrigerant, the delivery pressure and the saturated suction that correspond to the refrigerant temperature inside the condenser and the evaporator.
- Step 10: Calculate the outlet of evaporator and condenser and the enthalpy of the air at the dryer with Eq. 5.9:

$$h = c_{pa}t + W(h_{fg} + c_{pvt}) \quad (5.9)$$

- Step 11: Calculate the cooling load on the evaporator and the refrigerant flow rate requirement:

$$\text{Cooling load} = q_{ma}(h_{do} - h_{eo}) \quad (5.10)$$

$$q_{mr} = \text{Cooling load}/(Vh) \quad (5.11)$$

- Step 12: Calculate the required power of the compressor and the piston displacement with Eq. 5.12:

$$V_p = q_{mr} \times \frac{v_{r1}}{\eta_v} \quad (5.12)$$

- Step 13: Calculate the heating load on the internal condenser and the flow rate of the refrigerant in both the internal and the external condenser.

$$\text{Heating load} = q_{ma}(h_{di} - h_{eo}) \quad (5.13)$$

$$q_{mr,intc} = \text{Heating load}/(Vh) \quad (5.14)$$

$$q_{mr,extc} = q_{mr} - q_{mr,intc} \quad (5.15)$$

- Step 14: Calculation of SMER, COP, and dryer efficiency.

$$SMER = \frac{q_{mwd}}{P_{comp} + P_{fan}} \quad (5.16)$$

$$COP = \text{Heating load} / E_{co} \quad (5.17)$$

$$\eta_d = \frac{t_{di} - t_{do}}{t_{di} - t_w} \quad (5.18)$$

- Step 15: Calculated the heat transfer coefficient of the air-side and the refrigerant side, the LMTD values and the overall heat transfer coefficient for both the evaporator and the condenser. Determine the evaporator and the condenser requirement for the surface area on the outside of the finned tube.
- Step 16: Calculate the required capillary length for the desired pressure drop. Determine the total pressure and power of the fan.
- Step 17: Finally, based on manufacturer's handbook, select the appropriate compressor, evaporator, condenser, capillary tube and fan to match the calculated values.

The above mathematical equations of different components of a heat pump assisted dryer are essential for design calculations, simulation of results, and performance evaluation of the dryer.

5.1.2 Desiccant Wheel

Desiccant drying systems have been introduced as attractive alternatives to conventional vapour compression systems due to their advantages of utilizing low temperature energy and of providing an environmentally-conscious operation [78-82].

A system (Fig 5.1) operating on the drying mode was constructed for this purpose. In the process side, desiccant wheel adsorbs moisture from the space air resulting in dehumidification and heating of ambient air. Evaporator reduces the temperature of process air. The cool and dry process air leaving evaporator is passed through a desiccant wheel, which adds moisture to the air, reducing its temperature further to provide design state for the conditioned air. Hot air from the conditioned space passes through condenser and desiccant wheel in its return path resulting in the regeneration side of desiccant wheel operation. The temperature of the air from the ambient air is increased through condenser and desiccant wheel together with heating and humidification. The heat transfer in desiccant wheel, which operates the outcome

of condenser, produces sensible hot air. Hot and dry air is used for the regeneration of rotary desiccant wheel with further moisture absorption, i.e. humidification resulting in wet and cooled air for the termination of the operation cycle.

A mathematical model is developed which can be used to analyse the desiccant wheel performance for different operating parameters. The model can be better understood by referring to the schematic setup is shown in Figure 5.1.

Desiccant wheel efficiency and its operational performance is determined by the combination of its mass and heat transfer. The effectiveness of the air stream dehumidification system are influenced by these two processes, in addition, they also give different definitions of the efficiency. First one is the thermal effectiveness, given by Eq. 5.19:

$$\varepsilon_{DW,1} = \frac{T_3 - T_2}{T_5 - T_2} \quad (5.19)$$

The inlet process air, T_2 , outlet process air T_3 and the inlet regeneration air temperature T_5 are presented in Figures 5.1, with the desiccant wheel performance being illustrated in terms of calorific. The definition given by Eq. 5.19 is in fact derived from the assumption that a desiccant wheel is a heat exchanger, and the relation is deduced from the effectiveness of a heat exchanger. Eq. 5.20 gives the regeneration effectiveness of the desiccant wheel:

$$\varepsilon_{DW,2} = \frac{(\omega_2 - \omega_3)h_{fg}}{h_5 - h_4} \quad (5.20)$$

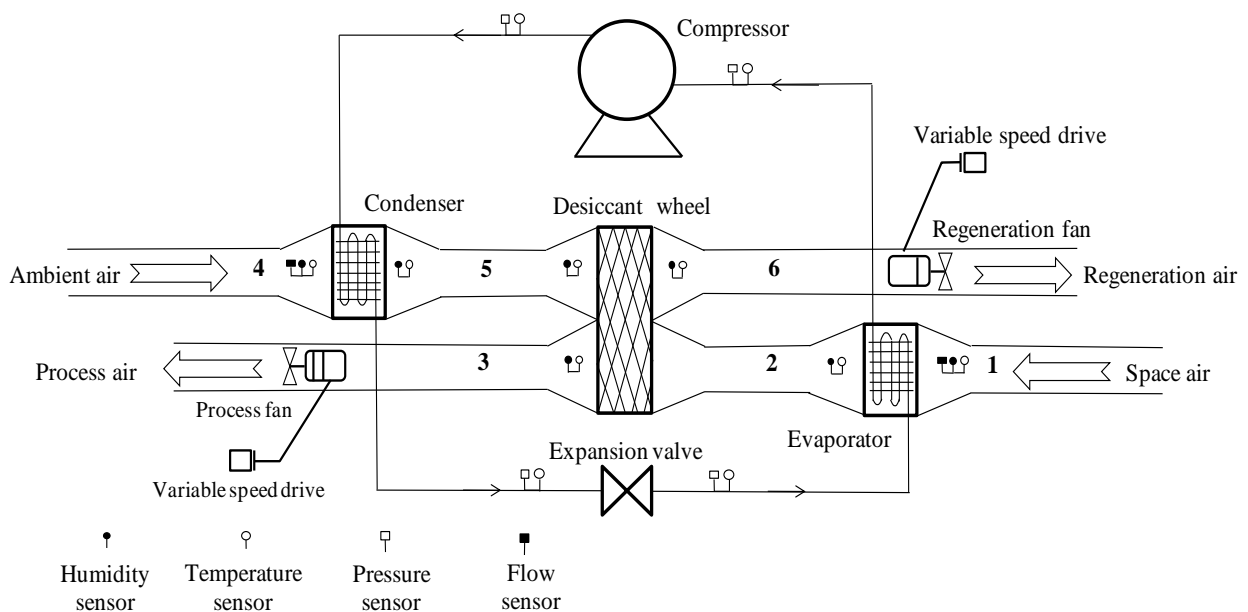


Fig 5.1 A Schematic Figure of Desiccant Wheel Experimental Setup

w is the specific humidity and h is the vaporisation latent heat of water. Although Eq. 5.20 can be used to calculate the regeneration heat consumption of evaporation of the adsorbed water, it would not yield a useful outcome when the mass flow rate of process air and regeneration are not equal, since the equation is dimensionless. An alternative to Eq.5.20 is thus proposed to amend this issue. Eq.5.21 includes more parameters to account for a more realistic condition.

$$\varepsilon_{DW,3} = \frac{\dot{q}_{m \text{ Process}}(w_2 - w_3)h_{fg}}{\dot{q}_{m \text{ Regeneration}}(h_5 - h_4)} = \frac{\dot{Q}_{\text{Latent}}}{\dot{Q}_{\text{Regeneration}}} \quad (5.21)$$

where \dot{Q}_{latent} is the vaporisation latent heat rate of adsorbed water and $\dot{Q}_{\text{Regeneration}}$ is the input heat of regeneration rate. Eq.5.22 takes into consideration the dehumidification process / mass transfer of the desiccant wheel for its effectiveness:

$$\varepsilon_{DW,4} = \frac{\omega_2 - \omega_3}{\omega_2 - \omega_{3,ideal}} \quad (5.22)$$

$w_{2,ideal}$ is the ideal outlet of air stream of desiccant wheel. An ideal desiccant wheel has a value of zero for $w_{2,ideal}$, which means that the air is completely dehumidified. Eq.5.22 is the most useful in desiccant wheel optimisation and is generally considered the reference function.

The wheel material, construction, wheel speed, temperature and humidity of inlet air and the regeneration air temperature determine the difference between the enthalpy of inlet and outlet air. Eq. 5.23 is a new expression that considers the importance of the enthalpy deviation, and is called the adiabatic desiccant wheel effectiveness:

$$\varepsilon_{DW,5} = 1 - \frac{(h_3 - h_2)}{h_2} = \frac{2h_2 - h_3}{h_2} \quad (5.23)$$

The ideal state of the desiccant is achieved by a completely adiabatic operation according to Eq.5.23. Only in this condition 100% efficiency would be reached. This concept according to psychrometric chart is shown in Figure 5.2.

sensible heat, a slight increase in the enthalpy takes places, and this air is hot at state B, thus needs to be cooled down before being used to cool the conditioned area.

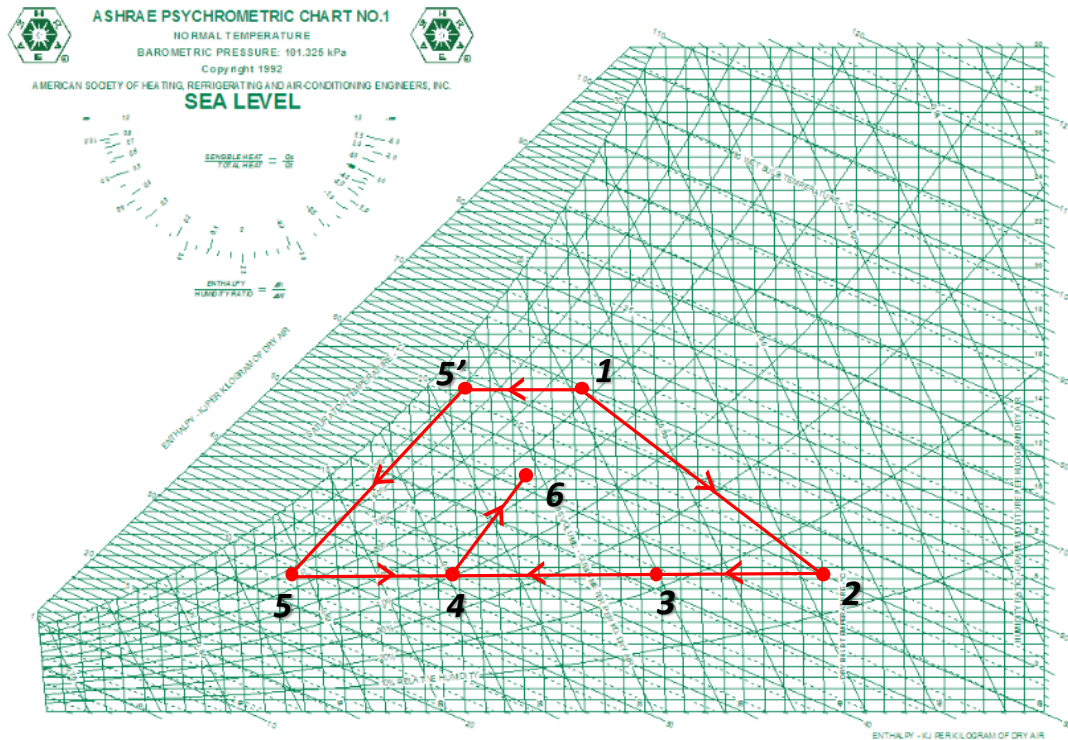


Fig 5.3 Desiccant Dehumidification Air Process

5.2.2 Cooling process

2-3: Heat loss or post-cooling – at the rotary heat wheel enters the dehumidified outdoor air, for which heat is exchanged with the exhaust air stream from the conditioned space. The hot and dry outdoor air is cooled down in this process, whereas the cold exhaust air is pre-heated for desiccant wheel reactivation.

3-4: Supplemental cooling – further cooling with a conventional direct-expansion vapour compression cooling system is needed for the air leaving the rotary heat wheel before it is allowed to enter the conditioned space.

4-6: Space cooling load – at state E, the exhaust air leaves the conditioned space.

5.2.3 Sensible cooling process

1: Intake – at point A on the psychrometric chart, hot and humid outdoor air enters the evaporator coil of a conventional vapour compression system.

1-5': Sensible cooling – at a point where the hot and humid outdoor air is sufficiently cooled and reaches saturation, it can then be used in the conditioned space, but as it is saturated with moisture, it cannot be circulated. In order to remove the

moisture in the air, it must be cooled to below its dew-point temperature.

5.2.4 Dehumidification and reheat process

5'-5: Dehumidification – the saturated air stream is continuously being cooled by the evaporator, which also condenses the moisture at the same time to reduce the humidity and the dry-bulb. When the requirement for humidity is low, meaning less than 5.82g/kg of dry air, it is essential to cool the air to less than 6.1°C to condense enough moisture.

5-4: Reheat – the cold and dry air stream is either mixed with hotter air, or alternatively, reheated to the circulation temperature that is desired (state 4).

4-6: Cooling load – at state E, the exhaust air exits the conditioned space.

5.2.5 Regeneration process

6-7: Heat recovery – Part of the heat lost in step 2-3 is recovered in this process as the exhaust air stream enters the rotary heat wheel. Heat is exchanged between the air stream and the hot and dry air that leaves the desiccant wheel shown in Figure 5.4.

7-8: Heat addition – further heating of the hot exhaust air is carried out for raising the vapour pressure to a degree that is high enough at the desiccant.

8-9: Reactivation – the hot exhaust air stream dries, and then it reactivates the saturated desiccant.

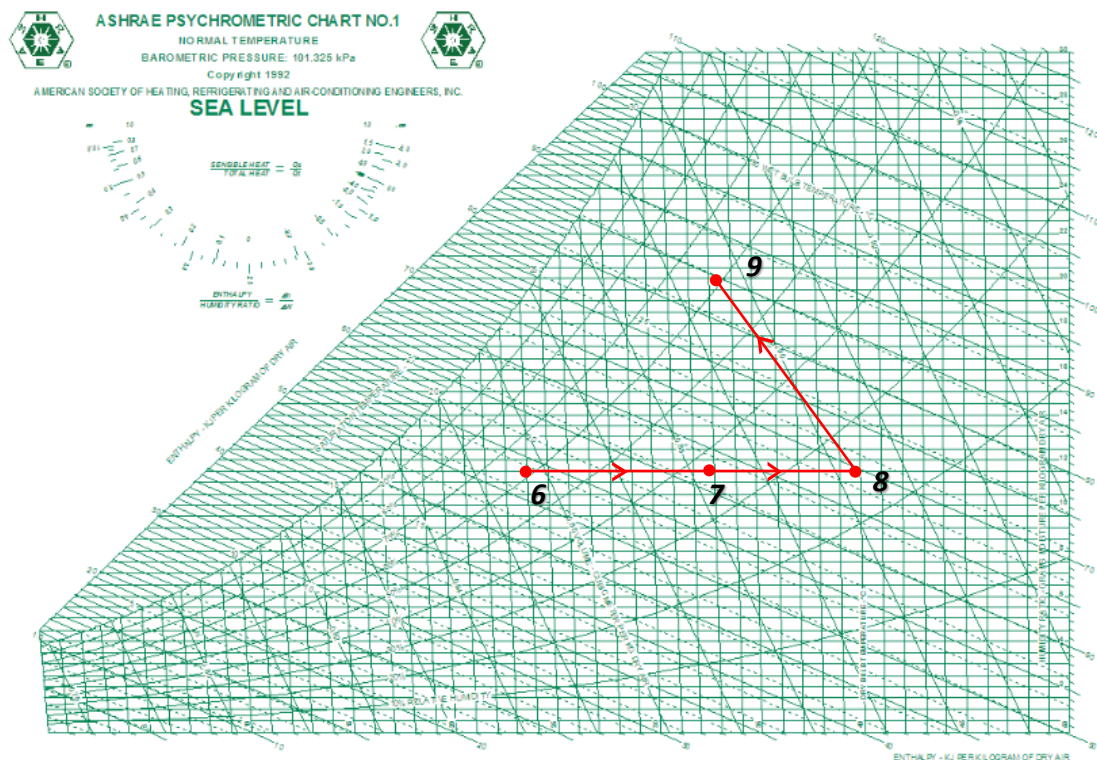


Fig 5.4 Desiccant Reactivation Air Process

The differences of the two systems in which they conduct dehumidification are shown in the psychrometric processes. Step 5-4 is the part of the process which exhibits the amount of energy saved by the system, of which depends mainly on the hybrid system's ability to shift part of the cooling load to a low-grade thermal source, at the same time eliminating reheat. The increased air pressure drop through the desiccant and sensible wheel leads to a manual increase in the fan power. The hybrid system and the desiccant based systems all provide energy conservation, as well as other benefit.

1. Due to part of the cooling load being shifted to the desiccant system, the size of the conventional system in the desiccant systems are often able to be reduced, which saves energy and also decreases the demand of electricity, sometimes even reducing the initial capital investment.
2. It is possible to replace some vapour compression system with cheaper evaporative cooling systems that are either direct or indirect.
3. The control of temperature in conventional cooling systems is done directly, and the humidity is left to fluctuate, whereas the temperature and humidity in a hybrid system are both independently controlled.
4. The conventional cooling systems can dehumidify the air to a dew-point temperature that is above 0°C, and desiccant-based systems can achieve a reduction in moisture much below 0°C.
5. The precise humidity control of the desiccant-based systems is able to improve indoor air quality. For desiccant-based system, the problem of microbial growth in the ducts and condensate drain pans that occurs in humid climates is usually not of concern, because there exists an insignificant amount of water on the post-desiccant cooling coil and the pans and ducts that follow.
6. Hybrid systems can provide several things all year round, for example, the boiler that is used for reactivation can be used for comfort heating, and the heat wheel can be used to recover energy.
7. The desiccant systems can be used to compensate for the replacement of CFC-11, CFC-12, and CFC-22 refrigerants with HCFC-123 and HCFC-134a. The new refrigerants provide only 90% of the existing capacity.

5.2.6 Energy Savings Mechanism in Hybrid System

Desiccant wheel heat pump drying system uses vapour compression refrigeration especially under conditions involving high latent loads. It can be used either in a stand-alone system or coupled judiciously with a vapour compression

system to achieve high performance over a wide range of operating conditions. The potential of energy savings in hybrid system is due to making use of exhaust heat from condenser. In this section, the analyses of a detailed study of desiccant wheel heat pump hybrid drying systems are presented.

Desiccant based hybrid dehumidification system is a process that combines a vapour compression machine and a desiccant system, which is illustrated in Figure 5.5. Moisture is removed by the desiccant, and the sensible heat load is shared between the vapour compression system and the heat exchanger.

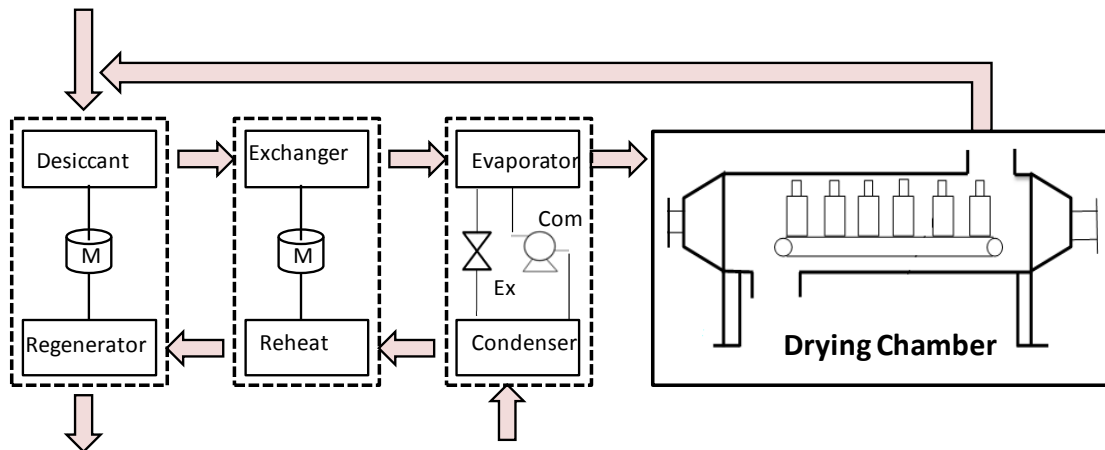


Fig 5.5 Hybrid Desiccant Drying System

Both the sensible load from the heat transfer into space and the latent load from moisture generation in space need to be met in all dehumidification systems. To meet these loads, cooling-based dehumidifier systems use vapour compression refrigeration, for example, the air needs to be dehumidified by cooling it below its dew point to meet the latent load, and the evaporator temperature becomes lower when the latent heat load becomes higher. The evaporator temperature must remain above 0°C, so constant heating is necessary in cooling-based dehumidifier systems, which also means low energy efficiency and large mass flow rates due to the limited moisture removal per unit mass of air.

A material that has a high affinity for water is used in simple desiccant systems to deal with latent heat loads. In such a system, process air is made to come in contact with the material for moisture absorption and adsorption. Consequently, the heat that is released in both processes heats up the air. The heat exchanger and the evaporative cooler cool the air afterwards. Simple desiccant systems are well suited to meet latent heat loads.

Figure 5.6 is a psychrometric chart that plots together the characteristics of all the mentioned systems. Air is directly cooled and dehumidified from state 1 to state 5 in the cooling-based dehumidifier system. This is achieved by passing the air over a coil that contains circulating refrigerant. State 5 is not found to be lying on the room sensible heat factor line in high latent load applications, therefore reheating the cold air from state 5 to 4 would have to be done to meet the load requirements.

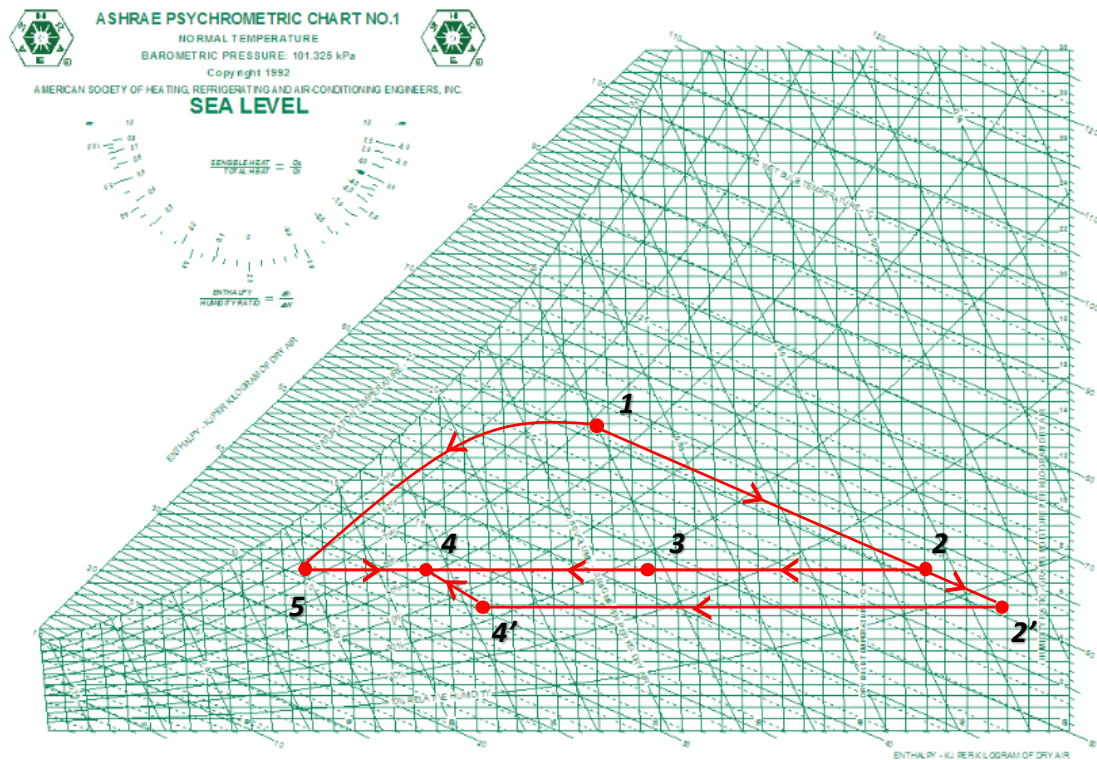


Fig 5.6 Hybrid Desiccant Dehumidification on Psychrometric Chart

The mixed air at state 1 is dehumidified to very low moisture content, 2', in a simple desiccant system. Air that is heated in the process is sent to state 4' to be cooled by the method of indirect evaporative cooling. At state 4 this air is further cooled with direct evaporative cooling. The psychrometric chart shows detailed calculations for deciding upon the most energy- and cost-effective system, which depends on the performance of the dehumidifier and the coolers etc.

Figures (5.7-5.9) are hybrid system configurations for drying, they are Air Mixing Cycle, Air Recirculation Cycle and Air Exchange Cycle, and the figures compare their performance with the conventional drying system.

Figure 5.7 shows that only the outside air at state 1 passes through the dehumidifier in the Air Mixing Cycle. At state 2, the dehumidified air is cooled by indirect evaporative cooling before it is mixed with the recirculated room air at state.

Further sensible cooling of the mixed air at state 4 takes places in a chilled water coil at states 4-5 until the RSHF line is reached. The heat of the waste condenser is used to preheat the air from states 1-7, and this step regenerates and recycles the desiccant. Further heating after state 7 is supplied by other supplementary heat sources. The air that passed through the desiccant now carries moisture and is cooled, at state 9 it is expelled out of the system.

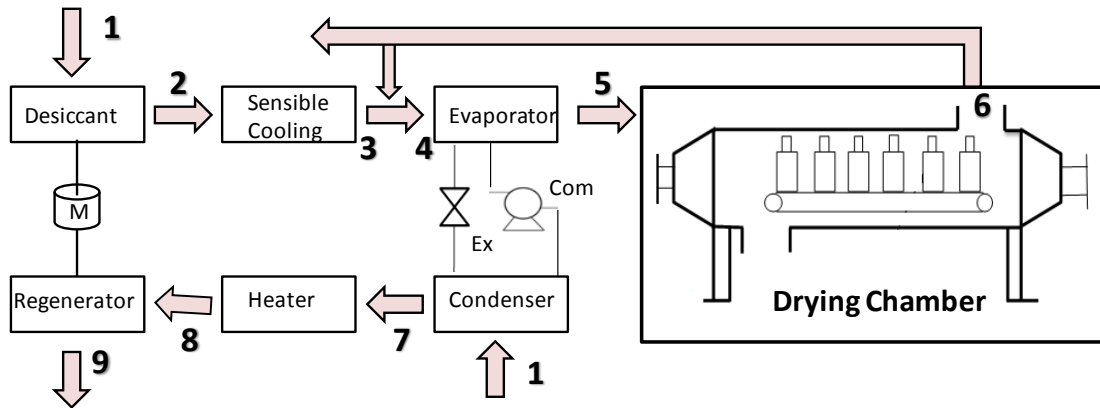


Fig 5.7 (a) Schematic Diagram and Plot of Air Mixing Cycle

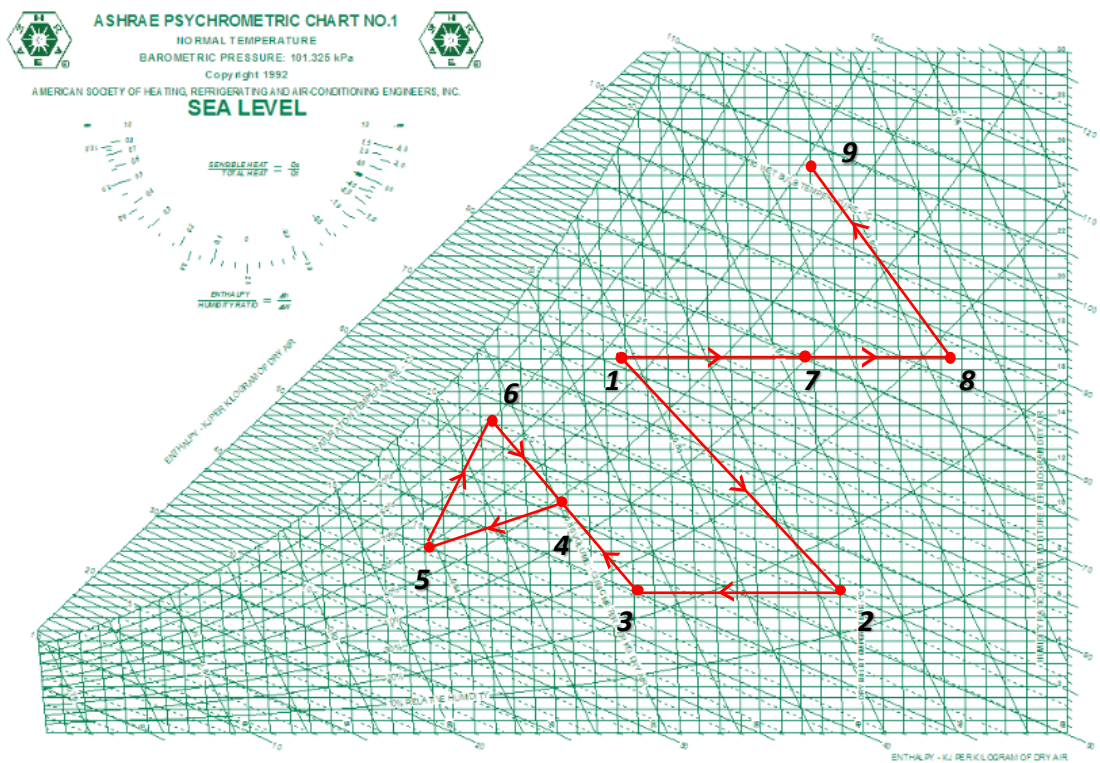


Fig 5.7 (b) Schematic Diagram and Plot of Air Mixing Cycle

Figure 5.8 shows that the Air Recirculation Cycle is different from the Air Mixing Cycle, for its state 2 of recirculated air and the outside air is passed through the dehumidifier. Larger volumes of air thus results, therefore the size of the

dehumidifier is larger for a bigger capacity to handle the amount of air. However, when comparing figures 5.7 and 5.8, it reveals that the total amount of moisture that needs to be removed per kilogram of air is significantly smaller, so the regeneration temperature required is lower than the temperature in the Air Mixing Cycle.

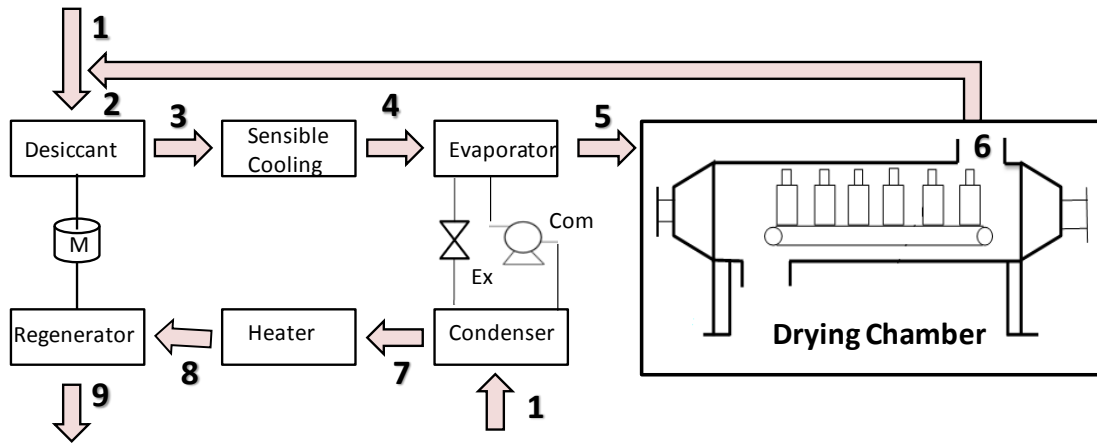


Fig 5.8 (a) Schematic Diagram and Plot of Air Recirculation Cycle

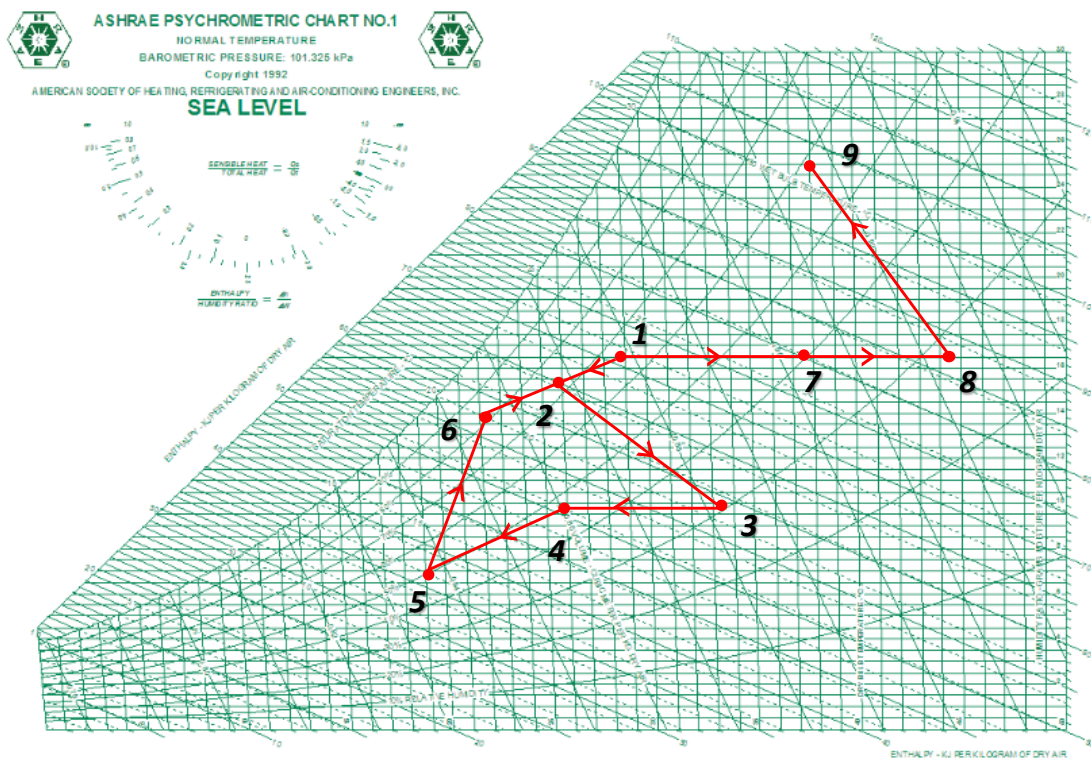


Fig 5.8 (b) Schematic Diagram and Plot of Air Recirculation Cycle

Figure 5.9 shows the Air Exchange Cycle, which is essentially a variant of the drying cycle. There is no indirect evaporative cooler used to cool the hot dehumidified air in the heat exchanger, instead, ambient air is used to help. In addition, the condenser heat is not reused anywhere, but the ambient air used is heated again to the regeneration temperature in the auxiliary heater.

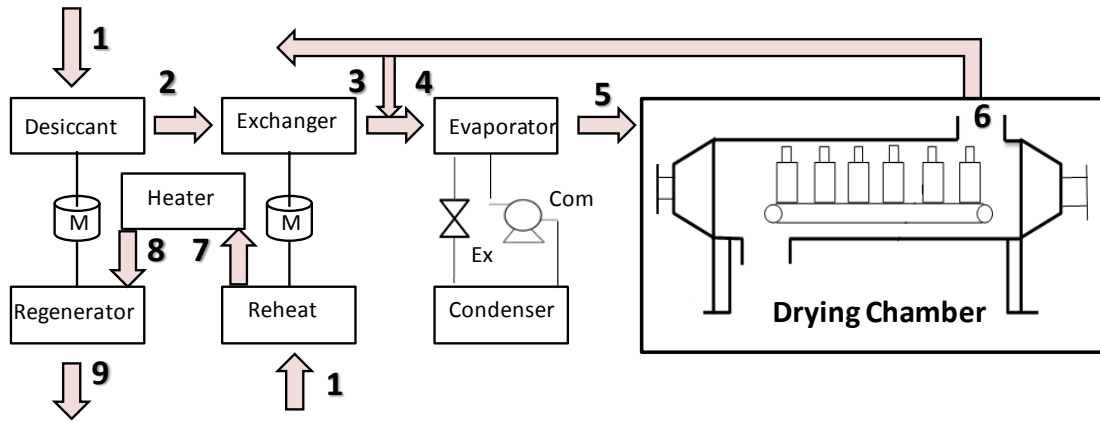


Fig 5.9 (a) Schematic Diagram and Plot of Air Exchange Cycle

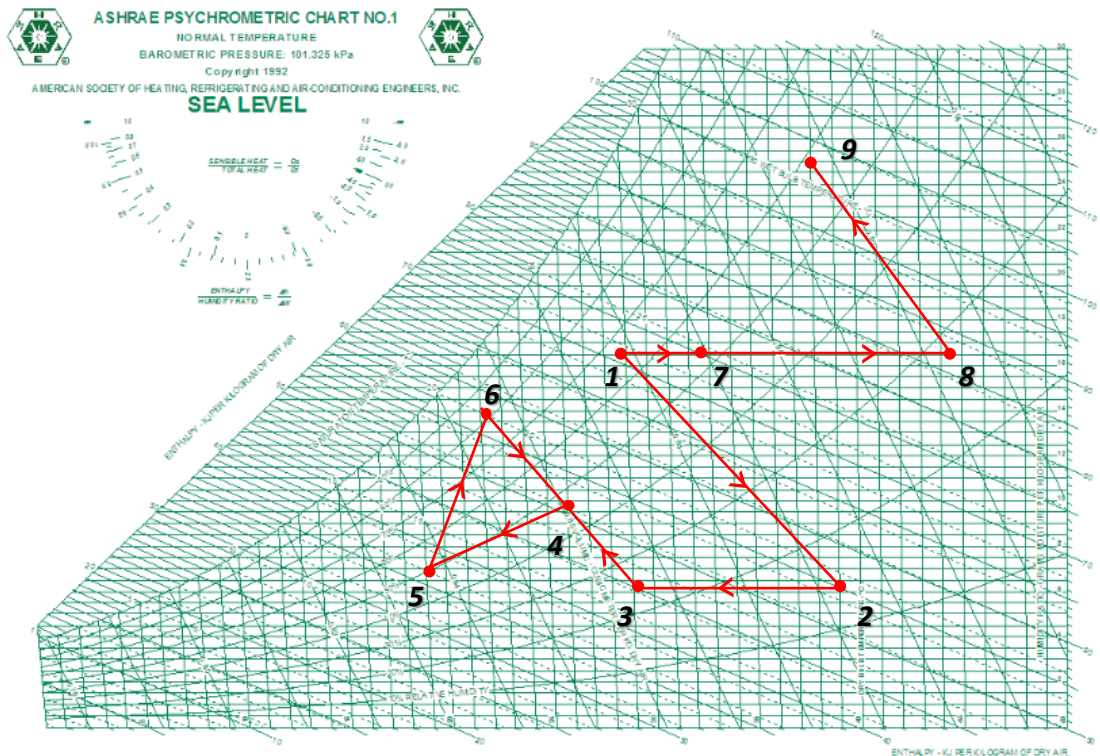


Fig 5.9 (b) Schematic Diagram and Plot of Air Exchange Cycle

Comparing to the cooling-based dehumidification systems, these cycles produce energy savings ranging from 56.6 to 66% in conditions of 30°C, 0.016 kg/kg da, RSHF of 0.35 and space conditions of 24°C, 0.0104 kg/kg da. The SHF was over 0.9 whilst drying high sensible heat load, and in high latent load, it varied from 0.3 to 0.5. Depending on the season, energy savings could range from 24 to 40% in high sensible heat load applications.

5.3. Summary

The purpose for the different case studies in this chapter is to explore various paths for a system to achieve different outcomes. The mechanisms are shown graphically and in their corresponding psychrometric charts. This is a necessary introduction to the development of the research's prototype as I demonstrate a few drying methods that meet different needs. Depending on the nature of the product and cost analysis, one can decide which mechanism to employ for drying.

The models can be used for design and for the analysis of the complete hybrid system. From the simulations that I have done, it was theoretically found that hybrid system consisting of heat pump and desiccant wheel offers the highest energy savings when compared with individual systems. A practical system can now be developed from this finding.

Chapter 6 Design & Construction of a Hybrid Dryer

The performance of three hybrid cycles (which are Air Mixing Cycle, Air Recirculation Cycle and Air Exchange Cycle) for typical drying space conditions has been evaluated using a detailed procedure for the analysis of rotary desiccant dehumidifier, the most commonly employed industrial dehumidifier, based on the analogy method of Psychrometric Analysis. Effect of space room sensible heat factor, mixing air ratio, and regeneration temperature has also been studied. The results show that desiccant wheel heat pump assisted hybrid drying system can give substantial energy savings as compared to based cooling conventional vapour compression refrigeration and single desiccant wheel systems in most commonly encountered situations. Following the findings in the previous chapters a heat pump desiccant wheel dehumidifier as a hybrid dryer is constructed.

6.1 Description of the System

Figure 6.1 shows the system which uses a refrigerant circuit in conjunction with a heat reactivated desiccant wheel to provide efficient drying capability. Due to the capabilities of the desiccant wheel, the unit can continue to provide substantial capacity and low supply dew point conditions. Air dehumidification can be achieved by two stages: (I) cooling the air below its dew point and removing moisture by condensation from evaporator and (II) sorption by a desiccant material. The heat pump desiccant dehumidifier is used and the simple analysis using the drying efficiency model is employed in the drying process. The steady-state drying process can be assumed in the loop-type dryer due to their continuous process, but the steady state cannot be obtained in an open-type dryer such as a conveyer dryer. During the constant rate period, the drying process might be a steady state in the open-type dryer. In the present study a steady state is assumed. The variables used in the analysis such as temperature, relative humidity, enthalpy, are the averaged values in a given state. The local variations of the variables are not considered in the heat exchangers, pipes, air flows with a pressure-enthalpy (P-h) diagram.

As shown in Figure 6.1, a fan sends the coolant airflow from the ambient air at state 4 into the condenser. The air at the condenser outlet is at a high temperature and low relative humidity. The air passing through the condenser is related only to sensible heat transfer, the absolute humidity is kept to be constant while the air is heated in the condenser.

Once the compressor is switched on, the condenser is heated to a high temperature and the evaporator is cooled to a very low temperature. The desiccant wheel is a rotating wheel that is in contact with both segments of the machine that is important in regulating the air temperature. The upper part is isolated from the lower part.

The ambient temperature air inside the product chamber is drawn in at (1) and is cooled by the evaporator. As it reaches (2), the portion of the rotating desiccant wheel that came from the upper part heats it up to an ambient temperature again. Ambient air is drawn from the atmosphere at (4) and relatively dry air at approximately ambient pressure is fed to the desiccant regenerator at (5) from the condenser, and as the air meets the rotating desiccant wheel, the hot air is rapidly cooled down by the section of the wheel that has been in the lower segment of the machine. The air thus gains moisture in a nearly isenthalpic process and exits at state 6 with much higher water content. There is also a slight increase in the entropy of the air due to addition of the moisture. The moist air exiting the regenerator desiccant is still relatively hot and nearly at ambient pressure.

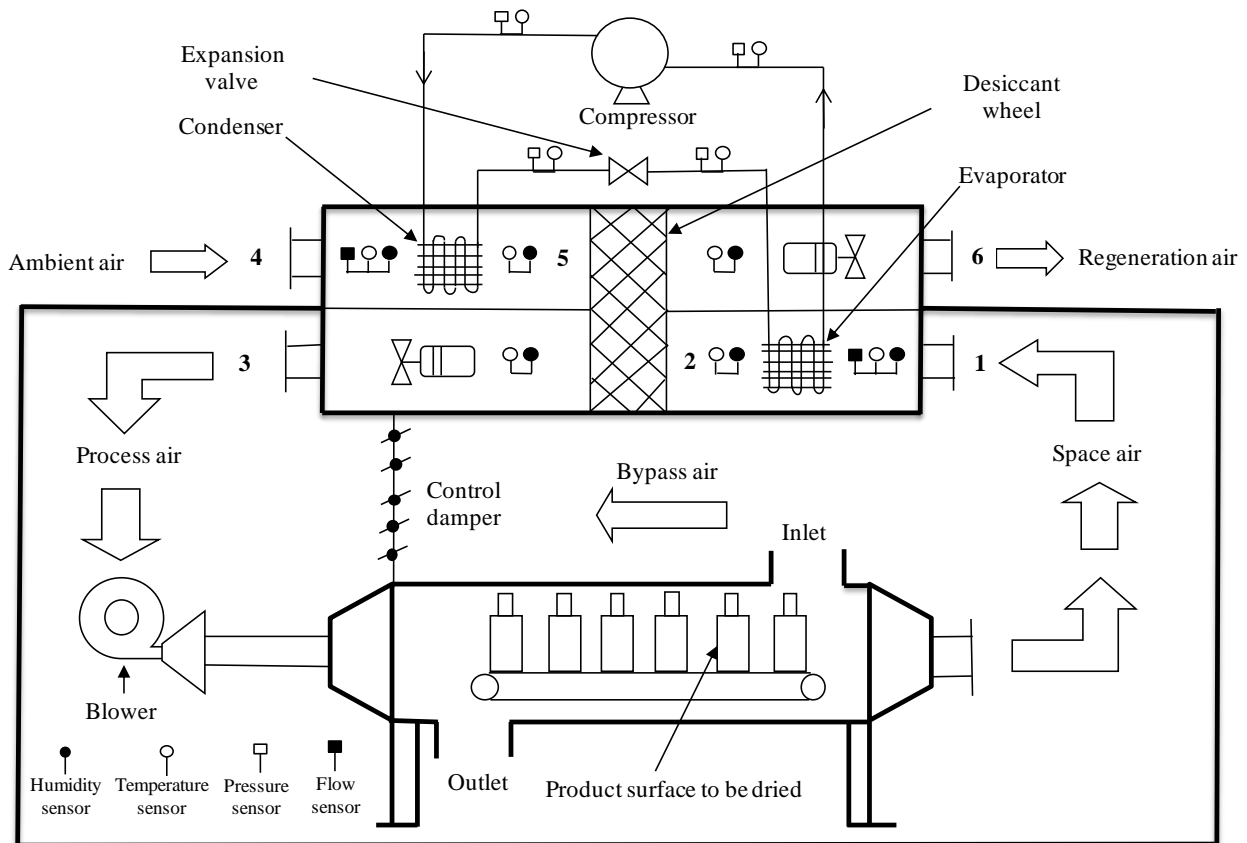


Fig 6.1 Hybrid System Combining Heat Pump and Desiccant Dehumidifier

For drying air cycle a fan is also necessary to provide the evaporation airflow from the dryer air at state 1. The moist drying air from the dryer enters the evaporator where the air is dehydrated as the moist condense on the surface of the evaporator. Thus, the latent heat of condensation is recovered from the moist air in the evaporator. At the evaporator outlet at state 2 the air temperature is nearly saturated but is also very cool and low humidity ratio. Then the air through desiccant material comes into contact with the desiccant wheel, and exits the dehumidifier hot and dry at state 3. The wheel is then rotated so that the desiccant portion that has picked up moisture is exposed to hot reactivation air and its moisture removed. Figure 6.2 shows that a drying process heat pump desiccant dehumidifier on the psychrometric chart. As the desiccant removes the moisture from the air, desiccant releases heat and warms the air, i.e., latent heat becomes sensible heat. To re-use the desiccant, it must be regenerated or reactivated through a process in which moisture is driven off by heat from condenser waste heat. The dried warm air can obtain desirable condition by sensible condenser.

To increase the economic practicality of such a hybrid system, the combined system utilises the heat dissipated by the condenser heat energy in regenerating the desiccant wheel. The location of the compressor and expansion valve in the cycle tends to enhance this heat recovery by creating relatively large temperature differences.

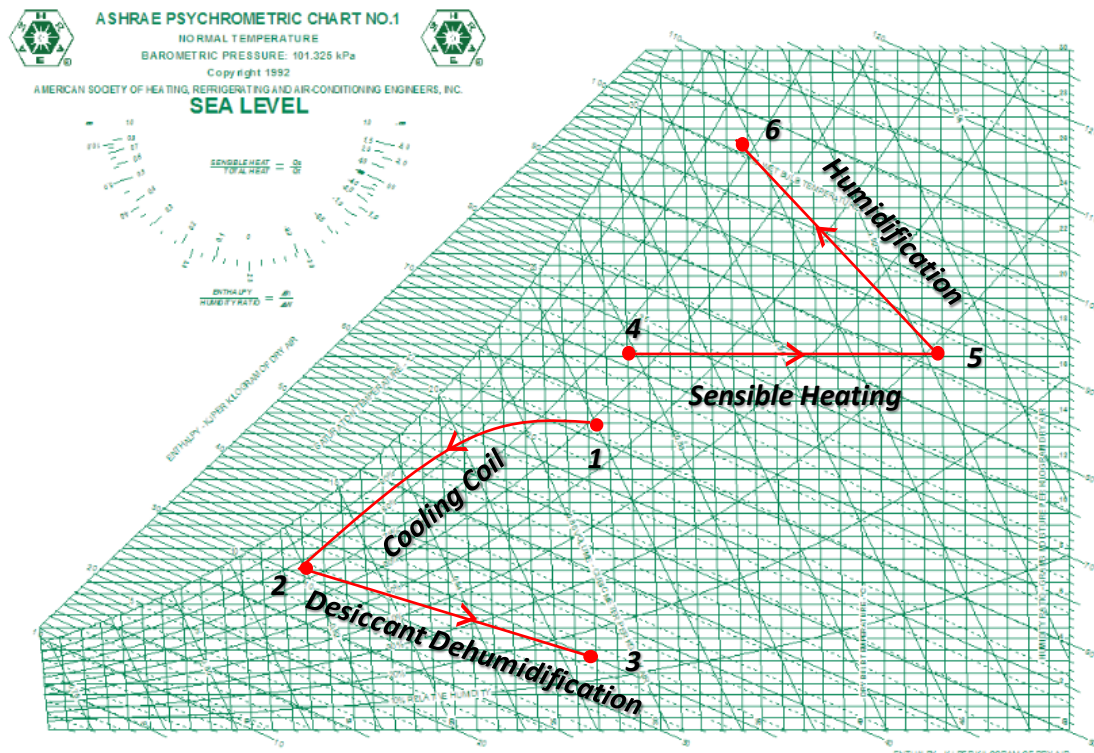


Fig 6.2 Hybrid Dryer Drying Process on the Psychrometric Chart

6.2 Experiment Setup

The photo of the hybrid system experimental equipment is shown Figure 6.3. A heat pump desiccant dehumidifier was developed on the basis of the design parameters obtained from the mathematical model in Chapter 4/5. The honeycombed silica gel composite desiccant wheels were used in this experiment. It can work well under lower regeneration temperature and achieve higher dehumidification capacity. Hydraulic diameter of each honeycomb channel is 2.1 mm and it is coated with a 2 mm thick silica gel layer. Therefore the air channel walls are coated adequately desiccant material and are capable of removing the moisture from the passing process air. The ratio of regeneration section to adsorption section is 1/4. Desiccant wheel has a diameter of 32 cm and is 20 cm long. The wheel speed is 24.5 revolutions per hour. For analysis the process and regeneration air-flow rates were chosen such that the condensed water at the evaporator will not be blown out of the water collector and that the temperature of the condenser will be too low.

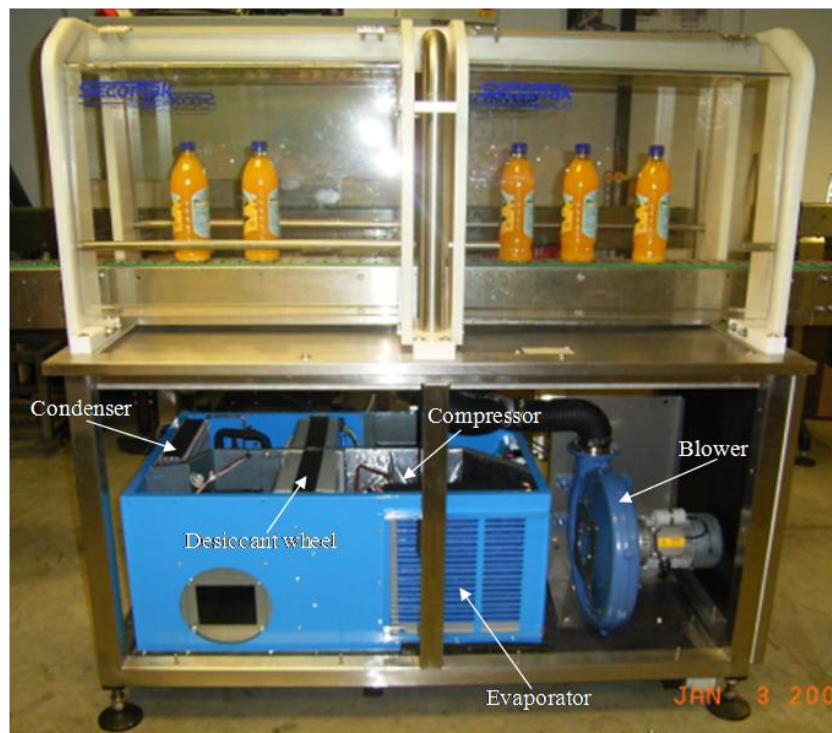


Fig 6.3 Hybrid System Experimental Equipment

Instrumentation & Measurement

In the constructed test system equal amounts of m_a in the process and regeneration sides were used due to the absence of the conditioned space. Tests were conducted to determine the influence of three design parameters namely cooling capacity, airflow rate and COP of heat pump cycle on the following performance parameters:

The specific cooling capacity of space air

$$\Delta H = (h_1 - h_2) \quad (6.1)$$

Total moisture removal capacity of dehumidification space air

$$q_{mw} = q_{ma}(w_1 - w_3) \quad (6.2)$$

The cooling capacity of desiccant wheel heat pump assisted and COP

$$Q_c = q_{ma} \times \Delta H \quad (6.3)$$

$$COP = \frac{Q_c}{P_{comp}} \quad (6.4)$$

Based on a detailed uncertainty analysis taking into account the accuracies of the sensors/ instruments, errors in various parameters are estimated and are shown in Table 6.1 and Table 6.2 show the measured and calculated properties for experimental test.

Measurements for the process and regeneration air streams include inlet and outlet dry bulb temperature (DBT) using ‘T’ type thermocouples ($\pm 0.1^\circ\text{C}$), relative humidity using RH sensors ($\pm 0.5\%$ RH) and air flow rates using hotwire anemometer (± 0.02 m/s). The refrigerant side measurements include refrigerant temperatures using ‘T’ type thermocouples ($\pm 0.1^\circ\text{C}$), and pressures using inductive pressure transmitters (± 0.05 bar) at inlet and outlet of evaporator, condenser and compressor, and power consumed by the compressor using a Watt transducer (± 20 W). Table 6.1 shows the parameters to be measured for analysing the system and Table 6.2 show the measured and calculated properties for experimental test.

Table 6.1 Measured Parameters

Measured parameter	Unit	Measuring range	Accuracy
Drying temperature	$^\circ\text{C}$	0-50	± 0.1
Ambient temperature	$^\circ\text{C}$	0-50	± 0.1
Relative humidity	%	0-100	± 0.5
Air volocity	m/s	0.1-20	± 0.02
Ambient pressure	mbar	0-2000	± 0.05
Electrical energy	kWh	0-1000	$\pm 20\text{W}$

The inaccuracies of the equipment are absolute errors given by the manufacturers. Experimental errors are neglected because as long as the controlled parameters, such as the temperature and pressure, are kept at an atmospheric scale, the deviations are tolerable as miniscule temperature fluctuations do not affect the drying performance.

Table 6.2 Measured and Calculated Properties for Experimental Test

	Measured		Calculated		
	Humidity	Temperature	Humidity	Enthalpy	Dew Point
	(%)	(°C)	(g/kg)	(kJ/kg)	(°C)
Inlet space air	54.2	19.3	7.57	38.6	9.7
Outlet evaporator air	81.1	8.5	5.6	22.63	5.4
Outlet process air	14.2	26.2	2.99	33.96	-2.8
Inlet ambient air	46.4	23.2	8.24	44.28	11.1
Outlet condenser air	14.4	44.1	8.24	65.6	11.1
Outlet Regeneration air	34.3	43.8	19.68	94.84	24.6

Figure 6.3 shows the heat pump cycle p-h diagrams. The system was designed to have a refrigeration capacity of about 3.5 kW in the compressor, obtained with the conditions such as the heat release rate of the condenser of 12kW, heat rate at the evaporator 7.5 kW. The average condensing temperature of 60°C, average evaporating temperature of 7°C, superheating at 11°C, the sub cooling at 7°C and the COP of the heat pump cycle is 3.43.

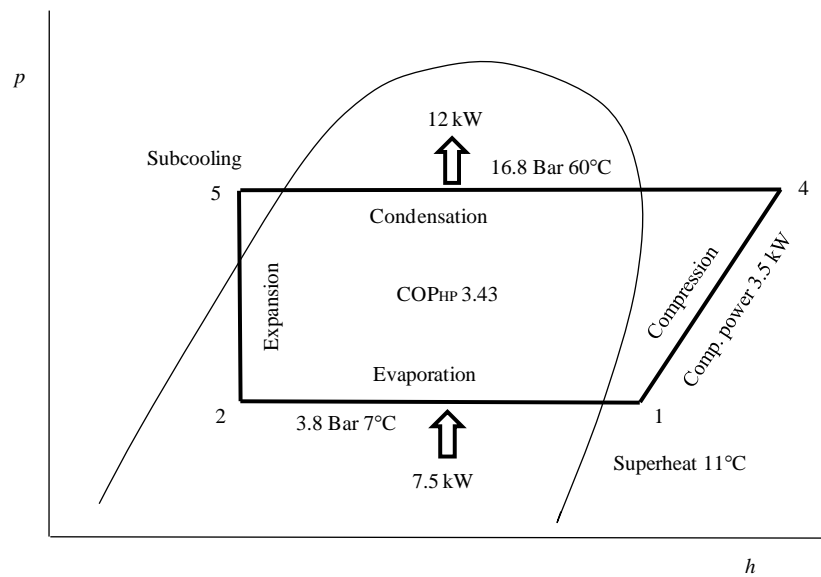


Fig 6.3 Heat Pump R134a Refrigerant Cycle

6.3 Summary

In this chapter a heat pump desiccant wheel dehumidifier hybrid dryer is constructed, the unit can continue to provide substantial capacity and low supply dew point conditions for rapid surface drying applications. The results of the effect of various parameters on the performance of the systems will be discussed in next chapter.

The desiccant wheel integrated heat pump is driven by a cooling load of 7.5 kW nominal cooling capacity. During the experiments, the space air (or process air) of desiccant wheel, is equal to return air, termed as regeneration air of the wheel. The return/regeneration air is controlled at $19.3/23.2 \pm 0.3$ °C DBT and $54.2/46.4\% \pm 1\%$ RH. The tests are envisaged to assess the influence of design parameters, namely, inlet air temperature, air flow rate, COP of heat pump cycle and regeneration air temperature on the performance of the desiccant wheel heat pump assisted drying unit. These are varied respectively from 18 to 32 °C, 900-1600 m³/h, 2.5-5.5 and 38-56 °C, the corresponding variations in the system performance are discussed.

Chapter 7 Results and Discussion

This chapter presents the theoretical results based on ideal hybrid system as a bench mark for comparison of real results.

7.1 Realisation of the Operation Cycle of Hybrid System

Psychrometric diagram of a real hybrid system shown in Figure 7.1 was considered as a bench mark for comparing the results of various test cases. Firstly the processes in the two units of the hybrid system were considered separately and then both processes are considered in series within a full cycle. In this approach, particular consideration was given to 1-2 and 4-5 processes occurring in heat pump; 2-3 and 5-6 processes occurring in desiccant wheel.

In an ideal cycle for a steady state operation of the desiccant wheel, the lines representing operations through 2-2' and 5-5' states as shown in Figure 7.1 are approximately parallel to Enthalpy lines. However calculated realized cycles deviate from the ideal cycle as can be seen from the psychrometric diagrams of one of the test cases. The deviation of realized cycle from an ideal cycle may be due to a number of factors such as characteristics of the system, however the realization of the cycle significantly has influenced by the m_a , and T_R . The behaviour of the processes in heat pump between states 1-2 and 4-5 was similar to that for the ideally expected case in most of the test cases. However the processes in desiccant wheel between states 2-2' and 5-5' have shown a considerable deviation from heat transfer process of constant enthalpy, the realized cycle follows the path 2-3 and 5-6.

The observed behaviours of test cases are governed by the specific combination of the operation parameters. Meanwhile inspections of the data resulted in the following estimations:

1. The processes occurring in desiccant wheel were influenced by regeneration and dehumidification air temperature with a critical magnitude of regeneration air temperature, which can be suggested as $T_R \geq 50$ °C. Temperature above 50 °C will greatly reduce the efficiency of the condenser.
2. Heat pump cycle was almost of secondary importance in comparison with desiccant wheel efficiency regarding both the complete cycle and operation through desiccant wheel.

- The magnitude of air flow rate was the dominant parameter under the major influence of regeneration air temperature with an expected relationship of $T_R = F(m_a)$ for the overall cycle realization.

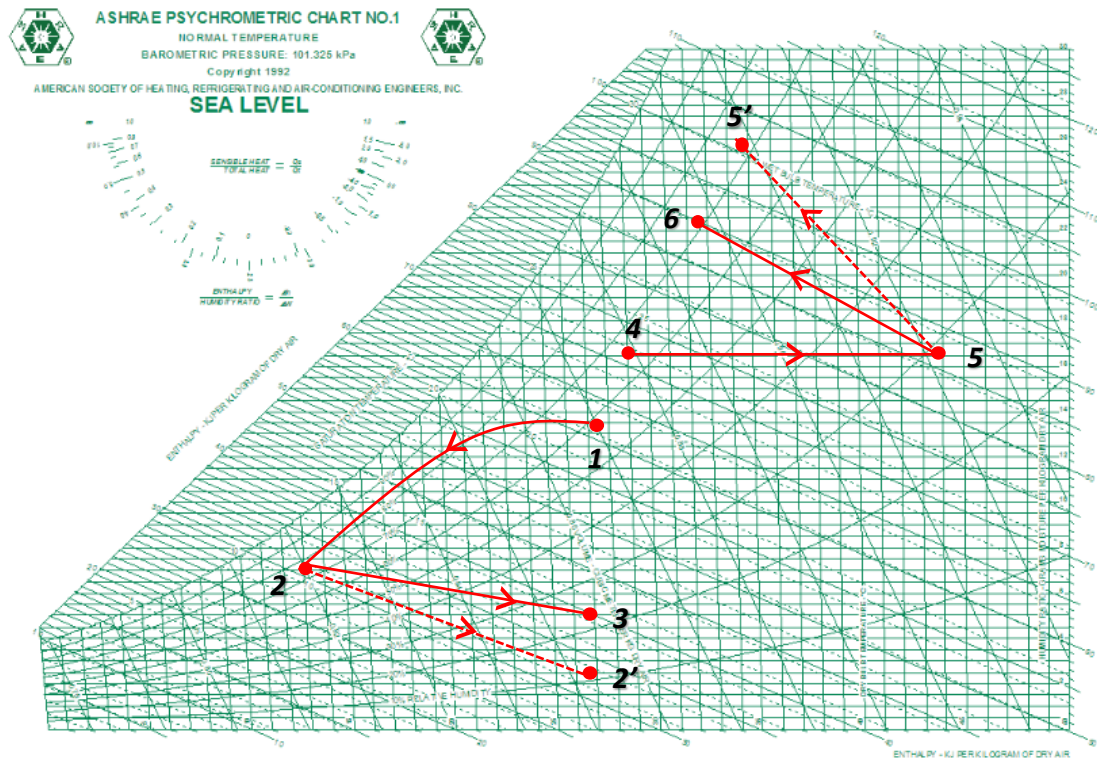


Fig 7.1 Psychrometric Representation of the Realized Cycle Test Results of Hybrid System

Figure 7.2 shows the schematic of the hybrid system and the test conditions at different stages in the system. Following conditions of the air used are considered: at the evaporator inlet: the DBT of 19.3°C and RH of 54.2%, air flow rate of 1300 m³/h. The air is dehydrated and cooled down in the evaporator. Then the air enters the desiccant at DBT of 8.5 °C and RH increases to 81.1% and due to the temperature rise in desiccant, leaves the desiccant at DBT of 26.2 °C and at very low RH of 14.2%.

The volumetric flow rate of the air varies slightly due to the density change with temperature, but the mass flow rate is kept constant because the air flow system is assumed to be closed. On the condenser side, the ambient air conditions are DBT 23.2 °C and RH of 46.4% inlet the condenser. Then regeneration air is heated to sensible reheat to DBT of 44.1 °C before passing through the desiccant wheel, where desiccant material picks up moisture from the process air and transports to the hot regenerated air. The air leaving the desiccant wheel is DBT of 43.8 °C and RH of 34.3% exhausted to the ambient, the humidity ratio of regeneration air is increased and its temperature decreases.

The results of the effect of various parameters on the performance of the systems are presented in the following sections.

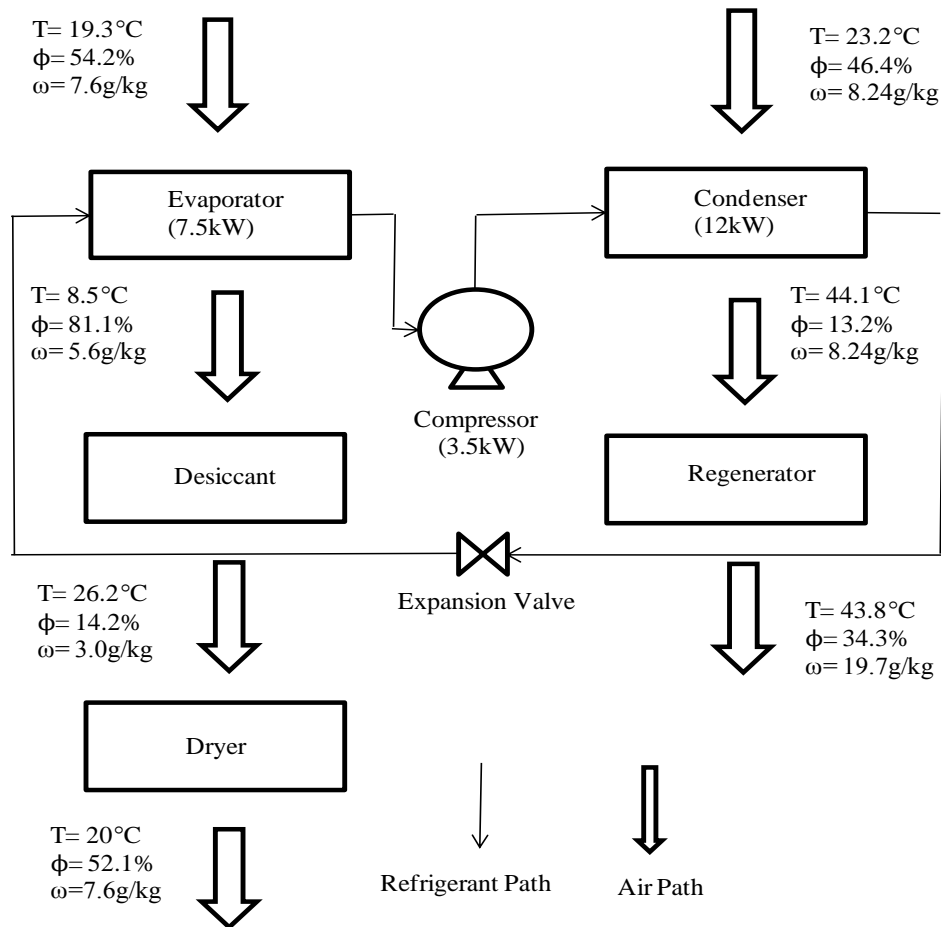


Fig 7.2 Hybrid System Drying Air Process

7.2 Effect of Inlet Air Temperature

Comparisons between single refrigerant circuit system, single desiccant wheel system and hybrid system operating in tandem are shown in Figure 7.3. These three systems are tested at the following conditions, airflow rate $1300 \text{ m}^3/\text{h}$, relative humidity = 60% and outlet air dew point temperature kept at $5.6 \text{ }^\circ\text{C}$. The variation in input energy required for each system with respect to inlet air temperature from $20 \text{ }^\circ\text{C}$ to $30 \text{ }^\circ\text{C}$ is plotted.

It shows that the input energy required for all systems increases with the inlet air temperature due to increased driving potential for mass transfer. However, the energy demand for the hybrid system is less than the other two individual systems at all inlet temperatures. It is evident that the energy requirement is reduced and 39% energy can be saved via the hybrid system. This improvement in heat recovery may be associated

with the greater heat transfer area for heat transferring with the drying air. The evaporator undertakes a part of the cooling duty to cool the air to dew-point temperature. In this way, the desiccant could dedicate more of its surface for latent heat recovery. In a physical sense, the hybrid system may be viewed to have enlarged the mechanical boundaries for heat recovery in a drying air cycle.

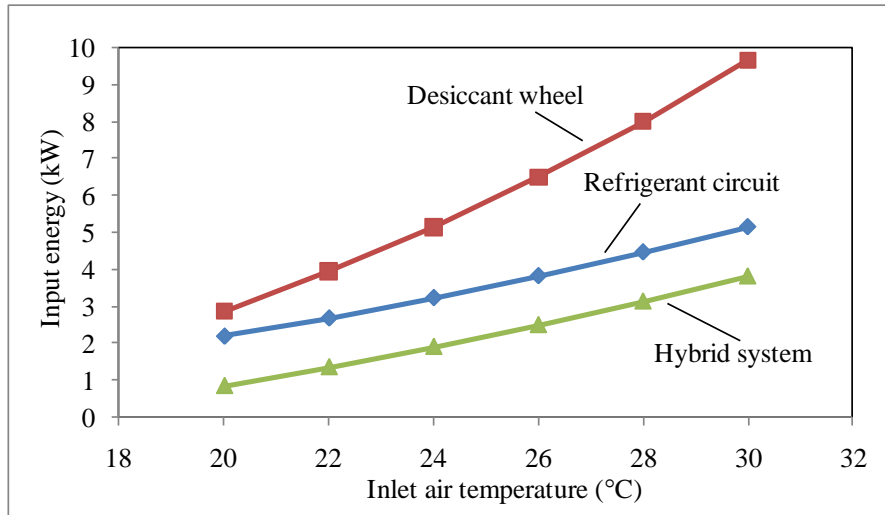


Fig 7.3 Effect of inlet air temperature on input energy required

Figure 7.4 shows that the SMER of the refrigerant circuit system is more than that of the desiccant wheel system but less than that of hybrid system throughout the range of inlet air temperature as the hybrid system was gradually activated. The addition of desiccant wheel improved the system performance in terms of SMER. The introduction of the desiccant wheel not only gained moist air from evaporator but also provided additional sensible heating to the air without the need of an auxiliary heater.

The gradual activation of the hybrid system improved SMER in the range of 37–42%. The additional advantage gained in terms of system performance is by employing both dehumidification and regeneration. This observation may be attributed to the finite rate of heat transfer in the heat exchangers as the air interacted with more heat exchangers.

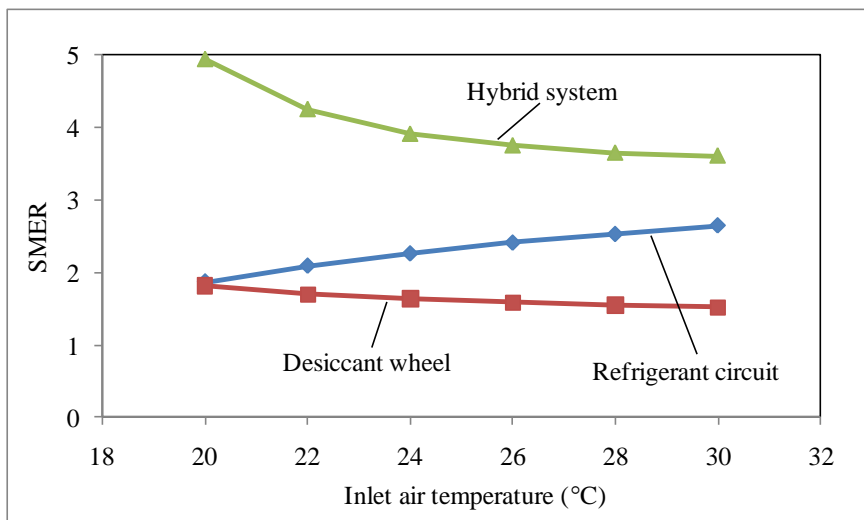


Fig 7.4 Effect of inlet air temperature on SMER

Figure 7.5 presents the effect of inlet temperature on sensible heat for all three systems. It is observed that due to the moisture transfer from inlet air to outlet air via the hybrid system the sensible heat rise in the inlet air is significant. It also reveals that this free heat supply by condenser heat release is comparable to the amount of heat energy that is required in the refrigerant circuit system. In addition, the desiccant wheel further dehumidifies the outlet air. Both input energy and sensible heat collectively enhance the effectiveness of the system, the sensible heat transfer is found to be between 2.58 and 6.26 kW, based on the condenser heat release in the desiccant wheel.

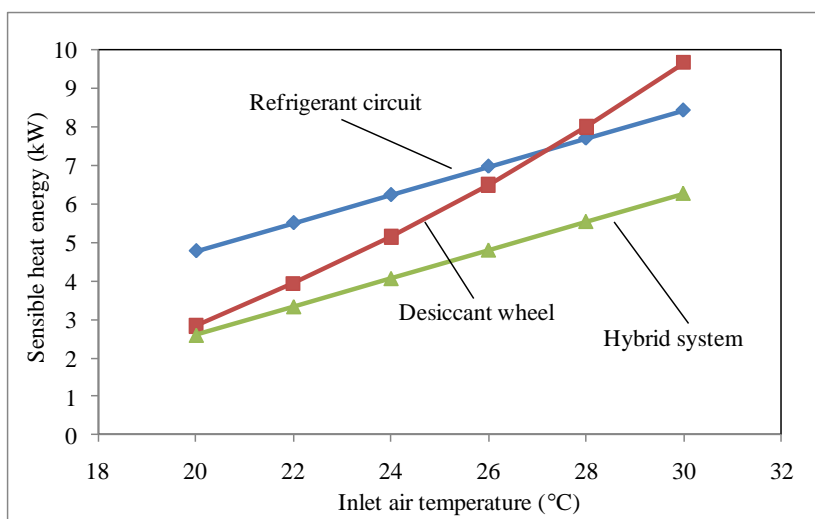


Fig 7.5 Effect of inlet air temperature on sensible heat energy

Figure 7.6 shows that the drying performance, the total moisture removal capacity in drying process increases with the inlet air temperature as expected. The inlet air relative humidity and the outlet air dew point temperature were kept at 60 % and 5.6 °C respectively. Therefore, the drying rate increases almost linearly with the inlet air temperature.

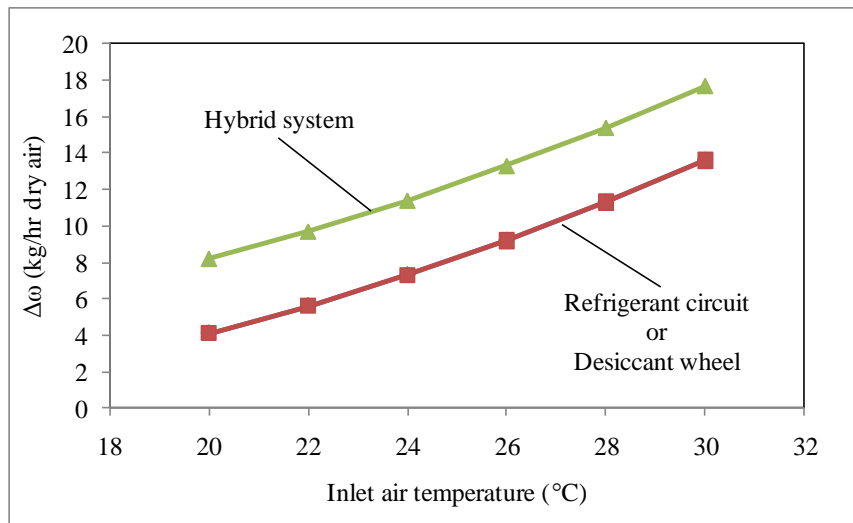


Fig 7.6 Effect of inlet air temperature on total moisture removal capacity

Figure 7.7 shows the airflow rate 1300 m³/h, relative humidity = 60% and outlet air dew point temperature kept at 5.6 °C, which are the outcomes read directly off the psychrometric chart. The variation for each system with respect to inlet air temperature from 20 °C to 30 °C is plotted in psychrometric chart. Table 7.1 (A) (B) (C) (D) shows the result of three systems using psychrometric Analysis state point and process report.



ASHRAE PSYCHROMETRIC CHART NO. 1

NORMAL TEMPERATURE

BAROMETRIC PRESSURE: 101.325 kPa

Copyright 1992

AMERICAN SOCIETY OF HEATING, REFRIGERATING AND AIR-CONDITIONING ENGINEERS, INC.



SEA LEVEL

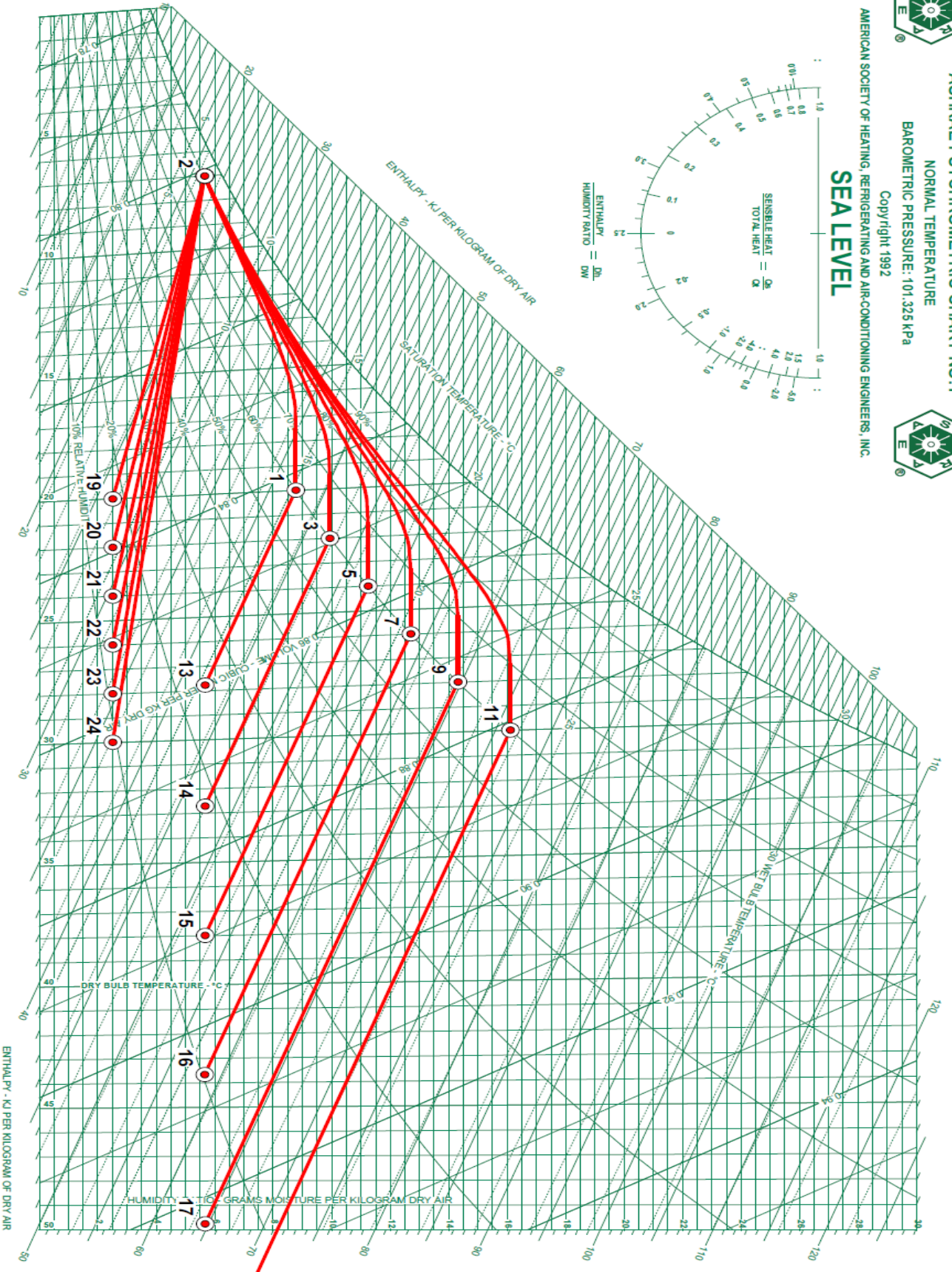
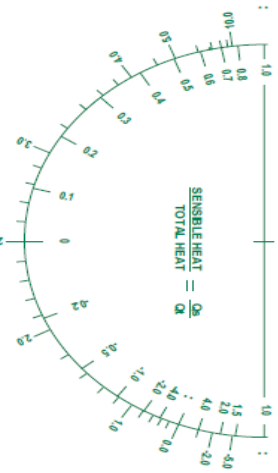


Fig 7.7 Psychrometric Chart

Table 7.1 (A) State Point & Process Report

STATE POINT & PROCESS REPORT

Report Date: Tuesday, March 15, 2011
Project Information:

Altitude: 0 (Meters)
Barometric Pressure: 760.001 (mm Hg)
Atmospheric Pressure: 101.325 (kPa)

1. 1

STATE POINT DATA

Air Flow (Standard) (kg/hr)	Dry Bulb (°C)	Wet Bulb (°C)	Relative Humidity (%)	Humidity Ratio (g/kg)	Specific Volume (cu.m/kg)	Enthalpy (kJ/kg)	Dew Point (°C)	Density (kg/cu.m)	Vapor Pressure (mm Hg)	Absolute Humidity (g/cu.m)
1,300.0	20.000	15.135	60.0	6.77	0.842	42.357	12.0093	1.1984	10.5267	10.418

2. 2

STATE POINT DATA

Air Flow (Standard) (kg/hr)	Dry Bulb (°C)	Wet Bulb (°C)	Relative Humidity (%)	Humidity Ratio (g/kg)	Specific Volume (cu.m/kg)	Enthalpy (kJ/kg)	Dew Point (°C)	Density (kg/cu.m)	Vapor Pressure (mm Hg)	Absolute Humidity (g/cu.m)
1,300.0	7.000	6.303	90.8	5.66	0.801	21.254	5.6000	1.2563	6.8232	7.066

Process: Cooling Coil

Start Point Name	Total Cooling (kW/hr)	Total Energy (W/hr)	Sensible Energy (W/hr)	Latent Energy (W/hr)	Dehumidification (kg/hr)	Sensible Heat Ratio	Enthalpy/ Humidity Ratio (kJ/kg / g/kg)
1	-7.619	-7,619	-4,765	-2,854	-4.0	0.625	6.759

3. 3

STATE POINT DATA

Air Flow (Standard) (kg/hr)	Dry Bulb (°C)	Wet Bulb (°C)	Relative Humidity (%)	Humidity Ratio (g/kg)	Specific Volume (cu.m/kg)	Enthalpy (kJ/kg)	Dew Point (°C)	Density (kg/cu.m)	Vapor Pressure (mm Hg)	Absolute Humidity (g/cu.m)
1,300.0	22.000	16.866	60.0	9.94	0.849	47.363	13.8879	1.1895	11.9041	11.702

4. 2

STATE POINT DATA

Air Flow (Standard) (kg/hr)	Dry Bulb (°C)	Wet Bulb (°C)	Relative Humidity (%)	Humidity Ratio (g/kg)	Specific Volume (cu.m/kg)	Enthalpy (kJ/kg)	Dew Point (°C)	Density (kg/cu.m)	Vapor Pressure (mm Hg)	Absolute Humidity (g/cu.m)
1,300.0	7.000	6.303	90.8	5.66	0.801	21.254	5.6000	1.2563	6.8232	7.066

Process: Cooling Coil

Start Point Name	Total Cooling (kW/hr)	Total Energy (W/hr)	Sensible Energy (W/hr)	Latent Energy (W/hr)	Dehumidification (kg/hr)	Sensible Heat Ratio	Enthalpy/ Humidity Ratio (kJ/kg / g/kg)
3	-9.426	-9,426	-5,499	-3,927	-5.6	0.583	6.082

5. 5

STATE POINT DATA

Air Flow (Standard) (kg/hr)	Dry Bulb (°C)	Wet Bulb (°C)	Relative Humidity (%)	Humidity Ratio (g/kg)	Specific Volume (cu.m/kg)	Enthalpy (kJ/kg)	Dew Point (°C)	Density (kg/cu.m)	Vapor Pressure (mm Hg)	Absolute Humidity (g/cu.m)
1,300.0	24.000	18.597	60.0	11.24	0.857	52.725	15.7656	1.1806	13.4364	13.120

6. 2

STATE POINT DATA

Air Flow (Standard) (kg/hr)	Dry Bulb (°C)	Wet Bulb (°C)	Relative Humidity (%)	Humidity Ratio (g/kg)	Specific Volume (cu.m/kg)	Enthalpy (kJ/kg)	Dew Point (°C)	Density (kg/cu.m)	Vapor Pressure (mm Hg)	Absolute Humidity (g/cu.m)
1,300.0	7.000	6.303	90.8	5.66	0.801	21.254	5.6000	1.2563	6.8232	7.066

Process: Cooling Coil

Start Point Name	Total Cooling (kW/hr)	Total Energy (W/hr)	Sensible Energy (W/hr)	Latent Energy (W/hr)	Dehumidification (kg/hr)	Sensible Heat Ratio	Enthalpy/ Humidity Ratio (kJ/kg / g/kg)
5	-11.362	-11,362	-6,232	-5,130	-7.3	0.548	5.620

7. 7

STATE POINT DATA

Air Flow (Standard) (kg/hr)	Dry Bulb (°C)	Wet Bulb (°C)	Relative Humidity (%)	Humidity Ratio (g/kg)	Specific Volume (cu.m/kg)	Enthalpy (kJ/kg)	Dew Point (°C)	Density (kg/cu.m)	Vapor Pressure (mm Hg)	Absolute Humidity (g/cu.m)
1,300.0	26.000	20.331	60.0	12.69	0.864	58.481	17.6422	1.1717	15.1383	14.683

8. 2

STATE POINT DATA

Air Flow (Standard) (kg/hr)	Dry Bulb (°C)	Wet Bulb (°C)	Relative Humidity (%)	Humidity Ratio (g/kg)	Specific Volume (cu.m/kg)	Enthalpy (kJ/kg)	Dew Point (°C)	Density (kg/cu.m)	Vapor Pressure (mm Hg)	Absolute Humidity (g/cu.m)
1,300.0	7.000	6.303	90.8	5.66	0.801	21.254	5.6000	1.2563	6.8232	7.066

Process: Cooling Coil

Start Point Name	Total Cooling (kW/hr)	Total Energy (W/hr)	Sensible Energy (W/hr)	Latent Energy (W/hr)	Dehumidification (kg/hr)	Sensible Heat Ratio	Enthalpy/ Humidity Ratio (kJ/kg / g/kg)
7	-13.440	-13,440	-6,965	-6,475	-9.1	0.518	5.273

Table 7.1 (B) State Point & Process Report

STATE POINT & PROCESS REPORT

9. 9

STATE POINT DATA

Air Flow (Standard) (kg/hr)	Dry Bulb (°C)	Wet Bulb (°C)	Relative Humidity (%)	Humidity Ratio (g/kg)	Specific Volume (cu.m/kg)	Enthalpy (kJ/kg)	Dew Point (°C)	Density (kg/cu.m)	Vapor Pressure (mm Hg)	Absolute Humidity (g/cu.m)
1,300.0	28.000	22.068	60.0	14.31	0.872	64.671	19.5177	1.1629	17.0251	16.404

10. 2

STATE POINT DATA

Air Flow (Standard) (kg/hr)	Dry Bulb (°C)	Wet Bulb (°C)	Relative Humidity (%)	Humidity Ratio (g/kg)	Specific Volume (cu.m/kg)	Enthalpy (kJ/kg)	Dew Point (°C)	Density (kg/cu.m)	Vapor Pressure (mm Hg)	Absolute Humidity (g/cu.m)
1,300.0	7.000	6.303	90.8	5.66	0.801	21.254	5.6000	1.2563	6.8232	7.066

Process: Cooling Coil

Start Point Name	Total Cooling (kW/hr)	Total Energy (W/hr)	Sensible Energy (W/hr)	Latent Energy (W/hr)	Dehumidification (kg/hr)	Sensible Heat Ratio	Enthalpy/ Humidity Ratio (kJ/kg / g/kg)
9	-15.674	-15,674	-7,698	-7,977	-11.3	0.491	4.999

11. 11

STATE POINT DATA

Air Flow (Standard) (kg/hr)	Dry Bulb (°C)	Wet Bulb (°C)	Relative Humidity (%)	Humidity Ratio (g/kg)	Specific Volume (cu.m/kg)	Enthalpy (kJ/kg)	Dew Point (°C)	Density (kg/cu.m)	Vapor Pressure (mm Hg)	Absolute Humidity (g/cu.m)
1,300.0	30.000	23.807	60.0	16.11	0.881	71.340	21.3921	1.1541	19.1135	18.295

12. 2

STATE POINT DATA

Air Flow (Standard) (kg/hr)	Dry Bulb (°C)	Wet Bulb (°C)	Relative Humidity (%)	Humidity Ratio (g/kg)	Specific Volume (cu.m/kg)	Enthalpy (kJ/kg)	Dew Point (°C)	Density (kg/cu.m)	Vapor Pressure (mm Hg)	Absolute Humidity (g/cu.m)
1,300.0	7.000	6.303	90.8	5.66	0.801	21.254	5.6000	1.2563	6.8232	7.066

Process: Cooling Coil

Start Point Name	Total Cooling (kW/hr)	Total Energy (W/hr)	Sensible Energy (W/hr)	Latent Energy (W/hr)	Dehumidification (kg/hr)	Sensible Heat Ratio	Enthalpy/ Humidity Ratio (kJ/kg / g/kg)
11	-18.082	-18,082	-8,431	-9,651	-13.6	0.466	4.772

13. 13

STATE POINT DATA

Air Flow (Standard) (kg/hr)	Dry Bulb (°C)	Wet Bulb (°C)	Relative Humidity (%)	Humidity Ratio (g/kg)	Specific Volume (cu.m/kg)	Enthalpy (kJ/kg)	Dew Point (°C)	Density (kg/cu.m)	Vapor Pressure (mm Hg)	Absolute Humidity (g/cu.m)
1,300.0	27.783	15.212	24.4	5.66	0.860	42.365	5.6087	1.1695	6.8273	6.582

Process: Desiccant Dehumidification

Start Point Name	Total Energy (W/hr)	Sensible Energy (W/hr)	Latent Energy (W/hr)	Dehumidification (kg/hr)	Sensible Heat Ratio	Enthalpy/ Humidity Ratio (kJ/kg / g/kg)	Sensible Energy Per Dehumidification (kJ/kg)
1	3	2,853	-2,850	-4.0	1081.889	-0.020	-2,558

14. 14

STATE POINT DATA

Air Flow (Standard) (kg/hr)	Dry Bulb (°C)	Wet Bulb (°C)	Relative Humidity (%)	Humidity Ratio (g/kg)	Specific Volume (cu.m/kg)	Enthalpy (kJ/kg)	Dew Point (°C)	Density (kg/cu.m)	Vapor Pressure (mm Hg)	Absolute Humidity (g/cu.m)
1,300.0	32.716	16.977	18.4	5.66	0.874	47.374	5.6087	1.1506	6.8273	6.476

Process: Desiccant Dehumidification

Start Point Name	Total Energy (W/hr)	Sensible Energy (W/hr)	Latent Energy (W/hr)	Dehumidification (kg/hr)	Sensible Heat Ratio	Enthalpy/ Humidity Ratio (kJ/kg / g/kg)	Sensible Energy Per Dehumidification (kJ/kg)
3	4	3,928	-3,924	-5.6	1117.167	-0.020	-2,562

15. 15

STATE POINT DATA

Air Flow (Standard) (kg/hr)	Dry Bulb (°C)	Wet Bulb (°C)	Relative Humidity (%)	Humidity Ratio (g/kg)	Specific Volume (cu.m/kg)	Enthalpy (kJ/kg)	Dew Point (°C)	Density (kg/cu.m)	Vapor Pressure (mm Hg)	Absolute Humidity (g/cu.m)
1,300.0	37.994	18.746	13.7	5.66	0.889	52.733	5.6087	1.1311	6.8273	6.366

Process: Desiccant Dehumidification

Start Point Name	Total Energy (W/hr)	Sensible Energy (W/hr)	Latent Energy (W/hr)	Dehumidification (kg/hr)	Sensible Heat Ratio	Enthalpy/ Humidity Ratio (kJ/kg / g/kg)	Sensible Energy Per Dehumidification (kJ/kg)
5	2	5,130	-5,127	-7.3	2188.375	-0.019	-2,565

16. 16

STATE POINT DATA

Table 7.1 (C) State Point & Process Report

STATE POINT & PROCESS REPORT

Air Flow (Standard) (kg/hr)	Dry Bulb (°C)	Wet Bulb (°C)	Relative Humidity (%)	Humidity Ratio (g/kg)	Specific Volume (cu.m/kg)	Enthalpy (kJ/kg)	Dew Point (°C)	Density (kg/cu.m)	Vapor Pressure (mm Hg)	Absolute Humidity (g/cu.m)
1,300.0	43.669	20.517	10.1	5.65	0.905	58.469	5.5834	1.1109	6.8153	6.241

Process: Desiccant Dehumidification

Start Point Name	Total Energy (W/hr)	Sensible Energy (W/hr)	Latent Energy (W/hr)	Dehumidification (kg/hr)	Sensible Heat Ratio	Enthalpy/ Humidity Ratio (kJ/kg / g/kg)	Sensible Energy Per Dehumidification (kJ/kg)
7	-4	6,476	-6,481	-9.2	-1473.600	-0.016	-2,565

17. 17

STATE POINT DATA

Air Flow (Standard) (kg/hr)	Dry Bulb (°C)	Wet Bulb (°C)	Relative Humidity (%)	Humidity Ratio (g/kg)	Specific Volume (cu.m/kg)	Enthalpy (kJ/kg)	Dew Point (°C)	Density (kg/cu.m)	Vapor Pressure (mm Hg)	Absolute Humidity (g/cu.m)
1,300.0	49.761	22.308	7.4	5.66	0.923	64.680	5.6087	1.0899	6.8273	6.134

Process: Desiccant Dehumidification

Start Point Name	Total Energy (W/hr)	Sensible Energy (W/hr)	Latent Energy (W/hr)	Dehumidification (kg/hr)	Sensible Heat Ratio	Enthalpy/ Humidity Ratio (kJ/kg / g/kg)	Sensible Energy Per Dehumidification (kJ/kg)
9	3	7,977	-7,973	-11.2	2474.909	-0.019	-2,572

18. 18

STATE POINT DATA

Air Flow (Standard) (kg/hr)	Dry Bulb (°C)	Wet Bulb (°C)	Relative Humidity (%)	Humidity Ratio (g/kg)	Specific Volume (cu.m/kg)	Enthalpy (kJ/kg)	Dew Point (°C)	Density (kg/cu.m)	Vapor Pressure (mm Hg)	Absolute Humidity (g/cu.m)
1,300.0	56.328	24.100	5.4	5.66	0.942	71.348	5.6087	1.0682	6.8273	6.012

Process: Desiccant Dehumidification

Start Point Name	Total Energy (W/hr)	Sensible Energy (W/hr)	Latent Energy (W/hr)	Dehumidification (kg/hr)	Sensible Heat Ratio	Enthalpy/ Humidity Ratio (kJ/kg / g/kg)	Sensible Energy Per Dehumidification (kJ/kg)
11	3	9,651	-9,648	-13.6	3293.800	-0.019	-2,575

19. 19

STATE POINT DATA

Air Flow (Standard) (kg/hr)	Dry Bulb (°C)	Wet Bulb (°C)	Relative Humidity (%)	Humidity Ratio (g/kg)	Specific Volume (cu.m/kg)	Enthalpy (kJ/kg)	Dew Point (°C)	Density (kg/cu.m)	Vapor Pressure (mm Hg)	Absolute Humidity (g/cu.m)
1,300.0	20.000	8.799	17.3	2.50	0.833	26.442	-4.9356	1.2028	3.0301	2.999

Process: Desiccant Dehumidification

Start Point Name	Total Energy (W/hr)	Sensible Energy (W/hr)	Latent Energy (W/hr)	Dehumidification (kg/hr)	Sensible Heat Ratio	Enthalpy/ Humidity Ratio (kJ/kg / g/kg)	Sensible Energy Per Dehumidification (kJ/kg)
2	1,873	4,737	-2,865	-4.1	2,530	-1.661	-4,175

20. 20

STATE POINT DATA

Air Flow (Standard) (kg/hr)	Dry Bulb (°C)	Wet Bulb (°C)	Relative Humidity (%)	Humidity Ratio (g/kg)	Specific Volume (cu.m/kg)	Enthalpy (kJ/kg)	Dew Point (°C)	Density (kg/cu.m)	Vapor Pressure (mm Hg)	Absolute Humidity (g/cu.m)
1,300.0	22.000	9.706	15.3	2.50	0.839	28.461	-4.9356	1.1946	3.0301	2.979

Process: Desiccant Dehumidification

Start Point Name	Total Energy (W/hr)	Sensible Energy (W/hr)	Latent Energy (W/hr)	Dehumidification (kg/hr)	Sensible Heat Ratio	Enthalpy/ Humidity Ratio (kJ/kg / g/kg)	Sensible Energy Per Dehumidification (kJ/kg)
2	2,602	5,466	-2,865	-4.1	2,101	-2.301	-4,815

21. 21

STATE POINT DATA

Air Flow (Standard) (kg/hr)	Dry Bulb (°C)	Wet Bulb (°C)	Relative Humidity (%)	Humidity Ratio (g/kg)	Specific Volume (cu.m/kg)	Enthalpy (kJ/kg)	Dew Point (°C)	Density (kg/cu.m)	Vapor Pressure (mm Hg)	Absolute Humidity (g/cu.m)
1,300.0	24.000	10.586	13.5	2.50	0.845	30.480	-4.9356	1.1866	3.0301	2.959

Process: Desiccant Dehumidification

Start Point Name	Total Energy (W/hr)	Sensible Energy (W/hr)	Latent Energy (W/hr)	Dehumidification (kg/hr)	Sensible Heat Ratio	Enthalpy/ Humidity Ratio (kJ/kg / g/kg)	Sensible Energy Per Dehumidification (kJ/kg)
2	3,331	6,195	-2,865	-4.1	1,860	-2.941	-5,454

22. 22

STATE POINT DATA

Air Flow (Standard) (kg/hr)	Dry Bulb (°C)	Wet Bulb (°C)	Relative Humidity (%)	Humidity Ratio (g/kg)	Specific Volume (cu.m/kg)	Enthalpy (kJ/kg)	Dew Point (°C)	Density (kg/cu.m)	Vapor Pressure (mm Hg)	Absolute Humidity (g/cu.m)
1,300.0	26.000	11.441	12.0	2.50	0.851	32.499	-4.9356	1.1787	3.0301	2.939

Process: Desiccant Dehumidification

Table 7.1 (D) State Point & Process Report

STATE POINT & PROCESS REPORT

Start Point Name	Total Energy (W/hr)	Sensible Energy (W/hr)	Latent Energy (W/hr)	Dehumidification (kg/hr)	Sensible Heat Ratio	Enthalpy/ Humidity Ratio (kJ/kg / g/kg)	Sensible Energy Per Dehumidification (kJ/kg)
2	4,059	6,924	-2,865	-4.1	1.706	-3.580	-6.094

23. 23

STATE POINT DATA

Air Flow (Standard) (kg/hr)	Dry Bulb (°C)	Wet Bulb (°C)	Relative Humidity (%)	Humidity Ratio (g/kg)	Specific Volume (cu.m/kg)	Enthalpy (kJ/kg)	Dew Point (°C)	Density (kg/cu.m)	Vapor Pressure (mm Hg)	Absolute Humidity (g/cu.m)
1,300.0	28.000	12.272	10.7	2.50	0.856	34.518	-4.9356	1.1708	3.0301	2.920

Process: Desiccant Dehumidification

Start Point Name	Total Energy (W/hr)	Sensible Energy (W/hr)	Latent Energy (W/hr)	Dehumidification (kg/hr)	Sensible Heat Ratio	Enthalpy/ Humidity Ratio (kJ/kg / g/kg)	Sensible Energy Per Dehumidification (kJ/kg)
2	4,788	7,653	-2,865	-4.1	1.598	-4.220	-6.734

24. 24

STATE POINT DATA

Air Flow (Standard) (kg/hr)	Dry Bulb (°C)	Wet Bulb (°C)	Relative Humidity (%)	Humidity Ratio (g/kg)	Specific Volume (cu.m/kg)	Enthalpy (kJ/kg)	Dew Point (°C)	Density (kg/cu.m)	Vapor Pressure (mm Hg)	Absolute Humidity (g/cu.m)
1,300.0	30.000	13.080	9.5	2.50	0.862	36.537	-4.9356	1.1631	3.0301	2.901

Process: Desiccant Dehumidification

Start Point Name	Total Energy (W/hr)	Sensible Energy (W/hr)	Latent Energy (W/hr)	Dehumidification (kg/hr)	Sensible Heat Ratio	Enthalpy/ Humidity Ratio (kJ/kg / g/kg)	Sensible Energy Per Dehumidification (kJ/kg)
2	5,517	8,382	-2,865	-4.1	1.519	-4.859	-7.373

Figure 7.8 shows the comparison between the hybrid system, desiccant wheel and the refrigerant circuit (heat pump) operating at the refrigerant load of 7.5 kW cooling capacity. The supply air DPT increases with the inlet temperature due to increased driving potential for mass transfer. Further, the supply air DPT of the hybrid system is lower than that of the refrigerant circuit and desiccant wheel at all inlet temperatures. This is because the hybrid system reduced the sensible and latent load on the cooling coil, resulting in reheat and dehumidification on desiccant wheel. In other words, the potential for sensible heat transfer is reduced, while the potential for moisture transfer is increased.

It is observed that supply air DPT of the hybrid system is lowered by about -20 °C compared with that the refrigerant circuit and desiccant wheel, which enables to maintain low humidity in the dryer.

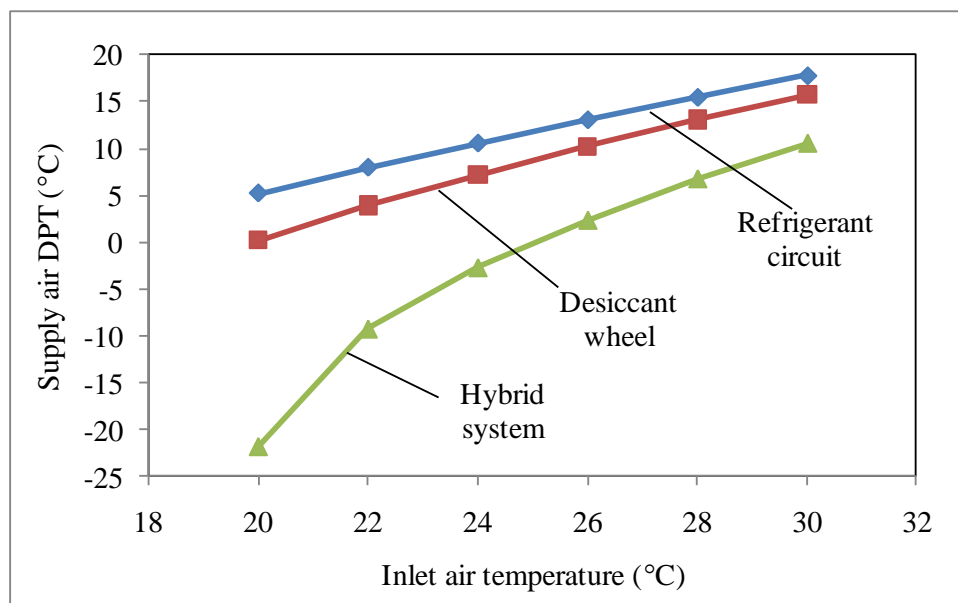


Fig 7.8 Effect of inlet air temperature on DPT

Figure 7.9 shows that the supply air DBT of the hybrid system is more than that of refrigerant circuit but less than that of desiccant wheel throughout the range of inlet air temperature. The hybrid system basically converts the latent load to sensible load by absorbing moisture and releasing heat to air. Hence its supply air DBT is always by approximately 13 °C higher throughout the range. However, it is less by about 12 °C when compared to that of the desiccant wheel. Thus the hybrid system is far better than single refrigerant circuit in providing low humidity, while the single desiccant wheel cannot provide low humidity at all. Thus the hybrid system can reach to minus twenty

one Celsius degree is far better than single refrigerant circuit in providing low humidity, while the single desiccant wheel cannot provide low humidity at all.

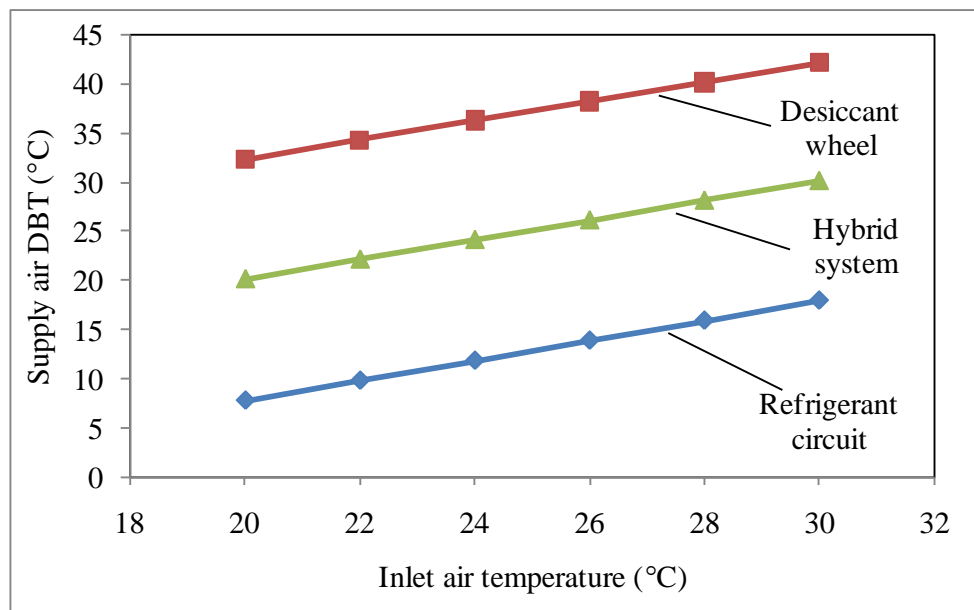


Fig 7.9 Effect of inlet air temperature on DBT

Figure 7.10 shows the airflow rate $1300 \text{ m}^3/\text{h}$, relative humidity = 60% and the same refrigerant circuit load 7.5 kW cooling capacity, which were outcomes read directly off the psychrometric chart. The variation for each system with respect to inlet air temperature from $20 \text{ }^\circ\text{C}$ to $30 \text{ }^\circ\text{C}$ is plotted in psychrometric chart. Table 7.2 (A) (B) (C) (D) shows the result of three systems using Psychrometric Analysis state point and process report.



ASHRAE PSYCHROMETRIC CHART NO. 1

NORMAL TEMPERATURE

BAROMETRIC PRESSURE: 101.325 kPa

Copyright 1992

AMERICAN SOCIETY OF HEATING, REFRIGERATING AND AIR-CONDITIONING ENGINEERS, INC.



SEA LEVEL

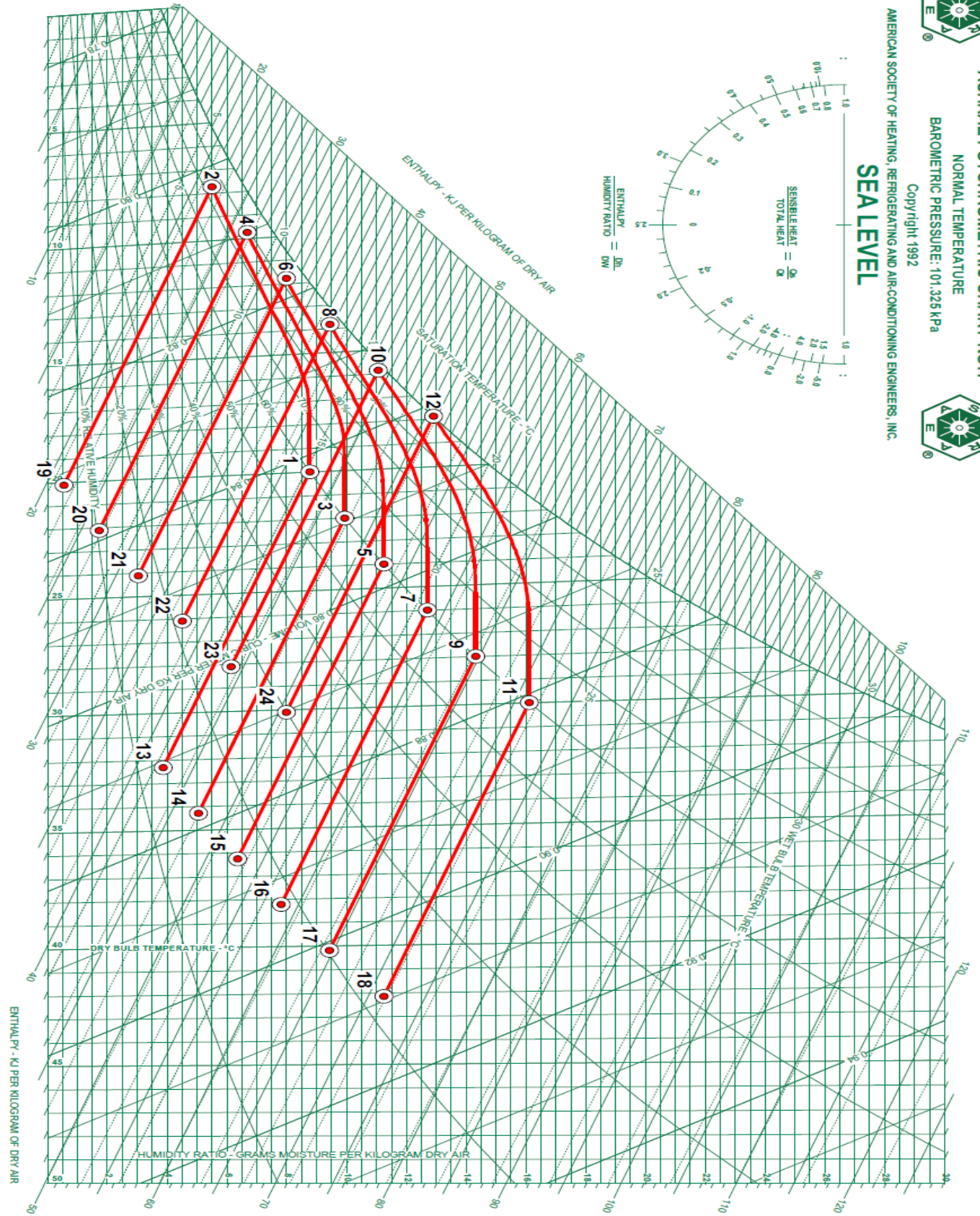


Fig 7.10 Psychrometric Chart

Table 7.2 (A) State Point & Process Report

STATE POINT & PROCESS REPORT

Report Date: Tuesday, March 15, 2011
 Project Information:

Altitude: 0 (Meters)
 Barometric Pressure: 760.001 (mm Hg)
 Atmospheric Pressure: 101.325 (kPa)

1.1

STATE POINT DATA

Air Flow (Standard) (kg/hr)	Dry Bulb (°C)	Wet Bulb (°C)	Relative Humidity (%)	Humidity Ratio (g/kg)	Specific Volume (cu.m/kg)	Enthalpy (kJ/kg)	Dew Point (°C)	Density (kg/cu.m)	Vapor Pressure (mm Hg)	Absolute Humidity (g/cu.m)
1,300.0	20.000	15.135	60.0	8.77	0.842	42.357	12.0093	1.1984	10.5267	10.418

2.2

STATE POINT DATA

Air Flow (Standard) (kg/hr)	Dry Bulb (°C)	Wet Bulb (°C)	Relative Humidity (%)	Humidity Ratio (g/kg)	Specific Volume (cu.m/kg)	Enthalpy (kJ/kg)	Dew Point (°C)	Density (kg/cu.m)	Vapor Pressure (mm Hg)	Absolute Humidity (g/cu.m)
1,300.0	7.721	6.466	84.0	5.50	0.802	21.584	5.1916	1.2531	6.6322	6.850

Process: Cooling Coil

Start Point Name	Total Cooling (kW/hr)	Total Energy (W/hr)	Sensible Energy (W/hr)	Latent Energy (W/hr)	Dehumidification (kg/hr)	Sensible Heat Ratio	Enthalpy/ Humidity Ratio (kJ/kg / g/kg)
1	-7.500	-7,500	-4,500	-3,000	-4.3	0.600	6.328

3.3

STATE POINT DATA

Air Flow (Standard) (kg/hr)	Dry Bulb (°C)	Wet Bulb (°C)	Relative Humidity (%)	Humidity Ratio (g/kg)	Specific Volume (cu.m/kg)	Enthalpy (kJ/kg)	Dew Point (°C)	Density (kg/cu.m)	Vapor Pressure (mm Hg)	Absolute Humidity (g/cu.m)
1,300.0	22.000	16.866	60.0	9.94	0.849	47.363	13.8879	1.1895	11.9041	11.702

4.4

STATE POINT DATA

Air Flow (Standard) (kg/hr)	Dry Bulb (°C)	Wet Bulb (°C)	Relative Humidity (%)	Humidity Ratio (g/kg)	Specific Volume (cu.m/kg)	Enthalpy (kJ/kg)	Dew Point (°C)	Density (kg/cu.m)	Vapor Pressure (mm Hg)	Absolute Humidity (g/cu.m)
1,300.0	9.747	8.796	88.7	6.67	0.810	26.590	7.9686	1.2433	8.0298	8.235

Process: Cooling Coil

Start Point Name	Total Cooling (kW/hr)	Total Energy (W/hr)	Sensible Energy (W/hr)	Latent Energy (W/hr)	Dehumidification (kg/hr)	Sensible Heat Ratio	Enthalpy/ Humidity Ratio (kJ/kg / g/kg)
3	-7.500	-7,500	-4,500	-3,000	-4.2	0.600	6.337

5.5

STATE POINT DATA

Air Flow (Standard) (kg/hr)	Dry Bulb (°C)	Wet Bulb (°C)	Relative Humidity (%)	Humidity Ratio (g/kg)	Specific Volume (cu.m/kg)	Enthalpy (kJ/kg)	Dew Point (°C)	Density (kg/cu.m)	Vapor Pressure (mm Hg)	Absolute Humidity (g/cu.m)
1,300.0	24.000	18.597	60.0	11.24	0.857	52.725	15.7656	1.1806	13.4364	13.120

6.6

STATE POINT DATA

Air Flow (Standard) (kg/hr)	Dry Bulb (°C)	Wet Bulb (°C)	Relative Humidity (%)	Humidity Ratio (g/kg)	Specific Volume (cu.m/kg)	Enthalpy (kJ/kg)	Dew Point (°C)	Density (kg/cu.m)	Vapor Pressure (mm Hg)	Absolute Humidity (g/cu.m)
1,300.0	11.776	11.101	92.4	7.97	0.817	31.951	10.5933	1.2335	9.5834	9.758

Process: Cooling Coil

Start Point Name	Total Cooling (kW/hr)	Total Energy (W/hr)	Sensible Energy (W/hr)	Latent Energy (W/hr)	Dehumidification (kg/hr)	Sensible Heat Ratio	Enthalpy/ Humidity Ratio (kJ/kg / g/kg)
5	-7.500	-7,500	-4,500	-3,000	-4.2	0.600	6.345

7.7

STATE POINT DATA

Air Flow (Standard) (kg/hr)	Dry Bulb (°C)	Wet Bulb (°C)	Relative Humidity (%)	Humidity Ratio (g/kg)	Specific Volume (cu.m/kg)	Enthalpy (kJ/kg)	Dew Point (°C)	Density (kg/cu.m)	Vapor Pressure (mm Hg)	Absolute Humidity (g/cu.m)
1,300.0	26.000	20.331	60.0	12.69	0.864	58.481	17.6422	1.1717	15.1383	14.683

8.8

STATE POINT DATA

Air Flow (Standard) (kg/hr)	Dry Bulb (°C)	Wet Bulb (°C)	Relative Humidity (%)	Humidity Ratio (g/kg)	Specific Volume (cu.m/kg)	Enthalpy (kJ/kg)	Dew Point (°C)	Density (kg/cu.m)	Vapor Pressure (mm Hg)	Absolute Humidity (g/cu.m)
1,300.0	13.808	13.381	95.5	9.43	0.825	37.707	13.1018	1.2238	11.3096	11.435

Process: Cooling Coil

Start Point Name	Total Cooling (kW/hr)	Total Energy (W/hr)	Sensible Energy (W/hr)	Latent Energy (W/hr)	Dehumidification (kg/hr)	Sensible Heat Ratio	Enthalpy/ Humidity Ratio (kJ/kg / g/kg)
7	-7.500	-7,500	-4,500	-3,000	-4.2	0.600	6.356

Table 7.2 (B) State Point & Process Report

STATE POINT & PROCESS REPORT

9. 9

STATE POINT DATA

Air Flow (Standard) (kg/hr)	Dry Bulb (°C)	Wet Bulb (°C)	Relative Humidity (%)	Humidity Ratio (g/kg)	Specific Volume (cu.m/kg)	Enthalpy (kJ/kg)	Dew Point (°C)	Density (kg/cu.m)	Vapor Pressure (mm Hg)	Absolute Humidity (g/cu.m)
1,300.0	28.000	22.068	60.0	14.31	0.872	64.671	19.5177	1.1629	17.0251	16.404

10. 10

STATE POINT DATA

Air Flow (Standard) (kg/hr)	Dry Bulb (°C)	Wet Bulb (°C)	Relative Humidity (%)	Humidity Ratio (g/kg)	Specific Volume (cu.m/kg)	Enthalpy (kJ/kg)	Dew Point (°C)	Density (kg/cu.m)	Vapor Pressure (mm Hg)	Absolute Humidity (g/cu.m)
1,300.0	15.844	15.635	97.9	11.06	0.833	43.897	15.5143	1.2140	13.2219	13.274

Process: Cooling Coil

Start Point Name	Total Cooling (kW/hr)	Total Energy (W/hr)	Sensible Energy (W/hr)	Latent Energy (W/hr)	Dehumidification (kg/hr)	Sensible Heat Ratio	Enthalpy/ Humidity Ratio (kJ/kg / g/kg)
9	-7.500	-7,500	-4,500	-3,000	-4.2	0.600	6.365

11. 11

STATE POINT DATA

Air Flow (Standard) (kg/hr)	Dry Bulb (°C)	Wet Bulb (°C)	Relative Humidity (%)	Humidity Ratio (g/kg)	Specific Volume (cu.m/kg)	Enthalpy (kJ/kg)	Dew Point (°C)	Density (kg/cu.m)	Vapor Pressure (mm Hg)	Absolute Humidity (g/cu.m)
1,300.0	30.000	23.807	60.0	16.11	0.881	71.340	21.3921	1.1541	19.1135	18.295

12. 12

STATE POINT DATA

Air Flow (Standard) (kg/hr)	Dry Bulb (°C)	Wet Bulb (°C)	Relative Humidity (%)	Humidity Ratio (g/kg)	Specific Volume (cu.m/kg)	Enthalpy (kJ/kg)	Dew Point (°C)	Density (kg/cu.m)	Vapor Pressure (mm Hg)	Absolute Humidity (g/cu.m)
1,300.0	17.890	17.890	100.0	12.90	0.841	50.657	17.8900	1.2042	15.3766	15.330

Process: Cooling Coil

Start Point Name	Total Cooling (kW/hr)	Total Energy (W/hr)	Sensible Energy (W/hr)	Latent Energy (W/hr)	Dehumidification (kg/hr)	Sensible Heat Ratio	Enthalpy/ Humidity Ratio (kJ/kg / g/kg)
11	-7.467	-7,467	-4,498	-2,969	-4.2	0.602	6.412

13. 13

STATE POINT DATA

Air Flow (Standard) (kg/hr)	Dry Bulb (°C)	Wet Bulb (°C)	Relative Humidity (%)	Humidity Ratio (g/kg)	Specific Volume (cu.m/kg)	Enthalpy (kJ/kg)	Dew Point (°C)	Density (kg/cu.m)	Vapor Pressure (mm Hg)	Absolute Humidity (g/cu.m)
1,300.0	32.317	15.253	12.8	3.86	0.870	42.356	0.2497	1.1534	4.6683	4.434

Process: Desiccant Dehumidification

Start Point Name	Total Energy (W/hr)	Sensible Energy (W/hr)	Latent Energy (W/hr)	Dehumidification (kg/hr)	Sensible Heat Ratio	Enthalpy/ Humidity Ratio (kJ/kg / g/kg)	Sensible Energy Per Dehumidification (kJ/kg)
1	0	4,500	-4,500	-6.4	-15358.000	-0.018	-2.556

14. 14

STATE POINT DATA

Air Flow (Standard) (kg/hr)	Dry Bulb (°C)	Wet Bulb (°C)	Relative Humidity (%)	Humidity Ratio (g/kg)	Specific Volume (cu.m/kg)	Enthalpy (kJ/kg)	Dew Point (°C)	Density (kg/cu.m)	Vapor Pressure (mm Hg)	Absolute Humidity (g/cu.m)
1,300.0	34.290	16.991	15.0	5.03	0.878	47.368	3.9467	1.1452	6.0788	5.736

Process: Desiccant Dehumidification

Start Point Name	Total Energy (W/hr)	Sensible Energy (W/hr)	Latent Energy (W/hr)	Dehumidification (kg/hr)	Sensible Heat Ratio	Enthalpy/ Humidity Ratio (kJ/kg / g/kg)	Sensible Energy Per Dehumidification (kJ/kg)
3	1	4,500	-4,498	-6.4	3071.600	-0.019	-2.561

15. 15

STATE POINT DATA

Air Flow (Standard) (kg/hr)	Dry Bulb (°C)	Wet Bulb (°C)	Relative Humidity (%)	Humidity Ratio (g/kg)	Specific Volume (cu.m/kg)	Enthalpy (kJ/kg)	Dew Point (°C)	Density (kg/cu.m)	Vapor Pressure (mm Hg)	Absolute Humidity (g/cu.m)
1,300.0	36.261	18.725	16.9	6.34	0.885	52.727	7.2454	1.1370	7.6428	7.166

Process: Desiccant Dehumidification

Start Point Name	Total Energy (W/hr)	Sensible Energy (W/hr)	Latent Energy (W/hr)	Dehumidification (kg/hr)	Sensible Heat Ratio	Enthalpy/ Humidity Ratio (kJ/kg / g/kg)	Sensible Energy Per Dehumidification (kJ/kg)
5	1	4,500	-4,499	-6.4	7679.000	-0.018	-2.564

16. 16

STATE POINT DATA

Table 7.2 (C) State Point & Process Report

STATE POINT & PROCESS REPORT

Air Flow (Standard) (kg/hr)	Dry Bulb (°C)	Wet Bulb (°C)	Relative Humidity (%)	Humidity Ratio (g/kg)	Specific Volume (cu.m/kg)	Enthalpy (kJ/kg)	Dew Point (°C)	Density (kg/cu.m)	Vapor Pressure (mm Hg)	Absolute Humidity (g/cu.m)
1,300.0	38.227	20.462	18.6	7.80	0.893	58.482	10.2729	1.1289	9.3805	8.740

Process: Desiccant Dehumidification

Start Point Name	Total Energy (W/hr)	Sensible Energy (W/hr)	Latent Energy (W/hr)	Dehumidification (kg/hr)	Sensible Heat Ratio	Enthalpy/ Humidity Ratio (kJ/kg / g/kg)	Sensible Energy Per Dehumidification (kJ/kg)
7	0	4,499	-4,499	-6.4	15358.000	-0.018	-2,567

17. 17

STATE POINT DATA

Air Flow (Standard) (kg/hr)	Dry Bulb (°C)	Wet Bulb (°C)	Relative Humidity (%)	Humidity Ratio (g/kg)	Specific Volume (cu.m/kg)	Enthalpy (kJ/kg)	Dew Point (°C)	Density (kg/cu.m)	Vapor Pressure (mm Hg)	Absolute Humidity (g/cu.m)
1,300.0	40.192	22.200	20.2	9.43	0.901	64.673	13.0965	1.1207	11.3056	10.468

Process: Desiccant Dehumidification

Start Point Name	Total Energy (W/hr)	Sensible Energy (W/hr)	Latent Energy (W/hr)	Dehumidification (kg/hr)	Sensible Heat Ratio	Enthalpy/ Humidity Ratio (kJ/kg / g/kg)	Sensible Energy Per Dehumidification (kJ/kg)
9	1	4,500	-4,499	-6.3	7679.000	-0.018	-2,571

18. 18

STATE POINT DATA

Air Flow (Standard) (kg/hr)	Dry Bulb (°C)	Wet Bulb (°C)	Relative Humidity (%)	Humidity Ratio (g/kg)	Specific Volume (cu.m/kg)	Enthalpy (kJ/kg)	Dew Point (°C)	Density (kg/cu.m)	Vapor Pressure (mm Hg)	Absolute Humidity (g/cu.m)
1,300.0	42.150	23.938	21.6	11.24	0.909	71.336	15.7624	1.1126	13.4338	12.362

Process: Desiccant Dehumidification

Start Point Name	Total Energy (W/hr)	Sensible Energy (W/hr)	Latent Energy (W/hr)	Dehumidification (kg/hr)	Sensible Heat Ratio	Enthalpy/ Humidity Ratio (kJ/kg / g/kg)	Sensible Energy Per Dehumidification (kJ/kg)
11	-1	4,499	-4,500	-6.3	-3838.750	-0.017	-2,574

19. 19

STATE POINT DATA

Air Flow (Standard) (kg/hr)	Dry Bulb (°C)	Wet Bulb (°C)	Relative Humidity (%)	Humidity Ratio (g/kg)	Specific Volume (cu.m/kg)	Enthalpy (kJ/kg)	Dew Point (°C)	Density (kg/cu.m)	Vapor Pressure (mm Hg)	Absolute Humidity (g/cu.m)
1,300.0	20.113	6.533	3.7	0.54	0.831	21.586	-21.6778	1.2037	0.6586	0.652

Process: Desiccant Dehumidification

Start Point Name	Total Energy (W/hr)	Sensible Energy (W/hr)	Latent Energy (W/hr)	Dehumidification (kg/hr)	Sensible Heat Ratio	Enthalpy/ Humidity Ratio (kJ/kg / g/kg)	Sensible Energy Per Dehumidification (kJ/kg)
2	0	4,500	-4,500	-6.4	15358.000	-0.018	-2,533

20. 20

STATE POINT DATA

Air Flow (Standard) (kg/hr)	Dry Bulb (°C)	Wet Bulb (°C)	Relative Humidity (%)	Humidity Ratio (g/kg)	Specific Volume (cu.m/kg)	Enthalpy (kJ/kg)	Dew Point (°C)	Density (kg/cu.m)	Vapor Pressure (mm Hg)	Absolute Humidity (g/cu.m)
1,300.0	22.112	8.881	10.4	1.72	0.838	26.591	-9.2297	1.1947	2.0870	2.051

Process: Desiccant Dehumidification

Start Point Name	Total Energy (W/hr)	Sensible Energy (W/hr)	Latent Energy (W/hr)	Dehumidification (kg/hr)	Sensible Heat Ratio	Enthalpy/ Humidity Ratio (kJ/kg / g/kg)	Sensible Energy Per Dehumidification (kJ/kg)
4	0	4,500	-4,500	-6.4	-999.000	-0.018	-2,537

21. 21

STATE POINT DATA

Air Flow (Standard) (kg/hr)	Dry Bulb (°C)	Wet Bulb (°C)	Relative Humidity (%)	Humidity Ratio (g/kg)	Specific Volume (cu.m/kg)	Enthalpy (kJ/kg)	Dew Point (°C)	Density (kg/cu.m)	Vapor Pressure (mm Hg)	Absolute Humidity (g/cu.m)
1,300.0	24.112	11.199	16.3	3.03	0.846	31.948	-2.6671	1.1858	3.6721	3.585

Process: Desiccant Dehumidification

Start Point Name	Total Energy (W/hr)	Sensible Energy (W/hr)	Latent Energy (W/hr)	Dehumidification (kg/hr)	Sensible Heat Ratio	Enthalpy/ Humidity Ratio (kJ/kg / g/kg)	Sensible Energy Per Dehumidification (kJ/kg)
6	-1	4,500	-4,501	-6.4	-3839.750	-0.017	-2,540

22. 22

STATE POINT DATA

Air Flow (Standard) (kg/hr)	Dry Bulb (°C)	Wet Bulb (°C)	Relative Humidity (%)	Humidity Ratio (g/kg)	Specific Volume (cu.m/kg)	Enthalpy (kJ/kg)	Dew Point (°C)	Density (kg/cu.m)	Vapor Pressure (mm Hg)	Absolute Humidity (g/cu.m)
1,300.0	26.110	13.491	21.4	4.50	0.854	37.708	2.3723	1.1768	5.4376	5.272

Process: Desiccant Dehumidification

Table 7.2 (D) State Point & Process Report

STATE POINT & PROCESS REPORT

Start Point Name	Total Energy (W/hr)	Sensible Energy (W/hr)	Latent Energy (W/hr)	Dehumidification (kg/hr)	Sensible Heat Ratio	Enthalpy/ Humidity Ratio (kJ/kg / g/kg)	Sensible Energy Per Dehumidification (kJ/kg)
8	0	4,500	-4,500	-6.4	-999.000	-0.018	-2,545

23. 23

STATE POINT DATA

Air Flow (Standard) (kg/hr)	Dry Bulb (°C)	Wet Bulb (°C)	Relative Humidity (%)	Humidity Ratio (g/kg)	Specific Volume (cu.m/kg)	Enthalpy (kJ/kg)	Dew Point (°C)	Density (kg/cu.m)	Vapor Pressure (mm Hg)	Absolute Humidity (g/cu.m)
1,300.0	28.110	15.752	25.9	6.13	0.862	43.897	6.7530	1.1679	7.3889	7.116

Process: Desiccant Dehumidification

Start Point Name	Total Energy (W/hr)	Sensible Energy (W/hr)	Latent Energy (W/hr)	Dehumidification (kg/hr)	Sensible Heat Ratio	Enthalpy/ Humidity Ratio (kJ/kg / g/kg)	Sensible Energy Per Dehumidification (kJ/kg)
10	0	4,500	-4,500	-6.4	-999.000	-0.018	-2,548

24. 24

STATE POINT DATA

Air Flow (Standard) (kg/hr)	Dry Bulb (°C)	Wet Bulb (°C)	Relative Humidity (%)	Humidity Ratio (g/kg)	Specific Volume (cu.m/kg)	Enthalpy (kJ/kg)	Dew Point (°C)	Density (kg/cu.m)	Vapor Pressure (mm Hg)	Absolute Humidity (g/cu.m)
1,300.0	30.110	18.014	29.9	7.98	0.870	50.659	10.6037	1.1590	9.5900	9.175

Process: Desiccant Dehumidification

Start Point Name	Total Energy (W/hr)	Sensible Energy (W/hr)	Latent Energy (W/hr)	Dehumidification (kg/hr)	Sensible Heat Ratio	Enthalpy/ Humidity Ratio (kJ/kg / g/kg)	Sensible Energy Per Dehumidification (kJ/kg)
12	1	4,498	-4,498	-6.4	7676.500	-0.018	-2,552

7.3 Effect of Airflow Rate

The flow rate of the drying air is an important parameter in the drying system which uses the air flow and it is closely related to the air velocity in the drying process. The high air velocity causes the water to evaporate rapidly but the quality of the products might be degraded. The low air velocity causes the drying rate to decrease and then the productivity also decreases. Thus, an appropriate flow rate should be determined for the dryer operation in the optimum condition to achieve a high quality product.

In this section, experiments were conducted to study the effect of regulating the airflow rate by the control damper. The three systems were tested at the following conditions, airflow rate from 1000m³/h to 1500m³/h, inlet air temperature fixed at 25°C, relative humidity = 60% and outlet air dew point temperature kept at 5.6°C.

Figure 7.11 illustrates that in all three systems the input power energy increases significantly with airflow rate. However the rate of increase in input energy in the hybrid system is significantly less when compared the rate of increase in input energy for the desiccant wheel but when compared with the refrigerant circuit system the rate of increase is similar. However the input energy for hybrid system is the least of all the systems. This is because condenser heat release is more than the heat recovered by the evaporator

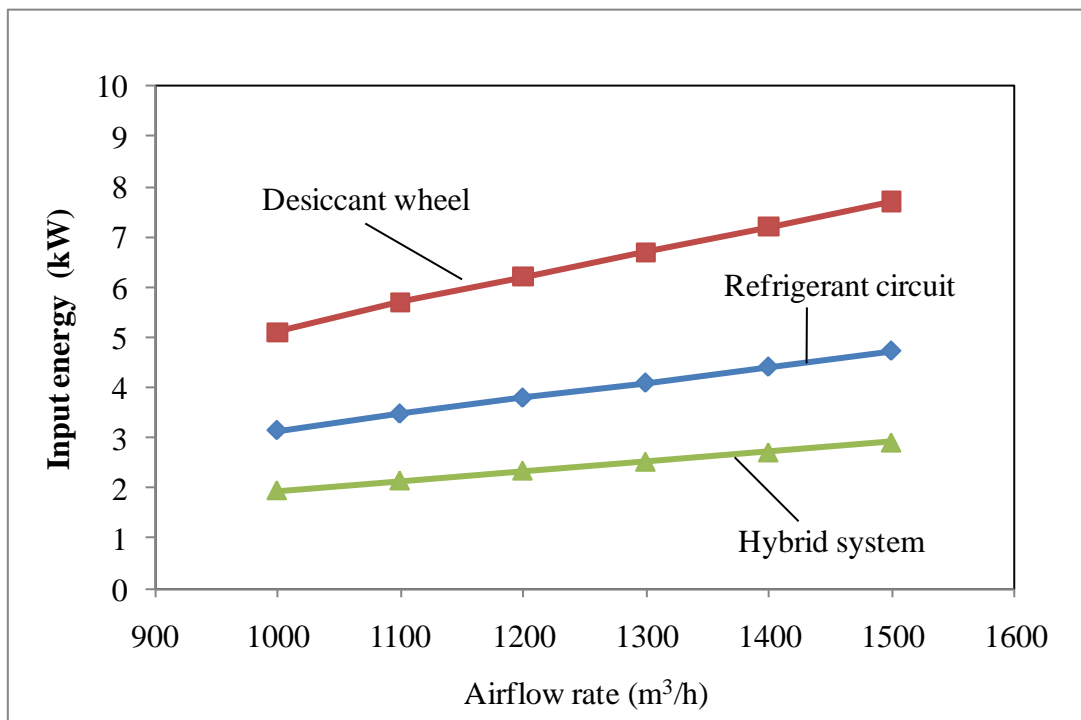


Fig 7.11 Effect of airflow rate on input energy required

Figure 7.12 shows there is no change in the SMER when the airflow rate is increased though all three systems. This is because as the airflow rate increases the input power energy also increases in the system to meet the change in the humidity ratio.

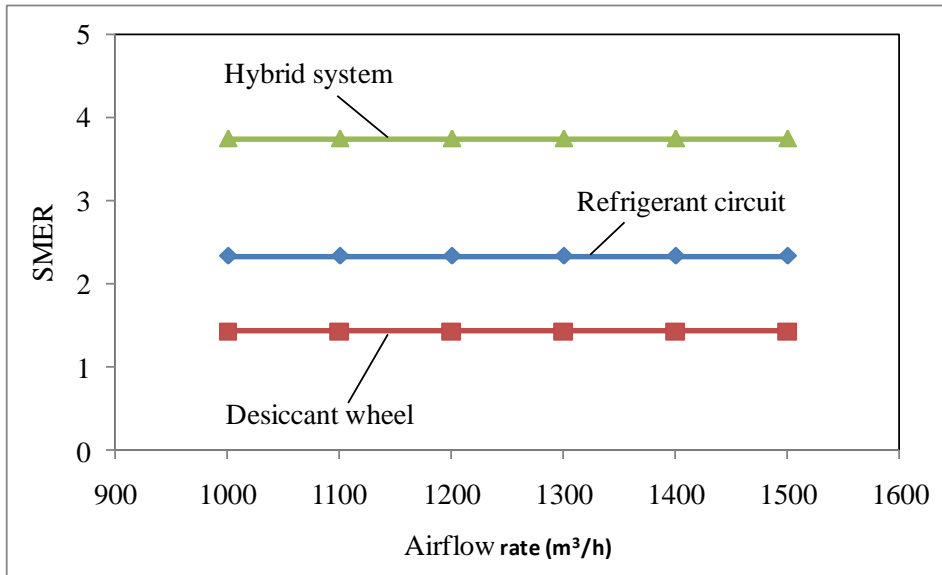


Fig 7.12 Effect of airflow rate on SMER

Figure 7.13 shows that the sensible heat energy increases with the airflow rate for all three systems, which is attributed to a small residence time. In the case of hybrid system (desiccant wheel is integrated system); the desiccant wheel further dehumidifies the air. The sensible heat energy required is lower by about 1.5 kW when compared with that of desiccant wheel systems.

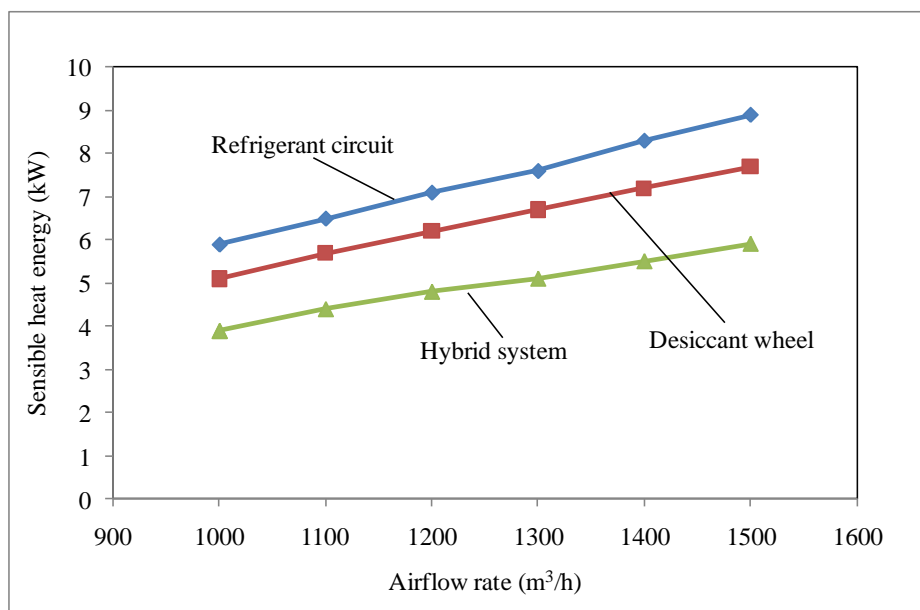


Fig 7.13 Effect of airflow rate on sensible heat energy

The variation in dew point temperature with respect to air flow rate is compared in Figure 7.14 for the three systems. It is evident that the DPT increases with the increasing airflow rate in all three systems, which is attributed to a short residence time. The hybrid system integrated refrigerant circuit and desiccant wheel is driven by the same refrigerant circuit load of 7.5 kW cooling capacity. In the case of hybrid system, the integrated desiccant wheel further dehumidifies the air and the dew point temperature is lowered by about -3.7 °C compared with that of refrigerant circuit and desiccant wheel signifying the effectiveness of the former for achieving low humidity air.

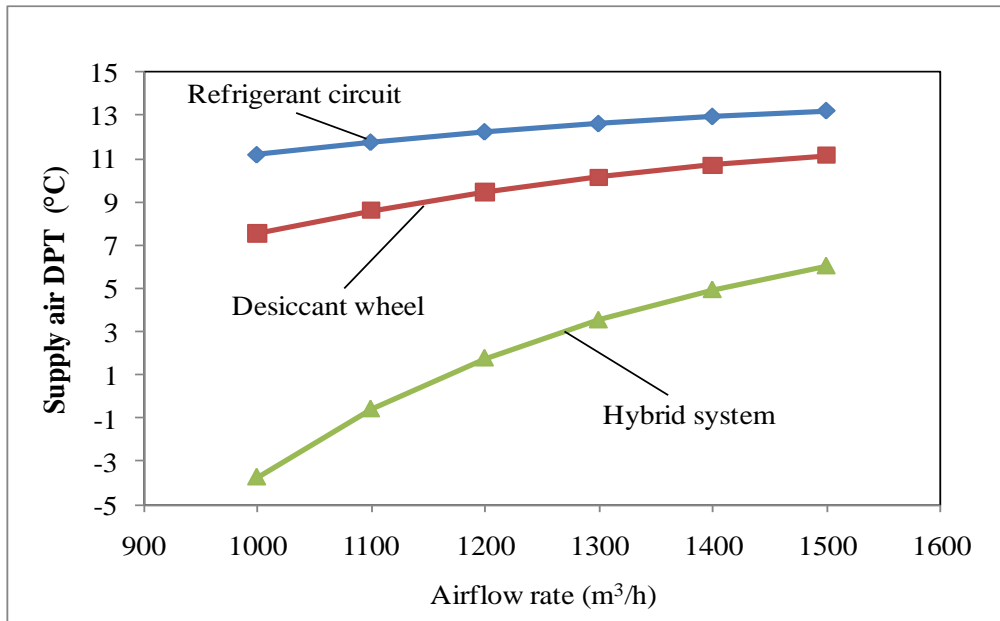


Fig 7.14 Effect of airflow rate on DPT

Figure 7.15 depicts the correlations between the airflow rate and the supply air temperature. It can be seen that the supply temperature of the hybrid system is higher than that of the refrigerant circuit but less than that of desiccant wheel throughout the range of the airflow rate. The hybrid system basically converts the latent load to a sensible load by absorbing moisture and releasing heat to air. Hence its supply air temperature is always higher by about 15 °C throughout the range. However, it is less by about 13 °C compared with that of the desiccant wheel. Thus the hybrid system is far better than single refrigerant circuit in providing low humidity, while the single desiccant wheel cannot provide low humidity at all. The hybrid system integrated refrigerant circuit and desiccant wheel is driven by the same refrigerant circuit load of 7.5 kW cooling capacity can deliver lower dew point temperature compare to other two systems.

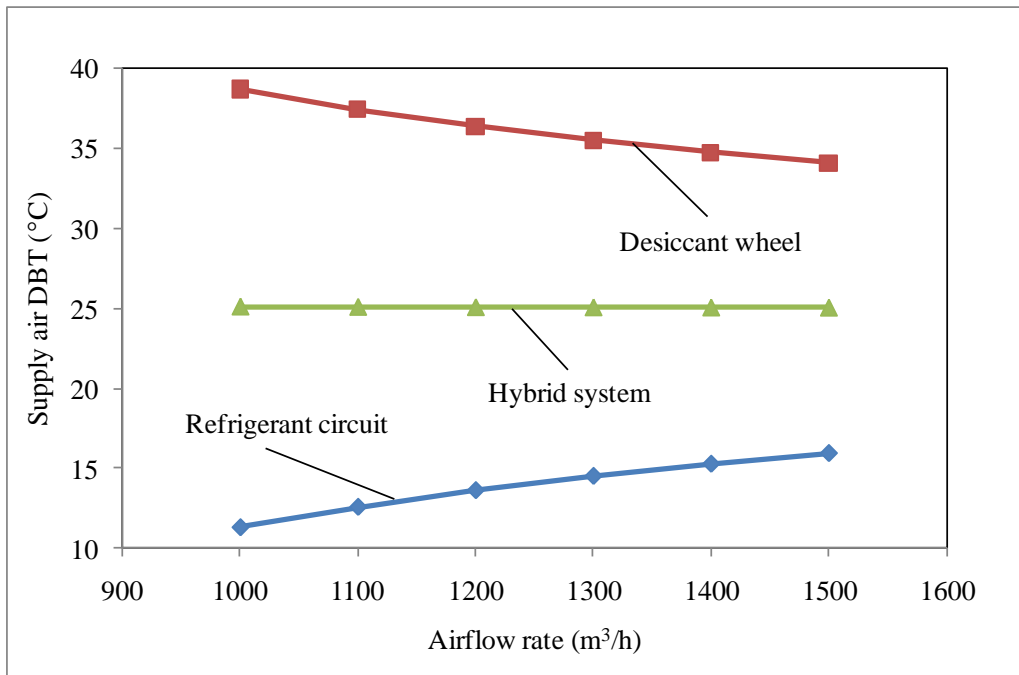


Fig 7.15 Effect of airflow rate on DBT

Figure 7.16 shows the airflow rate from 1000m³/h to 1500m³/h, inlet air temperature fixed at 25°C, relative humidity = 60% and outlet air dew point temperature kept at 5.6°C., the variation for each system is plotted in psychrometric chart. Table 7.3 shows the result of three systems state point and process report.

Figure 7.17 shows the airflow rate from 1000m³/h to 1500m³/h, inlet air temperature fixed at 25°C, relative humidity = 60% and the same refrigerant circuit load of 7.5 kW cooling capacity, which were outcomes read directly off the psychrometric chart. The variation for each system is plotted in psychrometric chart. Table 7.4 (A) (B) (C) (D) shows the result of three systems using Psychrometric Analysis state point and process report.



ASHRAE PSYCHROMETRIC CHART NO. 1

NORMAL TEMPERATURE

BAROMETRIC PRESSURE: 101.325 kPa

Copyright 1992

AMERICAN SOCIETY OF HEATING, REFRIGERATING AND AIR-CONDITIONING ENGINEERS, INC.



SEA LEVEL

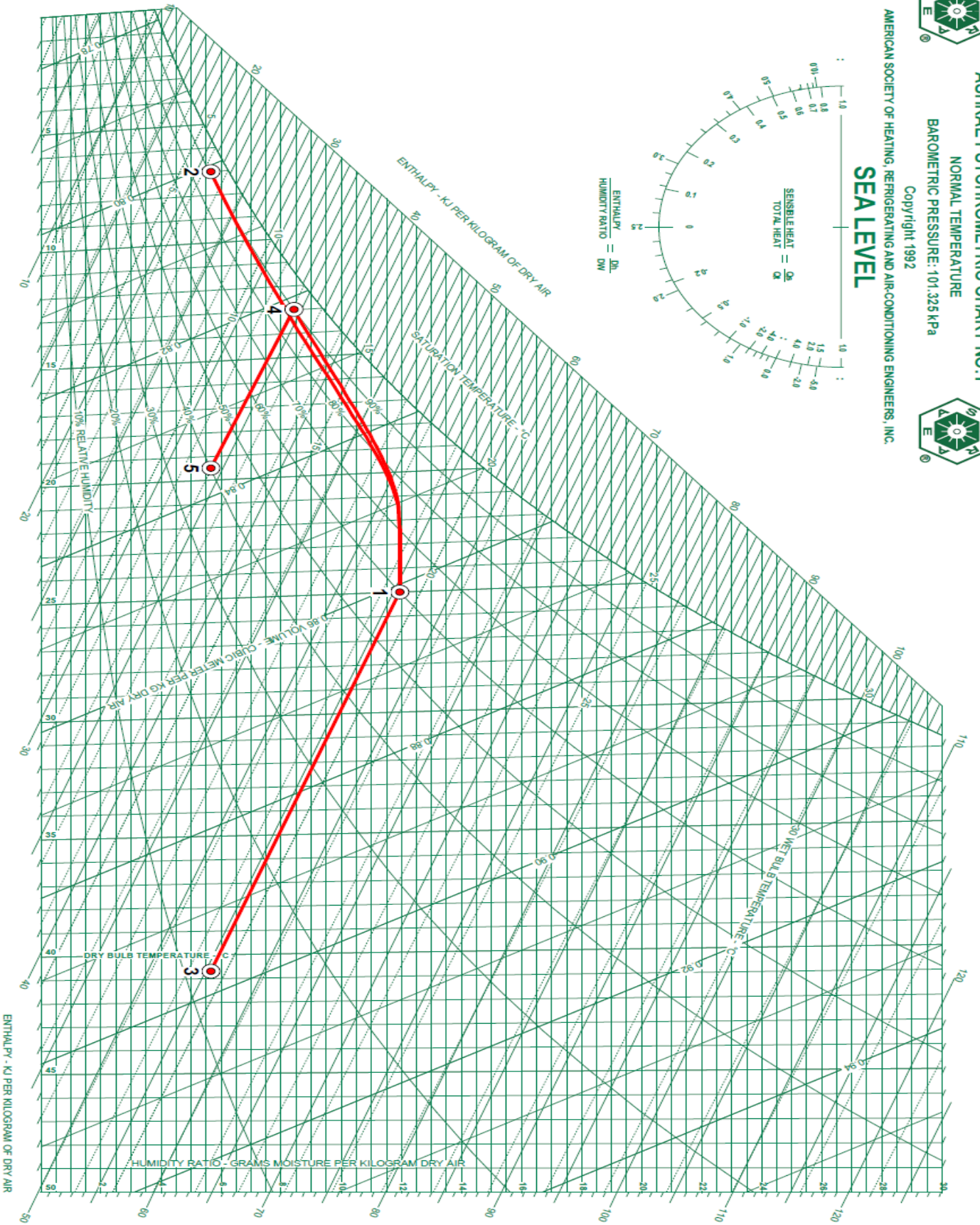
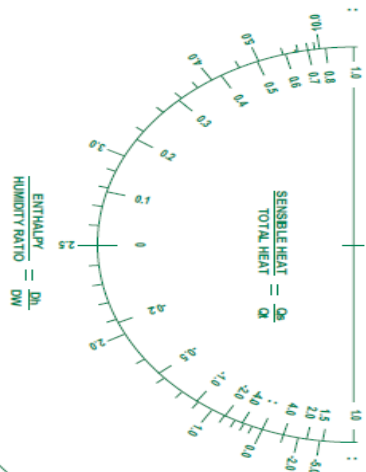


Fig 7.16 Psychrometric Chart

Table 7.3 State Point & Process Report

STATE POINT & PROCESS REPORT

Report Date: Tuesday, March 15, 2011
 Project Information:

Altitude: 0 (Meters)
 Barometric Pressure: 760.001 (mm Hg)
 Atmospheric Pressure: 101.325 (kPa)

1. 1

STATE POINT DATA

Air Flow (Standard) (kg/hr)	Dry Bulb (°C)	Wet Bulb (°C)	Relative Humidity (%)	Humidity Ratio (g/kg)	Specific Volume (cu.m/kg)	Enthalpy (kJ/kg)	Dew Point (°C)	Density (kg/cu.m)	Vapor Pressure (mm Hg)	Absolute Humidity (g/cu.m)
1,300.0	25.000	19.464	60.0	11.95	0.861	55.552	16.7040	1.1762	14.2653	13.882

2. 2

STATE POINT DATA

Air Flow (Standard) (kg/hr)	Dry Bulb (°C)	Wet Bulb (°C)	Relative Humidity (%)	Humidity Ratio (g/kg)	Specific Volume (cu.m/kg)	Enthalpy (kJ/kg)	Dew Point (°C)	Density (kg/cu.m)	Vapor Pressure (mm Hg)	Absolute Humidity (g/cu.m)
1,300.0	7.000	6.303	90.8	5.66	0.801	21.254	5.6000	1.2563	6.8232	7.066

Process: Cooling Coil

Start Point Name	Total Cooling (kW/hr)	Total Energy (W/hr)	Sensible Energy (W/hr)	Latent Energy (W/hr)	Dehumidification (kg/hr)	Sensible Heat Ratio	Enthalpy/Humidity Ratio (kJ/kg / g/kg)
1	-12.382	-12,382	-6,598	-5,784	-8.2	0.533	5.435

3. 3

STATE POINT DATA

Air Flow (Standard) (kg/hr)	Dry Bulb (°C)	Wet Bulb (°C)	Relative Humidity (%)	Humidity Ratio (g/kg)	Specific Volume (cu.m/kg)	Enthalpy (kJ/kg)	Dew Point (°C)	Density (kg/cu.m)	Vapor Pressure (mm Hg)	Absolute Humidity (g/cu.m)
1,300.0	40.700	19.606	11.9	5.66	0.897	55.471	5.6000	1.1214	6.8232	6.307

Process: Desiccant Dehumidification

Start Point Name	Total Energy (W/hr)	Sensible Energy (W/hr)	Latent Energy (W/hr)	Dehumidification (kg/hr)	Sensible Heat Ratio	Enthalpy/Humidity Ratio (kJ/kg / g/kg)	Sensible Energy Per Dehumidification (kJ/kg / g/kg)
1	-29	5,755	-5,784	-8.2	-198.394	-0.005	-2,552

4. 4

STATE POINT DATA

Air Flow (Standard) (kg/hr)	Dry Bulb (°C)	Wet Bulb (°C)	Relative Humidity (%)	Humidity Ratio (g/kg)	Specific Volume (cu.m/kg)	Enthalpy (kJ/kg)	Dew Point (°C)	Density (kg/cu.m)	Vapor Pressure (mm Hg)	Absolute Humidity (g/cu.m)
1,300.0	13.000	12.067	90.0	8.42	0.821	34.323	11.4000	1.2279	10.1112	10.252

Process: Cooling Coil

Start Point Name	Total Cooling (kW/hr)	Total Energy (W/hr)	Sensible Energy (W/hr)	Latent Energy (W/hr)	Dehumidification (kg/hr)	Sensible Heat Ratio	Enthalpy/Humidity Ratio (kJ/kg / g/kg)
1	-7.664	-7,664	-4,421	-3,243	-4.6	0.577	6.002

5. 5

STATE POINT DATA

Air Flow (Standard) (kg/hr)	Dry Bulb (°C)	Wet Bulb (°C)	Relative Humidity (%)	Humidity Ratio (g/kg)	Specific Volume (cu.m/kg)	Enthalpy (kJ/kg)	Dew Point (°C)	Density (kg/cu.m)	Vapor Pressure (mm Hg)	Absolute Humidity (g/cu.m)
1,300.0	19.500	11.971	40.1	5.66	0.836	33.946	5.6000	1.2026	6.8232	6.764

Process: Desiccant Dehumidification

Start Point Name	Total Energy (W/hr)	Sensible Energy (W/hr)	Latent Energy (W/hr)	Dehumidification (kg/hr)	Sensible Heat Ratio	Enthalpy/Humidity Ratio (kJ/kg / g/kg)	Sensible Energy Per Dehumidification (kJ/kg / g/kg)
4	-136	2,382	-2,519	-3.6	-17.486	0.119	-2,406



ASHRAE PSYCHROMETRIC CHART NO. 1

NORMAL TEMPERATURE

BAROMETRIC PRESSURE: 101.325 kPa

Copyright 1992

AMERICAN SOCIETY OF HEATING, REFRIGERATING AND AIR-CONDITIONING ENGINEERS, INC.



SEA LEVEL

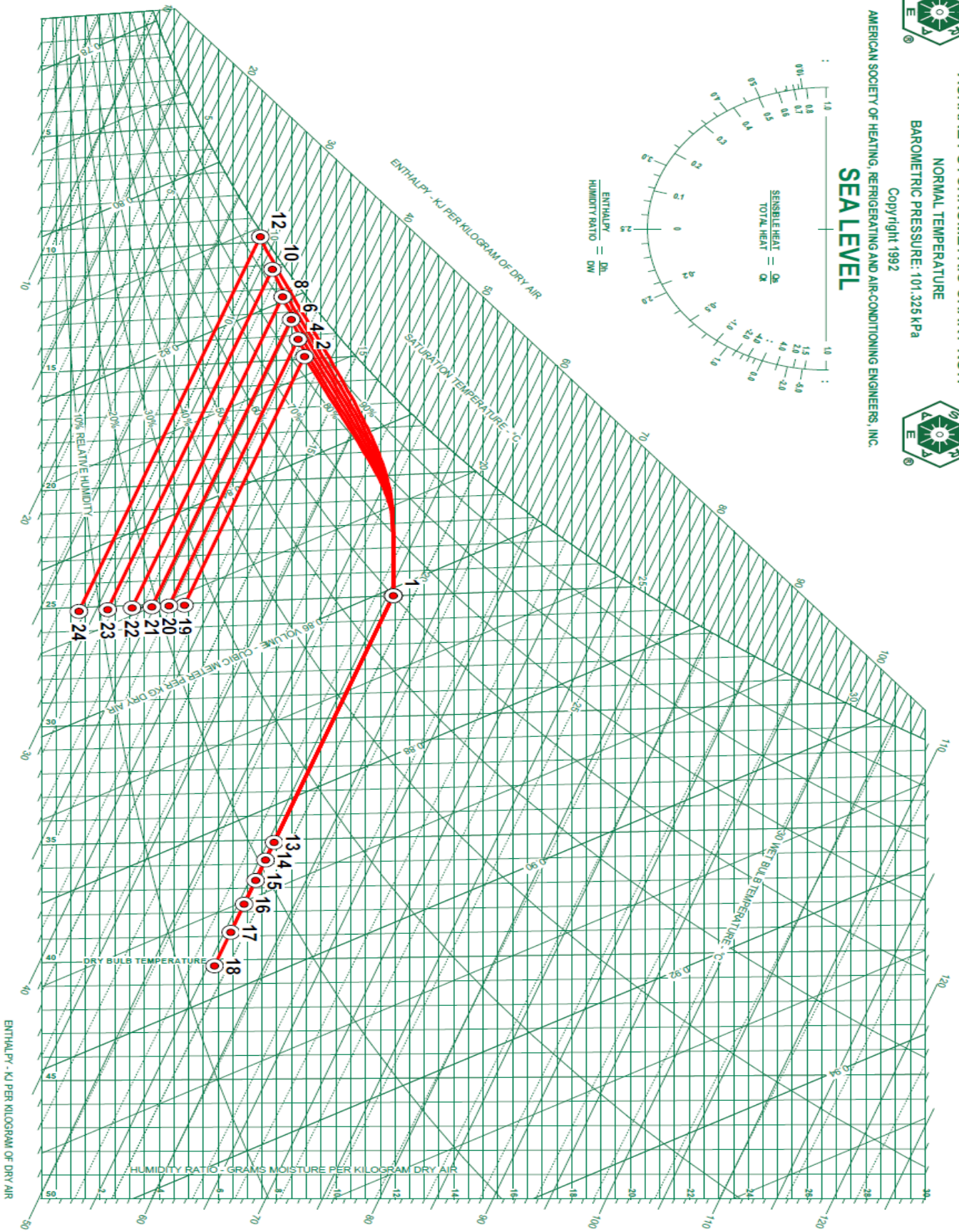
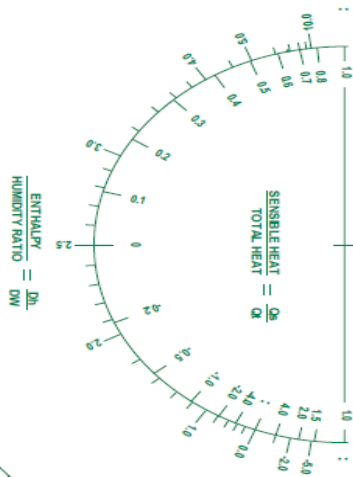


Fig 7.17 Psychrometric Chart

Table 7.4 (A) State Point & Process Report

STATE POINT & PROCESS REPORT

Report Date: Tuesday, March 15, 2011
 Project Information:

Altitude: 0 (Meters)
 Barometric Pressure: 760.001 (mm Hg)
 Atmospheric Pressure: 101.325 (kPa)

1. 1

STATE POINT DATA

Air Flow (Standard) (kg/hr)	Dry Bulb (°C)	Wet Bulb (°C)	Relative Humidity (%)	Humidity Ratio (g/kg)	Specific Volume (cu.m/kg)	Enthalpy (kJ/kg)	Dew Point (°C)	Density (kg/cu.m)	Vapor Pressure (mm Hg)	Absolute Humidity (g/cu.m)
1,500.0	25.000	19.464	60.0	11.95	0.861	55.552	16.7040	1.1762	14.2653	13.882

2. 2

STATE POINT DATA

Air Flow (Standard) (kg/hr)	Dry Bulb (°C)	Wet Bulb (°C)	Relative Humidity (%)	Humidity Ratio (g/kg)	Specific Volume (cu.m/kg)	Enthalpy (kJ/kg)	Dew Point (°C)	Density (kg/cu.m)	Vapor Pressure (mm Hg)	Absolute Humidity (g/cu.m)
1,500.0	14.894	13.330	84.3	8.93	0.827	37.547	12.2791	1.2195	10.7155	10.793

Process: Cooling Coil

Start Point Name	Total Cooling (kW/hr)	Total Energy (W/hr)	Sensible Energy (W/hr)	Latent Energy (W/hr)	Dehumidification (kg/hr)	Sensible Heat Ratio	Enthalpy/ Humidity Ratio (kJ/kg / g/kg)
1	-7.500	-7,500	-4,300	-3,200	-4.5	0.573	5.952

3. 1

STATE POINT DATA

Air Flow (Standard) (kg/hr)	Dry Bulb (°C)	Wet Bulb (°C)	Relative Humidity (%)	Humidity Ratio (g/kg)	Specific Volume (cu.m/kg)	Enthalpy (kJ/kg)	Dew Point (°C)	Density (kg/cu.m)	Vapor Pressure (mm Hg)	Absolute Humidity (g/cu.m)
1,400.0	25.000	19.464	60.0	11.95	0.861	55.552	16.7040	1.1762	14.2653	13.882

4. 4

STATE POINT DATA

Air Flow (Standard) (kg/hr)	Dry Bulb (°C)	Wet Bulb (°C)	Relative Humidity (%)	Humidity Ratio (g/kg)	Specific Volume (cu.m/kg)	Enthalpy (kJ/kg)	Dew Point (°C)	Density (kg/cu.m)	Vapor Pressure (mm Hg)	Absolute Humidity (g/cu.m)
1,400.0	14.168	12.829	86.2	8.71	0.825	36.249	11.9059	1.2227	10.4552	10.557

Process: Cooling Coil

Start Point Name	Total Cooling (kW/hr)	Total Energy (W/hr)	Sensible Energy (W/hr)	Latent Energy (W/hr)	Dehumidification (kg/hr)	Sensible Heat Ratio	Enthalpy/ Humidity Ratio (kJ/kg / g/kg)
1	-7.505	-7,505	-4,300	-3,205	-4.5	0.573	5.947

5. 1

STATE POINT DATA

Air Flow (Standard) (kg/hr)	Dry Bulb (°C)	Wet Bulb (°C)	Relative Humidity (%)	Humidity Ratio (g/kg)	Specific Volume (cu.m/kg)	Enthalpy (kJ/kg)	Dew Point (°C)	Density (kg/cu.m)	Vapor Pressure (mm Hg)	Absolute Humidity (g/cu.m)
1,300.0	25.000	19.464	60.0	11.95	0.861	55.552	16.7040	1.1762	14.2653	13.882

6. 6

STATE POINT DATA

Air Flow (Standard) (kg/hr)	Dry Bulb (°C)	Wet Bulb (°C)	Relative Humidity (%)	Humidity Ratio (g/kg)	Specific Volume (cu.m/kg)	Enthalpy (kJ/kg)	Dew Point (°C)	Density (kg/cu.m)	Vapor Pressure (mm Hg)	Absolute Humidity (g/cu.m)
1,300.0	13.329	12.253	88.6	8.47	0.822	34.786	11.4890	1.2265	10.1710	10.300

Process: Cooling Coil

Start Point Name	Total Cooling (kW/hr)	Total Energy (W/hr)	Sensible Energy (W/hr)	Latent Energy (W/hr)	Dehumidification (kg/hr)	Sensible Heat Ratio	Enthalpy/ Humidity Ratio (kJ/kg / g/kg)
1	-7.497	-7,497	-4,300	-3,197	-4.5	0.574	5.956

7. 1

STATE POINT DATA

Air Flow (Standard) (kg/hr)	Dry Bulb (°C)	Wet Bulb (°C)	Relative Humidity (%)	Humidity Ratio (g/kg)	Specific Volume (cu.m/kg)	Enthalpy (kJ/kg)	Dew Point (°C)	Density (kg/cu.m)	Vapor Pressure (mm Hg)	Absolute Humidity (g/cu.m)
1,200.0	25.000	19.464	60.0	11.95	0.861	55.552	16.7040	1.1762	14.2653	13.882

8. 8

STATE POINT DATA

Air Flow (Standard) (kg/hr)	Dry Bulb (°C)	Wet Bulb (°C)	Relative Humidity (%)	Humidity Ratio (g/kg)	Specific Volume (cu.m/kg)	Enthalpy (kJ/kg)	Dew Point (°C)	Density (kg/cu.m)	Vapor Pressure (mm Hg)	Absolute Humidity (g/cu.m)
1,200.0	12.351	11.555	91.3	8.18	0.819	33.056	10.9709	1.2309	9.8273	9.986

Process: Cooling Coil

Start Point Name	Total Cooling (kW/hr)	Total Energy (W/hr)	Sensible Energy (W/hr)	Latent Energy (W/hr)	Dehumidification (kg/hr)	Sensible Heat Ratio	Enthalpy/ Humidity Ratio (kJ/kg / g/kg)
1	-7.497	-7,497	-4,300	-3,197	-4.5	0.574	5.956

Table 7.4 (B) State Point & Process Report

STATE POINT & PROCESS REPORT

9. 1

STATE POINT DATA

Air Flow (Standard) (kg/hr)	Dry Bulb (°C)	Wet Bulb (°C)	Relative Humidity (%)	Humidity Ratio (g/kg)	Specific Volume (cu.m/kg)	Enthalpy (kJ/kg)	Dew Point (°C)	Density (kg/cu.m)	Vapor Pressure (mm Hg)	Absolute Humidity (g/cu.m)
1,100.0	25.000	19.464	60.0	11.95	0.861	55.552	16.7040	1.1762	14.2653	13.882

10. 10

STATE POINT DATA

Air Flow (Standard) (kg/hr)	Dry Bulb (°C)	Wet Bulb (°C)	Relative Humidity (%)	Humidity Ratio (g/kg)	Specific Volume (cu.m/kg)	Enthalpy (kJ/kg)	Dew Point (°C)	Density (kg/cu.m)	Vapor Pressure (mm Hg)	Absolute Humidity (g/cu.m)
1,100.0	11.192	10.701	94.4	7.83	0.815	30.991	10.3232	1.2362	9.4121	9.603

Process: Cooling Coil

Start Point Name	Total Cooling (kW/hr)	Total Energy (W/hr)	Sensible Energy (W/hr)	Latent Energy (W/hr)	Dehumidification (kg/hr)	Sensible Heat Ratio	Enthalpy/ Humidity Ratio (kJ/kg / g/kg)
1	-7.503	-7,503	-4,300	-3,203	-4.5	0.573	5.949

11. 1

STATE POINT DATA

Air Flow (Standard) (kg/hr)	Dry Bulb (°C)	Wet Bulb (°C)	Relative Humidity (%)	Humidity Ratio (g/kg)	Specific Volume (cu.m/kg)	Enthalpy (kJ/kg)	Dew Point (°C)	Density (kg/cu.m)	Vapor Pressure (mm Hg)	Absolute Humidity (g/cu.m)
1,000.0	25.000	19.464	60.0	11.95	0.861	55.552	16.7040	1.1762	14.2653	13.882

12. 12

STATE POINT DATA

Air Flow (Standard) (kg/hr)	Dry Bulb (°C)	Wet Bulb (°C)	Relative Humidity (%)	Humidity Ratio (g/kg)	Specific Volume (cu.m/kg)	Enthalpy (kJ/kg)	Dew Point (°C)	Density (kg/cu.m)	Vapor Pressure (mm Hg)	Absolute Humidity (g/cu.m)
1,000.0	9.799	9.651	98.2	7.42	0.811	28.538	9.5307	1.2425	8.9251	9.151

Process: Cooling Coil

Start Point Name	Total Cooling (kW/hr)	Total Energy (W/hr)	Sensible Energy (W/hr)	Latent Energy (W/hr)	Dehumidification (kg/hr)	Sensible Heat Ratio	Enthalpy/ Humidity Ratio (kJ/kg / g/kg)
1	-7.502	-7,502	-4,300	-3,202	-4.5	0.573	5.951

13. 13

STATE POINT DATA

Air Flow (Standard) (kg/hr)	Dry Bulb (°C)	Wet Bulb (°C)	Relative Humidity (%)	Humidity Ratio (g/kg)	Specific Volume (cu.m/kg)	Enthalpy (kJ/kg)	Dew Point (°C)	Density (kg/cu.m)	Vapor Pressure (mm Hg)	Absolute Humidity (g/cu.m)
1,500.0	35.125	19.567	22.3	7.89	0.884	55.542	10.4361	1.1402	9.4833	8.925

Process: Desiccant Dehumidification

Start Point Name	Total Energy (W/hr)	Sensible Energy (W/hr)	Latent Energy (W/hr)	Dehumidification (kg/hr)	Sensible Heat Ratio	Enthalpy/ Humidity Ratio (kJ/kg / g/kg)	Sensible Energy Per Dehumidification (kJ/kg)
1	-4	4,300	-4,304	-6.1	-1048.214	-0.016	-2.563

14. 14

STATE POINT DATA

Air Flow (Standard) (kg/hr)	Dry Bulb (°C)	Wet Bulb (°C)	Relative Humidity (%)	Humidity Ratio (g/kg)	Specific Volume (cu.m/kg)	Enthalpy (kJ/kg)	Dew Point (°C)	Density (kg/cu.m)	Vapor Pressure (mm Hg)	Absolute Humidity (g/cu.m)
1,400.0	35.854	19.575	20.6	7.60	0.886	55.541	9.8834	1.1377	9.1390	8.581

Process: Desiccant Dehumidification

Start Point Name	Total Energy (W/hr)	Sensible Energy (W/hr)	Latent Energy (W/hr)	Dehumidification (kg/hr)	Sensible Heat Ratio	Enthalpy/ Humidity Ratio (kJ/kg / g/kg)	Sensible Energy Per Dehumidification (kJ/kg)
1	-4	4,300	-4,304	-6.1	-978.333	-0.015	-2.563

15. 15

STATE POINT DATA

Air Flow (Standard) (kg/hr)	Dry Bulb (°C)	Wet Bulb (°C)	Relative Humidity (%)	Humidity Ratio (g/kg)	Specific Volume (cu.m/kg)	Enthalpy (kJ/kg)	Dew Point (°C)	Density (kg/cu.m)	Vapor Pressure (mm Hg)	Absolute Humidity (g/cu.m)
1,300.0	36.696	19.587	18.9	7.27	0.888	55.551	9.2309	1.1348	8.7468	8.190

Process: Desiccant Dehumidification

Start Point Name	Total Energy (W/hr)	Sensible Energy (W/hr)	Latent Energy (W/hr)	Dehumidification (kg/hr)	Sensible Heat Ratio	Enthalpy/ Humidity Ratio (kJ/kg / g/kg)	Sensible Energy Per Dehumidification (kJ/kg)
1	0	4,300	-4,300	-6.1	-14675.000	-0.018	-2.565

16. 16

STATE POINT DATA

Table 7.4 (C) State Point & Process Report

STATE POINT & PROCESS REPORT

Air Flow (Standard) (kg/hr)	Dry Bulb (°C)	Wet Bulb (°C)	Relative Humidity (%)	Humidity Ratio (g/kg)	Specific Volume (cu.m/kg)	Enthalpy (kJ/kg)	Dew Point (°C)	Density (kg/cu.m)	Vapor Pressure (mm Hg)	Absolute Humidity (g/cu.m)
1,200.0	37.679	19.597	16.9	6.88	0.890	55.549	8.4249	1.1315	8.2827	7.731

Process: Desiccant Dehumidification

Start Point Name	Total Energy (W/hr)	Sensible Energy (W/hr)	Latent Energy (W/hr)	Dehumidification (kg/hr)	Sensible Heat Ratio	Enthalpy/ Humidity Ratio (kJ/kg / g/kg)	Sensible Energy Per Dehumidification (kJ/kg)
1	-1	4,299	-4,300	-6.1	-4891.333	-0.018	-2,565

17. 17

STATE POINT DATA

Air Flow (Standard) (kg/hr)	Dry Bulb (°C)	Wet Bulb (°C)	Relative Humidity (%)	Humidity Ratio (g/kg)	Specific Volume (cu.m/kg)	Enthalpy (kJ/kg)	Dew Point (°C)	Density (kg/cu.m)	Vapor Pressure (mm Hg)	Absolute Humidity (g/cu.m)
1,100.0	38.844	19.610	14.8	6.42	0.893	55.551	7.4198	1.1275	7.7346	7.192

Process: Desiccant Dehumidification

Start Point Name	Total Energy (W/hr)	Sensible Energy (W/hr)	Latent Energy (W/hr)	Dehumidification (kg/hr)	Sensible Heat Ratio	Enthalpy/ Humidity Ratio (kJ/kg / g/kg)	Sensible Energy Per Dehumidification (kJ/kg)
1	0	4,300	-4,300	-6.1	-14675.000	-0.018	-2,565

18. 18

STATE POINT DATA

Air Flow (Standard) (kg/hr)	Dry Bulb (°C)	Wet Bulb (°C)	Relative Humidity (%)	Humidity Ratio (g/kg)	Specific Volume (cu.m/kg)	Enthalpy (kJ/kg)	Dew Point (°C)	Density (kg/cu.m)	Vapor Pressure (mm Hg)	Absolute Humidity (g/cu.m)
1,000.0	40.244	19.627	12.6	5.87	0.896	55.558	6.1299	1.1229	7.0782	6.552

Process: Desiccant Dehumidification

Start Point Name	Total Energy (W/hr)	Sensible Energy (W/hr)	Latent Energy (W/hr)	Dehumidification (kg/hr)	Sensible Heat Ratio	Enthalpy/ Humidity Ratio (kJ/kg / g/kg)	Sensible Energy Per Dehumidification (kJ/kg)
1	2	4,300	-4,298	-6.1	2445.833	-0.019	-2,566

19. 19

STATE POINT DATA

Air Flow (Standard) (kg/hr)	Dry Bulb (°C)	Wet Bulb (°C)	Relative Humidity (%)	Humidity Ratio (g/kg)	Specific Volume (cu.m/kg)	Enthalpy (kJ/kg)	Dew Point (°C)	Density (kg/cu.m)	Vapor Pressure (mm Hg)	Absolute Humidity (g/cu.m)
1,000.0	25.075	13.423	24.5	4.85	0.851	37.552	3.4213	1.1807	5.8578	5.698

Process: Desiccant Dehumidification

Start Point Name	Total Energy (W/hr)	Sensible Energy (W/hr)	Latent Energy (W/hr)	Dehumidification (kg/hr)	Sensible Heat Ratio	Enthalpy/ Humidity Ratio (kJ/kg / g/kg)	Sensible Energy Per Dehumidification (kJ/kg)
2	2	4,300	-4,298	-6.1	2096.429	-0.019	-2,548

20. 20

STATE POINT DATA

Air Flow (Standard) (kg/hr)	Dry Bulb (°C)	Wet Bulb (°C)	Relative Humidity (%)	Humidity Ratio (g/kg)	Specific Volume (cu.m/kg)	Enthalpy (kJ/kg)	Dew Point (°C)	Density (kg/cu.m)	Vapor Pressure (mm Hg)	Absolute Humidity (g/cu.m)
1,000.0	25.087	12.920	21.9	4.33	0.850	36.239	1.8378	1.1810	5.2340	5.092

Process: Desiccant Dehumidification

Start Point Name	Total Energy (W/hr)	Sensible Energy (W/hr)	Latent Energy (W/hr)	Dehumidification (kg/hr)	Sensible Heat Ratio	Enthalpy/ Humidity Ratio (kJ/kg / g/kg)	Sensible Energy Per Dehumidification (kJ/kg)
4	-4	4,300	-4,304	-6.1	-1048.214	-0.016	-2,543

21. 21

STATE POINT DATA

Air Flow (Standard) (kg/hr)	Dry Bulb (°C)	Wet Bulb (°C)	Relative Humidity (%)	Humidity Ratio (g/kg)	Specific Volume (cu.m/kg)	Enthalpy (kJ/kg)	Dew Point (°C)	Density (kg/cu.m)	Vapor Pressure (mm Hg)	Absolute Humidity (g/cu.m)
1,000.0	25.100	12.348	19.0	3.75	0.850	34.775	-0.1271	1.1813	4.5363	4.413

Process: Desiccant Dehumidification

Start Point Name	Total Energy (W/hr)	Sensible Energy (W/hr)	Latent Energy (W/hr)	Dehumidification (kg/hr)	Sensible Heat Ratio	Enthalpy/ Humidity Ratio (kJ/kg / g/kg)	Sensible Energy Per Dehumidification (kJ/kg)
6	-4	4,299	-4,304	-6.1	-978.267	-0.016	-2,541

22. 22

STATE POINT DATA

Air Flow (Standard) (kg/hr)	Dry Bulb (°C)	Wet Bulb (°C)	Relative Humidity (%)	Humidity Ratio (g/kg)	Specific Volume (cu.m/kg)	Enthalpy (kJ/kg)	Dew Point (°C)	Density (kg/cu.m)	Vapor Pressure (mm Hg)	Absolute Humidity (g/cu.m)
1,000.0	25.119	11.662	15.5	3.07	0.849	33.062	-2.5202	1.1817	3.7177	3.617

Process: Desiccant Dehumidification

Table 7.4 (D) State Point & Process Report

STATE POINT & PROCESS REPORT

Start Point Name	Total Energy (W/hr)	Sensible Energy (W/hr)	Latent Energy (W/hr)	Dehumidification (kg/hr)	Sensible Heat Ratio	Enthalpy/ Humidity Ratio (kJ/kg / g/kg)	Sensible Energy Per Dehumidification (kJ/kg)
8	2	4,300	-4,298	-6.1	2445.833	-0.019	-2,543

23. 23

STATE POINT DATA

Air Flow (Standard) (kg/hr)	Dry Bulb (°C)	Wet Bulb (°C)	Relative Humidity (%)	Humidity Ratio (g/kg)	Specific Volume (cu.m/kg)	Enthalpy (kJ/kg)	Dew Point (°C)	Density (kg/cu.m)	Vapor Pressure (mm Hg)	Absolute Humidity (g/cu.m)
1,000.0	25.143	10.812	11.4	2.25	0.848	30.997	-6.1586	1.1822	2.7282	2.654

Process: Desiccant Dehumidification

Start Point Name	Total Energy (W/hr)	Sensible Energy (W/hr)	Latent Energy (W/hr)	Dehumidification (kg/hr)	Sensible Heat Ratio	Enthalpy/ Humidity Ratio (kJ/kg / g/kg)	Sensible Energy Per Dehumidification (kJ/kg)
10	1	4,300	-4,299	-6.1	2935.200	-0.019	-2,541

24. 24

STATE POINT DATA

Air Flow (Standard) (kg/hr)	Dry Bulb (°C)	Wet Bulb (°C)	Relative Humidity (%)	Humidity Ratio (g/kg)	Specific Volume (cu.m/kg)	Enthalpy (kJ/kg)	Dew Point (°C)	Density (kg/cu.m)	Vapor Pressure (mm Hg)	Absolute Humidity (g/cu.m)
1,000.0	25.172	9.760	6.4	1.27	0.847	28.529	-12.6133	1.1828	1.5422	1.500

Process: Desiccant Dehumidification

Start Point Name	Total Energy (W/hr)	Sensible Energy (W/hr)	Latent Energy (W/hr)	Dehumidification (kg/hr)	Sensible Heat Ratio	Enthalpy/ Humidity Ratio (kJ/kg / g/kg)	Sensible Energy Per Dehumidification (kJ/kg)
12	-3	4,300	-4,302	-6.2	-1630.556	-0.016	-2,535

7.4 Influence of Varying Operation Parameters in Desiccant Wheel

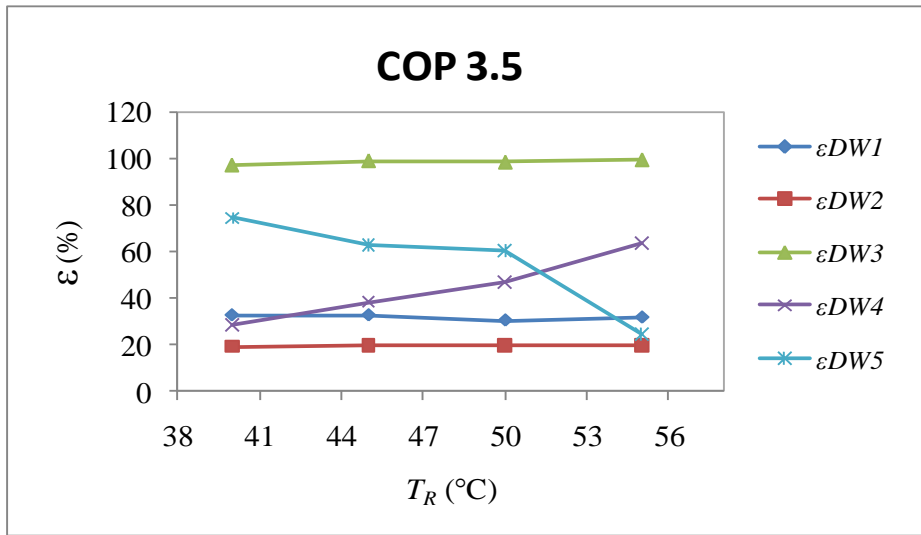
Process air enthalpy deviation has been observed in some theoretical and experimental studies. Difference between the enthalpy at the inlet air and the outlet air of the desiccant wheel is due to the properties of the desiccant material, construction of the desiccant wheel, regeneration air temperature, wheel speed and obviously temperature and humidity of the inlet air.

Figures 7.18 (a) (b) show the variation in the DW efficiency with respect to regeneration air temperature T_R for COP value of 3.5 and air flow rate $300\text{m}^3/\text{h}$. It is evident from these graphs that different definitions of DW efficiency suggest different trends in the variation of efficiency with respect to T_R . For example ϵ_{DW1} , ϵ_{DW2} and ϵ_{DW3} apparently do not change with any change in T_R whereas ϵ_{DW4} and ϵ_{DW5} show a clear variation in the efficiency of the DW, ϵ_{DW4} improves with the increasing regeneration temperature due to a better performance of desorption process at a higher temperature. Therefore the humidity adsorption capacity enhances, humidity adsorption enhancement accordingly causes an improvement in Dehumidification Effectiveness ϵ_{DW4} (Eq.5.22), but Adiabatic Effectiveness ϵ_{DW5} (Eq.5.23), passes through a descending trend line. On the other side input heat to the wheel increases due to the regeneration temperature.

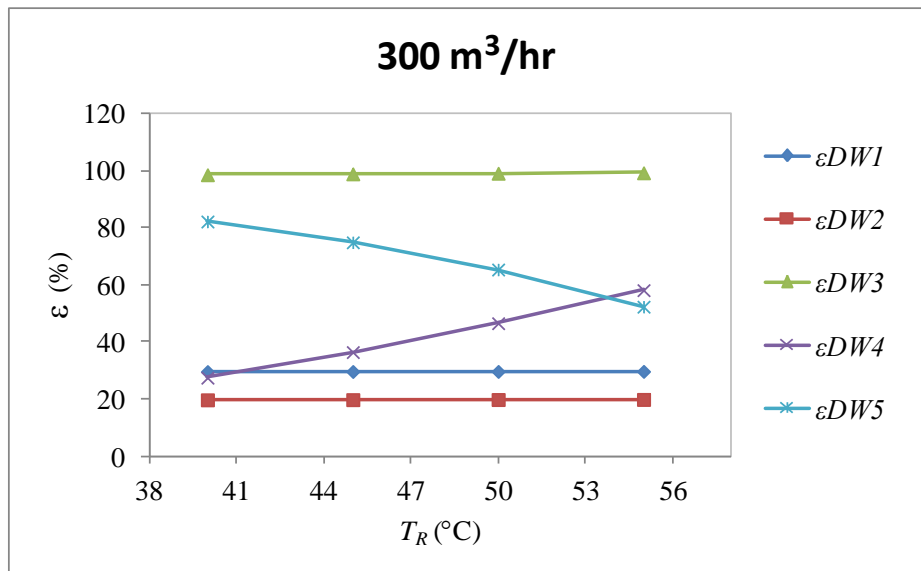
In Figure 7.18 (c) the variation in DW efficiency with respect to the COP is shown. As it can be seen with increasing the COP, Adiabatic Effectiveness ϵ_{DW5} (Eq.5.23), reduces but the other efficiencies apparently increase. Whereas ϵ_{DW3} reaches an optimum point at COP of 3.5, the occurrence of this optimum value is because of the related regeneration and process air flow rate. Considering the observed enthalpy increase in the process air passing through the desiccant wheel ϵ_{DW5} decreases by an amount of the enthalpy deviation, therefore the ϵ_{DW4} increased due to the inverse effects.

Figure 7.18 (d) shows that the air flow rate increases, heat is carried from the regeneration side to the process side, the ϵ_{DW4} increase and the dehumidification efficiency improves due to the smaller time intervals for the humidification and dehumidification.

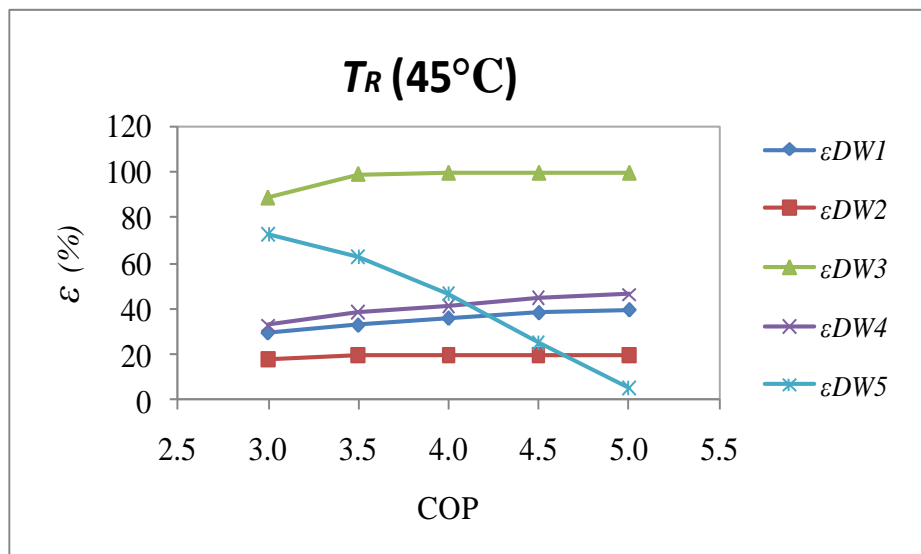
As can be seen in all Figure 7.18 the modified desiccant regeneration efficiency ϵ_{DW3} has an optimum point, because in ϵ_{DW3} equation include more parameters (i.e. mass flow rate of process and regeneration air), hence represent a more realistic condition.



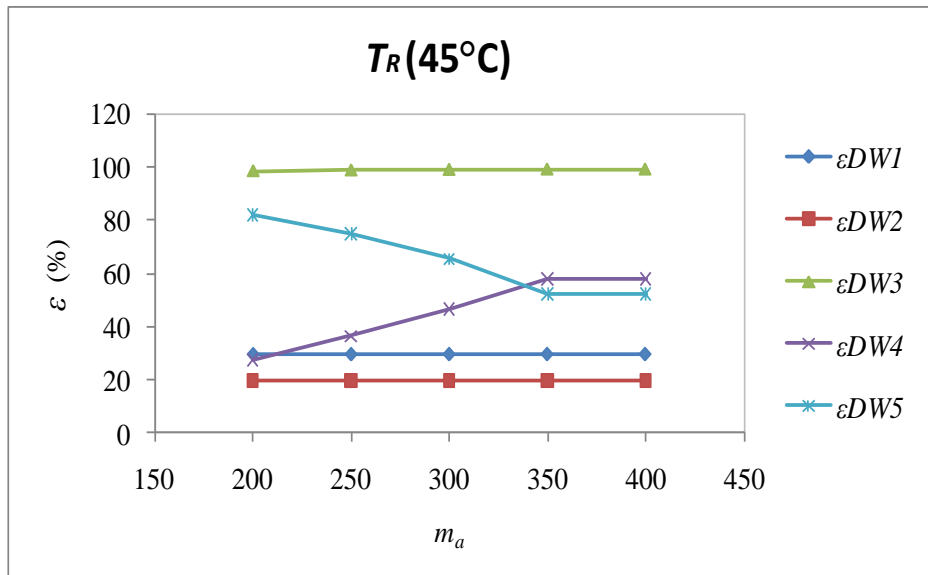
(a)



(b)



(c)



(d)

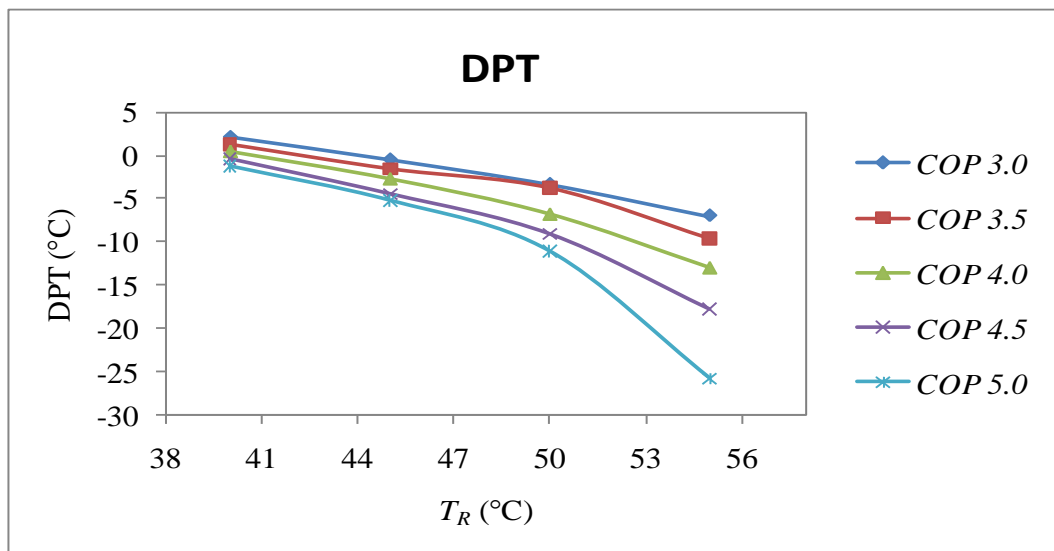
Fig 7.18 Variation of DW efficiency (ϵ) with different T_R , COP and m_a

7.5 Influence of Varying Operation Parameters in Heat Pump

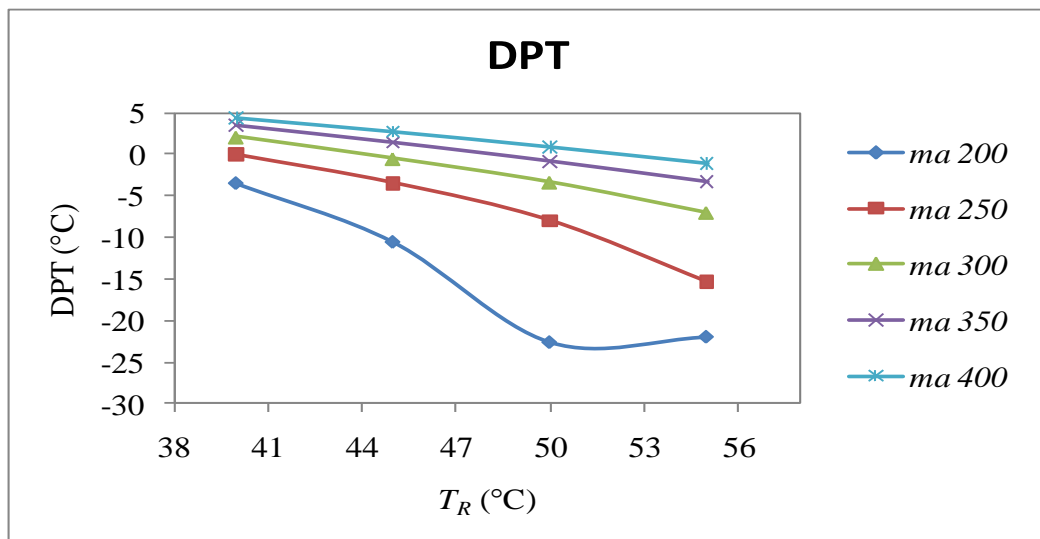
Heat pump operation parameters, regeneration temperature T_R and air mass flow rate m_a were varied respectively from 40 °C - 55 °C and 200 m³/h - 400 m³/h and the corresponding variations in the system performance are discussed in the following sections.

Figures 7.19 (a) and (b) show the expected trend that DPT of the process air decreases with increasing T_R . This is essential because the heat release in the condenser increases with COP, and a reduction of in the process air flow rate increases the residence time, which results in a decrease in DPT.

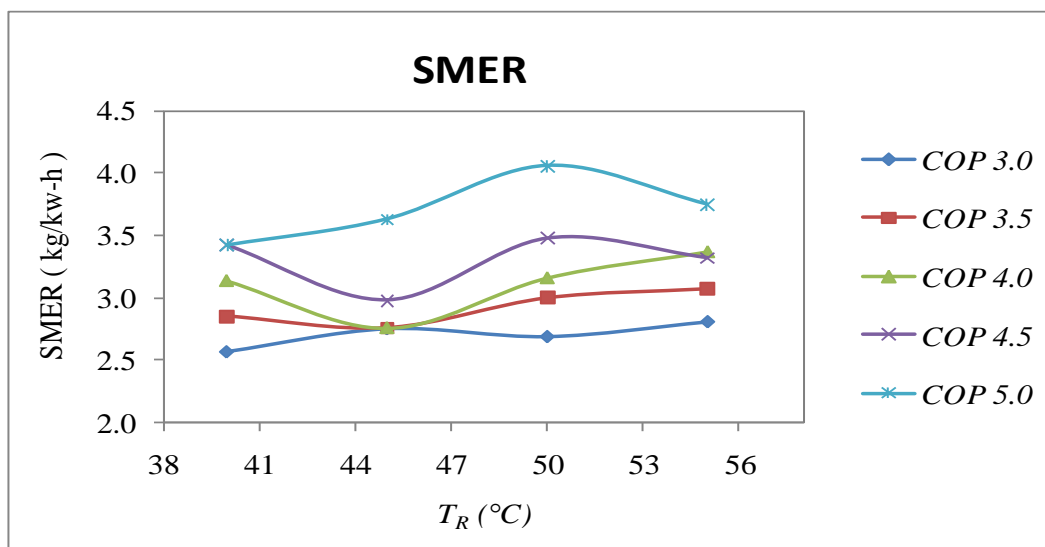
Figure 7.19 (c) illustrates that the relationships between T_R and SMER for different COP. The process air specific humidity is directly related to DPT and hence the former increases with an increase in air flow. Thus the total moisture removal capacity decreases with airflow rate. However, this decrease is more than that compensated by an increase in the airflow rate, thereby the total moisture removal capacity which is the product of specific moisture removal capacity and the air mass flow rate increases as evident in Figure 7.19 (d).



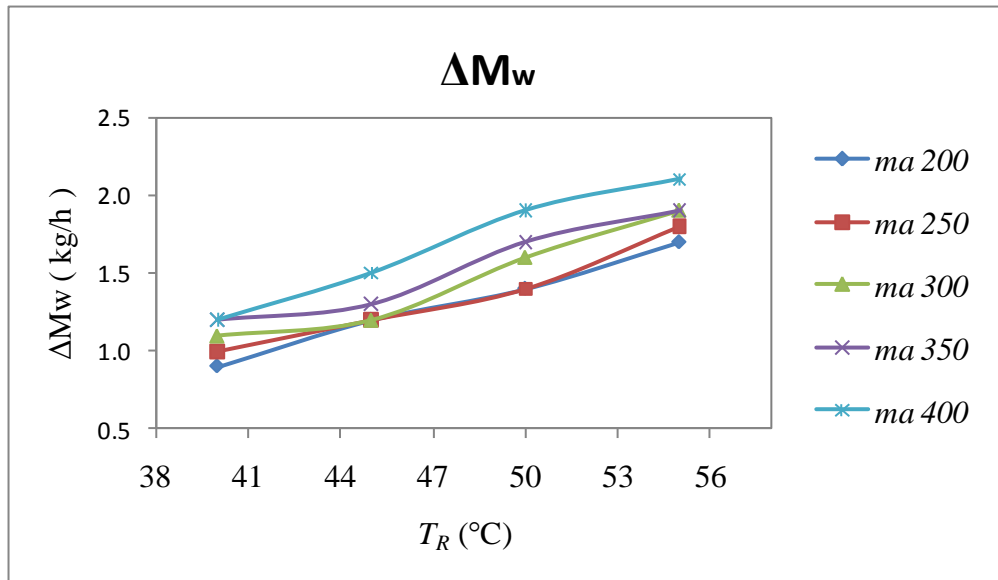
(a)



(b)



(c)



(d)

Fig 7.19 Variation of DPT, SMER and ΔM_w with T_R for different COP and m_a

7.6 Summary

In this chapter the test results of a hybrid dehumidifier system are presented and discussed. The performance of the hybrid system is compared with single refrigerant circuit system and single desiccant wheel system for a range of operating parameters, i.e. inlet air temperature, airflow rate and regeneration temperature. The hybrid system enhances energy efficiency, SMER and supplies a low dew point temperature. The hybrid system is found to be more energy efficient compared to the single system of desiccant wheel and refrigerant circuit.

The system operates cost-effectively because the waste heat from the condenser is used for regeneration of the desiccant wheel. In the presented design the total energy demand for the regeneration of the desiccant wheel is met by the waste heat from the condenser. This results in reducing of the overall energy requirement by up to 40%. The present study confirms the importance of improving heat recovery to improve the performance of desiccant wheel heat-pump-assisted drying systems.

Chapter 8 Conclusions and Recommendations for Future Work

8.1 Conclusions

The aim of the research project was to develop an energy efficient system particularly for rapid drying applications. The motivation for the research was due to the real problems faced by beverage packaging industry where drying occurs at low dew point temperatures¹. The drying process is influenced by the desired drying temperature of the product and the properties of the process air and by the ambient conditions. In certain environment conditions the production is adversely affected. Drying is a very energy intensive activity, thus it is important for drying industry to reduce energy consumption, in order to save cost and decrease carbon footprint.

8.1.1 Overall Performance of the Hybrid Drying System

A hybrid dehumidification system consisting of a heat pump desiccant dehumidifier assisted mechanical drying system is proposed for rapid drying applications. The main conclusion of this research is that significant energy savings can be made by the hybrid system presented in this thesis. The heat dissipated by the heat pump condenser is used as regeneration heat by the desiccant wheel thereby increasing the utilisation of the waste energy and overall efficiency. The overall heat pump and desiccant wheel dehumidification system efficiency is considered to be representative of the hybrid system and can be used as a reliable performance parameter for comparison of similar systems.

It is shown in Table 8.1 and Table 8.2 that the specific moisture extraction rate (SMER) for conventional heat pump cycle is 1.9-2.7 kg/kWh, SMER for desiccant wheel is 1.8-1.5 kg/kWh whereas the hybrid system achieves SMER > 3.6 kg/kWh. The present research confirms the importance of improving heat recovery to improve the performance of hybrid drying systems. Error values were not included as explained before: the inaccuracies of the equipment are absolute errors given by the manufacturers. Experimental errors are neglected because as long as the controlled parameters, such as the temperature and pressure, are kept at an atmospheric scale, the deviations are tolerable.

1) ¹ Field testing of the proposed system is underway by a drying equipment manufacturer.

Table 8.1 Comparing three drying systems of effect inlet air temperature

Parameter	Heat Pump cycle	Desiccant wheel	Hybrid system
Input energy (kW)	2.2~5.1	2.9~9.7	0.8~3.8
SMER (kg water/kWh)	1.9~2.7	1.8~1.5	5~3.6
$\Delta\omega$ (kg/h)	4.1~13.6	4.1~13.6	8.2~17.7
DPT (°C)	5.2~17.9	0.3~15.7	-21.7~10.5
DBT (°C)	7.2~17.9	32.3~42.2	20.1~30.1

Table 8.2 Comparing three drying systems of effect airflow rate

Parameter	Heat Pump Cycle	Desiccant wheel	Hybrid system
Input energy (kW)	3.2~6.7	5.7~7.7	2~2.9
SMER (kg water/kWh)	2.3	1.4	3.7
$\Delta\omega$ (kg/h)	7.3~11	7.3~11	7.3~11
DPT (°C)	11.2~13.2	7.5~11.2	-3.7~6
DBT (°C)	11.3~15.9	38.7~34	25

8.1.2 Theoretical & Experimental Analysis of Various Parameters

A prototype model of the hybrid dryer was designed and fabricated. The experimental facility consisted of a heat pump desiccant dehumidifier with R134a as the refrigerant which used the heat dissipated by the condenser. A theoretical approach is presented and mathematical models are developed which can be used to optimise the design parameters of the hybrid system and also of singular components of the system. The analysis of the experimental data was conducted to determine the practical relationship between the operational parameters (COP, m_a and T_R) performance parameters (SMER, DPT and ϵ) of the system. The observed behaviours of test cases are suggested to be governed by the specific combination of the operation parameters. The critical observation of the mathematical analysis resulted in the following conclusions:

- 1) The increase in regeneration temperature, T_R (40-55°C) results in an increase in the sorption heat and increase in mass flow rate, m_a (200-400 m³/h) result in smaller time intervals between adsorption and desorption processes. Therefore all performance parameters i.e. COP, DPT, SMER and efficiency are improved. However, adiabatic efficiency of the desiccant wheel, ϵ_{DW5} shows a decrease with increasing temperature. This is due to the fact that heat transfer occurs from the regeneration side to the process side.
- 2) The processes occurring in desiccant wheel are influenced by T_R with a critical magnitude of $T_R \geq 50$ °C.
- 3) m_a was almost of secondary importance in comparison with COP for the

complete cycle operation and as well as for DW.

- 4) Increasing airflow rate over the cooling coil and desiccant wheel are found to improve the system performance in terms of moisture removal capacity, which is increased from 7.3 to 11 kg/h when airflow rate is increased from 1000 to 1500 m³/h.

Overall the results show that in the hybrid system, desiccant dehumidification can work under much lower regeneration temperature. The hybrid system can supply air at a lower dew temperature than the other two drying systems. Heat pump cycle can be efficiently utilised to drive such a dehumidification cycle. The energy consumption is also low because of fully utilising the heat dissipated by the condenser in regenerating the desiccant wheel.

8.1.3 Other Practical Implications

Further important conclusions are drawn following the experimental evaluation of the hybrid system:

- 1) Up to 30% to 60% more heat energy can be saved depending on moisture levels in ambient and process air by using hybrid system compared to conventional drying methods.
- 2) The addition of desiccant wheel in refrigerant circuit improved the system performance in terms of SMER in the range of 12–20%. The introduction of the desiccant wheel is not only to provide efficient drying capability and low supply dew point conditions but also provides additional sensible heating to the air without the incorporation of an auxiliary heater.
- 3) Regulating the airflow of the control damper is found to be an effective method to regulate the humidity of the drying air while enhancing the amount of heat recovered from the drying air.

8.2 Recommendations for Future Work

For development of sustainable energy, three important technological changes are required: energy economies on the demand side, efficiency improvements in the energy production, and using various sources of renewable energy. In this regard, a hybrid system improves energy efficiency and needs less electric power consumption, so this system is appropriate to sustainable development concept. In this study, the future recommendations which suggest from the results of the present study are listed

as follows:

- 1) To undertake the integration of the drying variables and the performance variables of low energy methods for product specific drying. There is no standard model for all drying processes, therefore it is essential to adapt to specific cases.
- 2) To develop an optimal low energy drying mathematical model for a low energy approach which meets varying loads during high speed production line such as those experienced in industrial drying applications. Time consumption during drying is an important factor. Product's surface must be dried in the least amount of time in a rapid mass production.
- 3) To further modify of the hybrid system that includes a range of latent energy reclaimed to reduce power consumption.
- 4) Improvements of low regeneration temperature desiccant wheel drying system as lower temperature implies a higher energy saving.
- 5) Use of compound desiccant materials to develop high performance desiccant drying system. This is to potentially developing a new material to further improve the current model.
- 6) Developing a standardised testing procedure for rotary desiccant based dehumidification efficient.

The hybrid dehumidification drying system is designed based on the high moisture loads and not on sensible loads, even though the system is capable of providing sensible cooling and heating. The system design is based on the latent cooling load therefore for designing the system for a particular application, its sensible cooling and heating capacity must be checked. If the sensible cooling capacity is inadequate then adding an external system, such as thermal wheel, heat exchanger at exhaust air to meet the additional load can be considered. In this regard, a hybrid system can meet varying loads during high speed production line such as those experienced in industrial drying applications.

References

1. Mujumdar Arun S, Handbook of Industrial Drying, third edition. 2007 by Taylor & Francis Group, LLC
2. Djaeni M and Boxtel A. J, Energy Efficient Multistage Zeolite Drying for Heat-Sensitive Products. *Drying Technology* 2009, 27 (5), 271-272
3. Stefano De Antonellis et al. Simulation and energy efficiency analysis of desiccant wheel systems for drying processes, *International Journal of Energy*, 37, 336-345, 2012
4. Baker C.G.J. Baker and Reay R. D, Energy Usage for Drying in Selected U.K. Industrial Sectors, *Proceeding of 3rd International Drying Symposium*, 1:201-209 (1982).
5. Toei R, *Course Notes on Drying Technology*, Asian Institute of Technology, Bangkok, Thailand, 1980.
6. Sloan C.E, *Drying systems and equipment*, *Chem. Eng.*, 19, 1967.
7. McCormick, P.Y., *Chemical Engineering Handbook*, 5th ed. (J.H. Perry, Ed.), McGraw-Hill, New York, 1973.
8. Scheper G.W, The vortex tube; internal flow data and a heat transfer theory. *J ASRE Refrig Eng* 1951; 59:985–9.
9. Mujumder A.S, *Advance in Drying*, Vol. 1 (1980), Vol. 2 (1982), Vol. 3 (1984), Hemisphere, New York.
10. Keey R.B, *Drying: Principles and Practice*, Pergamon Press, Oxford, 1972.
11. Keey R.B, *Introduction to Industrial Drying Operation*, 1st ed., Pergamon Press, New York, 1978, chap. 2.
12. Dittman, F.W., How to classify a drying process, *Chem. Eng.*, 17, 106–108, 1977.
13. Lang R.W, *Proceeding of the First International Drying Symposium* (Mujumder A.S. Mujumder, Ed.), Montreal Science Press, Princeton, NJ, 1978.
14. Strumiłło Czesław, Jones Peter L, and ZŻyła Romuald, Energy Aspects in Drying Energy Aspects in Drying, *Handbook of Industrial Drying*, Mujumdar Arun S, third edition. 2007 by Taylor & Francis Group, LLC.

15. Larreture A and Laniau M, Experimental verification of a heat pump assisted continuous dryer simulation model. *International Journal of Energy Research* 1993, 17, 19–28.
16. Richardson A.S and Jenson W.M.P, Energy Research and Development Adm., Aerojet Nuclear Company, Report No. E (10-1)-1375 (1976).
17. Bakker-Arkema F.W, Lerew L.E., Boer S.W. de, and Roth M.G., Research Report No. 224, Michigan State University, Agricultural Experiment Station (January 1, 1974).
18. Danilov O.L and Leontchik B.I, *Energy Economic in Thermal Drying* Energoatomizdat, Moscow (1986), (in Russian)
19. Bahu R.E, Baker C.G.J, and Reay D, Energy Balances on Industrial Dryers- A Route to Fuel Conservation, International Meeting, Energy Saving in Drying Process- Application to Industry and Agriculture, Liege, Belgium, 4-6 October, pp. A 1.1 (1983).
20. Strumillo C and Zylla R, Optimization of Heat Pump Dehumidifier, in *Proceedings of the 4th International Drying Symposium, Vol. 2*, R. Toei and Mujumdar A.S. (Eds.), Kyoto, pp. 739–747 (1984).
21. Zylla R and Strumillo C., Heat Pumps in Drying, in *Drying '87*, A.S. Mujumdar (Ed.), Hemisphere, pp. 129–141 (1987).
22. Michael J. Moran, *Introduction to Thermal Systems Engineering: Thermodynamics, Fluid Mechanics, and Heat Transfer*, Wiley (September 17, 2002) | ISBN: 0471204900
23. Harriman, L.G, *The Dehumidification Handbook Second Edition*, ISBN 0-9717887-0-7, Munters Corporation, 2002.
24. Ronak Daghigh , Mohd Hafidz Ruslan, Mohamad Yusof Sulaiman and Kamaruzzaman Sopian, Review of solar assisted heat pump drying systems for agricultural and marine products, *Renewable and Sustainable Energy Reviews*, 2010, 14 (9), 2564–2579
25. Will Catton, , Gerry Carrington and Zhifa Sun, Exergy analysis of an isothermal heat pump dryer, *Energy*, 36 (8) , 4616–4624, 2011
26. Geeraert B, *Nato Advance Study Institute Series, Series E, Applied Science*, 1(15), 219, 1976.
27. Strumillo C. and Zylla R, *Drying '85*, Mujumdar, A.S. (Ed.), Elsevier Science, Amsterdam, 21, 1985.

28. M. Mohanraj, Performance of a solar-ambient hybrid source heat pump drier for copra drying under hot-humid weather conditions, *Energy for Sustainable Development*, Volume 23, 2014, 165 - 169
29. Zafer Erbay and Arif Hepbasli, Application of conventional and advanced exergy analyses to evaluate the performance of a ground-source heat pump (GSHP) dryer used in food drying, *Energy Conversion and Management*, Volume 78, 2014, 499 - 507
30. M.I. Fadhel, K. Sopian and W.R.W. Daud, Performance analysis of solar-assisted chemical heat-pump dryer, *Solar Energy*, Volume 84, Issue 11, 2010, 1920 - 192
31. Chua K.J and Chou, S.K, A modular approach to study the performance of a two-stage heat pump system for drying. *Applied Thermal Engineering* 2005, 25 (8-9), 1363-1379.
32. Pal U. S and Khan Md. K, Calculation Steps for the Design of Different Components of Heat Pump Dryers Under Constant Drying Rate Condition. *Drying Technology*, 2008 (26), 864–872
33. Perry J.H., *Chemical Engineering Handbook*, 5th ed., McGraw-Hill, New York, pp. 20. 7–20.8 (1990).
34. X. Jia, P. Jolly, S. Clements, Heat pump assisted continuous drying. Part 2: simulation results, *Int. J. Energy Res.*, 14 (1990), pp. 771–782
35. S. Clements, X. Jia, P. Jolly, Experimental verification of a heat pump assisted continuous dryer simulation model, *Int. J. Energy Res.*, 17 (1993), pp. 19–28
36. V. Minea, Drying heat pumps – Part I: System integration, *International Journal of Refrigeration*, Volume 36, Issue 3, 2013, 643 - 658
37. Jolly P, Jia, X and Clements S, Heat pump assisted continuous drying Part 1: Simulation model. *International Journal of Energy Research* 1990, 14, 757–770.
38. Jia, X, Jolly P and Clements S, Heat pump assisted continuous drying Part 2: Simulation results. *International Journal of Energy Research* 1990, 14, 771–782.
39. Teeboonma U, Tiansuwan J and Soponronnarit S, Optimisation of heat pump fruit dryers. *Journal of Food Engineering* 2003, 59, 369–377.
40. Prasertsan S and Saen-Saby P, Heat pump drying of agricultural materials. *Drying Technology* 1998, 16 (1&2), 235–250.
41. Prasertsan S.and Saen-Saby, P, Nyamsritraku P, Prateepchaikul G, Heat pump dryer Part 2: Results of the simulation. *International Journal of Energy Research* 1997, 21, 1–20.

42. Achariyaviriya S, Sophonronnarit S and Terdyothin A, Mathematical model development and simulation of heat pump fruit dryer. *Drying Technology* 2000, 18 (1–2), 479–491.
43. Adapa P.K, Sokbansanj S and Schoenau G.J, Performance study of a re-circulating cabinet dryer using a house hold dehumidifier. *Drying Technology* 2002, 20 (8), 1673-1689.
44. Adapa, P.K, Schoenau G.J and Sokhansanj S, Performance study of a heat pump dryer system for specialty crops Part 1: Development of simulation model. *International Journal of Energy Research* 2002, 26, 1001–1019.
45. Krokida,M.K and Bisharat G.I, Heat recovery from dryer exhaust air. *Drying Technology* 2004, 22 (7), 1661–1674.
46. Sarkar J, Bhattacharyya S.and Ram G. M, Transcritical CO₂ heat pump dryer: Part 1. Mathematical model and simulation. *Drying Technology* 2006, 24, 1583–1591.
47. Saensabai P and Prasertsan S, The effect of refrigerant circuitry on the condenser coil performance. *Proceeding of the 2nd Regional Conference on Energy Technology Towards a Clean Environment*, 12–14 February 2003, Phuket, Thailand, 464–470.
48. Saensabai P and Prasertsan S., Effects of component arrangement and ambient and drying conditions on the performance of heat pump dryers. *Drying Technology* 2003, 21 (1), 103–127.
49. Liang S.Y, Wong T.N and Nathan, G.K., Numerical and experimental studies of refrigerant circuitry of evaporator coils. *International Journal of Refrigeration* 2001, 24, 823–833.
50. Alosaimy AS, Hamed Ahmed M. Theoretical and experimental investigation on the application of solar water heater coupled with air humidifier for regeneration of liquid desiccant. *Energy* 2011;36:3992–4001.
51. XiongZQ,DaiYJ,WangRZ.Investigationon atwo-stagesolarliquid- desiccant (LiBr)dehumidificationsystemassistedbyCaCl₂ solution. *Applied Thermal Engineering*2009;29:1209–15.
52. Ahmed MH, Kattab NM, Fouad M. Evaluation and optimization of solar desiccant wheel performance. *Renewable Energy* 2005;30:305–25.

53. Lu SM, Shyu RJ, Yan WJ, Chung TW. Development and experimental validation of two novel solar desiccant–dehumidification–regeneration systems. *Energy* 1995;20(8):751–7.
54. De Antonellis Stefano, Maria Joppolo Cesare, Molinaroli Luca, Pasini Alberto. Simulation and energy efficiency analysis of desiccant wheel systems for drying processes. *Energy* 2012;37:336–45.
55. Zaltash A, Petrov AY, Rizy DT, Labinov SD, Vineyard EA, Linkous RL. Laboratory R&D on integrated energy systems (IES). *Applied Thermal Engineering*. 2006;26:28–35.
56. Bassuoni MM. An experimental study of structured packing dehumidifier/regenerator operating with liquid desiccant. *Energy* 2011;36:2628–38.
57. Mandegari MAli, Pahlavanzadeh H. Introduction of a new definition for effectiveness of desiccant wheels. *Energy* 2009;34:797–803.
58. Yao Ye, Zhang Weijiang, He Beixing. Investigation on the kinetic models for the regeneration of silica gel by hot air combined with power ultrasonic. *Energy Conversion and Management* 2011;52:3319–26.
59. Yao Ye. Using power ultrasound for the regeneration of dehumidizers in desiccant air-conditioning systems: a review of prospective studies and unexplored issues. *Renewable and Sustainable Energy Reviews* 2010;14:1860–73.
60. Li B, Lin QY, Yan YY. Development of solid desiccant dehumidification using electro-osmosis regeneration method for HVAC application. *Building and Environment* 2012;48:128–34.
61. Roula Ghazal, Christian Ghiaus, Gray-box identification of thermal transfer coefficients of desiccant wheels, *Energy and Buildings* 70 (2014) 384–397
62. Xinli Wang , Wenjian Cai , Jiangang Lu , Youxian Sun , Lei Zhao, Model-based optimization strategy of chiller driven liquid desiccant dehumidifier with genetic algorithm, *Energy*, Volume 82, 2015, 939 – 948
63. Ping Tao, Bing Liao, Yun Tan, A primary study on the water absorbing/releasing performance of molecular sieve desiccant, *Procedia Engineering* 27 (2012) 781 – 786
64. Chih-Hao Chen, Chien-Yeh Hsu, Chih-Chieh Chen, Sih-Li Chen, Silica gel polymer composite desiccants for air conditioning systems, *Energy and Buildings*, Volume 101, 15, 2015, 122–132

65. M. Goldsworthy, S.D. White, Limiting performance mechanisms in desiccant wheel dehumidification, *Applied Thermal Engineering*, Volume 44, 2012, 21–28
66. Giovanni Angrisani, Carlo Roselli, Maurizio Sasso, Effect of rotational speed on the performances of a desiccant wheel, *Applied Energy*, Volume 104, 2013, 268–275
67. Carpinlioglu Melda Ozdinc and Yildirim Murtaza. A methodology for the performance evaluation of an experimental desiccant cooling system. *International Communications in Heat and Mass Transfer*, Vol. 32, pp. 1400–1410, 2005.
68. Ali Mandegari M. and Pahlavanzadeh H. Introduction of a new definition for effectiveness of desiccant wheels, *Energy*. Vol. 34, pp. 797–803, 2009.
69. Kanoglu Mehmet, Carpinlioglu Melda Ozdinc and Yildirim Murtaza. Energy and exergy analyses of an experimental open-cycle desiccant cooling system. *Applied Thermal Engineering*, Vol. 24, pp. 919–932, 2004.
70. Jia C. X., Dai Y. J., Wu J. Y. and Wang R. Z. Use of compound desiccant to develop high performance desiccant cooling system. *International Journal of Refrigeration*, Vol. 30, pp. 345- 353, 2007.
71. Jae Dong Chung, Dae-Young Lee, Effect of desiccant isotherm on the performance of desiccant wheel, *International Journal of Refrigeration*, Volume 32, Issue 4, 2009, 720–726
72. Pascal Stabat and Dominique Marchio., Heat-and-mass transfers modelled for rotary desiccant dehumidifiers. *Applied Energy* 85 (2008) 128–142.
73. Harriman, L. 1996. *Applications Engineering Manual for Desiccant Systems*. American Gas Cooling Center, Arlington, Virginia.
74. Harriman, L.G, 1990, *The Dehumidification Handbook*, 2nd Edition, Munters Cargocaire, Amesbury, MA.
75. Harriman, L.G, Editor. 1990. *The Dehumidification Handbook*. 2nd Edition, published by Munters Cargocaire, Amesbury, Massachusetts.
76. Harriman, L.G, January 1994, "Field Experience with Desiccant Systems," *Engineered Systems*, pp. 63-68.
77. Ranque G,J, Method and apparatus for obtaining from a fluid under pressure two outputs of fluid at different temperatures. US patent 1:952,281, 1934.
78. Ranque G.J, Experiments on expansion in a vortex with simultaneous exhaust of hot air and cold air. *J Phys Radium (Paris)* 1933; 4:112–4S-115, June. Also translated as General Electric Co., Schenectady Works Library 1947; T.F. 3294.

79. Hilsch R, The use of expansion of gases in a centrifugal field as a cooling process. *Rev Sci Instrum* 1947; 18 (2):108–13.
80. Smith Eiamsa-ard and Pongjet Promvonge, Review of Ranque-Hilsch effect in vortex tubes. 2007.
81. Bruno TJ, Applications of the vortex tube in chemical analysis Part I: introductory principle. *Am Lab* 1993; 25:15–20.
82. Bruno TJ, Applications of the vortex tube in chemical analysis. Process control and quality 3. Amsterdam: Elsevier Science Publishers BV; 1992. p. 195–207.
83. Comassar S, The vortex tube. *J Am Soc Naval Eng* 1951;63:99–108
84. Curley W and McGree Jr R. Bibliography of vortex tubes. *Refriger Eng* 1951;59 (2):191–3.
85. Vennos S.L.N, An experimental investigation of the gaseous vortex. PhD thesis. Rensselaer Polytechnic Institute, 1968.
86. Scheller W.A and Brown G.M, The Ranque–Hilsch vortex tube. *J Ind Eng Chem* 1957; 49(6):1013–6.
87. Williams D.T, Ranque-Hilsch Vortex Tube for Refrigeration in Developing Communities, CA USA 2005
88. Dhar P. L. and Singh S. K. Studies on solid desiccant based hybrid air-conditioning systems. *Applied Thermal Engineering*. Vol. 21, pp. 119-134, 2001.
89. Lazzarin Renato M. and Castellotti Francesco. A new heat pump desiccant dehumidifier for supermarket application, *Energy and Buildings*. Vol. 39, pp. 59–65, 2007.
90. Subramanyam N., Maiya M. P. and Srinivasa Murthy S. Application of desiccant wheel to control humidity in air-conditioning systems. *Applied Thermal Engineering*, Vol. 24, pp. 2777–2788, 2004.
91. Subramanyam N, Maiya M P and Srinivasa Murthy S. Parametric studies on a desiccant assisted air-conditioner, *Applied Thermal Engineering*. Vol. 24, pp. 2679–2688, 2004.
92. Ghali K, Othmani M and Ghaddar N. Energy consumption and feasibility study of a hybrid desiccant dehumidification air conditioning system on Beirut. *International Journal of Green Energy*. Vol. 5, pp. 360-372, 2008.
93. Lee Kong Hoon and Kim Ook Joong. Investigation on Drying Performance and Energy Savings of the Batch-Type Heat Pump Dryer, *Drying Technology*. Vol. 27, pp. 565-573, 2009.

94. Pesaran Ahmad A. A Review of Desiccant Dehumidification Technology.
Prepared for Proceedings of EPRI's Electric Dehumidification: Energy Efficient
Humidity Control for Commercial and Institutional Buildings Conference, New
Orleans, Louisiana , NREL/TP-472-7010, June 2-3, 1993

List of Publications

- Wang W.C, Calay R.K, Chen Y.K, Experimental study of an energy efficient hybrid system for surface drying. Applied Thermal Engineering 2011, 31, 425-431.
- Wang W.C, Calay R.K, Chen Y.K, Investigation on surface drying and energy savings of the hybrid dryer. Innovative Materials for Processes in Energy Systems 2010, ISBN 978-981-08-7614-2, IMPRES004, 153-160.
- Calay R.K, Wang W.C, A study of an energy efficient building ventilation system. 12th International Conference on Air Distribution in Rooms 2011, ROOMVENT 2011.
- Wang W.C, Calay R.K, Chen Y.K, Experimental evaluation of the performance of a low dew point dehumidification system. 10th International Energy Agency Heat Pump Conference 2011.



Experimental study of an energy efficient hybrid system for surface drying

W.C. Wang, R.K. Calay*, Y.K. Chen

Sustainable Energy Technology Centre, University of Hertfordshire, Hatfield, Herts AL10 9AB, UK

ARTICLE INFO

Article history:

Received 19 February 2010
Accepted 16 September 2010
Available online 24 September 2010

Keywords:

Dehumidification
Drying
Heat recovery

ABSTRACT

Rapid surface drying is an important and energy intensive process in food and beverage packaging industry. Usually these products are dried at low dew-point temperatures (DPT) -10 to -20 °C and low dry ball temperatures (DBT) 20 – 30 °C for product quality optimization. The conveyor moves at very high speeds and it is necessary to expose as much of the drying surface to the drying effect in a shortest time possible. Re-condensation is a big problem in these systems and a good drying system is that preserves the quality of the product and is energy efficient. This paper presents a feasibility study to obtain the design parameters of a hybrid dryer suited for rapid drying applications. Drying process of a re-circulation heat pump is integrated with rotary dehumidifier (desiccant wheel) system. The system employed a refrigerant circuit in conjunction with a heat reactivated desiccant wheel to provide efficient drying capability and supply low DPT conditions. To increase the economic practicality of such a hybrid system, the combined system utilises the heat dissipated by the condenser in regenerating the desiccant wheel. The study shows that the proposed hybrid system can deliver supply air at much lower DPT compared to the single refrigerant circuit and a desiccant wheel. By operating the combined system in tandem, greater amount of dehumidification could be realised due to the improved ratio of latent to total load at the hybrid. Up to 60% heat energy can be saved in rapid surface drying applications by using the proposed hybrid system.

© 2010 Elsevier Ltd. All rights reserved.

1. Introduction

Drying process is an energy intensive activity and plays a significant role in many industrial applications such as food, textile and paper and in many other processing industries. Rapid surface drying is a special form of drying which is widely used in food and beverage packaging industry such as bottles, cans and food packets and pouches. Usually these products are dried at low dew-point temperatures (DPT) -10 ~ -20 °C and low dry ball temperatures (DBT) 20 – 30 °C for product quality optimization. The big issue in these applications is re-condensation and the moisture interference with the drying processes which adversely affects the product quality and reduces production process speeds. For example, when the cider is bottled cold it quickly causes condensation to form on the neck and body of the bottles' surface. This moisture must be completely removed prior to labeling, coating, date stamps or the label can easily slip out of alignment and water can collect under the foil wrap around the neck presenting possible hygiene concerns to customers. Drying is very rapid; compressed air is blown over the bottle on the conveyor belt, which moves at very high speeds (e.g. up to 2000 bottles per minute). Therefore, firstly it

is necessary to expose as much of the drying surface to the drying effect in a shortest time possible. Secondly, energy consumption is a concern for all industries. Typically the energy efficiency for various drying applications is between 20 and 60% depending on the type of dryer and product used for drying [1]. The excessive energy consumption is not acceptable when the non-replenishable resources such as gas and oil are used. Use of hydrocarbon fuels also has problems such as CO₂ emission. For drying industry there are economic implications due to rising cost of energy. Therefore innovative methods are sought to develop low energy or efficient drying systems. A drying process involves heat and mass transfer in a dynamic process and how to achieve proper drying conditions is an important research field. The optimized drying time and energy consumption would result in an ideal drying condition. Table 1 shows the most promising options for energy savings that can then be selected [2].

This study investigates a feasibility of using a hybrid dryer suited for rapid drying applications. Analytical and experimental studies were performed to obtain the design parameters for the proposed hybrid system. A combination of a dehumidifier with a heat pump is a possible energy efficient alternative method that can be applied for drying and dehumidification. The dehumidification method dries a surface by cooling the air below its dew point and causing it to condense out the water vapor. Alternatively a desiccant adsorption

* Corresponding author. Tel.: +44 1707 281098; fax: +44 1707 285086.
E-mail address: r.k.calay@herts.ac.uk (R.K. Calay).

Nomenclature

\dot{W}_{comp}	Compressor power requirement (kW)
H	Enthalpy of refrigerant (kJ/kg)
\dot{Q}_c	Heat transfer rate of condenser (kW)
\dot{Q}_e	Heat transfer rate of evaporator (kW)
\dot{m}_a	Mass flow rate of air (kg/s)
h	Enthalpy of air (kJ/kg dry air)
h_{fg}	Latent heat of vaporization (kJ/kg dry air)
ε	Effectiveness of desiccant wheel
w	Humidity ratio of air (kg water/kg dry air)
\dot{m}_r	Mass flow rate of refrigerant (kg/s)
\dot{m}_w	Moisture removal capacity (kg/s)
COP	Coefficient of performance
DBT	Dry ball temperature (°C)
DPT	Dew-point temperature (°C)

DW	Desiccant wheel
HP	Heat pump
RH	Relative humidity (%)
SHR	Ratio of sensible load to total load
SMER	Specific moisture extraction rate (kg/kWh)

Subscripts

1	Space air inlet or refrigerant outlet at evaporator
2	Space air inlet at desiccant wheel or refrigerant inlet at evaporator
3	Process air outlet at desiccant wheel
4	Ambient air inlet or refrigerant inlet at condenser
5	Ambient air inlet at desiccant wheel or refrigerant outlet at condenser
6	Regeneration air outlet at desiccant wheel

system such as a rotary dehumidifier can be used. Both technologies have wide application in building service applications for air conditioning system [3–7]. The use of regeneration heating in desiccant rotary dryers has a limitations in energy saving. But waste heat energy could be useful normal energy source if it were used so that electrical heating with its implications of use of natural resources may not be necessary.

The role of heat pump desiccant dehumidifier is to turn up the heat recovery by the heat pump cycle. In general, the moist air with a certain temperature at the outlet of the dryer is not discharged to the outside but circulated through heat exchangers such as the evaporator. The evaporator recovers the sensible and latent heat from the moist air by condensing water vapor. The recovered energy utilizes the heat dissipated by the condenser in regenerating the desiccant wheel. The desiccant wheel, which removes water vapor from the air by desiccant material, is analogous to water vapor condensing on evaporator surface. The latent heat corresponding to the extracted water liberated into the surrounding air is analogous to energy recovery through the condenser of a heat pump dryer.

The surface drying plays essential role in food packaging, labeling of bottles and cans. The aim of the current paper is to introduce a hybrid system for surface drying consisting of heat pump desiccant dehumidifier. The heat pump cycle and desiccant dehumidification was developed and investigated for the thermal and drying performance of wet surface bottles. A surface drying process is controlled by three variables, temperature, humidity rate and direction of air flow rate from external conditions. Thus, the values of these three variables should be optimized to obtain the maximum efficiency and drying performance [8]. Design parameters of the proposed dryer

were obtained by simulating the heat pump cycle and drying process.

The refrigerant R134a is used in the heat pump system. In order to examine the performance, the COP of the heat pump cycle, the specific moisture extraction rate (SMER) of the drying process, the dehydration rate in the evaporator and desiccant, the temperature and relative humidity (RH) of drying air are estimated and compared for given conditions. The thermal properties of the moist air used in the analysis are obtained from the wet surface bottles on high speed conveyor line as the test material in the surface drying process.

2. Hybrid system descriptions

Fig. 1. shows a heat pump desiccant dehumidifier proposed in this study. The system utilises a refrigerant circuit in conjunction with a heat reactivated desiccant wheel to provide efficient drying capability. Due to the capabilities of the desiccant wheel, the unit can continue to provide substantial capacity and low supply DPT conditions. Process air dehumidification can be achieved by two steps: cooling the air below its dew point and removing moisture by condensation from evaporator and adsorption by a desiccant material [9].

The heat pump desiccant dehumidifier is used and the simple analysis using the drying efficiency model is employed in the drying process. The steady-state drying process can be assumed in the loop-type dryer due to their continuous process, but the steady state cannot be obtained in an open-type dryer such as a conveyer dryer. During the constant rate period, the drying process might be steady state in the open-type dryer. In the present study a steady state is assumed. The variables used in the analysis such as temperature, relative humidity, and enthalpy, are the averaged values in a given state. The local variations of the variables are not considered in the heat exchangers, pipes, air flows with a pressure-enthalpy ($p-h$) diagram.

For process air side a fan provides the evaporation air flow from the space air at state 1. The moist space air from the dryer enters the evaporator where the air is dehydrated as the moist condense on the surface of the evaporator. Thus, the latent heat of condensation is recovered from the moist air in the evaporator. At the evaporator outlet at state 2 the air temperature is nearly saturated but is also very cool and low humidity ratio. Then the air through desiccant material comes into contact with the desiccant wheel, and exits the dehumidifier hot and dry at state 3. The wheel is then rotated so that the desiccant portion that has picked up moisture is exposed to hot reactivation air and its moisture removed.

Table 1

Potential energy savings for selected U.K. industries.

Option	Potential energy savings		Penetration rating ^a
	(109 MJ/y)	(% Total)	
Heat recovery from dryer exhaust (other than heat pump)	18.9	15	High
Heat pumps (closed cycle)	8.9	6	Medium
Vapor compression	26.2	20	Low
Better instrumentation and control	4.3	3	Medium/high
Optimization of dryer design and operation	11	9	High
Improved dewatering of feedstock	5.3	4	High

^a Penetration rate is a guess of the degree of penetration of the potential market for the development that will eventually be achieved.

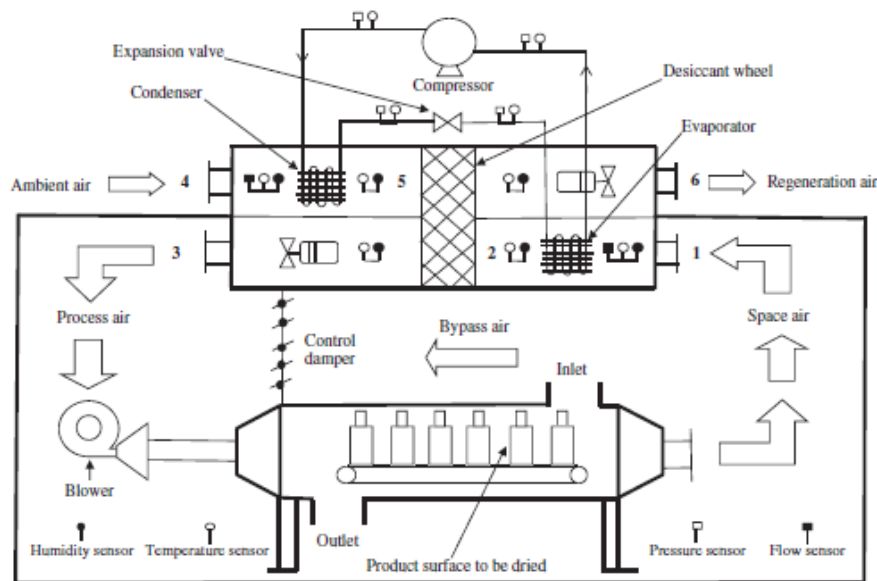


Fig. 1. Hybrid system combining heat pump and desiccant dehumidifier.

A fan is also necessary to provide the coolant air flow from the ambient air 4 into the condenser. The air at the condenser outlet is at high temperature and low RH. The air passing through the condenser is related only to sensible heat transfer, the absolute humidity is kept to be constant while the air is heated in the condenser. Hot and relatively dry air at approximately ambient pressure is supplied to the desiccant regenerator at state 5. The air gains moisture in a nearly isenthalpic process and exits more humid state 6. There is also a slight increase in the entropy of the air due to the moisture addition. The moist air exiting the regenerator desiccant is still relatively hot and nearly at ambient pressure. Fig. 2 shows that heat pump desiccant dehumidifier drying process on the psychrometric chart.

As the desiccant removes the moisture from the air, desiccant releases heat and warms the air, i.e., latent heat becomes sensible heat. To re-use the desiccant, it must be regenerated or reactivated through a process in which moisture is driven off by heat from condenser waste heat. The dried warm air can obtain desirable condition by sensible condenser.

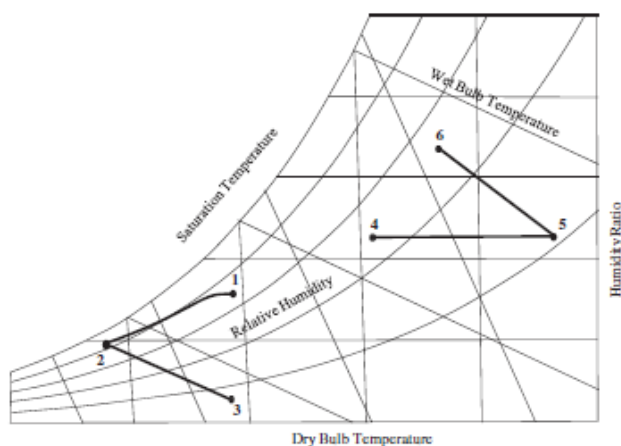


Fig. 2. Psychrometric diagram of an ideal heat pump desiccant dehumidifier with defined state points.

To increase the economic practicality of such a hybrid system, the combined system utilizes the waste heat from the condenser coil to drive moisture off of the desiccant wheel, no extra energy is required to provide increased dehumidification performance. By using the exhaust airstream to remove all heat rejected by the refrigeration system, no additional condenser fans or remote condensers are required. The location of the compressor and expansion valve in the cycle tends to enhance this heat recovery by creating relatively large temperature differences.

3. Experimental test system and measurements

By employing the mathematical model developed by Subramanyam et al. [5,6]. It is known that system performance is mainly governed by the design and operating parameters of heat pump and desiccant wheel. The other parameters of primary importance are inlet process air DBT, RH, and process air flow rate. An optimal choice of these parameters will reduce the regeneration heat required for a given load and operation cost in terms of minimizing air flow rate in process sides. The refrigerant R134a is used in the heat pump system. In order to examine the performance, the input energy of the heat pump cycle, the SMER of the dehumidification process, the dehumidify rate in the evaporator and desiccant, the DPT and of dehumidification air are estimated and compared for given conditions. The thermal properties of the moist air used in the analysis are obtained from the moisture air space in the dehumidification process. The photo of the hybrid system experimental equipment is shown Fig. 3.

A model of a heat pump system of the refrigerant cycle is generated in order to simulate the process close to the real one. The modelling is done using the adiabatic efficiency applied to the isentropic compression process. The given operating conditions are used to design the heat pump cycle. The pressure, temperature, quality, and enthalpy at each cycle point are determined from the modelling. Then the compressor power, the heat transfer rate of the condenser and evaporator, and the air flow rate of process drying air are worked out.

As the refrigerant passes through the evaporator, heat transfer from the refrigerated space results in the vaporization of the refrigerant [10]

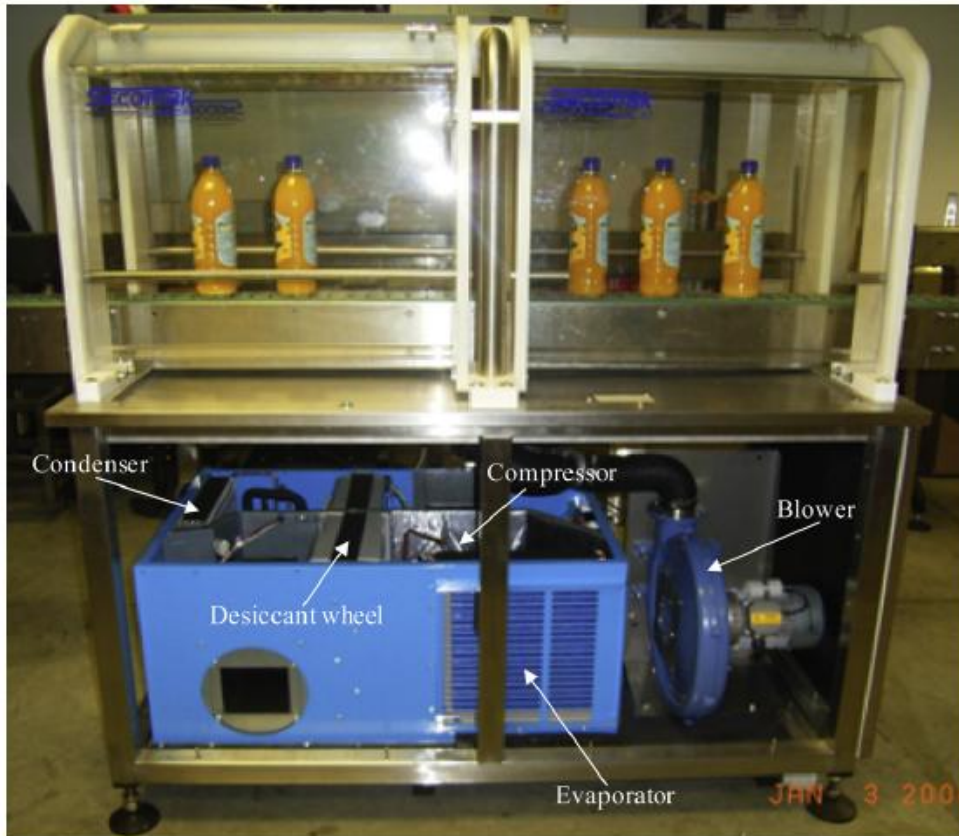


Fig. 3. The photo of the hybrid system experimental equipment.

$$\dot{Q}_e = \dot{m}_r(H_1 - H_2) \quad (1)$$

The cooling capacity of process drying air [11]

$$\dot{Q}_e = \dot{m}_a(h_1 - h_2) \quad (2)$$

Moisture removal capacity of process air in heat pump integrated desiccant wheel is

$$\dot{m}_w = \dot{m}_a(w_1 - w_3) \quad (3)$$

The refrigerant passes through the condenser, where the refrigerant condenses and there is heat transfer from the refrigerant to the cooler surroundings

$$\dot{Q}_c = \dot{m}_r(H_4 - H_5) \quad (4)$$

The heat release rate in heat pump of the condenser of regeneration air

$$\dot{Q}_c = \dot{m}_a(h_5 - h_4) \quad (5)$$

Finally, the energy balance of the heat pump dryer system is given by

$$\dot{Q}_c = \dot{Q}_e + W_{\text{comp}} \quad (6)$$

The dehumidification performance of the system is evaluated by the COP of the heat pump and the SMER of the process air [13]

$$\text{COP} = \frac{Q_c}{W_{\text{comp}}} \quad (7)$$

$$\text{SMER} = \frac{\dot{m}_w}{W_{\text{comp}}} \quad (8)$$

The moisture air dehumidification occurring in desiccant wheel and its operation can be considered by combination of its heat and mass transfer. Considering that the mass flow rates of process air and regeneration air are not equal. Hence for having a more realistic condition, that includes mass air flow rate of regeneration and process air parameters, the modified regeneration desiccant efficient is given by [12–15]

$$\varepsilon_{\text{DW}} = \frac{\dot{m}_{\text{process}}(\omega_2 - \omega_3)h_{\text{fg}}}{\dot{m}_{\text{Regeneration}}(h_5 - h_4)} = \frac{Q_{\text{Latent}}}{Q_{\text{Regeneration}}} \quad (9)$$

where Q_{latent} is the vaporization latent heat rate of the adsorbed water and $Q_{\text{regeneration}}$ is the input heat of regeneration rate.

4. Experiment setup

A heat pump desiccant dehumidifier was developed on the basis of the design parameters obtained from the energy modelling approach analysis. Temperatures and pressures of the refrigerant at several points of the system were measured during drying to determine the performance of the heat pump system. Using the

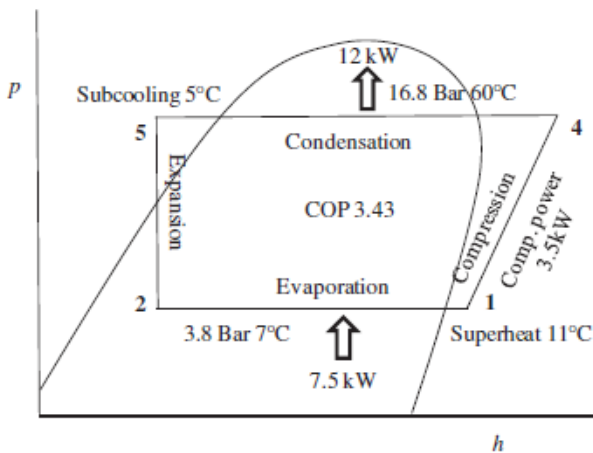


Fig. 4. Heat pump R134a refrigerant cycle.

temperatures, pressure, thermodynamic relations and properties, cycle of the heat pump can be drawn and the COP of the cycle can approximately be evaluated. For a given set of operating conditions, data is taken under steady-state conditions. Measurements for the process and regeneration air streams include inlet and outlet air temperature using a series of high accuracy T type thermocouples sensors ($\pm 0.1^\circ\text{C}$). The upper limit of measured temperature is 250°C , the lower limit is -75°C , relative humidity using RH sensor range from 0% to 100% and its linearity error is ($\pm 1.5\%$). Air flow

rates using hotwire anemometer range from 0.2 m/s to 20 m/s accuracy ($\pm 5\% + 1\text{d}$). Power consumed by the compressor using 10VA maximum watt transducer accuracy is ($\pm 0.2\%$).

The honeycombed silica gel composite desiccant wheels were used in this experiment. It can work well under lower regeneration temperature and achieve higher dehumidification capacity. The air channel coated with abundant desiccant materials is capable of removing the moisture from the passing process air. Hydraulic diameter of each honeycomb channel is 2.1 mm and it is coated with a 2 mm thick silica gel layer. The portion of regeneration section to adsorption section is 1/4. Diameter of the wheel is 32 cm, with a length of 20 cm. The desiccant wheel speed is 24.5 rpm. The process and regeneration air flow rates were chosen 1300 and 1000 m^3/h respectively.

Fig. 4 shows the heat pump cycle $p-h$ diagrams. The system was designed to have a refrigeration capacity of about 3.5 kW in the compressor, obtained with the conditions such as the heat release rate of the condenser of 12 kW, heat rate at the evaporator 7.5 kW. The average condensing temperature 60°C , average evaporating temperature 7°C , superheating at 11°C , the sub cooling at 5°C and the COP of the heat pump cycle is 3.43.

5. Results and conclusion

Fig. 5 shows the schematic of the hybrid system and the sample results. The states of the drying air are determined with psychrometric relations illustrated in Fig. 2. The air conditions used in the analysis of the drying process are the DBT of 19.3°C and RH of 54.2% at the evaporator inlet, sensible heat ration (SHR) 0.7, air flow rate

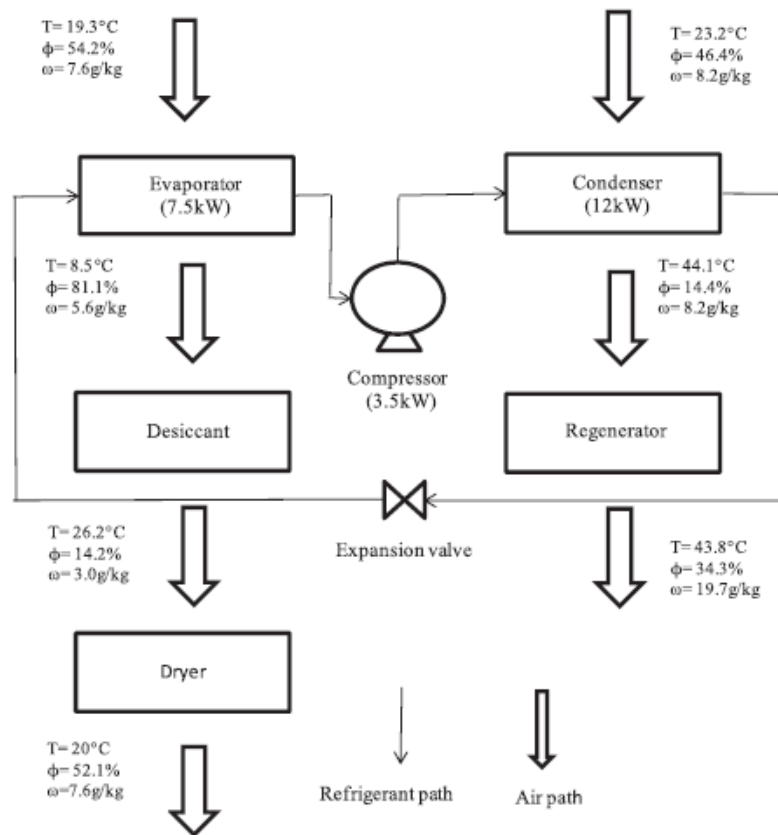


Fig. 5. Hybrid system drying air process.

of 1300 m³/h, and the air is dehydrated and cooled down in the evaporator. Then the air enters the desiccant at DBT of 8.5 °C and RH increases to 81.1% and due to the temperature rise in desiccant, leaves the desiccant at DBT of 26.2 °C and at very low RH of 14.2%. The volumetric flow rate of the air varies slightly due to the density change with temperature, but the mass flow rate is kept constant because the air flow system is assumed to be closed. On the other side, ambient air conditions DBT of 23.2 °C and RH of 46.4% inlet the condenser, then only sensible reheat to DBT of 44.1 °C before passing through the desiccant wheel, in which desiccant material pickup moisture from the process air and transports to the hot regenerated air. The air leaving the desiccant wheel is DBT of 43.8 °C and RH of 34.3% exhausted to the ambient, the humidity ratio of regeneration air is increased and its temperature decreases.

5.1. Effect of inlet air temperature

Comparisons between single refrigerant circuit system, single desiccant wheel system and hybrid system operating in tandem are shown in Fig. 6. These three systems are tested at the following conditions, air flow rate 1300 m³/h, RH = 60% and outlet air DPT keep at 5.6 °C. The variation in input energy required for each system with respect to inlet air DBT from 20 °C to 30 °C is plotted. It shows that the input energy required for all systems increases with the inlet air temperature due to increased driving potential for mass transfer. However the energy demand for the hybrid system is less than the other two single systems at all inlet temperatures. It is clear that the energy requirement is reduced can be saved via the hybrid system. It is suggested that this improvement in heat recovery may be associated with the greater heat transfer area for heat transferring with the drying air and that the evaporator undertook a part of the cooling duty to cool the air to dew-point temperature. Therefore, the desiccant could dedicate more of its surface for latent heat recovery. In a physical sense, the hybrid system may be equivalent to have enlarged the mechanical boundaries for heat recovery in a drying air cycle. Fig. 6 also shows that the SMER of the refrigerant circuit system is more than that of the desiccant wheel system but less than that of hybrid system throughout the range of inlet air temperature as the hybrid system was gradually activated. The addition of desiccant wheel improved the system performance in terms of SMER. It is evident that an introduction of the desiccant wheel not only gained moist air from evaporator but also provided additional sensible heating to the air without an auxiliary heater. The gradual activation of the hybrid system improved SMER in the range of 37–42%. The additional advantage gained in terms of system performance is by employing both dehumidification and regeneration. It is suggested that this outcome may be attributed to the finite rate of heat transfer in the heat exchangers as the air interacted with more heat exchangers.

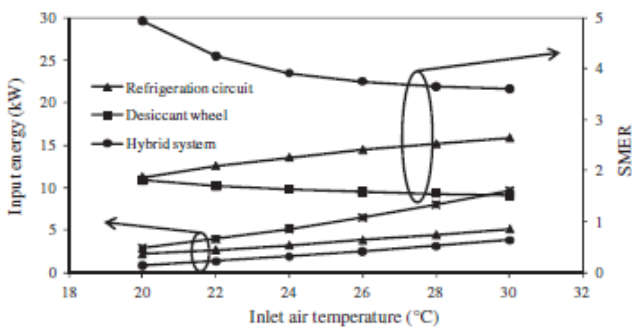


Fig. 6. Effect of inlet air temperature on input energy required and SMER.

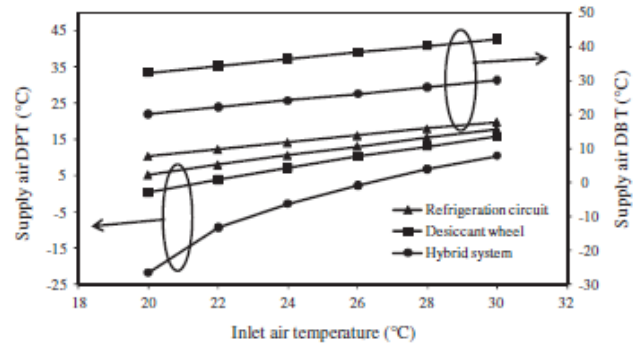


Fig. 7. Effect of inlet air temperature on DPT and DBT.

Fig. 7 shows the hybrid system integrated refrigerant circuit and desiccant wheel are driven by the same refrigerant circuit load 7.5 kW cooling capacity. The supply air DPT increases with the inlet temperature rate due to increased driving potential for mass transfer. Further, the supply air DPT of the hybrid system is lower than that of the refrigerant circuit and desiccant wheel at all inlet temperature rates. This is because the hybrid system decreased the sensible and latent load on the cooling coil, resulting in reheat and dehumidification on desiccant wheel. In other words, the potential for sensible heat transfer is reduced, while the potential for moisture transfer is increased. It is observed that supply air DTB of the hybrid system is lowered by about –20 °C compared to that the refrigerant circuit and desiccant wheel, which enables to maintain low humidity in the dryer. Fig. 7 also shows that the supply air DBT of the hybrid system is more than that of refrigerant circuit but less than that of desiccant wheel throughout the range of inlet air temperature rate. The hybrid system basically converts the latent load to sensible load by absorbing moisture and releasing heat to air. Hence its supply air temperature is always more by about 20 °C throughout the range. However, it is less by about 13 °C compared to that of the desiccant wheel. Thus the hybrid system is far better than single refrigerant circuit in providing low humidity, while the single desiccant wheel cannot provide low humidity at all.

5.2. Effect of air flow rate

It is well known that the air flow rate of the drying air is a key parameter in a drying system [7]. The flow rate uses the air flow and is closely related to the air velocity in the drying process. Although the high air velocity results in a fast evaporation of water, the quality of the products might be degraded. The low air velocity causes the drying rate to decrease so that the productivity will

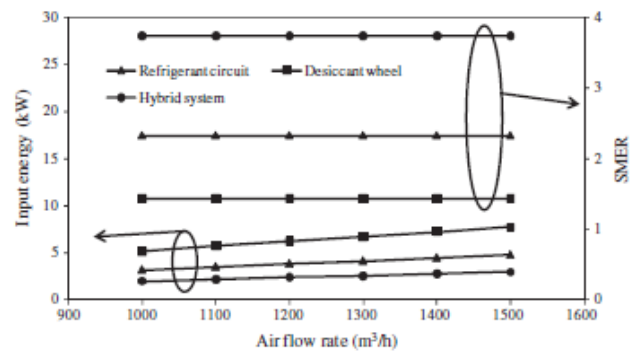


Fig. 8. Effect of air flow rate on input energy required and SMER.

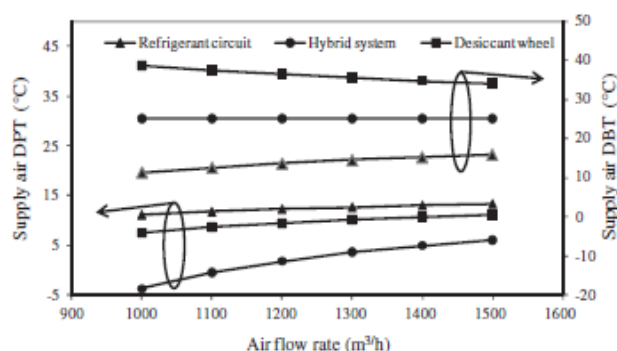


Fig. 9. Effect of air flow rate on DPT and DBT.

decrease. Therefore, the appropriate flow rate for a dryer operation in the optimized conditions should be determined in order to achieve a requested high efficiency. In this section, experiments were conducted to study the effect of regulating the process air flow rate by the control damper. The three systems were tested at the following conditions, process air flow rate from 1000 m³/h to 1500 m³/h, inlet air DBT fixed at 25 °C, RH = 60% and outlet air DPT kept at 5.6 °C.

Fig. 8 illustrates that in all three systems the input power energy increase significantly with air flow rate. However the rate of increase in input energy in the hybrid system is significantly less when compared to the rate of increase in input energy for the desiccant wheel but when compared with the refrigerant circuit system the rate of increase is similar. However the input energy for hybrid system is the least of all the systems. This is because condenser heat release is more than the heat recovered by evaporator. There is no change in the SMER when the air flow rate is increased though all three systems. This is because as the air flow rate increases the input power energy also increases in the system to meet the change in the humidity ratio (Fig. 8).

The variation in DPT with respect to air flow rate is compared in Fig. 9 for the three systems. The DPT increases with the increasing air flow rate in all three systems, which is attributed to a short residence time. The hybrid system integrated refrigerant circuit and desiccant wheel are driven by same refrigerant circuit load 7.5 kW cooling capacity. In the case of hybrid system, the integrated desiccant wheel further dehumidifies the DPT is lowered by about -3.7 °C compared to that of refrigerant circuit and desiccant wheel signifying the effectiveness of the former for achieving low humidity air. Fig. 9 also depicts correlations between the air flow rate and the supply air DBT. It can be seen that the supply DBT of the hybrid system is more than that of the refrigerant circuit but less than that of desiccant wheel throughout the range of air flow rate.

6. Conclusions

A prototype heat pump desiccant dehumidifier assisted mechanical drying system was designed, fabricated, and tested for enhancing the drying efficiency. The system operates cost-effectively because energy required for the regeneration of the desiccant wheel is recycled from the condenser waste heat. The system is integrally designed and controlled for superior performance in even the highest humidity load conditions. The present study confirms the importance of improving heat recovery to improve the performance of heat-pump-assisted drying systems. Adopting the modular approach of increasing the complexity of the heat pump

cycle, the following key conclusions may be drawn from the present investigation:

1. By utilising the waste heat from the condenser coil to drive moisture off of the desiccant wheel, up to 30% to 60% more heat energy can be saved by hybrid system depending on SHR in comparison to a system consisting of single refrigerant circuit or desiccant wheel.
2. The addition of desiccant wheel in refrigerant circuit improves the system performance in terms of SMER in the range of 12–20%. The introduction of the desiccant wheel is not only to provide efficient drying capability and low supply dew-point conditions but also provides additional sensible heating to the air without the incorporation of an auxiliary heater thus achieving a very high energy efficiency,
3. Regulating the air flow of the control damper is found to be an effective method to regulate the humidity of the drying air while enhancing the amount of energy recovered from the drying air thus avoiding the need for cooling and reheating air.
4. Increasing the air flow rate over the cooling coil and desiccant wheel was found to improve the system performance in terms of moisture removal capacity, which was increased from 7.3 to 11 kg/h when air flow rate is increased from 1000 to 1500 m³/h.

Acknowledgements

The authors thank Mr. David Dell from Secomak Limited, U.K. for providing support for experimental facilities.

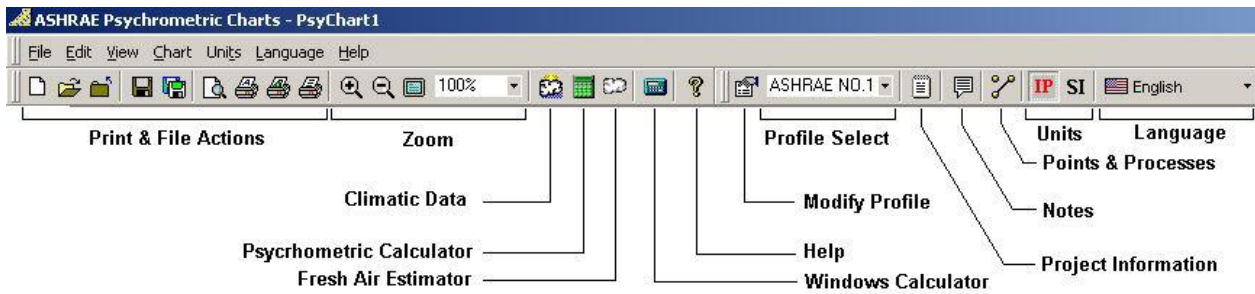
References

- [1] S. Mujumdar Arun, in: Handbook of Industrial Drying, third ed. Taylor & Francis Group, LLC, 2007, pp. 3–32.
- [2] C.G.J. Baker, D. Reay, Energy usage for drying in selected U.K. Industrial sectors, *Proceeding of Third International Drying Symposium 1* (1982) 201–209.
- [3] P.I. Dhar, S.K. Singh, Studies on solid desiccant based hybrid air-conditioning systems, *Applied Thermal Engineering* 21 (2001) 119–134.
- [4] M. Lazzarin Renato, Castellotti Francesco, A new heat pump desiccant dehumidifier for supermarket application, *Energy and Buildings* 39 (2007) 59–65.
- [5] N. Subramanyam, M.P. Maiya, S. Srinivasa Murthy, Application of desiccant wheel to control humidity in air-conditioning systems, *Applied Thermal Engineering* 24 (2004) 2777–2788.
- [6] N. Subramanyam, M.P. Maiya, S. Srinivasa Murthy, Parametric studies on a desiccant assisted air-conditioner, *Applied Thermal Engineering* 24 (2004) 2679–2688.
- [7] K. Ghali, M. Othmani, N. Ghaddar, Energy consumption and feasibility study of a hybrid desiccant dehumidification air conditioning system on Beirut, *International Journal of Green Energy* 5 (2008) 360–372.
- [8] Lee Kong Hoon, Kim Ook Joong, Investigation on drying performance and energy savings of the batch-type heat pump dryer, *Drying Technology* 27 (2009) 565–573.
- [9] Pesaran Ahmad, A., A review of desiccant dehumidification technology. Prepared for proceedings of EPRI's electric dehumidification: energy efficient humidity control for commercial and institutional buildings conference, New Orleans, Louisiana, NREL/TP-472-7010; June 2–3, 1993.
- [10] U.S. Pal, M.K. Khan, Calculation steps for the design of different components of heat pump dryers under constant drying rate condition, *Drying Technology* 26 (2008) 864–872.
- [11] Carpinlioglu Melda Ozdinc, Yildirim Murtaza, A methodology for the performance evaluation of an experimental desiccant cooling system, *International Communications in Heat and Mass Transfer* 32 (2005) 1400–1410.
- [12] K.J. Chua, S.K. Chou, A modular approach to study the performance of a two-stage heat pump system for drying, *Applied Thermal Engineering* 25 (2005) 1363–1379.
- [13] M. Ali Mandegari, H. Pahlavanzadeh, Introduction of a new definition for effectiveness of desiccant wheels, *Energy* 34 (2009) 797–803.
- [14] Kanoglu Mehmet, Carpinlioglu Melda Ozdinc, Yildirim Murtaza, Energy and exergy analyses of an experimental open-cycle desiccant cooling system, *Applied Thermal Engineering* 24 (2004) 919–932.
- [15] C.X. Jia, Y.J. Dai, J.Y. Wu, R.Z. Wang, Use of compound desiccant to develop high performance desiccant cooling system, *International Journal of Refrigeration* 30 (2007) 345–353.

Appendix-B ASHRAE Psychrometric Chart

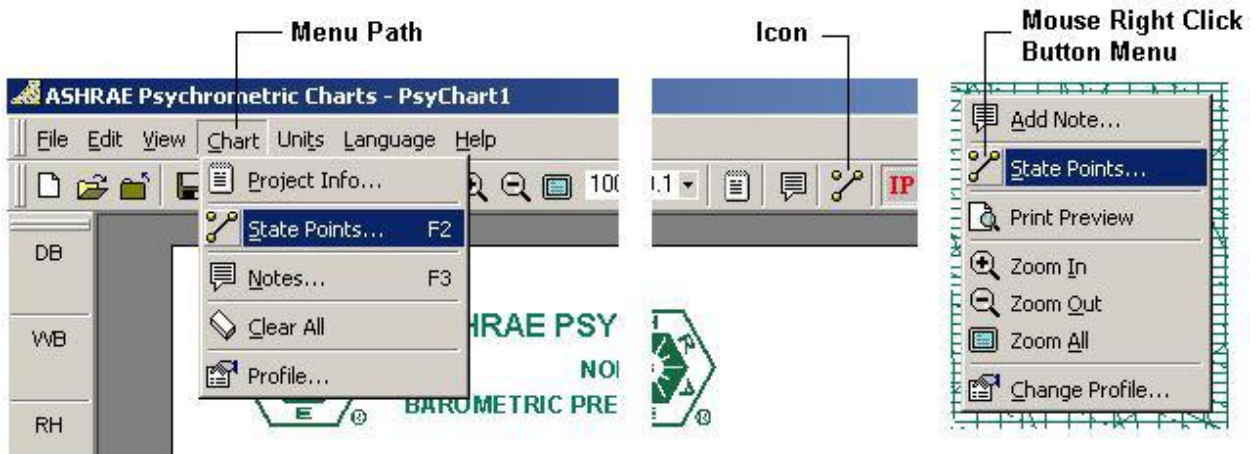
Menus and Toolbars

The Psychrometric Analysis services via a standard Windows menu and tool bar system. Each component of the system can be dragged and docked to the top, bottom, left or right sides of the Psychrometric Chart Window, or can become floating menus positioned anywhere within the Psychrometric Window.

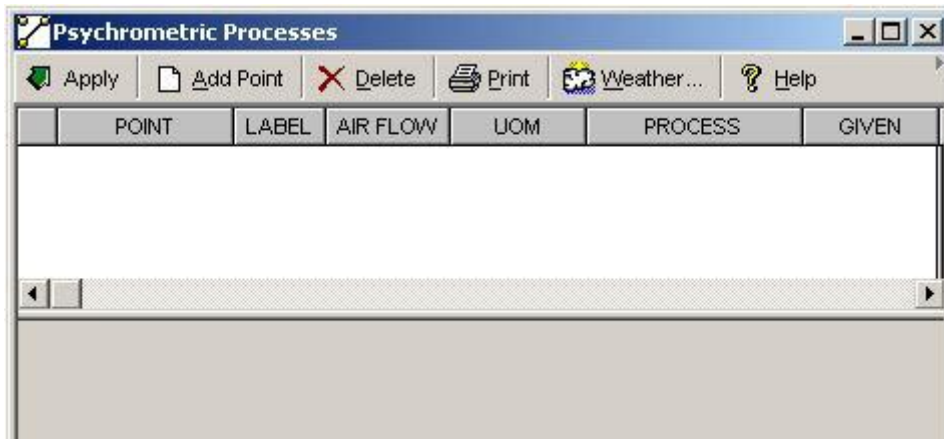


State Point and Process Line Plotting

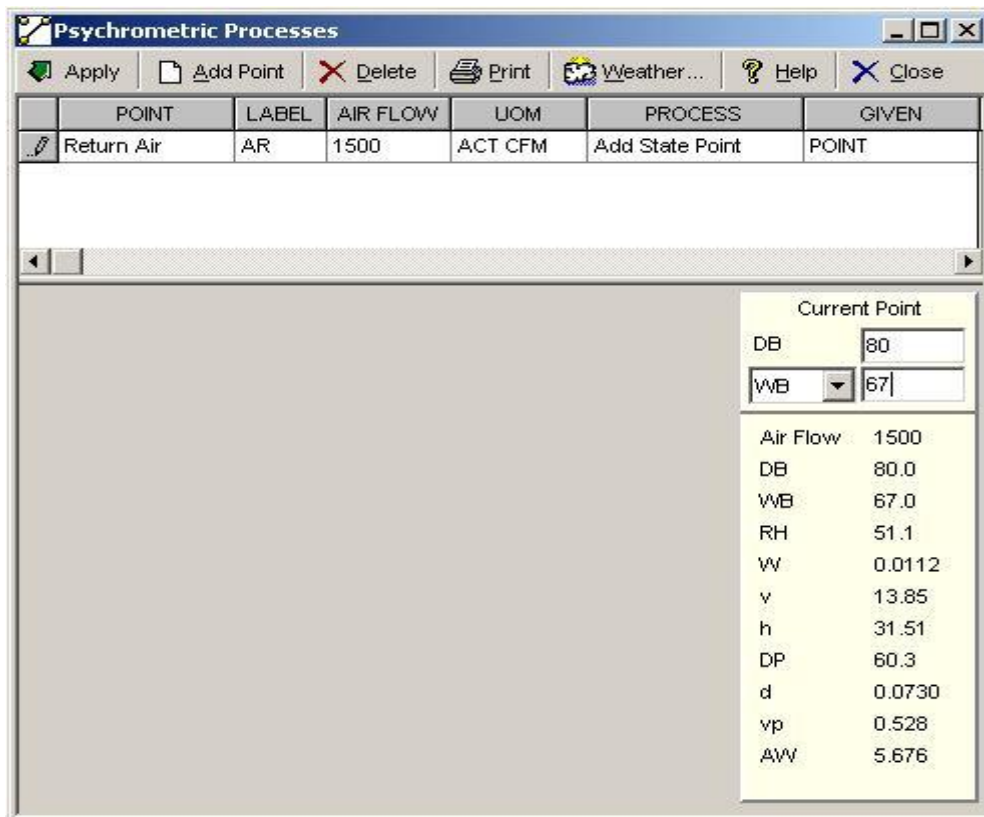
1. Activate "Psychrometric Processes" by any of the three methods shown below:



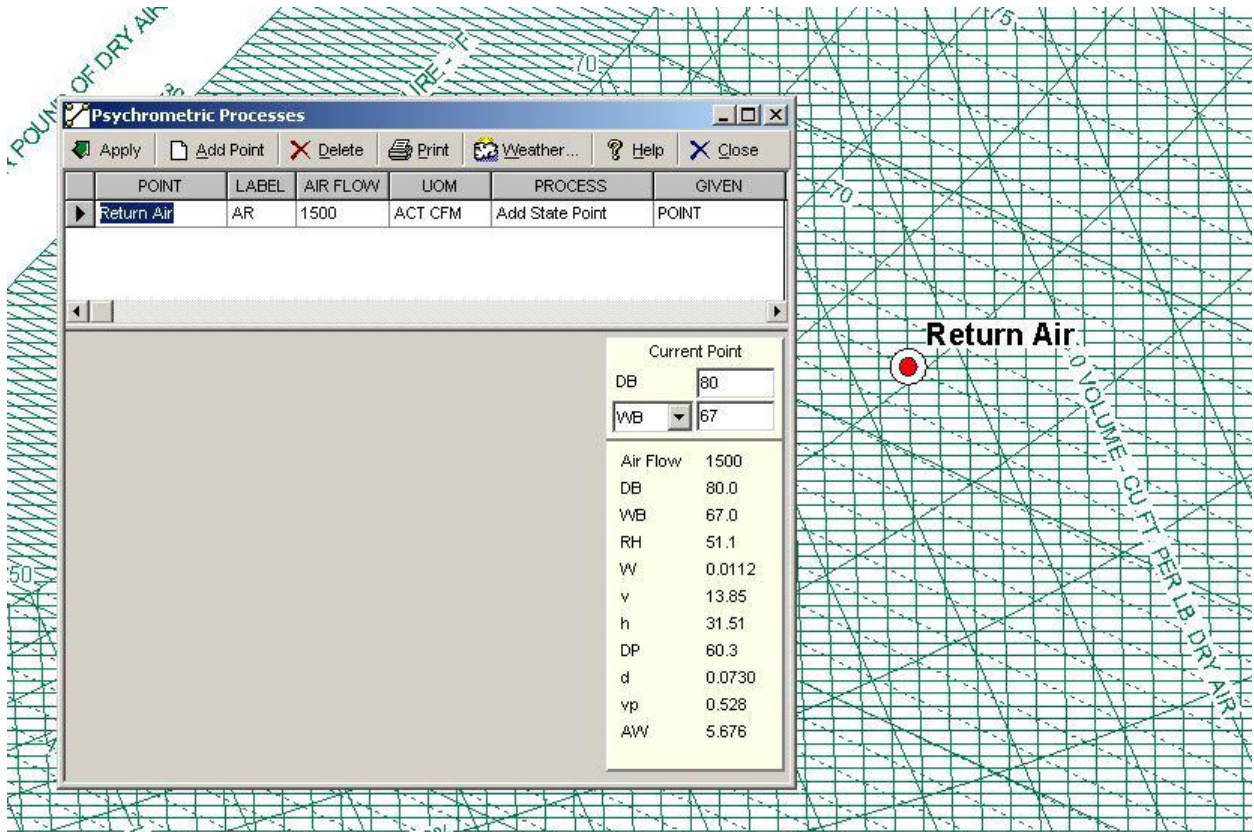
2. The Psychrometric Processes window appears with blank data fields.



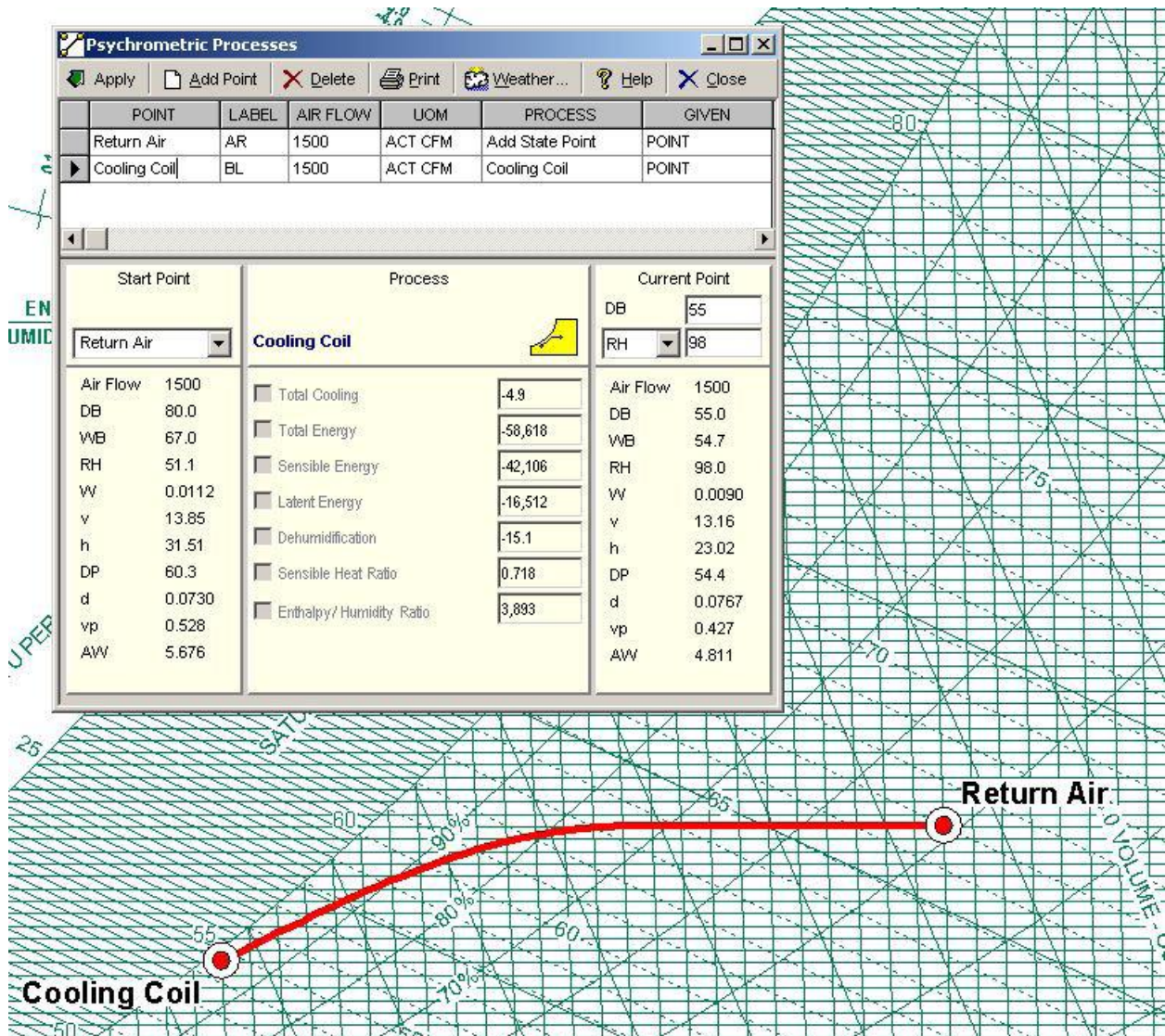
3. To enter a new point, click the Add Point button. Fill in the grid information as needed (point name, point label location, enter the airflow, select air flow units, select process and select given option). If this is the first point, the only process offered is "Add State Point" since there are no other points to create a process with. Click on the "Current Point" panel and enter dry bulb temperature, enter moisture value and select moisture property from the drop-down box.



4. Click on the Apply button and the point is plotted to the chart.

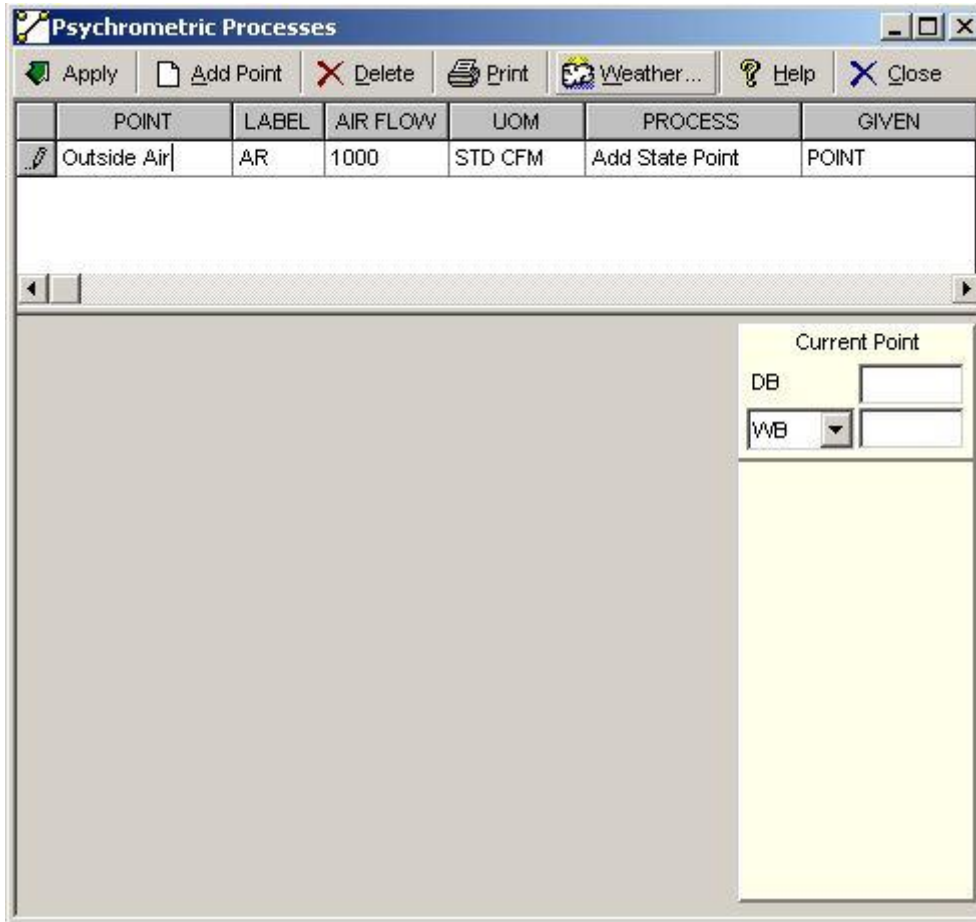


5. Click the Add Point button again to continue adding new points. Adding more than one point enables additional PROCESSES to be selected in the grid. The given column will also be enabled, after the first point is entered, to allow entering either the end point, calculating the process energy or entering the process energy and calculating the end point. After each successive point, click the Apply button to plot the point and process to the chart.



Additional processes can be added to complete any system. If you need to make changes you may do so to any point by just clicking on the proper grid row, make any desired changes and simply click "Apply" and the point and connecting processes are automatically updated.

6. To apply a Climatic Data weather point to the chart, simply click on the Weather icon to access the Climatic Data Window.



7. Select the geographic location by country, state and city. Select the desired outside design condition (for Summer Cooling: 0.4%, 1% or 2%) (for Winter Heating: 99.6% or 99%).

Psychrometric Processes

POINT	LABEL	AIR FLOW	UOM	PROCESS	GIVEN
Outside Air	AR	1000	STD CFM	Add State Point	POINT

Current Point
DB:
WB:

Climatic Data - ASHRAE 1997 Fundamentals

COOLING USA 1,033 Elevation, Feet English (IP)
 HEATING Georgia 33.65 North Latitude Metric (SI)
 WIND Atlanta 84.42 West Longitude Apply

SUMMER COOLING

	DB °F	MWB °F	WB °F	MDB °F	DP °F	MDB °F
0.4%	93	75	77	88	74	82
1%	91	74	76	87	73	81
2%	88	73	75	85	72	80

Average Annual Max. DB °F 96 Std. Dev. °F 3 Mean Daily Range DB °F 17

WINTER HEATING

	DB °F	RH %	Coldest Month	WS mph	MCD °F	Average Annual Min. DB °F	Std. Dev. °F
99.6%	18	50	0.4%	23	37	9	7
99%	23	50	1%	21	36		

WIND

	MCWS mph	PWD deg.
Coincident with 0.4% DB (cooling)	9	300
Coincident with 99.6% DB (heating)	12	320
Annual Design Values	1% 22 mph, 2% 19 mph, 5% 17 mph	

8. To apply this design condition as a State Point, simply click the Apply button in the upper left hand of the Window and then close the Climatic Data Window to return to State Points & Processes.

Psychrometric Processes

POINT	LABEL	AIR FLOW	UOM	PROCESS	GIVEN
Outside Air	AR	1000	STD CFM	Add State Point	POINT

Current Point
DB: 93
WB: 75

Air Flow 1000
DB 93.0
WB 75.0
RH 43.7
W 0.0146
v 14.25
h 38.42
DP 67.7
d 0.0712
vp 0.684
AW 7.173

Climatic Data - ASHRAE 1997 Fundamentals

COOLING USA 1,033 Elevation, Feet English (IP)
 HEATING Georgia 33.65 North Latitude Metric (SI)
 WIND Atlanta 84.42 West Longitude Apply

SUMMER COOLING

	DB °F	MWB °F	WB °F	MDB °F	DP °F	MDB °F
0.4%	93	75	77	88	74	82
1%	91	74	76	87	73	81
2%	88	73	75	85	72	80

Average Annual Max. DB °F 96 Std. Dev. °F 3 Mean Daily Range DB °F 17

WINTER HEATING

	DB °F	RH %	Coldest Month	WS mph	MCD °F	Average Annual Min. DB °F	Std. Dev. °F
99.6%	18	50	0.4%	23	37	9	7
99%	23	50	1%	21	36		

WIND

	MCWS mph	PWD deg.
Coincident with 0.4% DB (cooling)	9	300
Coincident with 99.6% DB (heating)	12	320
Annual Design Values	1% 22 mph, 2% 19 mph, 5% 17 mph	

Appendix-C Auxiliary Calculations

Atmospheric Pressure

$$P = \text{Atm} \times (1 - 6.8753 \times 10^{-6} \times Z)^{5.2559}$$

P = inches of Mercury

$$\text{Atm} = 29.921299597519$$

Z = elevation in feet

Water Vapor Saturation Pressure

For $311.67^{\circ}\text{R} \leq T < 491.67^{\circ}\text{R}$

$$pws = \exp(C_1 \div T + C_2 + C_3 \times T + C_4 \times T^2 + C_5 \times T^3 + C_6 \times T^4 + C_7 \times \ln(T))$$

T = absolute temperature, $^{\circ}\text{R} = ^{\circ}\text{F} + 459.67$

$$C_1 = -1.0214165 \times E^4$$

$$C_2 = -4.8932428 \times E^0$$

$$C_3 = -5.3765794 \times E^{-3}$$

$$C_4 = 1.9202377 \times E^{-7}$$

$$C_5 = 3.5575832 \times E^{-10}$$

$$C_6 = -9.0344688 \times E^{-14}$$

$$C_7 = 4.1635019 \times E^0$$

For $491.67^{\circ}\text{R} < T < 851.67^{\circ}\text{R}$

$$pws = \exp(C_8 \div T + C_9 + C_{10} \times T + C_{11} \times T^2 + C_{12} \times T^3 + C_{13} \times \ln(T))$$

T = absolute temperature, $^{\circ}\text{R} = ^{\circ}\text{F} + 459.67$

$$C_8 = -1.0440397 \times E^4$$

$$C_9 = -1.1294650 \times E^1$$

$$C_{10} = -2.7022355 \times E^{-2}$$

$$C_{11} = 1.2890360 \times E^{-5}$$

$$C_{12} = -2.4780681 \times E^{-9}$$

$$C_{13} = 6.5459673 \times E^0$$

Saturated Humidity Ratio

$$W_s = \frac{0.62198 \times f \times P_{ws}}{p - f \times P_{ws}}$$

P = total pressure of moist air

f = enhancement factor

P_{ws} = pressure of saturated pure water

Enhancement Factor

f = calculated in accordance with Hyland and Wexler (1973, "The Second")

Humidity Ratio

For $t^* > 32^{\circ}F$

$$W = \frac{(1093 - 0.556 \times t^*) \times W_s - c_p \times (t - t^*)}{1093 + 0.444 \times t - t^*}$$

t^* = thermodynamic wet-bulb temperature of moist air, $^{\circ}F$

t = dry-bulb temperature of moist air, $^{\circ}F$

c_p = specific heat of moist air, Btu/lb $^{\circ}F$

W = humidity ratio of moist air at saturation at thermodynamic wet-bulb temperature

For $t^* \leq 32^{\circ}F$

$$W = \frac{(1061 + 0.444 \times t^* - (-143.34 + 0.5 \times (t^* - 32))) \times W_s - c_p \times (t - t^*)}{1061 + 0.444 \times t^* - (-143.34 + 0.5 \times (t^* - 32))}$$

t^* = thermodynamic wet-bulb temperature of moist air, $^{\circ}F$

t = dry-bulb temperature of moist air, $^{\circ}F$

c_p = specific heat of moist air, Btu/lb $^{\circ}F$

W^* = humidity ratio of moist air at saturation at thermodynamic wet-bulb Temperature

Specific Heat

$$c_p = -2.0921943 \times 10^{-14} \times t^4 + 2.5588383 \times 10^{-11} \times t^3 + 1.2900877 \times 10^{-8} \times t^2 + 5.8045267 \times 10^{-5} \times t + 0.2395$$

t = dry-bulb temperature of moist air, $^{\circ}F$

Specific Volume

$$v = \frac{0.7543 \times (t + 459.67) + (1 + 1.6078 \times W)}{P}$$

t = dry-bulb temperature of moist air⁰F

W = humidity ratio of moist air, mass of water per unit mass of dry air

P = total pressure of moist air

Enthalpy

$$h = c_p \times t + W \times (1061 + 0.444 \times t)$$

t = dry-bulb temperature of moist air⁰F

W = humidity ratio of moist air, mass of water per unit mass of dry air

c_p = specific heat of moist air, Btu/lb⁰F

Wet Bulb

Iterative calculation calling Humidity Ratio function

Dew Point

Iterative calculation calling Saturated Humidity Ratio function